KAUNAS UNIVERSITY OF TECHNOLOGY

ERNESTA AUGUSTINIENĖ

GENETICALLY ENCODED BIOSENSORS FOR METABOLIC ENGINEERING AND IMPROVED BIOSYNTHESIS OF ORGANIC AND PHENOLIC ACIDS

Doctoral dissertation
Technological Sciences, Chemical Engineering (T 005)

Kaunas, 2023

This doctoral dissertation was prepared at Kaunas University of Technology, Faculty of Chemical Technology, Department of Silicate Technology during the period of 2019–2023.

Scientific Supervisor:
Prof. Dr. Kęstutis BALTAKYS (Kaunas University of Technology, Technological Sciences, Chemical Engineering, T 005).

Scientific Advisor:
Prof. Dr. Naglis MALYS (Kaunas University of Technology, Technological Sciences, Chemical Engineering, T 005).

Edited by: English language editor Dr. Armandas RUMŠAS (Publishing House *Technologija*), Lithuanian language editor Aurelija Gražina RUKŠAITĖ (Publishing House *Technologija*).

The official defense of the dissertation will be held at 10 a.m. on 17 October 2023 at the public meeting of Dissertation Defense Board of Chemical Engineering Science Field in Rectorate Hall of Kaunas University of Technology.

Address: K. Donelaičio 73 - 402, Kaunas, LT-44249, Lithuania
Phone: (+370) 608 28 527; e-mail: doktorantura@ktu.lt

Doctoral dissertation was sent on 15 September 2023.

The doctoral dissertation is available on the internet at http://ktu.edu and at the library of Kaunas University of Technology (Gedimino 50, LT-44239, Kaunas, Lithuania).

KAUNO TECHNOLOGIJOS UNIVERSITETAS

ERNESTA AUGUSTINIENĖ

GENETIŠKAI UŽKODUOTI BIOJUTIKLIAI METABOLINEI INŽINERIJAI IR PATOBULINTAI ORGANINIŲ IR FENOLINIŲ RŪGŠČIŲ BIOSINTEZEI

Daktaro disertacija
Technologijos mokslai, Chemijos inžinerija (T 005)

2023, Kaunas

Disertacija rengta 2019–2023 metais Kauno technologijos universiteto Cheminės technologijos fakultete, Silikatų technologijos katedroje.

Mokslinis vadovas:
prof. dr. Kęstutis BALTAKYS (Kauno technologijos universitetas, technologijos mokslai, chemijos inžinerija, T 005).

Mokslinis konsultantas:
prof. dr. Naglis MALYS (Kauno technologijos universitetas, technologijos mokslai, chemijos inžinerija, T 005).

Redagavo: anglų kalbos redaktorius dr. Armandas RUMŠAS (leidykla „Technologija“), lietuvių kalbos redaktorė Aurelija Gražina RUKŠAITĖ (leidykla „Technologija“).

Chemijos inžinerijos mokslo krypties disertacijos gynimo taryba:
prof. dr. Daiva LESKAUSKAITĖ (Kauno technologijos universitetas, technologijos mokslai, chemijos inžinerija, T 005) – **pirmininkė**;
doc. dr. Anatolijus EISINAS (Kauno technologijos universitetas, technologijos mokslai, chemijos inžinerija, T 005);
dr. Egidija RAINOSALO („Centria“ taikomųjų mokslų universitetas, Suomija, technologijos mokslai, chemijos inžinerija, T 005);
dr. Paulius Lukas TAMOŠIŪNAS (Vilniaus universitetas, gamtos mokslai, biochemija, N 004);
prof. dr. Petras Rimantas VENSKUTONIS (Kauno technologijos universitetas, technologijos mokslai, chemijos inžinerija, T 005).

Disertacija bus ginama viešame Chemijos inžinerijos mokslo krypties disertacijos gynimo tarybos posėdyje 2023 m. spalio 17 d. 10 val. Kauno technologijos universiteto Rektorato salėje.

Adresas: K. Donelaičio g. 73 - 402, Kaunas, LT-44249, Lietuva.
Tel. (+370) 608 28 527; el. paštas: doktorantura@ktu.lt

Disertacija išsiųsta 2023 m. rugsėjo 15 d.

Su disertacija galima susipažinti interneto svetainėje http://ktu.edu ir Kauno technologijos universiteto bibliotekoje (Gedimino g. 50, 44239 Kaunas).

CONTENTS

LIST OF TABLES

LIST OF FIGURES

LIST OF ABBREVIATIONS

ADP – adenosine diphosphate;
ALE – adaptive laboratory evolution;
ANF – absolute normalized fluorescence;
ATP – adenosine triphosphate;
BLAST – basic local alignment search tool;
D-nLDH – NAD-dependent D-lactate dehydrogenase;
DNA – deoxyribonucleic acid;
EMP – pathway Embden-Meyerhof-Parnas pathway;
FACS – fluorescence-activated cell sorting;
FAD – flavin adenine dinucleotide;
FMN – flavin mononucleotide;
FRET – Förster resonance energy transfer;
gDNA – genomic deoxyribonucleic acid;
GFP – green fluorescent protein;
HEPES – 4-(2-hydroxyethyl)-1-piperazineethanesulfonic acid;
HPLC – high-performance liquid chromatography;
iLDH – NAD-independent lactate dehydrogenase;
LAB – lactic acid bacteria;
LB – lysogeny broth;
LC-MS – liquid chromatography–mass spectrometry;
L-nLDH – NAD-dependent L-lactate dehydrogenase;
mcl-PHA – *mcl*-polyhydroxyalkanoate;
MICF – membrane integrated continuous fermentation;
MM – minimal medium;
MRS – De Man, Rogosa and Sharpe broth;
N/A – not available;
NAD^+ – nicotinamide adenine dinucleotide oxidized form;
NADH – nicotinamide adenine dinucleotide reduced form;
ND – protein homologue was not determined;
nLDH – NAD-dependent lactate dehydrogenase;
NS – no significant homology was found;
ORRF – organic-rich residual fraction obtained from saccharified wheat starch solution via the production of glucose syrup;
PCL – poly-ε-caprolactone;
PCR – polymerase chain reaction;
pDNR – plasmid deoxyribonucleic acid;
PGA – poly(glycolic acid);
PHB – polyhydroxybutyrate;
PLA – polylactic acid;
PLGA – poly(lactic-co-glycolic acid);
RBS – ribosome binding site;
RFP – red fluorescent protein;
RNA – ribonucleic acid;
SG-MM – minimal medium containing 0.4% sodium gluconate;

SHF – separated hydrolysis fermentation;
SSCF – simultaneous saccharification and co-fermentation;
SSF – simultaneous saccharification and fermentation;
TF – transcription factor;
TR – transcription regulator.

The abbreviations and sources of microorganism strains are represented in Table 2.2 (see the *Materials and Methods* Section).

INTRODUCTION

Synthetic biology was first mentioned in the early 20th century in the book of the medical scientist and biologist Stephane Leduc and defined as "…either we succeed in controlling a life phenomenon to the extent that we can evoke the same whenever we wish […] or else we manage to identify the numerical connection between experimental condition and the biological result"[1]. Thus, synthetic biology involves the development of new biological systems, or the transformation of the already existing ones for some useful purposes. Microorganisms, including bacteria, have sensing and regulatory devices based on the transcription regulator (TR) which can activate gene expression in response to changes in metabolite concentrations[2]. One of the directions in synthetic biology is the development of genetically encoded biosensors based on inducible gene expression systems consisting of TR and cognate inducible promoters[3]. Genetically encoded biosensors constitute a high-throughput analytical technique to understand mechanisms of the gene expression control. Future applications of biosensors include the monitoring of intra- and extracellular metabolite concentration, high-throughput screening for rapid strain evolution, dynamic pathway control, and adaptive laboratory evolution[4,5,6]. Genetically encoded small-molecule biosensors provide an opportunity to link the concentration of metabolites associated with phenotypes[5,7].

Organic acids, including L- and D-lactic acids, are an important platform used for the production of various compounds, including biodegradable bioplastics that can replace the traditional petroleum-based polymers [8,9]. The US *Department of Energy* identified lactic acid as one of the 10 most important high-value green chemicals [10]. There are many examples which describe the production of L- and D-lactic acid. The leading producer is LAB, reaching a yield of 1 g/g with traditional substrates[11,12,13,14,15,16]. Although several studies have successfully used lignocellulosic waste or residues from the agro-food industry for fermentation, the efficient production of L- and D-lactic acid from alternative substrates still remains a challenge. Meanwhile, phenolic acids are significant antioxidants and antimicrobial agents, basically used in pharmacy, cosmetics, and chemical industries, and it can also be utilized as precursors for the production of other value-added compounds, for example, catechol, vanillin, muconic and adipic acids, etc[17]. Hydroxycinnamic acids can be produced naturally by some bacteria and fungi, but in very low yields, and these compounds are often metabolic intermediates[18]. The development of metabolically modified strains is the main path for the efficient production of hydroxycinnamic acids.

The microbial fermentation of lactic acids and hydroxycinnamic acids takes precedence over alternative production methods. Fermentation does not require organic solvents, expensive precursors, or harsh reaction conditions. Furthermore, optically pure L- and D-acids can be obtained only by fermentation. Microbial cell factories require strains which can use not only the traditional substrates, but also low-cost, non-food alternatives, including glycerol, lignocellulose, and industrial residues. The transformation of alternative substrates, such as residues or wastes from the agro-food industry, into value-added materials not only ensures efficient production, but it

is also an integral part of the circular economy[19]. Pairing an appropriate microorganism to the right substrate is the actual bottleneck requiring the search for strains or the development of genetically modified microorganisms which could efficiently use components of agro-food waste and remain viable in the presence of inhibitors formed via lignocellulose treatment.

Rapid and high-throughput analytical methods are required to search for and develop bacterial strains and adapt inexpensive and non-food alternative substrates. The traditional analytical methods – although precise and applicable (for example, HPLC, LC-MS, and commercial enzymatic methods) – are low-throughput, expensive, and time-consuming. Therefore, it is useful to use genetically encoded biosensors which allow the rapid characterization of several thousand variants in a short time, and they offer the potential to be applied to the development and selection of microbial strains and substrates for the efficient production of lactic and hydroxycinnamic acids [20].

The aim of the thesis is to identify and develop inducible gene expression systems for lactic acids and naturally occurring hydroxycinnamic acids.

The **objectives of the thesis are** as follows**:**

1. To identify and characterize L- and D-lactic acids inducible gene expression systems from *E. coli* MG1655, *C. necator* H16, and *Pseudomonas* spp.;
2. To identify and characterize hydroxycinnamic acids inducible gene expression systems from *E. coli* MG1655, *A. baylyi* ADP1, *B. multivorans* ATCC BAA-247, *P. putida* KT2440, and *L. argentoratensis* DSM 16365;
3. To develop a genetically encoded biosensor BLA1 specific for L-lactic acid and genetically encoded biosensor BLA2 induced by both L- and D-lactic acids and compare their performance against analytical techniques;
4. To apply genetically encoded biosensor BLA2 to optimize the composition of the media with glucose syrup production residues for D-lactic acid fermentation by *L. lactis*.

Scientific novelty of the thesis

The identified lactic and hydroxycinnamic acids inducible systems have been characterized and specified, and their kinetics, dynamic range, specificity, as well as the broad-host-range applicability have been demonstrated. The elucidation of the systems mechanisms allows us to understand the functions of the genes and the regulation of gene expression and protein synthesis in various bacterial strains in the presence of changes in the intra- and extracellular environment. For the first time, lactic acid-inducible systems from *C. necator* H16 and *p*-coumaric acid-inducible system from *B. multivorans* ATCC BAA-247 have been characterized. Moreover, the broad-host-range applicability of the inducible system from *L. argentoratensis* DSM 16365, responding to several hydroxycinnamic acids, has been demonstrated. Optically pure L- and D-lactic acids and their mixture have been produced by using residues remaining after glucose syrup production by *Lactobacillus* spp. For the first time, genetically encoded biosensors BLA1 and BLA2 have been applied to detect L-

and D-lactic acid in fermentation samples with one of the L- or D-lactic acid enantiomers and with a mixture of them, and have been validated with the traditional analytical methods. A rapid and high-throughput method has been demonstrated for the optimization of media formulations containing low-cost alternative carbon sources.

The practical value of the work

Genetically encoded biosensors based on inducible gene expression systems are an essential tool for the microbial production of value-added compounds as they enable the controlling of native and heterologous genes and biosynthetic pathways, and are suitable for high-throughput strains screening. The developed lactic acid-inducible biosensors allow the detection of L- and D-lactic acid in a racemic mixture with sufficient accuracy as well as high performance, and at a relatively low cost. Genetically encoded biosensors can be a great tool for determining the optimal media composition with the glucose syrup industry residues for improved L- and D-lactic acid fermentation by *Lactobacillus* spp. The production of value-added chemicals from renewable bioresources could reduce the negative environmental impacts of conventional chemical plants and the challenges posed by depleted petroleum resources.

Statements presented for the defense of the dissertation

1. Lactic acids-inducible gene expression systems identified in *E. coli* MG1655, *C. necator* H16, and *Pseudomonas* spp. which were used for the construction of genetically encoded biosensors and developed biosensors were applied for the determination of L- and D-lactic acids in biological samples with one enantiomer of L- or D-lactic acid or with their mixture.
2. Hydroxycinnamic acids-inducible gene expression systems identified in *E. coli* MG1655, *A. baylyi* ADP1, *B. multivorans* ATCC BAA-247, *P. putida* KT2440, and *L. argentoratensis* DSM 16365 were applied to the development of genetically encoded biosensors.

Approval and publication of the research results

The results of the research have been presented in 3 scientific publications in journals indexed in the *Web of Science* with Impact Factor (JCR SCIE): one of them published in *Scientific Reports*, one in *Critical Reviews in Biotechnology*, and one in *Biomolecules*. The results of the research have also been submitted in two scientific publications in journals indexed in the *Web of Science* with Impact Factor (JCR SCIE). The results of the dissertation have been presented at 4 international conferences: *Open Readings 2021: 64th International Conference for Students of Physics and Natural Sciences* (2021, Lithuania), Open Readings 2022: 65th International Conference for Students of Physics and Natural Sciences (2022, Lithuania), *6th Applied Synthetic Biology in Europe* (2022, United Kingdom), and *VIII Baltic Genetics Congress* (2023, Lithuania).

Contribution of the author and co-authors

The author has developed and characterized genetically encoded biosensors. Naglis Malys advised on the progress of the experiment and the analysis of the results. Kęstutis Baltakys and Naglis Malys advised on the progress in the preparation of the manuscript. Edita Mažonienė and Jurgita Kailiuviene derived and analyzed the composition of the glucose syrup production industrial waste. Ilona Jonuškienė consulted on the planning of experiments related to lactic acid fermentation. Michail Syrpas advised on HPLC analysis.

Structure and outline of the dissertation

The dissertation consists of an introduction, a literature review, results and discussion, material and methods, conclusions, a list of references, a list of publications on the topic of the dissertation, and supplementary information. The list of references includes 234 sources. The main results are discussed in 152 pages and illustrated in 21 tables and 27 figures. Supplementary information includes 7 tables and 14 figures.

1. LITERATURE REVIEW

1.1. Why Genetically Encoded Biosensors?

Genetically encoded biosensors include whole cells or cellular components and are rapidly used for the detection and quantification of metabolites. Biosensors offer advantages over other alternative analytical tools. They are rapid, cost-effective, and allow determination of metabolite concentrations in real time *in vivo*[7,21]. Biosensors can serve in the development of organic and phenolic acids-producing strains, as well as in the search for alternative and inexpensive substrates for fermentation. This chapter summarizes on the construction and application possibilities of genetically encoded biosensors and overviews the developed and described biosensors for organic and phenolic acids.

1.1.1 Comparison of genetically encoded biosensors with HPLC and other analytical tools

Lactic acids and hydroxycinnamic acids can be quantified by using a variety of analytical methods, including colorimetry, enzymatic spectrophotometry, enzymatic colorimetry, enzymatic micro-assays, voltammetry, and enzyme-based biosensors, HPLC coupled with a photodiode array detector, proton nuclear magnetic resonance spectroscopy, and LC-MS. An overview, including the advantages and disadvantages, of the suggested analytical approaches for lactic acids and hydroxycinnamic acids is summarized in Table 1.1.

Among the analytical methods used for the determination of lactic acid and hydroxycinnamic acids, HPLC is the most commonly used despite its high operating costs[22,23]. This analytical tool is denoted by high sensitivity, resolution, and accuracy, and the limit of detection for lactic acid was 0.0061 mM with a linearity range of 0.025–5.0 mM[23], while the limit of detection of *p*-coumaric acid was 0.00018 mM with a linearity range of 0.0008–0.5 mM[29]. The determination of L- and D-lactic acids with HPLC requires expensive columns, which further increases the cost of the analysis[24]. L- and D-lactic acid determination with enzymatic methods is also an expensive and time-consuming method.

Unlike the aforementioned characterization techniques (Table 1.1), whole-cell biosensors enable high-throughput screening of strains, thus facilitating metabolic engineering and adaptive laboratory evolution. Gene or microorganism screening for the improved production of various compounds can accelerate the design-build-test-learn cycle[20,25,26]. The development of genetically encoded biosensors can be expanded in the areas of specificity, the operational range, and the limits of detection.

Table 1.1. Advantages and disadvantages of analytical methods for the determination of lactic acid and hydroxycinnamic acids

Compound	Method	Cost effectiveness	Time efficiency	Reliability	Throughput	Linear dynamic range, mM (limit of detection)	References
Lactic acid	colorimetric method	high	medium	high	low	variable (0.0015)	Manufacturer's manual[a]
Lactic acid	voltammetric method	high	medium	medium	low	11.9–188 (1.54)	[27]
L-lactic acid and D-lactic acid	enzymatic methods	low	low	high	low	0.0056–0.333 (0.0023)	Manufacturer's manual[b]
Lactic acid	proton nuclear magnetic resonance method	very low	very low	low	very low	ND	[28]
Lactic acid	chromatographic methods (e.g., HPLC)	very low	low	very high	very low	0.025–5.0 (0.0061)	[23]
p-Coumaric acid						0.0008–0.5 (0.00018)	[29]
Lactic acid	LC-MS	very low	low	very high	very low	0.0038–0.379 (<0.0001)	[30]
Lactic acid	enzyme-based biosensors	high	low	high	low	0.0001–5.0 (0.00145)	[31]
Caffeic acid						0.0025–0.0125 (0.0023)	[32]
L-lactic acid	inducible systems-based biosensors	high	medium	high	very high	0.08–4.0 (0.001-0.05)	[33]
p-Coumaric acid						0.1–1	[34]

[a]Lactate Assay Kit (Colorimetric), *Cell Biolabs*, USA, 2016; [b]D-/L-Lactic Acid (D-/L-Lactate) (Rapid) Assay Kit, *Megazyme*, Ireland.

1.1.2. Genetically encoded biosensors design

Complex genetic regulatory systems are found in the nature, and they are required for cells to understand the environmental conditions and detect various metabolites (intra- and extracellular). In such systems, the sensing of the target signal or metabolite is coupled to an actuator response, which alters the gene activity. These systems are used to construct genetically encoded biosensors to measure the concentrations of target metabolites and to translate the input into a useful output (e.g., fluorescent protein and biosynthetic pathway expression). Biosensors provide a method to detect, monitor, and regulate the cellular metabolic productivity[7,21]. There are three categories of genetically encoded small molecule biosensors: TR-based biosensors, riboswitches, and FRET-based biosensors[35]. In this work, the construction of biosensors based on TR is accomplished, and a flowchart of genetically encoded biosensor construction and investigation is represented in Fig. 1.1.

Gene transcription is regulated by TR, which contains an N-terminal domain (interacts with the promoter) and a C-terminal domain (interacts with the ligand). The N-terminal domain binds to specific DNA sequences in the promoters and controls the formation of RNA polymerase and promoter complex. These regulators can be activators and/or repressors. Repressors bind to the operator and prevent the formation of an RNA polymerase-promoter complex while the activators bind to the operator and promote the formation of a stable RNR polymerase-promoter complex [36,37]. Genetically encoded biosensors are based on inducible gene expression systems, whereas plasmid construction is composed of two essential components: a sensing unit which detects changes in the signal transduction and a reporting unit which converts these changes into a measurable form. The reporting unit typically consists of the fluorescent protein and is coupled to the sensing unit, and so the changes in the sensory block alter the fluorescence[21,36]. More than 100 different biosensors for ions, molecules, and enzymes are currently being developed[38]. A list of the published fluorescent biosensors, which includes more than 750 different biosensor variants, is available at *BiosensorDB.ucsd.edu*[21].

Several parameters must be optimized for an efficient performance of a biosensor: (1) minimized leakiness to allow accurate measurements at low signal levels; (2) maximized reporter expression level to allow signal detection in the presence of background noise and to achieve high levels of gene expression for sensing and control applications; (3) a high dynamic range allows more confident identification due to a high signal-to-noise ratio; (4) sensitivity; (5) sensing range; (6) specificity. Biosensors have been optimized by using directed evolution, mechanistic modelling, and rational engineering [39,40].

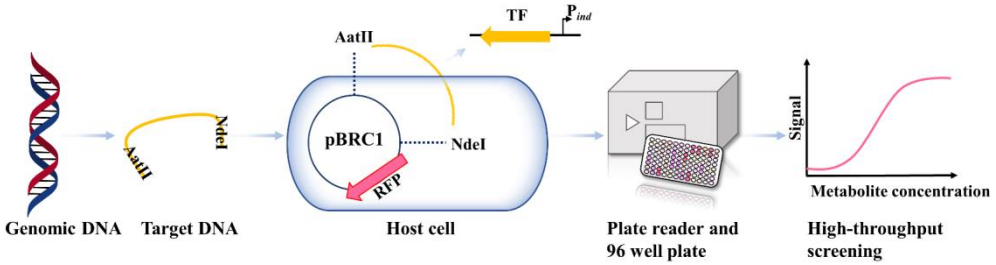

Fig. 1.1. Flowchart of the construction and investigation of genetically encoded biosensors

1.1.3. Established applications of genetically encoded biosensors

Although many publications describe the construction and characterization of transcriptional biosensors, only a few studies have reported the successful application of TR-based biosensors. The application of biosensors can be divided into several groups: biosensors for real-time monitoring, phenotype screening, dynamic pathway control, and adaptive evolution[7]. Table 1.2 represents the application of TR-based biosensors for more productive microbial acid production.

The biosensor can be used for phenotype screening when the detection of a target metabolite is coupled to the expression of fluorescent proteins. Screening campaigns are designed to identify improved producers from mutant libraries and select suitable synthetic pathway variants. The use of biosensors with FACS allows for ultra-high throughput screening at the single cell level and the isolation of producing single cells from very large libraries. The *trans*-cinnamic acid biosensor pSenCA was employed with FACS in *E. coli* for phenylalanine ammonia lyase variants with improved activity screening [41]. A lysine-specific biosensor consisting of a lysine-specific TF LysG and a reporter gene YFP was constructed and used to screen high lysine producers among the *C. glutamicum* library generated by chemical mutagenesis. With FACS analysis, highly improved mutant strains were screened [42]. The 3-hydroxypropionic acid biosensor generated a fluorescent signal that was proportional to 3-hydroxypropionic acid production during growth in the presence of interference components. This 3-hydroxypropionic acid biosensor can be widely used in applications of enzyme and metabolic engineering for the production of 3-hydroxypropionic acid [43].

Evolution approaches based on mutations and selections are a good tool for adapting microorganisms to stress conditions or for improving the formation of the target products. Adaptive laboratory evolution is a widely used and highly effective tool in metabolic engineering for creating industrial strains with superior properties. An experimental evolutionary method has been demonstrated to improve the production of metabolites using FACS. The L-valine producer *C. glutamicum* Δ*aceE* was equipped with an L-valine responsive sensor based on TF Lrp of *C. glutamicum*. The evolved strains featured a significantly higher growth rate, increased L-valine titers (25%), and a 3–4-fold reduction of by-product formation. Genome sequencing resulted in the identification of a loss-of-function mutation (UreD-E188*) in the gene

ureD (urease accessory protein), which was shown to increase L-valine production by up to 100%[44].

TF-based biosensors can be used to construct synthetic regulatory switches to dynamically regulate metabolic fluxes[45]. For example, Doong and colleagues provided an example of dual-regulation D-glucaric acid production in *E. coli* K-12 strains. First, it was necessary to dynamically knock down glycolytic flux and redirect carbon into the production of glucaric acid. Second, a biosensor for myo-inositol, which is an intermediate in the D-glucaric acid metabolism pathway, was applied. The use of both strategies resulted in a 4-fold increase in the titer (2 g/L) (see Table 1.2)[46].

Table 1.2. TR type small-molecule biosensors applied for the production of more productive microbial acids

Host chassis	Analyte	TFs	Field of application	Production increase (-fold)	Concentration (g/L)	Reference
E. coli K-12	*myo*-inositol	IpsA	improving D-glucaric acid production by using dynamic pathway regulation	4	2	[46]
S. cerevisiae CEN.PK113-11C	malonyl-CoA	FapR	improving 3-hydroxypropionic acid production by using dynamic pathway regulation	10	1	[47]
S. cerevisiae BY4741	muconic acid	Aro9p	improving muconic acid production by using ALE and metabolic engineering	3	0.5	[48]
P. putida KT2440	muconic acid	CatM	improving muconic acid production by using ALE	3	7	[49]

1.2. Organic Acids as Industrially Relevant Compounds

Organic acids, for example, glycolic, pyruvic, lactic, 3-hydroxypropionic, succinic, fumaric, itaconic, levulinic, muconic, adipic, and citric acid, are chemicals of top industrial importance which could be produced via microbial fermentation [50,51]. The opportunities to utilize renewable residual biomass as a feedstock to produce organic acids will further increase their production sustainability according to the circular economy principle[52]. This subsection presents the progress of lactic and glycolic acids in terms of their microbial fermentation, along with the catabolism principles in bacteria essential for developing genetically encoded biosensors.

1.2.1. Production of lactic acids and structurally similar compounds

Lactic acid (2-hydroxypropanoic acid) is a chiral organic acid that which exist in two enantiomeric forms: L-(+)-lactic acid and D-(–)-lactic acid. The presence of two optical isomers is attributed to an asymmetric carbon, which presents as a result of an adjacent hydroxyl and carboxyl group. These functional groups facilitate various chemical transformations, such as dehydration, esterification, oxidation, and hydrogenation. L- and D-lactic acids act as important platform chemicals from which numerous other substances can be derived: lactide, PLA, pyruvic acid, propylene glycol, etc. (Fig. 1.2)[8,53]. One of the most important compounds is PLA, a biodegradable and biocompatible plastic that can replace the traditional petroleum-based polymers, such as polyvinyl chloride, low-density polyethylene, linear low-density polyethylene, polypropylene, or polystyrene. PLA is widely available and is denoted by a low cost compared to other biodegradable polymers. However, the properties of PLA, such as crystallinity and high thermal tolerance, depend on the specific ratio of poly-L-lactic acid and poly-D-lactic acid in the mixture. The melting point of pure poly-L-lactic acid is 180 °C, while, for the blend of poly-L-lactic acid and poly-D-lactic acid, it is up to 230 °C[54,55]. It is also possible to blend PLA with PHB thus increasing the crystallinity and mechanical strength[56]. The reason to produce quality PLA is that it is not only important to produce optically pure L- and D-lactic acids efficiently, but that also it can be relevant produce PHB from various lignin derivatives. The global lactic acid market was valued at USD 2.9 billion in 2021, and is expected to reach USD 5.8 billion in 2030[57,58]. Meanwhile, PLA has become the dominant segment of the industrial lactic acid application due to its increasing use in the manufacturing of biodegradable and biocompatible products. The global PLA market size was USD 566.74 million in 2021, and it is expected to reach 2,709.61 million by 2030 according to a report by *Grand View Research*[59,60].

Glycolic acid (Fig. 1.2 (4)) is a small two-carbon α-hydroxy acid having alcohol and acid groups. This acid is used in various industries: in the textile industry as a dyeing and tanning agent; in the food industry as a flavor and a preservative, and in the pharmaceutical industry as a skin care agent. It is also used in industrial and household cleaning agents and adhesives, and is often included in emulsion polymers, solvents, and additives for inks and paints in order to improve the flow properties and gloss[9]. As with lactic acid, a biodegradable PGA polymer is produced from glycolic acid, and a PLGA copolymer for medical purposes can also be produced with lactic acid. The global glycolic acid market was valued at USD 468.2 million in 2019 and is projected to reach USD 820.3 million by 2027[96]. Glycolic acid is naturally produced by chemolithotrophic iron (*L. ferriphilum*, *A. ferrooxidans*, and *A. caldus*) and sulphur-oxidizing bacteria[97], a variety of yeast (*S. cerevisiae*, *P. naganishii* AKU 4267) [98,99], and acetic acid bacteria from ethylene glycol (*Acetobacter* sp.)[9]. However, glycolic acid can only be produced with the maximum yield by genetically modified microorganisms, for example, *E. cloacae*[100], *G. oxydans*[101], *E. coli*[102], and *K. lactis*[103].

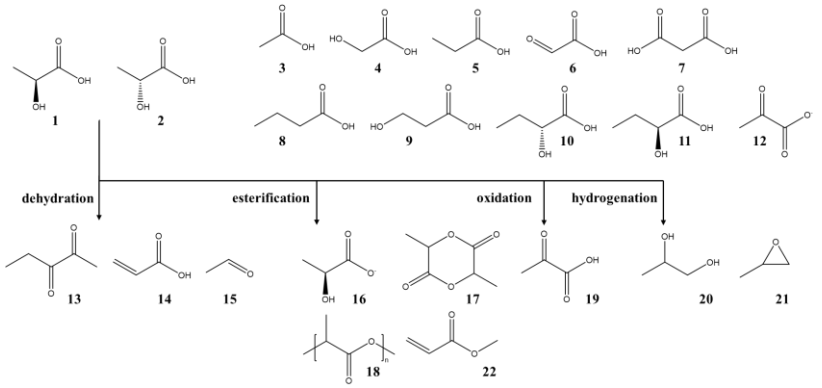

Fig. 1.2. Structurally similar compounds to L-lactic acid **(1)** and D-lactic acid **(2)**: acetic acid **(3)**, glycolic acid **(4)**, propionic acid **(5)**, glyoxylic acid **(6)**, malonic acid **(7)**, butyric acid **(8)**, 3-hydroxypropanoic acid **(9)**, D-2-hydroxybutyric acid **(10)**, L-2-hydroxybutyric acid **(11)**, pyruvate **(12)**, pentane-2,3-dione **(13)**, acrylic acid **(14)**, acetaldehyde **(15)**, lactates **(16)**, lactide **(17)**, PLA **(18)**, pyruvic acid **(19)**, propylene glycol **(20)**, propylene oxide **(21)**, methyl acrylate **(22)**

Lactic acid can be produced by chemical synthesis or fermentation. Fermentation takes precedence over chemical synthesis because it involves the fermentation of renewable raw feedstocks, does not use petroleum raw materials, and allows the production of optically pure L- and D-lactic acids by properly selecting the microorganism strains. Bacteria, filamentous fungi, yeast, and microalgae can naturally produce lactic acid. One of the most important producers in the industry is LAB, which includes the genera of *Lactococcus*, *Lactobacillus*, *Enterococcus*, *Pediococcus*, *Leuconostoc*, *Streptococcus*, *Bifidobacterium*, *Aerococcus*, *Tetragenecoccus*, *Vagococcus*, and *Carnobacterium*.

Naturally, microorganisms can produce lactic acid by homofermentation and heterofermentation from hexoses, pentoses, and glycerol. The theoretical yield of lactic acid is 100% from hexoses during homofermentation via the EMP pathway. One molecule of glucose is converted into two molecules of lactic acid generating two ATPs. Some LABs (*Enterococcus*, *Lactococcus*) can also utilize pentoses: three pentose molecules are converted into five molecules of lactic acid, and seven ATP molecules are also generated. In these reactions, the NAD^+/NADH state remains neutral (see Figs. 1.3a and 1.3b). Heterofermentative LAB (*Leuconostoc*, *Oenococcus*, *Weissella*, and some species of the *Lactobacillus* genus) converts only 50% of carbon into lactic acid via the phosphoketolase pathway, forming alongside one ATP molecule per hexose or pentose, and such by-products as ethanol or acetic acid (see Figs. 1.3d and 1.3e). LAB produces lactic acid with close to 100% yield from hexoses and pentoses [11,12,13,14,15,16]. *L. lactis* IO-1 can produce L-lactic acid from xylose with a titer of 20.62 g/L and a yield of 1 g/g[16]. It is important to note that no homolactic production by LAB of the D enantiomer form from pentoses has been reported to date to the best of the knowledge of the author of the thesis.

L-nLDH (EC 1.1.1.27) and D-nLDH (EC 1.1.1.28) enzymes catalyze the conversion of pyruvate to L- and D-lactic acids, respectively. The L-nLDH and D-nLDH enzymes encoding genes are established in different strains of LAB and some

other microorganisms[61]. The existence of both nLDH types in microorganism genomes results in the biosynthesis of both lactic acid enantiomeric forms, which prevents obtaining optically pure acids and requires genetic modification of the microorganism.

For the efficient production of L- and D-lactic acids, it is important to reduce the cost of the substrate material. The substrate should be inexpensive, readily available, and easily fermentable to a high product yield. Such crops as maize or rice are undesirable substrates because they impose an additional burden on agriculture. Therefore, a more sustainable option would be to use non-food substrates, such as glycerol, lignocellulose, and agro-food industries residues, including wastes [62,63,64,65]. In addition, there are possibilities to produce lactic acid from CH_4 or CO_2 [66,67,68,69].

Glycerol, a major by-product in the biodiesel manufacturing process, can be used as a carbon source for homo- and hetero-lactic acid fermentation. Bacteria can degrade glycerol in the *dhaK* pathway and/or the *glpK* pathway. Four ATP molecules are formed per three glycerol molecules through heterofermentation, and then one ATP molecule is formed per one glycerol molecule via homofermentation (see Figs. 1.3c and 1.3f)[70,71]. Among LAB, glycerol utilisation has been most extensively studied in *E. faecalis* and shown that this strain can produce L-lactic acid with a yield close to 1 g/g (Supplementary Table S1) [62,70]. The production of D-lactic acid using glycerol as a substrate by LAB has not yet been demonstrated. To enable the production of D-lactic acid using glycerol as a carbon source and achieve high yields, *E. coli* was engineered by disabling *pflB* along with other genes encoding enzymes involved in succinate, acetate, and ethanol formation, and additionally applying adaptive laboratory evolution (Table 1.3)[72].

Lignocellulose can also be used as an alternative substrate for lactic acid production, but it is important to highlight that, due to its complex structure, additional treatment is required before fermentation[73]. Chemical methods (e.g., acid or alkali treatment) or enzymatic (cellulases, β-glucosidases) are commonly used for pre-treatment [65,73,74]. The lignocellulosic treatment not only incurs the disadvantage of increasing the cost of lactic acid production, but also the process yields compounds which can inhibit the growth of microorganisms, including ionic liquid, furfural, and 5-hydroxymethylfurfural. Some bacteria can tolerate these compounds, *L. plantarum* SKL-22 can grow in the presence of 2% ionic liquid, and it is resistant against 10 g/L of furfural and 5-hydroxymethylfurfural [75]. However, this strain produces a racemic mixture of lactic acid. The production of D-lactic acid was reported by using *L. delbrueckii* subsp. *bulgaricus* strain from the lignocellulose treated with organic solvents, and it achieved a yield of 0.69 g/g and a productivity of 0.86 g/(Lh) [76]. A higher yield (0.93 g/g) of D-lactic acid was achieved with the *P. acidilatici* ZY15 strain after several genetic modifications enabling the ability of the strain to use xylose as a carbon source (Table 1.3)[77]. The efficient production of L-lactic acid from enzyme-saccharified hydrolysates of acid-impregnated steam explosion-treated plywood chips was demonstrated by using the *E. faecalis* SI strain (Supplementary Table S1). However, this study showed that *E. faecalis* SI used only glucose for L-lactic acid production, whereas the concentration of xylose in the substrate remained unchanged[78]. An interesting study was conducted by Johnson and Beckham (2015).

They showed the possibility of producing L-lactic acid from lignin derivatives, thus expanding the possibilities of utilizing lignocellulosic components[79]. Microalgae have also been studied as a promising feedstock for fermentative lactic acid production, as their walls are composed of cellulose and hemicellulose [64,80,81,82]. Optically pure L- and D-lactic acids have been obtained by using *Hydrodictyon reticulum* biomass with yields of 0.46 g/g and 0.46 g/g, respectively [80,81].

The use of agro-food industries residues for lactic acid fermentation can be a sustainable step in the circular economy [83,84]. Agro-food by-products in addition to carbohydrates may also contain lipids, proteins, vitamins, and minerals, which can positively affect the fermentation process. Orange peel [65], spent brewers' grain from beer production [85], gelatinized starchy waste [86], apple pomace [87], broken rice [88], cassava fibrous waste [89], sugarcane bagasse [90], and rice straw [91] have been used as feedstock for lactic acid production (Table 1.1 and Supplementary Table S1). Starch-rich waste can be used for the production of L-lactic acid with amylolytic microorganisms [86]. However, most of the residues are composed of lignocellulosic feedstock, which requires processing, as mentioned above. A fermentation strategy for sugarcane bagasse using *P. acidilactici* D01 strain adapted with laboratory evolution for the capacity of aldehyde inhibitor conversion was recently demonstrated. The pre-fermentation of water-soluble carbohydrates before the sugarcane bagasse pre-treatment allowed reducing the generation of 5-hydroxymethylfurfural and increasing the yield of D-lactic acid up to 0.58 g/g [90].

In conclusion, the use of alternative feedstock for lactic acid production, and especially the production of D-lactic acid, still remains a challenge. Consequently, more detailed studies on the productivity, tolerance, and the ability of the strains to utilize substrates of complex sugar composition are still needed.

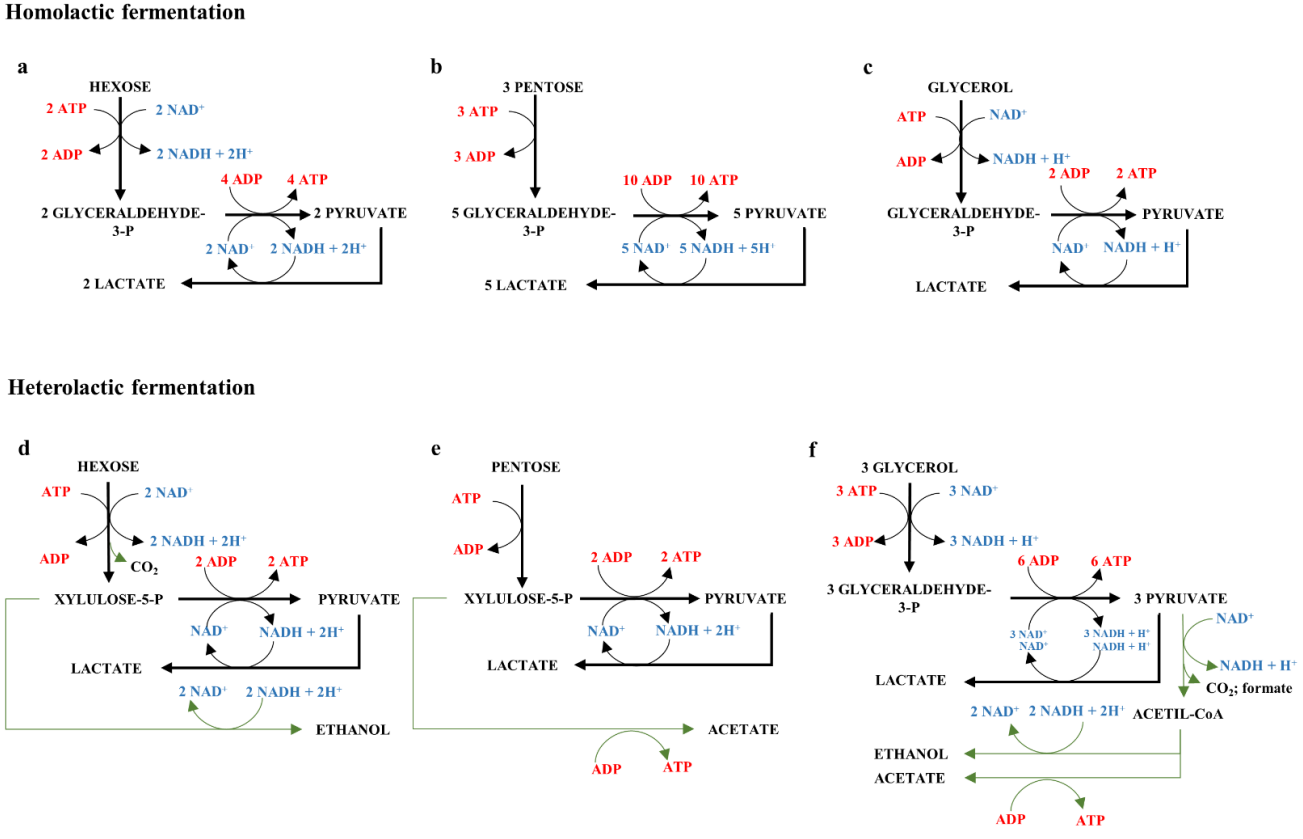

Fig. 1.3. Lactic acid fermentation from different carbon sources. Fermentation of hexoses **(a, d)**, pentoses **(b, e)**, and glycerol **(c, f)** to lactic acid. The formation of reduced and oxidized NAD co-factors is indicated in the blue font; ATP synthesis and consumption are indicated in the red font; the pathway of by-product formation is indicated by green arrows (based on [92,93]). Reprinted from [94] with permission of publisher

Table 1.3. D-lactic acid production by using alternative substrates

Microorganism (relevant characteristics)	Carbon source	Fermentation mode	Concentration (g/L)	Yield (g/g) consumed substrate	Productivity (g/(Lh))	References
L. delbrueckii subsp. bulgaricuscus ATCC 1184*2*	beechwood pre-treated with organic solvents	batch, SSF	62	**0.69**	0.86	[76]
L. delbrueckii sp. *delbrueckii* CECT 286	orange peel waste pre-treated with enzyme mixtures (glucose, fructose, galactose)	batch, SHF	96.34	**0.93**	3.70	[95]
L. delbrueckii JCM 1106	liquefacted broken rice with α-amylase and protease (glucose)	batch, SSF	79.0	**0.81**	3.59	[88]
L. delbrueckii subsp. delbrueckii NBRC 3202	enzyme hydrolyzed cassava fibrous waste (glucose)	batch, SHF	16.15	**0.5**	0.9	[89]
P. acidilactici XH11 (*P. acidilactici* D01 adaptive laboratory evolution)	water-soluble carbohydrates-rich sugarcane bagasse (glucose, fructose)	water-soluble carbohydrates pre-fermentation and one-pot SSCF	57.0	**0.58**	ND	[90]
L. delbrueckii subsp. delbrueckii NBRC 3202	rice straw (glucose) pretreated with liquid hot water and cellulase	continuous, MICF	46.6	**0.92**	18.56	[91]
Genetically engineered microorganisms						
E. coli EcoB-140B (BLac-2106 adaptive laboratory evolution)	glycerol	batch	100	**0.97**	1.85	[72]
P. acidilatici ZY15 (*P. acidilactici* ZP26::*xylAB*-Δ*pkt::*(*tkt_tal*) adaptive laboratory evolution)	biodetoxified corn stover pretreated with acid (glucose, xylose)	batch, SSF	97.3	**0.93**	1.01	[77]

1.2.2. Lactic acid and glycolic acid catabolism in bacteria

There are two types of lactate dehydrogenases in microbes, nLDHs and iLDHs. nLDHs use NADH as the cofactor (Figs. 1.4a, b), whereas iLDHs utilize flavins (Figs. 1.4c, d). The iLDHs, also called respiratory lactate dehydrogenases, are generally considered to the enzymes responsible for lactate oxidation in microbes. Most commonly, the operon associated with lactate utilization consists of lactate permease, L- and/or D-NAD-independent lactate dehydrogenase, and regulatory protein genes[104,105]. Those TFs which regulate such operons can be used in the development of genetically encoded biosensors. iLDHs are most widely described in *P. aeruginosa*[106], *P. stutzeri* A1501[107], and *E. coli* [108].

iLDHs are classified into D-iLDH and L-iLDH according to the substrate specificity. Most L-iLDHs belong to the *α*-hydroxy acid oxidizing flavoproteins family and use FMN as a cofactor. These dehydrogenases can be divided into three groups by the electron acceptor which can utilize (quinones, O_2, or cytochrome c). The potential grouping of D-iLDHs is similar. Most bacterial D-iLDHs use FAD as a cofactor and belong to the FAD-binding 4 family. According to the electron acceptor, it is divided into quinone-dependent, cytochrome *c*-dependent D-iLDH, and Fe-S D-iLDH [104,109].

Glycolate is metabolized in *E. coli* through oxidation to glyoxylate in a reaction catalyzed by glycolate oxidase. The structural genes of the *glc* locus are organized as an operon (*glcDEFGB*) and associated with the glycolate utilization in *E. coli*. They are known to contain *glcB* which encodes malate synthase G, the *glcDEF* genes needed for glycolate oxidase activity, and *glcG*, of an unknown function[110,111].

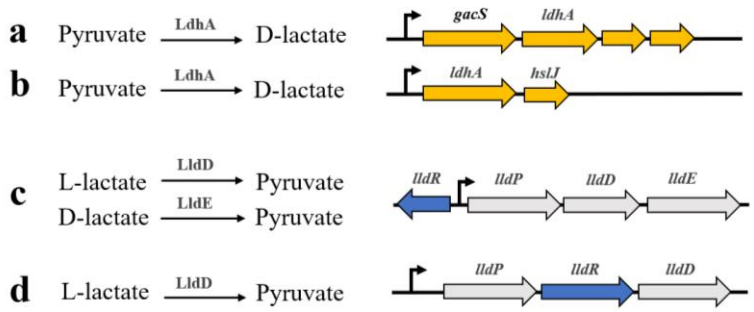

Fig. 1.4. The genome of *E. coli* and *P. aeruginosa* encodes several enzymes that interconvert pyruvate and lactate. **(left)** Reactions catalyzed by lactate dehydrogenases; **(right)** chromosomal loci encoding each of the corresponding enzymes. **(a)** pyruvate reduction during anaerobic survival catalyzed by *P. aeruginosa* LdhA; **(b)** pyruvate reduction during anaerobic survival catalyzed by *E. coli* LdhA; **(c)** oxidation of L- and D-lactate during aerobic growth by *P. aeruginosa* LldD and LldE; **(d)** oxidation of L-lactate during aerobic growth by *E. coli* LldD [106,105,108]

1.2.3. Lactic acid–inducible gene expression systems: prospect for biosensors

Genetically encoded biosensors enable high-throughput quantification by transducing the concentration of the target molecule into an easily measurable signal, such as fluorescence, luminescence, or absorbance[112]. This type of biosensors commonly consists of TF-based inducible gene expression systems functionally connected to a reporter or an antibiotic resistance gene[113]. This type of biosensor offers several advantages over any previously mentioned methods (Subsection *1.1.1*). It allows for the real-time monitoring of product formation and the measurement of the titer *in vivo*, is fast, inexpensive, specific, highly sensitive and suitable for high-throughput screening[112].

Several examples of lactic acid-inducible gene expression systems have been reported previously in *E. coli* MG1655 (*Ec*LldR/P_{lldP})[108], *C. glutamicum* ATCC 13032 (*Cg*LldR/P_{lldP})[114], *P. aeruginosa* XMG (*Pa*LldR/P_{lldP})[115], *B. subtilis* 168 (*Bc*LutR/P_{lutA})[116,117], *D. vulgaris* Hildenborough (*Dv*LurR/P_{por})[118], and *A. woodii* DSM 1030 (*Aw*LctA/P_{lctB})[119]. The systems are of two types. The first type was found in *E. coli* (*Ec*LldR/P_{lldP}) and *C. glutamicum* (*Cg*LldR/P_{lldP})[108,114], the LldR TF has a dual regulatory function, acting as an activator (in the presence of L-lactate) and as a repressor (in the absence of L-lactate). The second type was identified in *P. aeruginosa* (*Pa*LldR/P_{lldP}), *B. subtilis* (*Bc*LutR/P_{lutA}), *A. woodii* (*Aw*LctA/P_{lctB}) and *D. vulgaris* (*Aw*LctA/P_{lctB})[115,116,117,118,119], and the TFs of these systems acts as repressors. (Fig. 1.5)

The *E. coli* system *Ec*LldR/P_{lldP} (Fig. 1.5a) controls an *lldPRD* operon (formerly named *lct*) responsible for aerobic L-lactic acid metabolism. This operon encodes flavin adenine dinucleotide-dependent dehydrogenase (*lldD*), L-lactic acid-specific permease (*lldP*), and regulatory protein (*lldR*) belonging to the FadR subfamily[108,120]. The expression of *lldD*, *lldP* and *lldR* genes is increased by L-lactic acid, but not by D-lactic acid [121]. LldR binds to both O1 (positions –105 to –89) and O2 (positions +22 to +38) operators, leading to the DNA loop formation and transcription suppression when L-lactic acid is absent. If L-lactatic acid is present, this acid binds to *LldR* and promotes conformational changes, which can disrupt the DNA loop and allow for the formation of an open transcription complex[108]. Moreover, the expression of *lldD*, *lldP* and *lldR* genes increases under aerobic conditions and decreases under anaerobic conditions [108,122]. The principle of gene expression regulation by *C. glutamicum* ATCC 13032 system *Cg*LldR/P_{lldP} (Fig. 1.5b) is similar to *Ec*LldR/P_{lldP}.

The *Pa*LldR/P_{lldP} from *P. aeruginosa* PAO1 controls the *lldPDE* operon containing both the L-lactate dehydrogenase (*lldD*) and the D-lactate dehydrogenase (*lldE*) genes. The gene expression is activated here in the presence of either L- or D-lactic acid (Fig. 1.5c)[115]. The remaining *Bc*LutR/P_{lutA}, *Dv*LurR/P_{por}, and *Aw*LctA/P_{lctB} systems regulate lactate utilisation genes which are arranged in different and more complex operons (Fig. 1.5d–f). For example, *B. subtilis* sp. *subtilis* 168 has three genes *lutA*, *lutB*, *lutC* responsible for the lactate utilization, and the functions of these genes have not been fully investigated yet. Genes are thought to contain iron-sulfur clusters, and the oxidation of lactate occurs *via* a cytochrome-like electron transfer chain[116].

Several examples of lactic and glycolic acids genetically encoded biosensors have been described in the literature (Table 1.4). A L-lactic acid biosensor has been developed by using the *E. coli* inducible gene expression system[108]. This biosensor includes GFP as a reporter, which responds to the P_{lldP} promoter, and contains the *lldR* TF gene under the control of a constitutive promoter to lower the baseline GFP expression. The biosensor has shown a 60-fold induction with high sensitivity (with the lowest detection limit of ~0.05 mM). The developed sensor found application in monitoring the lactate content in mammalian cells (hybridoma cells, CHO-S, GS-CHO)[33]. A more sensitive L-lactic acid biosensor (featuring a limit of detection of 0.68 μM) was constructed by using *St*LldR TF from *S. typhimurium* LT2 combined with FRET. The biosensor $FILLac_{10N0C}$ was used in the analysis of fermentation samples and food products, and the obtained values showed high agreement with that of the commercial SBA-40D bioanalyzer[123]. A D-lactate biosensor has also recently been developed by using the *P. fluorescens* A506 inducible gene expression system. Approximately a 6-fold higher induction of 100 mM D-lactate than L-lactate was observed with a relatively broad (35–100 mM) dynamic range for D-lactic acid[124]. A glycolic acid biosensor was also recently reported. Its construction was designed based on TF GlcC and its responsive promoter P_{glcD} from *E. coli* MG1655. This biosensor was adapted for the rapid screening of preeminent glycolate producers from a large library[125].

Table 1.4. Genetically encoded biosensors for lactic and glycolic acids

Target molecule	Inducible systems or biosensor name	Host organism	Dynamic range	Application	Reference
L-lactic acid	*Ec*LldR/P_{lldP}	*E. coli*	0.05–14 mM	L-lactate determination in mammalian cell cultures	[33]
D-lactic acid	*Pd*PdhR/P_{lldP}	*P. denitrificans*	35–100 mM	ND	[124]
L-lactic acid	$FILLac_{10N0C}$	*S. typhimurium* LT2	0.00076–0.0517	L-lactate detection in bacterial fermentation and commercial foods samples	[123]
Glycolic acid	*Ec*GlcC/P_{ffs}	*E. coli*	0.1–200 mM	high-throughput screening	[125]

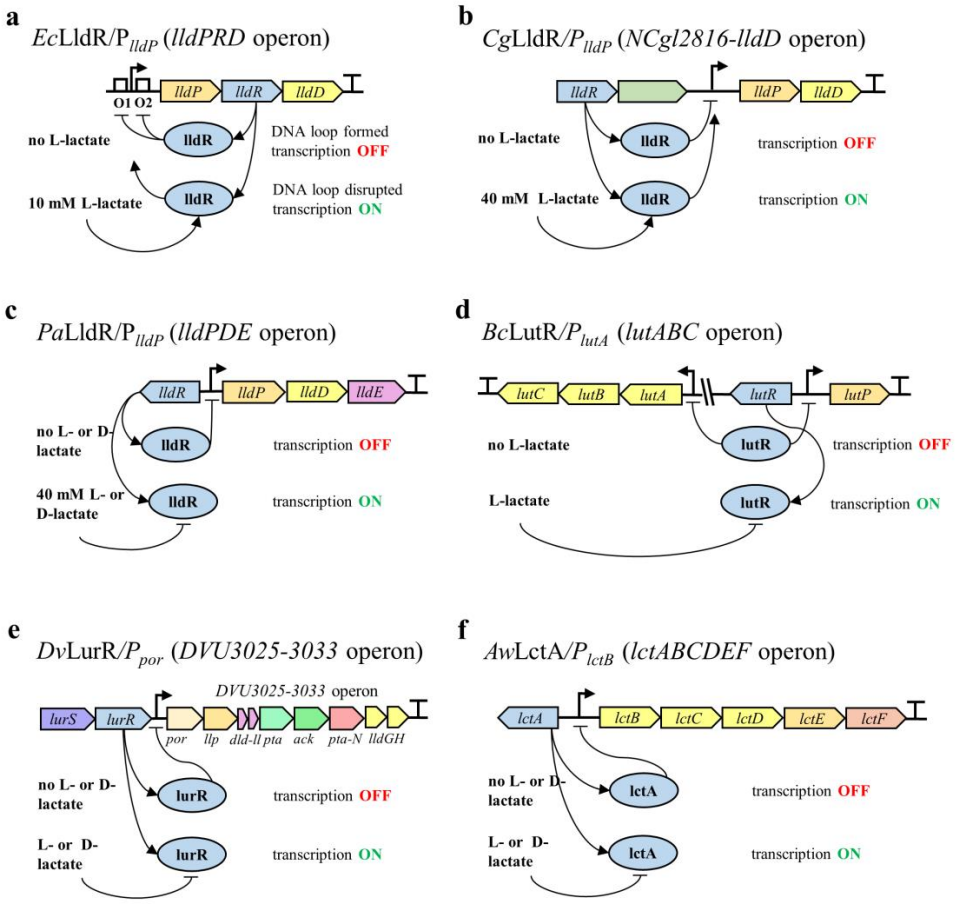

Fig. 1.5. D- and L-lactic acid inducible gene expression systems. **(a, b)**. Gene clusters in *E. coli* MG1655 and *C. glutamicum* ATCC 13032 encoding the enzymes required for L-lactic acid catabolism. The inducible gene expression systems are referred to as *Ec*LldR/P_{lldP} and *Cg*LldR/P_{lldP}, respectively, where LldR are a TRs (locus tags *b3604* and *WA5_2814*, respectively) [108]. **(c-f)** Gene clusters in *P. aeruginosa* XMG, *B. subtilis* sp. *subtilis* 168, *D. vulgaris* Hildenborough, and *A. woodii* DSM 1030 encoding the enzymes required for L- and D-lactic acid catabolism. The inducible systems are referred to as *Pa*LldR/P_{lldP}, *Bc*LutR/P_{lutA}, *Dv*LurR/P_{por}, and *Aw*LctA/P_{lctB}, where LldR, LutR, LurR, and LctA are a TR, respectively (locus tags *PA4769*, *BSU_34180*, *AWO_RS04405*) [115,116,117,118,119]. *LldP*, *lutP*, *lctE*: L-lactate permease gene; *lldD*, *lldGH*: L-lactate dehydrogenase gene; *lldE*, *dld-ll*: D-lactate dehydrogenase gene; *lutABC* operon (*lutA*: iron-sulfur oxidase subunit used in L-lactate utilization; *lutB*: component of an iron-sulfur oxidase linked to L-lactate utilization; *lutC*: component of an iron-sulfur oxidase for L-lactate utilization; *por*: pyruvate ferredoxin oxidoreductase gene; *llp*: lactate permease gene; *pta*: phosphotransacetylase gene; *ack*: acetate kinase gene; *lctB*: electron transfer flavoprotein subunit *beta*; *lctC*: electron transfer flavoprotein subunit *alpha*; *lctD*: FAD-binding oxidoreductase (putative lactate dehydrogenase) gene; *lctF*: nickel-dependent lactate racemase gene. Reprinted from [94] with a permission of the publisher

1.3. Phenolic Acids as Industrially Relevant Compounds

Phenolic acids are industrially relevant compounds with superior antioxidant properties used in food, pharmaceutical, cosmetic, and chemical industries. Phenolic acids are divided into hydroxybenzoic and hydroxycinnamic acids. The most commonly known hydroxybenzoic acids include *o*-hydroxybenzoic, *m*-hydroxybenzoic, *p*-hydroxybenzoic, vanillic, isovanillic, gallic, protocatechuic, syringic, gentisic, *α*-resorcylic, *β*-resorcylic, *γ*-resorcylic, orsellinic, and 6-methylsalicylic acids, while hydroxycinnamic acids include *o*-coumaric, *m*-coumaric, *p*-coumaric, ferulic, sinapic, and caffeic acids (Fig. 1.6). The global *o*-hydroxybenzoic acid market was valued at US$ 417.8 million in 2022 and is one of the largest market sizes among phenolic acids. This acid is the main component in the production of aspirin (acetylsalicylic acid), an analgesic and antiplatelet drug. Furthermore, *o*-hydroxybenzoic acid is increasingly used by cosmetic manufacturers and dermatologists due to its positive effect on acne-affected skin[126]. The protocatechuic acid market size is significantly smaller compared to that of salicylic acid, but it is likely to grow over time due to the potential to be used as a precursor for several other monomers such as catechol, vanillic acid, vanillin, muconic acid, and adipic acid[17].

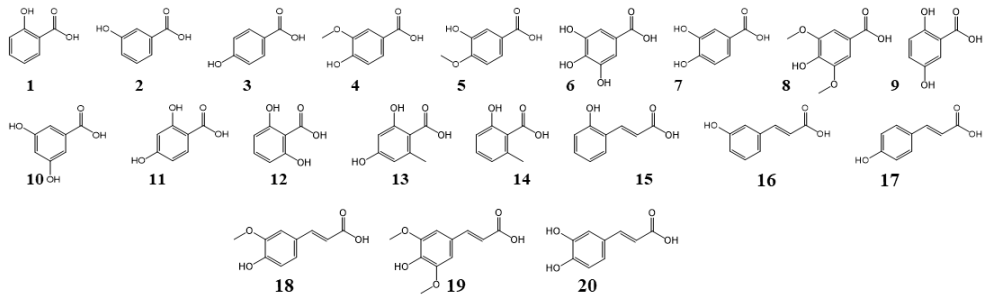

Fig. 1.6. Chemical structures of most commonly known phenolic acids: *o*-hydroxybenzoic acid **(1)**, *m*-hydroxybenzoic acid **(2)**, *p*-hydroxybenzoic acid **(3)**, vanillic acid **(4)**, isovanillic acid **(5)**, gallic acid **(6)**, protocatechuic acid **(7)**, syringic acid **(8)**, gentisic acid **(9)**, *α*-resorcylic acid **(10)**, *β*-resorcylic acid **(11)**, *γ*-resorcylic acid **(12)**, orsellinic acid **(13)**, 6-methylsalicylic acid **(14)**, *o*-coumaric acid **(15)**, *m*-coumaric acid **(16)**, *p*-coumaric acid **(17)**, ferulic acid **(18)**, sinapic acid **(19)**, and caffeic acid **(20)**

1.3.1. Production of hydroxycinnamic acids

Among hydroxycinnamic acids, *p*-coumaric acid is the main acid dominating the market with a size of US$ 134 million (in 2021). The demand for this acid has been growing every year, and it is predicted to reach to the levels of nearly US$ 200 million in 2031[127]. *p*-Coumaric acid is denoted by antimelanogenic properties and is suitable for use as a skin-lightening cosmetic ingredient[128]; it can also be used in the pharmaceutical industry; it prevents necrosis and cholestasis, and exhibits amoebostatic activity against *E. histolytica*[129]. *p*-Coumaric acid is chemically combined with PCL by synthesizing the copolymer-binding properties of polyphenols and polycaprolactones, thus enabling its application in biomedicine [130]. In addition, a strategy to produce *mcl*-PHA from lignin derivatives (aromatic mixture of *p*-

coumarate, ferulate, and benzoate) has been demonstrated, and a concentration of 0.582 g/L has been obtained for oxygen-unlimited conditions at a C/N ratio of 60 using *P. putida* KT2440 strain[131].

Phenolic acids are commonly extracted by organic solvents from plants-based raw materials; however, extraction is limited due to insoluble bound forms conjugated with cell wall components[18,132]. Chemical phenolic acid synthesis also encounters such bottlenecks as expensive precursors from petroleum (e.g., benzaldehydes) and harsh reaction conditions[133]. For these reasons, currently, attention is focused on the production of phenolic acids by using microbial factories. Microbial factories offer several significant advantages over extraction and chemical synthesis because of their fast growth rate, ease of cultivation, cost-effectiveness, and environmental friendliness. However, only some fungi (*R. oryzae* and *A. niger*) and bacteria (*P. aeruginosa*, *B. subtilis*, and *S. thermophile*) can naturally produce phenolic acids in low yields; therefore, it is necessary to use metabolic engineering to improve the bioproduction[18]. Metabolic engineering of microbial cells, such as *E. coli*, *P. putida*, *S. cerevisiae*, *Y. lipolytica*, *C. glutamicum* offers a sustainable and alternative way to produce phenolic acids[133,134,135]. The biotechnological production of *p*-coumarate and protocatechuate has been widely discussed in the literature. The *S. cerevisiae* diploid strain was adapted to produce 12.5 g/L of *p*-coumaric acid from glucose as a carbon source[136]. *C. glutamicum* PCA3 strain with strong P_{gapA} promoter for *qsuB* (3-dehydroshikimate dehydratase), *ubiC* (chorismate pyruvate lyase), and *pobA* (4-hydroxybenzoate hydroxylase) genes overexpression forms 82.7 g/L of protocatechuate from glucose[137]. Publications have demonstrated the future perspective of microbial platforms for the industrial bioproduction of phenolic acids from renewable sugars.

1.3.2. Phenolic acids metabolism pathways in bacteria

Metabolic pathways of phenolic acids have been discovered in various classes of bacteria, including proteobacteria, actinobacteria, and bacilli[138]. Gammaproteobacterium *P. putida* metabolize aromatic compounds and organic acids preferentially over glucose, while gammaproteobacteria *E. coli* and *B. subtilis* prefer glucose over other substrates. The mechanism of carbon catabolite repression allows microorganisms living in a consortium to mitigate the competition for energy and nutrients[139,140]. This allows us to conclude that the ability of bacteria to catabolize phenolic acids as a carbon source is related to the bacteria adaptation to survive in the natural environment.

Hydroxycinnamates can be catabolized in three different ways in bacteria. Phenolic acid decarboxylase (encoded by *padC* gene) converts hydroxycinnamates into vinyl derivatives in *B. subtilis*[141], phenolic acid reductase (encoded by *hcrAB* genes) from *L. plantarum* WCFS1 involved hydroxycinnamates reduction[142], and feruloyl-CoA synthase (encoded by *fcs* gene) from *P. fluorescens* BF13 and *A. baylyi* ADP1 transform the *p*-coumaric, caffeic, and ferulic acids to the respective intermediates *p*-hydroxybenzoic, protocatechuic, and vanillic acids, respectively[143,144]. *p*-Hydroxybenzoic and vanillic acids are converted to protocatechuic acid by the *p*-hydroxybenzoate hydroxylase encoded by *pobA* gene

and vanillate O-demethylase encoded by *vanAB* genes, respectively. Protocatechuic acid is further metabolized through the tricarboxylic acid cycle. *m*-Coumaric acid is the only hydroxycinnamic acid metabolized by *E. coli* MG1655 through a series of reactions involving enzymes encoded by the *mhpABCDEFT* cluster[145] (Fig. 1.7).

Unraveling the degradation pathways of phenolic acids in bacteria allows utilizing lignin derivatives as feedstock for the production of value-added products[7,138,146]. *P. putida* KT2440 was successfully applied for the production of lactic acid from *p*-coumarate[79], muconic acid from catechol, and polyhydroxyalkanoates from *p*-coumarate[138,147]. *P. putida* KT2440 cells factory is one of the promising routes to make lignin valorization sustainable.

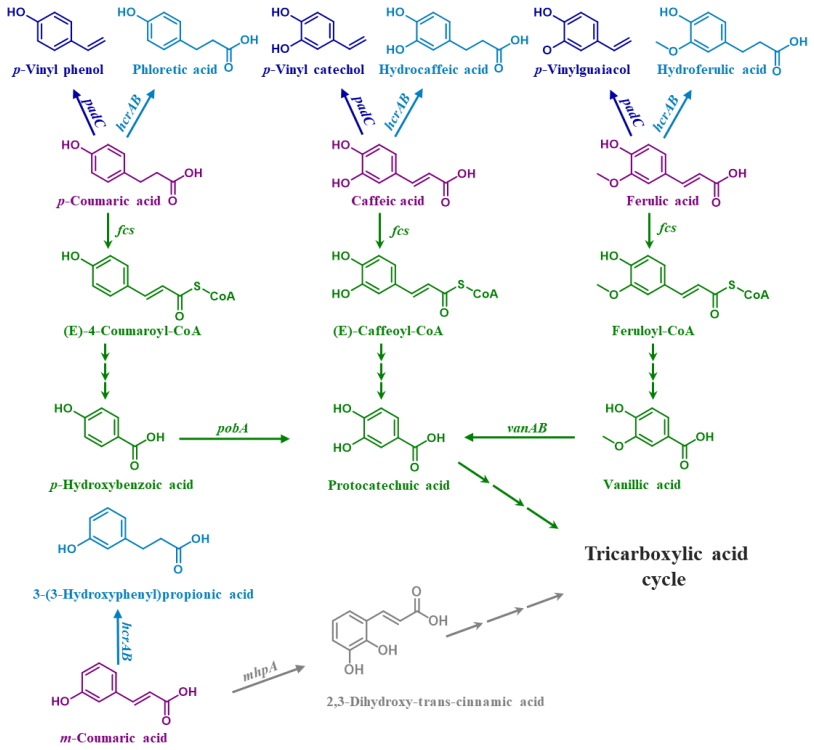

Fig. 1.7. Schematic representation of the metabolism of hydroxycinnamic acid (purple) by *Bacillus* sp. (dark blue), *Lactobacillus* sp. (light blue), *P. putida* and *A. baylyi* (green), and *E. coli* (gray). Genes encoding the corresponding enzymes are indicated above the arrows, and dashed arrows indicate several metabolic reactions. *padC*: phenolic acid decarboxylase from *Bacillus* sp.; *hcrAB*: phenolic acid reductase from *Lactobacillus* sp.; *fcs:* acyl-CoA ligase from *Pseudomonas* sp.; *mhpA*: 3-hydroxycinnamic acid hydroxylase from *E. coli* MG1655; *pobA*: *p*-hydroxybenzoate hydroxylase; *vanAB*: vanillate O-demethylase

1.3.3. Phenolic acids-inducible gene expression systems: prospects for biosensors

Phenolics acids-inducible systems were identified in gammaproteobacteria (*E. coli*, *P. putida*, *A. baylyi*, *A. chroococcum*), betaproteobacteria (*C. necator*, *C. testosterone*, *T. aromatica*), alphaproteobacteria (*Sphingobium* sp., *R. palustris*, *C. crescentus*), actinomycetia (*S. coelicolor*, *R. jostii*), and bacilli (*B. subtilis*). A detailed overview of the described hydroxybenzoic and hydroxycinnamic acids-inducible systems is presented in Supplementary Table S2. In recent years, more attention has been paid to the development of biosensors for hydroxybenzoic acid, such as *o*-hydroxybenzoic, *p*-hydroxybenzoic, vanillic, and protocatechuic acids. Biosensors for *p*-coumaric and ferulic acids have been the most widely discussed among hydroxycinnamic acids, but these biosensors were not specific as they showed induction with both *p*-coumaric and ferulic acids. It is also essential to highlight that, so far, no whole-cell biosensors have been developed for isovanillic, gentisic, *β*-resorcylic, orsellinic, 6-methylsalicylic, and *o*-coumaric acids (Supplementary Table S2). The application of phenolic acids-inducible systems as genetically encoded biosensors offers the potential to improve lignin valorization and expand the scope of the microbial cell factory, and it is a powerful tool to screen strains or enzymes[7,148,149]. For example, Li and colleagues developed a *p*-coumarate and ferulate auto-regulatory platform in *P. putida* and successfully applied it to protocatechuate production (12.7 g/L titer of protocatechuate was achieved)[150]. Another team of researchers demonstrated the sorting of yeast cells producing *p*-coumaric acid using *Ec*PadR *E. coli* biosensor cells[34]. Application of biosensors for lignocellulosic valorization was demonstrated with a ferulic acid biosensor (based *Sp*FerC/P_{LC} inducible system), and the activity of feruloyl esterases in different biomass sources has been determined[151].

1.4. Justification of the Thesis Aim and Objectives

The literature review showed the potential and broad application possibilities of organic and phenolic acids in various industries. The production of organic and phenolic acids via microbial fermentation is denoted by advantages over the chemical synthesis or extraction methods. Fermentation is cost-effective and environmentally friendly, microorganisms have a fast growth rate, and are easily cultured; moreover, optically pure L- and D-lactic acids can only be obtained by fermentation. However, efficient production requires natural or genetically modified strains capable of fermenting inexpensive and non-food substrates. Low-cost and high-throughput analytical methods, for example, genetically encoded biosensors, are required for the rapid screening of microbial strains across numerous substrates. In recent years, significant progress has been achieved in the development of organic and phenolic acid genetically encoded biosensors. Nevertheless, a biosensor specific for D-lactic acid has not been described, and the application of biosensors for the production of L- and D-lactic acids optimization has not been demonstrated. Several phenolic acid biosensors have been developed, but specificity and universality between different hosts evidently still remain a bottleneck.

2. MATERIALS AND METHODS

2.1. Identification of Gene Clusters in Bacterial Genomes

The identification of putative gene clusters responsible for organic and phenolic acids metabolism has been performed in the literature and the GenBank database (available at https://www.ncbi.nlm.nih.gov/)[152]. The available information about catabolic pathways has been analyzed in the KEGG Pathway Database (available at www.genome.jp/kegg/pathway.html[153]), and in the BRENDA database (available at www.brenda-enzymes.org[154]). The protein homologs encoded by target genes have been identified, and homology has been determined by using a BLAST (available at https://blast.ncbi.nlm.nih.gov/Blast.cgi).

2.2. Chemicals and Equipment

All chemicals used as inducers in the present study are listed in Table 2.1. The equipment used in this study was as follows: a biological safety cabinet *AC2-TUV* (*ESCO*, USA); a *Mastercycler Nexus X2* PCR thermocycler (*Eppendorf*, Germany); a *BioMate 160* spectrophotometer (*Thermo Fisher Scientific*, USA); a *MicroPulser* electroporation system (*Bio-Rad*, USA); a nanophotometer *N60/N50* (*Implen*, Germany); a *Lexicon II* ultra-low temperature freezer (*ESCO*, USA); an *Infinite M Nano*$^+$ plate reader (*Tecan*, Austria); a gel documentation system *Essential V6* (*UVITEC*, UK); a blue light transilluminator (*UVITEC*, UK); a *Dionex UltiMate 3000* HPLC system (*Thermo Fisher Scientific*, USA); a water bath *Grant TC120* (*Grant Instruments*, UK); a centrifuge *Eppendorf 5425* and *5804 R* (*Eppendorf*, Germany) ; a thermoblock (*VWR*, USA); a pH meter *FP20-Micro* (*Mettler Toledo*, USA); a balance *SPX2201* (*Ohaus*, USA); an analytical balance *ENTRIS224-1S* (*Sartorius*, Germany); a *multiSUB mini horizontal l*agarose gel electrophoresis system (*Cleaver Scientific*, UK); an autoclave *CV–EL* (*CertoCLAV*, Austria); an ice-making machine (*Brema*, Italy); an incubator *IN30* (*Memmert*, Germany); a shaking incubator *MaxQ 6000* (*Thermo Fisher Scientific*, USA); an automated pipetting system (*Gilson*, France); and a vortex mixer *V–1 plus* (*Biosan*, Latvia).

Table 2.1. Chemical compounds as inducers used in the present study

Chemical	Producer	Catalog number
Sodium L-lactate	*Alfa Aesar, Thermo Fisher Scientific*	L14500
Sodium D-lactate	*Sigma-Aldrich*	71716
3-Hydroxypropanoic acid solution, 30%	*Sigma-Aldrich*	792659
Sodium glyoxylate monohydrate	*Sigma-Aldrich*	G4502
Sodium pyruvate	*Sigma-Aldrich*	P8574
Sodium glycolate	*Alfa Aesar, Thermo Fisher Scientific*	A12341
o-Coumaric acid	*Sigma-Aldrich*	H22809
m-Coumaric acid	*Sigma-Aldrich*	H23007
p-Coumaric acid	*Sigma-Aldrich*	C9008
Ferulic acid	*Sigma-Aldrich*	128708
Sinapic acid	*Alfa Aesar*	A15676
Caffeic acid	*Sigma-Aldrich*	C0625
Chlorogenic acid	*TCI*	C0181

2.3. Bacteria Strains

All strains used in the present study are listed in Table 2.2.

Table 2.2. Bacterial strains used in the present study

Strain	Abbreviation	Characteristic	Source	Reference
Escherichia coli Top10	*E. coli* Top10	F- *mcrA* Δ(*mrr-hsd*RMS-*mcr*BC) Φ80*lac*ZΔM15 Δ *lac*X74 *rec*A1 *ara*D139 Δ(*araleu*)7697 *gal*U *gal*K *rps*L (StrR) *end*A1 *nup*G	Invitrogen	[155]
Escherichia coli DH5α	*E. coli* DH5α	F^- Φ80*lac*ZΔM15 Δ(*lac*ZYA-*arg*F) U169 *rec*A1 *end*A1 *hsd*R17(r_K^-, m_K^+) *pho*A *sup*E44 *thi*-1 *gyr*A96 *rel*A1 λ^-	Invitrogen	[156]
Escherichia coli MG1655	*E. coli* MG1655	wild type strain	DSM 18039	[157]
Cupriavidus necator H16	*C. necator* H16	wild type strain	DSM 428	[158]
Pseudomonas putida KT2440	*P. putida* KT2440	wild type strain	DSM 6125	[159]
Pseudomonas fluorescents NCTC10038	*P. fluorescents* NCTC10038	wild type strain	DSM 50090	[160]
Pseudomonas lactis DSM 29167	*P. lactis* DSM29167	wild type strain	DSM 29167	[161]
Acinetobacter baylyi ADP1	*A. baylyi* ADP1	wild type strain	DSM 24193	[162]
Burkholderia multivorans ATCC BAA-247	*B. multivorans* ATCC BAA-247	wild type strain	DSM 13243	[163]
Lactiplantibacillus argentoratensis DSM 16365	*L. argentoratensis* DSM 16365	wild type strain	DSM 16365	[164]
Lactobacillus delbrueckii subsp. *lactis* DSM 16365	*L. lactis*	wild type strain	DSM 16365	[165]
Lactobacillus amylovorus DSM 20532	*L. amylovorus*	wild type strain	DSM 20532	[166]
Lacticaseibacillus paracasei subsp. *paracasei* DSM 20312	*L. paracasei*	wild type strain	DSM 20312	[167]

2.4. Preparation of Nutrient Media

E. coli MG1655, *E. coli* Top 10, *E. coli* DH5α, *C. necator* H16, and *P. putida* KT2440 are cultured in liquid and solid LB medium. Mediums are prepared according to the manufacturer's protocols. LB broth (*Thermo Fisher Scientific*, USA) was prepared with 40 g of LB powder dissolved in 1000 ml of distilled water. LB agar medium (*Thermo Fisher Scientific*, USA) was prepared with 37 g of powder dissolved

in 1000 ml of distilled water. The mediums are autoclaved at 125 °C for 15 min at 1.5 atm pressure. If necessary, the medium was supplemented with the appropriate antibiotics. The preparation of antibiotic solutions is described in Table 2.3.

Table 2.3. Antibiotic solutions composition

Antibiotic	Initial concentration, mg/ml	Final concentration, µg/ml	Solvent
Tetracycline	15	12.5	distillate water
Gentamicine	10	10	distillate water
Chloramfenicol	50	25	ethanol

For reporter gene assays, *E. coli* Top 10, *E. coli* DH5α, and *P. putida* KT2440 were grown in MM with 0.4% glucose[168], the medium was prepared in sterile water supplemented with additional filtered sterile components (Table 2.4). A 5x M9 salt solution was prepared separately by dissolving the following salts as listed in (Table 2.5) in water, then adjusting the pH to 7.0, and sterilized by autoclaving for 15 min at 120 °C at 1.5 atm. The required antibiotic was added to the media before bacteria inoculation (Table 2.3).

Table 2.4. MM with 0.4 % glucose composition

Reagents	Initial concentration	Final concentration
M9 salts	5x	1x
$MgSO_4$	1 M	2 mM
$CaCl_2$	1 M	0.1 mM
glucose	20 %	0.4 %
thiamine	1 mg/ml	1 µg/ml
leucine	0.25 M	0.4 mM

Table 2.5. 5x M9 salts solution composition

Reagents	Concentration, g/L
Na_2HPO_4 x $7H_2O$	64
KH_2PO_4	15
NaCl	2.5
NH_4Cl	5

Table 2.6. SG-MM with 0.4% sodium gluconate composition

Reagent	Quantity, g	Final concentration, mM
Na_2HPO_4 x 12 H_2O	9	25
KH_2PO_4	1.5	11
NH_4Cl	1	18.7
$MgSO_4$ x 7 H_2O	0.2	0.8
$CaCl_2$ x 2 H_2O	0.02	0.14
Fe (III) NH_4-Citrate	0.0012	0.0046
Reagent	**Quantity, ml**	**Final concentration, %**
SL7 solution	1	0.1

For reporter gene assays, *C. necator* H16 was grown in SG-MM with 0.4% sodium gluconate [169]. The medium was prepared by dissolving the salts as listed in (Table 2.6) in 1000 ml of distilled water. The detailed composition of the SL7 solution is given in Table 2.7. The medium pH was adjusted at 7.0 and was filtrated by using a 0.22 µm filter. Subsequently, 20 mM sterile sodium gluconate was added to the

prepared medium. If necessary, the medium was also supplemented with the appropriate antibiotics (Table 2.3).

Table 2.7. SL7 solution composition

Reagent	**Quantity, mg**	**Final concentration, mM**
H_3BO_3	62	1
$CoCl_2$ x 6 H_2O	190	0.8
$CuCl_2$ x 2 H_2O	17	0.1
$MnCl_2$ x 4 H_2O	100	0.5
Na_2MoO_4 x 2 H_2O	36	0.15
$NiCl_2$ x 6 H_2O	24	0.1
$ZnCl_2$	70	0.5
Reagent	**Quantity, ml**	**Final concentration, mM**
HCl (w/v)	1.3	0.0156

2.5. Assembly of Constructs

A detailed construction description for each plasmid is provided in Supplementary Table S6.

2.5.1. Oligonucleotide primers

The oligonucleotide primers were designed *in silico* by using *SnapGene* software (*Insightful Science*, available at snapgene.com). This cloning simulation tool allowed vector assembly *in silico* as a control before the vector assembly in the laboratory. Oligonucleotide primers were synthesized by *Metabion* (Germany), *Sigma-Aldrich* (USA), and *Invitrogen* (USA) (Supplementary Table S7). To achieve the optimal HiFi assembly efficiency, 15–20 bp overlap regions between each fragment were designed.

2.5.2. PCR reactions and conditions

Phusion High-Fidelity DNA polymerase (*Thermo Fisher Scientific*, Lithuania) was used to amplify copies of a specific DNA sample and clone them into the pBRC1 vector prepared by restriction enzymes. DreamTaq master mix (*Thermo Fisher Scientific*, Lithuania) was used for colony screening after vector construction and transformation into *E. coli* Top10 competent cells. The PCR reactions were set up according to the manufacturer's protocol (Table 2.8 and Table 2.9). The thermocycler (*Eppendorf*, Germany) was used for PCR, and the reactions conditions are listed in Table 2.10.

Table 2.8. PCR reaction composition when using Phusion High-Fidelity DNA polymerase

Component	**Quantity, µl**	**Final concentration**
Water, nuclease-free	11.8	
5x Phusion GC buffer	4	1x
10 mM dNTPs	0.4	200 µM
Forward primer	1	0.5 µM
Reverse primer	1	0.5 µM
Template DNA	1	5 ng (for pDNA) 100 ng (for gDNA)
DMSO	0.6	3 %
Phusion DNA polymerase	0.2	0.02 U/µL

Table 2.9. PCR composition when using DreamTaq master mix

Component	Quantity, µl	Final concentration
Water, nuclease-free	6.4	
Forward primer	1	0.5 µM
Reverse primer	1	0.5 µM
Template DNA	1	1 µg
DMSO	0.6	3 %
2x DreamTaq PCR master mix	10	

Table 2.10. PCR conditions when using Phusion High-Fidelity DNA polymerase and DreamTaq master mix

Cycle step	Phusion High-Fidelity DNA polymerase		DreamTaq master mix		Cycles
	Temperature, °C	Time	Temperature, °C	Time	
Initial denaturation	98	1 min (for pDNA) 3 min (for gDNA)	95	3 min	1
Denaturation	98	10 s	95	30 s	35
Annealing	63	30 s	54	30 s	
Extension	72	1.30 min	72	1.30 min	
Final extension	72	10 min	72	10 min	1
Hold	4		4		

2.5.3. DNA ligation

Vector assembly was prepared in two ways: the first way was implemented by the restriction enzyme-based cloning procedure with T4 DNA Ligase (*Thermo Fisher Scientific*, Lithuania), whereas the other way was performed by HiFi DNA assembly (*New England Biolabs*, UK). The reactions were set up according to the manufacturer's protocol (see Table 2.11 and Table 2.12). Ligation with the T4 DNA ligase reaction mixture was incubated 2 h at room temperature, and 8 µL of the mixture was used for the transformation of 50 µL *E. coli* Top10 competent cells. The HiFi DNA assembly reaction mixture was incubated for 60 min in a thermocycler at 50 °C. Following the incubation, the samples were stored at -20 °C. Transformations were prepared with 5 µL of reaction mixture and 50 µL of *E. coli* Top10 competent cells. The competent cells preparations and transformations protocols are described in Section *2.6*.

Table 2.11. Reaction compositions for restriction enzyme-based cloning procedure

Component	Volume, µL
Water, nuclease-free*	11
Linear vector DNA**	5
Insert DNA**	1
T4 DNA ligase	1
10X DNA ligase buffer	2
Total volume	20

*****the volume of water can be adjusted to keep the indicated total reaction volume;
******the volume of DNA can be adjusted depending on the DNA concentration (50 ng for linear vector with two-fold excess of each insert).

Table 2.12. *NEBuilder* HiFi DNA assembly reaction protocol

Component	Volume, µL
Water, nuclease-free*	0.4
Linear vector DNA**	2
Insert DNA**	0.1
NEBuilder HiFi DNA Assembly Master Mix	2.5 µL
Total volume	5 µL

*****the volume of water can be adjusted to keep the indicated total reaction volume;
******the volume of DNA can be adjusted depending on the DNA concentration (25 ng for linear vector with two-fold excess of each insert).

2.5.4. Gel electrophoresis

Gel electrophoresis was performed by using an agarose gel electrophoresis system (*Cleaver Scientific*, UK). 1 % agarose (*Sigma-Aldrich*, USA) was diluted with 50x TAE buffer (*Thermo Scientific*, Lithuania), melted, and poured into an electrophoresis tank and mixed with 1 µL of *Midori Green Advance* (*NIPPON Genetics Europe*, Germany). *TriTrack DNA Loading Dye* 6x (*Thermo Fisher Scientific*, Lithuania) was added to the DNA samples for separation. DNA size marker *GeneRuler 1 kb DNA Ladder* (*Thermo Fisher Scientific*, Lithuania) was used for DNA size analyses. The power supply was programmed at 120 V for 15 min. The observation of separated DNA fragments was performed with a gel documentation system (*UVITEC*, UK). Excision of the fragments was performed by using a blue-light transilluminator (UVITEC, UK).

2.5.5. pDNA isolation

The *GeneJET* plasmid miniprep kit (*Thermo Fisher Scientific*, Lithuania) was used for the isolation of pDNR after the vector assembly and transformation into *E. coli* Top 10 or *E. coli* DH5α. The isolation procedure was performed according to the manufacturer's protocol. A single colony was inoculated with 6 ml of LB medium supplemented with chloramphenicol or tetracycline, depending on the antibiotic resistance gene contained in the pDNA. The bacteria culture was incubated for 16 h at 37 °C at 200 rpm and harvested by centrifugation at 8000 rpm for 2 min. The supernatant was discarded, and the cells were resuspended in 250 µL of the resuspension solution, and the cells suspension was transferred to a microcentrifuge tube. Additionally, 250 µL of the lysis solution and 350 µL of the neutralization solution were added to the resuspended cells, while mixing by inverting the tubes 6 times after each solution had been added and centrifuged for 10 min at 14000 rpm. The supernatant was transferred to the GeneJET spin column and centrifuged for 10 min at 14000 rpm, and the flow-through was discarded. 500 µL of the wash solution was added to the GeneJET spin column and centrifuged as described above. This step was repeated twice, and the empty column was centrifuged for an additional 1 min to remove ethanol. The GeneJET spin column was transferred to a fresh 1.5 ml microcentrifuge tube, and 30 µL of the elution buffer was added to the center of spin column. The tube was incubated for 2 min at room temperature and centrifugated for 2 min at 14000 rpm. The concentration of pDNR was verified with a nanophotometer (*Implen*, Germany) and stored at -20 °C.

2.5.6. Restriction enzymes for pDNA and PCR products digestion

In this work, pDNA and PCR products were prepared with *FastDigest* restriction enzymes (*Thermo Fisher Scientific*, Lithuania) for the vector assembly or for the vector verification according to the manufacturer's protocol. The compositions of the reactions are listed in Table 2.13. The prepared reaction mixture was mixed and incubated at 37 °C in a heat block (*VWR*, USA). The digestion reaction time and the inactivation temperature depend on the enzyme used; they are listed in Table 2.14. After enzyme inactivation, the reaction mixture was loaded into agarose gel, and electrophoresis was performed.

Table 2.13. Reaction compositions for pDNA and PCR products digestion

Component	**Volume, µL**	
	pDNA	**PCR product**
Water, nuclease-free*	15	16
10X FastDigest Green Buffer	2	3
DNA**	2	3
FastDigest enzyme (1)	1	1
FastDigest enzyme (2)	1	1
Total volume	20	30

*****the volume of water can be adjusted to keep the indicated total reaction volume;
******the volume of DNA can be adjusted depending on the DNA concentration (500 ng for DNA preparation for vector assembly and 200 ng for vector verification after assembly).

Table 2.14. *FastDigest* restriction enzymes (according to the manufacturer's protocol)

Restriction enzyme	**Thermal inactivation**	**Incubation time (in hours)**
AatII	80°C, 5 min	16
NdeI	65°C, 5 min	16
BamHI	80°C, 5 min	1
BglII	65°C, 5 min	2
EcoRI	80°C, 5min	0.5
MssI	65°C, 10 min	16
SacI	65°C, 5 min	16
ScaI	65°C, 10 min	16
SdaI	unnecessary	1
SgsI	65°C, 20 min	16
SpeI	unnecessary	16

2.6. Competent Cell Preparation and Transformation

E. coli Top10 and *E. coli* DH5α chemical competent cells were prepared by following the *Sambrook and Russell* protocol[168]. A single *E. coli* colony was inoculated in 5 ml of LB medium. 0.5 ml of overnight culture was added to 50 ml of LB medium in a 250 ml flask and incubated at 37 °C at 200 rpm for 2–3 hours until 0.4–0.8 OD_{600}. The culture was cooled on ice for 10 min and transferred to a 50 ml conical sterile tube and centrifuged for 6 min, at 4000 rpm at 4 °C. The supernatant was discarded, and the cells were resuspended in 15 ml of 0.1 M $MgCl_2$ by shaking on ice. The mixture was centrifuged for 6 min at 4000 rpm at 4 °C. The supernatant was discarded, and the cells resuspended in 15 ml of 0.1 M $CaCl_2$ by shaking on ice. The mixture was cooled on ice for 20 min and centrifuged under the same conditions

as described above. The supernatant was discarded, and the cells were resuspended in 3 ml of 0.1 M $CaCl_2$ with 15% glycerol by shaking on ice. *E. coli* Top10 and *E. coli* DH5α chemical competent cell aliquots were stored at -80°C.

For plasmid DNA or the ligation mix transformation (after HiFi DNA assembly or ligation with T4 DNA ligase), *E. coli* competent cells were thawed on ice, and 50 µL cells were mixed with 1–10 ng of plasmid DNA or 5 µL ligation mix. The mixture was cooled on ice for 5 min, heat shock was performed for 1.5 min at 42 °C, and again cooled on ice for 5 min. 1 ml of LB medium was added to the tubes and incubated for 1.5 h at 37 °C at 200 rpm. Subsequently, 100–200 µL cel culture was plated on an LB agar plate supplemented with 25 µg/ml chloramfenicol. Cultures were grown overnight at 37 °C.

C. necator H16 electrocompetent cells were prepared by following the Ausubel et al. protocol 170. Fresh *C. necator* H16 cells were inoculated in 10 ml of SOB medium supplemented with 10 µg/ml gentamicine and incubated overnight at 30 °C at 200 rpm. 10 µL overnight culture was added to 9.990 ml of SOB medium supplemented with 10 µg/ml gentamicine and incubated for 10–14 hours at 30 °C at 200 rpm. 1 ml of the overnight culture was added to 50 ml of SOB medium in 250 ml baffled flask and incubated for 2 h at 30 °C at 250 rpm at 0.2–0.3 OD_{600}. 25 ml of the culture was transferred to a 50 ml conical sterile tube and centrifuged for 10 min, at 7000 rpm at 4 °C. The supernatant was discarded, and the cells were resuspended in 10 ml of 1 mM HEPES buffer (pH=7.0). The mixture was centrifuged as before. The supernatant was discarded, and the cells were resuspended in 5 ml of 1 mM HEPES buffer (pH=7.0) and centrifuged as as explained above. The supernatant was then discarded, and the cells were resuspended in 2 ml of 1 mM HEPES buffer (pH=7.0) with 10% glycerol. *C. necator* H16 electrocompetent cells aliquots were stored at -80 °C.

P. putida KT2440 electrocompetent cells were prepared by following the Hanko et al. protocol 148. A single colony of *P. putida* KT2440 was inoculated in 5 ml of LB medium at 30 °C at 200 rpm. The overnight culture was centrifuged for 5 min, at 7000 rpm at 4 °C. The supernatant was discarded, the cells were resuspended in ice cold 5 ml of 10% glycerol, and was centrifuged as described above (this step was repeated twice). The supernatant was discarded, and the cells were resuspended in 3 ml of 10% glycerol. *P. putida* KT2440 electrocompetent cells aliquots were stored at -80 °C.

For pDNA electroporation in *C. necator* H16 or *P. putida* KT2440 cells, these cells were thawed on ice, and 100 µL electrocompetent cells with 100–500 ng transferred to the electroporation cuvette and incubated on ice for 2–5 min. Electroporation was performed with a micropulser electroporator at 2.5 kV, 200 Ω and 25 µF. After electroporation, 1 ml LB medium was added to the cell suspension and transfered into a 50 ml conical sterile tube. The cells were incubated for 2–3 h at 30 °C at 250 rpm. Subsequently, 100–200 µL cel culture was plated on an LB agar plate supplemented with 50 µg/ml chloramfenicol and 12.5 µg/ml tetracycline for *C. necator* H16 and *P. putida* KT2440, respectively. The cultures were grown for 1–3 days at 37 °C.

2.7. L- and D-lactic Acid Consumption Assay

C. necator H16 was grown with 44 mM L-lactate, D-lactate, and glycolate as the sole carbon source in MM (Table 2.6) for 48 hours. The samples were collected for the determination of lactate and glycolate at 6, 24, and 48 h. Bacterial growth was estimated by measuring the optical density of the samples. For HPLC analysis, the samples were centrifuged for 5 min at 15000 rpm, and the supernatants were stored at 80 °C. HPLC analysis is described in Section *2.11*.

2.8. Fluorescence Assay

Freshly grown bacterial cells from the agar plate were inoculated in 2 ml of the appropriate media containing the respective antibiotic in 50 ml tubes and incubated overnight at 30 °C at 200 rpm. After the incubation, the cultures were diluted to 0.05 OD_{600} and grown until 0.1–0.2 OD_{600}, and then transferred to a 96-well plate (*Corning Incorporated*, USA, or *Thermo Scientific*, USA). 142.5 µl of the cell culture and 7.5 µl of the selected inducer were added to each well of the 96-plate. The RFP fluorescence assay was accomplished by using an *Infinite M200 PRO* microplate reader (*Tecan*, Austria). The fluorescence bottom reading mode was applied for RFP excitation, and emitted light measurement using 585 and 620 nm wavelengths with 9 and 20 nm bandwidths, respectively, the gain factor was set at 120%, and the number of flashes was set at 20. Absorbance was measured at 600 nm wavelength with 9 nm bandwidth, and the number of flashes was set to 20. RFP fluorescence and absorbance were quantified over time for about 15–20 h, and their values were corrected for autofluorescence and autoabsorbance of the medium without cells, respectively.

The absolute normalized fluorescence values (*ANF*) obtained with inducers were calculated as previously described [148] by using Formula (1):

$$ANF = \frac{FL_{sample} - FL_{medium}}{OD_{sample} - OD_{medium}}; \quad (1)$$

where FL_{sample} is the RFP fluorescence of the sample, FL_{medium} is the RFP fluorescence of the medium, OD_{sample} is the optical density of the sample, and OD_{medium} is the optical density of the medium.

To obtain the system parameters, the *ANF* values were plotted as a function of the inducer concentration by using the software *GraphPad Prism 8* (*GraphPad Software, Inc.*, USA), and a non-linear least-squares fit was performed by using the Hill function (2) as previously described[113]:

$$ANF = b_{max} \times \frac{I^h}{K_m^h + I^h} + b_{min}; \quad (2)$$

where b_{max} is the maximum rate of RFP synthesis, b_{min} is the basal level of RFP synthesis, I is the concentration of the inducer, h is the Hill coefficient, and K_m is the inducer concentration that mediates the half-maximal reporter output.

The fold induction (dynamic range) was calculated by dividing the *ANF* value of the induced sample by the *ANF* value of the uninduced sample (Tables 3.1 and 3.2). Relative normalized fluorescence values (A.U.) as shown in Fig. 2.5 were obtained by subtracting the *ANF* values of the uninduced cells from the *ANF* values of cells

supplemented with the inducer. Relative normalized fluorescence (%) values as shown in Figs. 3.4, 3.10, and 3.11 were obtained by using *ANF* values at a specific inducer concentration as specified in Formula (3):

$$Relative\ normalized\ fluorescence\ (\%) = 100 \times \left(\frac{ANF - b_{min}}{b_{max}}\right). \quad (3)$$

2.9. Lactic Acid Fermentation

LAB cultures (*L. paracasei*, *L. amylovorus*, and *L. lactis*; Table 2.2) were grown for 24 h in the MRS medium (*VWR Chemicals*, USA) with 15 g/L agar (*Sigma Aldrich*, USA) and used as inoculum. *L. paracasei* was grown at 30 °C, while *L. amylovorus* and *L. lactis* were grown at 37 °C in MRS broth or ORRF with supplements without shaking in glass culture tubes. The growth curves were constructed by measuring the optical density at 600 nm (OD_{600}) of the bacteria cultures by using a spectrophotometer (*BioMate 160 UV-Vis* spectrophotometer, *Thermo Scientific*, USA).

ORRF was investigated as a potential substrate for the production of L- and D-lactic acid or a mixture of both by *L. paracasei*, *L. lactis*, and *L. amylovorus*, respectively. ORRF was obtained through the production of glucose syrup from *Roquette Amilina* (Lithuania). In the industry, starch solution was liquefied and saccharified by alpha-amylase and glucoamylases enzymes, and crude syrup was ultrafiltered by using 30 nm pore-size filters. ORRF was separated from proteins and fatty acids-rich undesired by-products remaining in the retentate by using a special separator (an undisclosed proprietary method of *Roquette Amilina*). For fermentation, the ORRF solution was prepared by dissolving soluble particles in distilled water at an initial concentration of 250 g/L and incubated for 1 h at 37 °C at 200 rpm. After incubation, the mixture was autoclaved at 125 °C for 15 min at 1.5 atm pressure, then, the mixture was cooled and centrifuged for 5 min at 11000 rpm. Water-insoluble substances were removed, thereby also losing some of the proteins and lipids. The supernatants were collected and used for bacteria cultivation. The final 200 g/L of the ORRF solution contained approximately 42 g/L of glucose.

For nutritional requirements, determination ORRF was supplemented with 10% MRS broth, 4 g/L of yeast extract (*Sigma-Aldrich*, USA), 8 g/L of meat extract (*Fluka Analytical*, USA), 1% vitamin supplement (*ATCC*, USA), and 0.1% *Tween 80* (*Applichem GmbH*, Germany). To determine the optimal amount of the nitrogen source, the culture media with ORRF was supplemented with different concentrations of yeast extracts (1 g/L, 5 g/L, 10 g/L, 15 g/L, 20 g/L, 30 g/L). In all cases of cultivation, the ORRF was additionally supplemented with salt solutions: 2 g/L of K_2HPO_4, 0.2 g/L of $MgSO_4$, and 0.05 g/L of $MnSO_4$.

2.10. ORRF Composition Analysis

Carbohydrate analysis in ORRF was performed with a *Dionex Ultimate 3000-4* HPLC system equipped with a refractive index detector (*Thermo Fisher Scientific*, USA), and chromatographic separation was achieved with an integrated *Aminex HPX-87H* column (300 × 7.8 mm) (*Bio-Rad*, USA). The analysis of lipids in ORRF was performed with the *Thermo Ultimate 3000-3* HPLC system equipped with an *ESA*

Corona Ultra CAD detector (*Thermo Scientific™ Dionex™*, USA) and the chromatographic separation was achieved with an integrated *Fortis C8* column (1.7 µm; 50 × 2.1 mm) (*Fortis Technologies*, UK). The protein amount of the ORRF sample was determined by using the Dumas method with a *Thermo Flash 2000* instrument (*Thermo Scientific*, USA) with a factor of 6.25. The biochemical compositions analysis of the ORRF was carried out in *Roquette Amilina*.

2.11. HPLC Analysis for Lactic Acid Quantification

HPLC analyses for lactic acid, glucose and glycolate detection were performed with an *Ultimate 3000* HPLC system coupled to a photodiode array (UV-VIS) detector (*Thermo Fisher Scientific*, USA), and an additionally connected *RefractoMax 521* refractive index detector (*Thermo Fisher Scientific*, USA). Chromatographic separation was achieved with a *Phenomenex Rezex*^{TM} ROA-organic acid H+ (8%) (150 × 7.8 mm) (*Phenomenex*, Germany) equipped with a security guard column, thermostated at 25 °C. The mobile phase A was aqueous 0.005 N H_2SO_4 with a flow rate of 0.5 ml/min 35 min. The detection was achieved at 210 nm. All chromatograms were recorded and analyzed by using *Chromeleon 7* software (*Thermo Fisher Scientific*, USA). Before the analysis, the samples were filtered by the passage through a 0.2 µm nylon filter (*UptiDisc*, Interchim).

2.12. Enzymatic L- and D-lactic acid determination method

For the determination of L- and D-lactic acid enantiomers, an enzymatic D-/L-Lactic Acid (D-/L-Lactate) (Rapid) assay kit (*Megazyme*, Ireland) was used, and the quantification of each lactate stereoisomer was carried out according to the manufacturer's recommendations.

2.13. L- and D-lactic Acid Determination with Biosensors BLA1 and BLA2

Biosensors BLA1 (*E. coli*/*Ec*LldR/P_{lldP}; pEA015 plasmid) and BLA2 (*P. putida*/*Pf*PdhR/P_{lldP}; pEA025 plasmid) were used to determine L- and D-lactic acid concentrations in biological samples. The analysis of fermentation supernatant samples was accomplished by using an *Infinite M200 PRO* (*Tecan*, Austria) microplate reader. Fermentation supernatant samples were diluted 5, 10, 15, 10, 20 or 30 times depending on the expected concentration of lactic acid. Fluorescence measurements and calculations were performed as described in Subsection *2.8*.

2.13.1 L- or D-lactic acid determination in biological sample with one of lactic acid enantiomers

The concentration of L-lactic acid produced by *L. paracasei* was determined with the biosensor BLA1, while D-lactic acid produced by *L. lactis* was determined with the biosensor BLA2. The absolute normalized fluorescence was calculated by using Formula (1). L- or D-lactic acid dose-response curves were plotted by using the Hill function (2).

2.13.2 L- and D-lactic acid determination in biological sample with a mixture of lactic acid enantiomers

L. amylovorus samples were analyzed with both biosensors BLA1 (for L-lactic acid determination) and BLA2 (for total DL-lactic acid determination) with additional recalculations, as described below. The total DL-lactic acid concentration was determined by using the biosensor BLA2. The biosensor BLA2 was tested with various concentrations of L- and D-lactic acid standards within the range of 0 to 20 mM over time, whereas the absolute normalized fluorescence values for various L-lactic acid (ANF_L) and D-lactic acid (ANF_D) concentrations were calculated by using Formula (1). The absolute normalized fluorescence values for the total concentration of DL-lactic acid (ANF_{DL}) were calculated by using Formula (4) and the attended *k* coefficient, calculated according to Formula (5). For the DL-lactic acid calibration curve, ANF_{DL} values were used to plot the Hill function (2).

$$ANF_{DL} = \frac{ANF_D + ANF_L}{k} \tag{4}$$

$$k = \frac{ANF_D}{ANF_L} \tag{5}$$

The concentration of L-lactic acid in *L. amylovorus* fermentation supernatant samples was determined by using the biosensor BLA1. The concentration of D-lactic acid in *L. amylovorus* fermentation supernatant samples was calculated by subtracting the concentration of L-lactic acid from the total concentration of DL-lactic acid. The specific D-lactic acid yield (SY_D) (Fig. 2.19) was calculated by using Formula (6):

$$SY_D = \frac{I_D}{OD \times I_{ORRF} \times I_{YE}}; \tag{6}$$

where I_D is the concentration of the D-lactic acid (g/L), OD is the optical density, I_{ORRF} is the concentration of ORRF (g/L), and I_{YE} is the concentration of the yeast extract (g/L).

2.14. Statistical Analysis

All experiments were performed by using two or three biological-experimental replicates. The standard error of the mean was determined for each experimental sample time point. Linear regression analysis and the nonparametric *t*-test were performed by using the software *GraphPad Prism 9*.

The Bland-Altman analysis[171] was performed by using *Microsoft Excel 2016*. The bias line as the mean difference ($\bar{d}$) was calculated by using Formula (7):

$$\bar{d} = \frac{(a-b)}{\left(\frac{(a+b)}{2}\right)} \times 100; \tag{7}$$

where *a* is the D-lactic acid concentration obtained with the enzymatic method, *b* is the D-lactic acid concentration obtained with a biosensor-based assay.

The 95% limits of agreement (*lower LoA* and *upper LoA*) were calculated by using Formulas (8–10):

$$lower\ LoA = \bar{d} - (1.96 \times s_d); \quad (8)$$

$$upper\ LoA = \bar{d} + (1.96 \times s_d); \quad (9)$$

$$s_d = \sqrt{\frac{\sum(d - \bar{d})^2}{(n-1)}}; \quad (10)$$

where s_d is the standard deviation, d is the sample value obtained with Formula (7), $\bar{d}$ is the mean of samples obtained with Formula (7), and n is the total number of observations.

3. RESULTS AND DISCUSSION

3.1. Lactic Acid-Inducible Gene Expression Systems

This section describes the identification, characterization, and specification of L-, D-lactic and glycolic acids inducible-gene expression systems from gammaproteobacteria *E. coli* MG1655 and *Pseudomonas* spp., and betaproteobacterium *C. necato*r H16. The putative lactic acid-inducible systems have been investigated for their response to L-, D-lactic, and glycolic acids, as well as structurally similar compounds (glyoxylate, 3-hydroxypropionate, and pyruvate), systems dynamics have been parameterized, broad-host-range applicability has been demonstrated, functional genes regulation and carbon catabolite repression has been discussed. The results of this Part *3.1* are included in the "Identification and characterization of L- and D-lactate-inducible systems from *Escherichia coli* MG1655, *Cupriavidus necator* H16 and *Pseudomonas* species" article published in the *Scientific Reports* Journal[172].

3.1.1. Identification of lactic acid-inducible gene expression systems

Previously, several lactate catabolism gene clusters had been characterized in *E. coli*[108,173], *P. aeruginosa*[115], and *P. fluorescens* strains[124]. In the present work, putative operons containing at least two genes related to lactic acid consumption and an adjacent promoter region and TF encoded gene have been identified in *E. coli* MG1655, *C. necator* H16, and *Pseudomonas* spp. The glycolic acid metabolism related gene clusters have also been included, as their involvement in D-lactic acid consumption had also been reported previously in[101]. The identified gene clusters have been grouped according to several rules; first, they have been divided into groups according to the type of enzyme. Second, the groups have been divided into subgroups (1, 2, and 3) based on the protein homology (with an identity of more than 40%) and the TF family (see Supplementary Table S3). Accordingly, Group I, representing FMN dependent L-iLDHs (EC 1.1.2.3) and FAD-dependent D-iLDHs (EC 1.1.2.4), Group II representing 3-component Fe-S iLDHs[174] (composed of two FAD-binding and Fe-S-bindings domains[109]), and Group III associated with the glycolate catabolism have been defined (Fig. 3.1).

E. coli MG1655, *P. aeruginosa* PAO1, *P. fluorescens* NCTC 10038, *P. lactis* DSM 29167 systems were assigned to Group I, and the functional genes of these systems are regulated by the GntR family TF. Operon *lldPRD* allocated in *E. coli* genome lacks the D-iLDH encoded gene, while operons from *P. putida* and *P. aeruginosa* consist of both L-iLDH and D-iLDH encoded genes; the other operons from *P. fluorescens* and *P. lactis* lack L-iLDH encoded gene (Fig. 3.1). L-iLDH and D-iLDH were encoded by *lldD* and *lldE*, respectively; these operons have an identity greater than 80% (see Supplementary Table S3).

C. necator H16 gene cluster *H16_RS19175-H16_RS19195*, assigned to Group II, has three genes *lldEGF* encoded proteins potentially related with lactic acid catabolism, with 34%, 40%, and 31% sequences identity to the 3-component Fe-S iLDH encoded by *ykgEFG* operon from *E. coli*, 32%, 40%, and 30% amino acid sequences identity to *lldEFG* operon genes from *S. oneidensis*[174], and 42%, 39%, and

28% sequences identity to *lutABC* operon genes from *B. subtilis*[116], respectively. *lldP* gene (*H16_RS19175*) encoded lactate permease exhibits a high homology with 65% and 63% identity to the *lldP* of *E. coli* (locus tag *b3603*) from Group I and to the *glcA* of *E. coli* (locus tag *B2975*) from Group III, respectively. *lldP* gene is the most conserved protein of lactate catabolism operons[104].

*Cn*GntR/$P_{H16\_RS19190}$ potential lactic acid utilization system from *C. necator* H16 includes iron-sulfur cluster-binding protein (locus tag *H16_RS19180*) and (Fe-S)-binding protein (locus tag *H16_RS19190*) and exhibits 40% and 40.5% sequences identity with *H16_RS06900* and *H16_RS06905* proteins, respectively, from *Cn*IclR/$P_{H16\_RS06900}$ system (see Supplementary Table S3). The TFs of Group II do not have significant similarity with each other and belong to different TFs families (GntR, AraC, and IclR). For this reason, all three systems were assigned to different Subgroups 1, 2, 3 of Group II.

Two analogous *E. coli* MG1655 and *P. putida* KT2440 glycolic acid catabolism-related gene clusters were involved in Subgroup 1 of Group III. Based on these cluster proteins, the glycolic acid cluster was also found in *C. necator* H16 genome. The main proteins encoded by *glcD*, *glcE*, *glcF* genes had greater than 47% sequences identity compared to the *E. coli* proteins (see Supplementary Table S3). It is essential to highlight that the *E. coli* and *P. putida* glycolic acid catabolism-related genes are potentially regulated by the GntR family TF, whereas *C. necator* genes are regulated by the LysR family TF. For this reason, *C. necator* genes cluster was assigned to Subgroup 2 of Group III. Eleven potential lactate-inducible systems, composed of TF genes and promoter regions, were identified in *E. coli* MG1655, *C. necator* H16, and *Pseudomonas* spp.

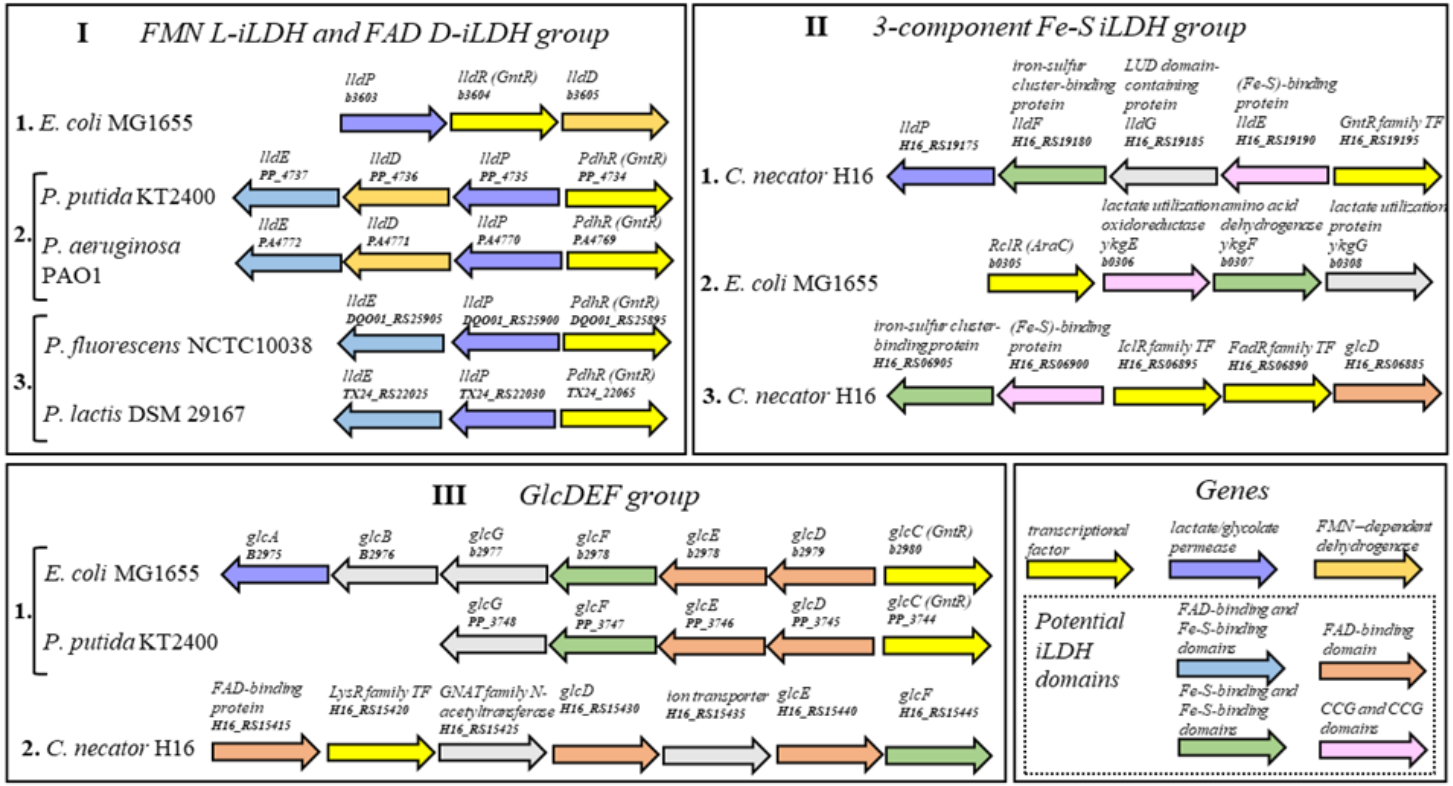

Fig. 3.1. Genomic organization of gene clusters containing lactic and glycolic acids catabolism-related operons and associated TR genes in *E. coli* MG1665, *C. necator* H16 and *Pseudomonas* spp. Only operons containing at least two lactic acid or glycolic acid catabolism-associated genes and adjacent TR gene are included. Locus tags, protein functions, and protein domains are indicated. This figure was used in[172]

3.1.2. Validation and evaluation of lactic acid-inducible systems

The utilization of lactic acid and glycolic acid by *E. coli* MG1665[108,110] and *P. putida* KT2440[101] had been previously demonstrated in several studies. To verify that *C. necator* H16 can catabolize L-, D-lactic and glycolic acids as the sole carbon source, a consumption assay was performed. *C. necator* H16 was grown with 44 mM L- and D-lactic acids, and 44 mM sodium glycolate as the sole carbon source for 48 hours. *C. necator* H16 fully consumed L-, D-lactic acids, and glycolate within 24 hours and reached an optical density OD_{600} higher than 1 (Fig. 3.2).

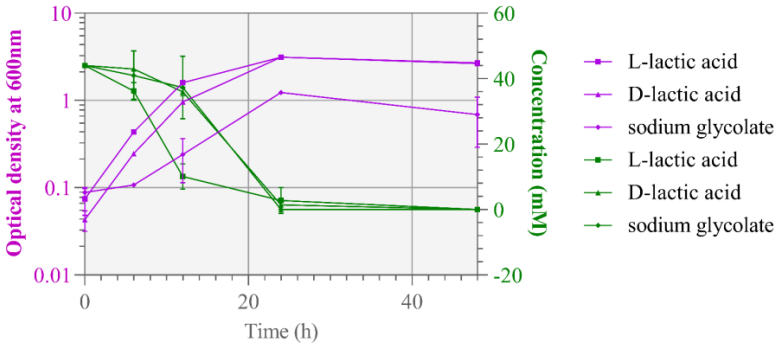

Fig. 3.2. The growth and carbon source consumption (L-lactate, D-lactate, and glycolate) of *C. necator* H16. The initial concentrations of L-lactate, D-lactate, and glycolate were 44 mM. Data is presented as mean ± SD, n = 3

The identified putative lactic acid-inducible systems (Fig. 3.1) were cloned into a modular reporter vector to examine their response to L-, D-lactic, and glycolic acids. For evaluation, two types of constructs with each inducible system were assembled: the promoter only version, and the TF with inducible promoter version, where TF was oriented in the opposite direction compared to RFP. The fluorescence output measurements were performed on the host cells of these systems, except for *P. aeruginosa* PAO1, *P. fluorescens* NCTC 10038, and *P. lactis* DSM 29167. These constructs were cloned into *P. putida* KT2440 cells (Fig. 3.3).

E. coli DH5α, *C. necator* H16, and *P. putida* KT2440 strains carrying the inducible systems were grown in MM, and the fluorescence output of the logarithmically growing cells was quantified at 6 h after the addition of the inducer. Of the eleven analyzed putative lactic acid inducible systems, two specific L-lactic acid systems were identified. As expected, the *Ec*LldR/P_{lldP} (pEA015) system was induced 15.9-fold by L-lactic acid. As it had been previously described, this system is induced 18.63-fold with 14 mM L-lactic acid. The results obtained in this study were consistent with the results in the Goers and team-presented publication[33].

Inducible systems *Cn*GntR/$P_{H16\_RS19190}$ (pEA007), *Ec*RclR/P_{b0306} (pEA032), and *Cn*IclR/$P_{H16\_RS06900}$ (pIE005) from Group II (Fig. 3.3) were compared. These systems are regulated by different types of TF, and 3-component iLDH proteins have less than 40% identity. This indicates genetic diversity within the species and different regulatory mechanisms of gene expression. *Cn*GntR/$P_{H16\_RS19190}$ (pEA007) showed 280.8-fold induction with L-lactic acid. It suggests that the GntR TF family is

involved in the regulation of L-lactic acid-related catabolism gene expression. *Ec*RclR/P_{b0306} (pEA032) was induced 2-fold with glycolic acid and the promoter P_{b0306} (*Ec*RclR/P_{b0306} system (pEA032)) expression is affected by the carbon catabolite repression in the presence of glucose and activated when L- and D-lactic acids are used as a carbon source (see Fig. 3.3c and Supplementary Fig. S1).

*Cn*IclR/$P_{H16\_RS06900}$ (pIE005) showed 2- and 3-fold induction with D-lactic acid and glycolic acid, respectively (Fig. 3.3c). To investigate whether IclR expression is inhibited under the tested conditions and whether IclR exerts an effect on the promoter $P_{H16\_RS06900}$ activation, the IclR gene was controlled by the strong synthetic promoter P_{13}^{175} and induced by the arabinose system (*Ec*AraC/P_{araBAD}). pEA014 and pEA028 constructs were assembled for this purpose (Supplementary Fig. S2a). A comparison of pIE005, pEA014, and pEA028 constructs' fluorescence outputs showed that IclR has no effect on the *Cn*IclR/$P_{H16\_RS06900}$ inducible system response to D-lactic acid and glycolic acid (see Supplementary Figs. S2b and S3b). For this reason, it was hypothesized that this system is regulated by other TFs. Two additional constructs with FadR TF (located downstream to the *iclR* (Fig. 3.1)) were constructed (pEA019 and pEA020) (see Supplementary Fig. S2a). The constructs with FadR TF did not show higher induction than the original constructs of this system (pIE005 and pIE004) (see Supplementary Fig. 2b). Furthermore, pIE005, pEA019, and pEA020 in *E. coli* host showed no response to either D-lactic or glycolic acids (see Supplementary Fig. S4). The obtained results indicate that it is unlikely that IclR or FadR is regulated by the *Cn*$P_{H16\_RS06900}$ promoter. The regulation of this system is still not entirely clear.

Inducible systems *Ec*GlcC/P_{b2979} (pEA004) and *Pp*GlcC/P_{PP_3745} (pEA012) assigned to Group III (Fig. 3.1) showed 4- and 15-fold induction with glycolic acid, respectively (Fig. 3.3d). To elucidate the regulation of *Cn*LysR/$P_{H16\_RS15430}$ glycolic acid-inducible system from *C. necator* H16, two $P_{H16\_RS15415}$ and $P_{H16\_RS15430}$ promoter regions (pEA022 and pEA023, respectively), LysR TF with additional genes and both $P_{H16\_RS15415}$ and $P_{H16\_RS15430}$ intergenic sequences (pEA021), and only a LysR TF with both $P_{H16\_RS15415}$ and $P_{H16\_RS15430}$ promoters (pEA030) were evaluated (see Supplementary Fig. S5a). The absolute normalized fluorescence results showed that $P_{H16\_RS15430}$ (pEA030) is induced 6-, 2-, and 4-fold with glycolic acid, L-, and D-lactic acids, respectively. Higher induction was observed with pEA021 construct, 8-, 3-, and 4-fold by glycolic acids, L-, and D-lactic acids, respectively (see Supplementary Fig. S5b).

a

System type	Origin	Regulator	Inducible system	Construct
I	*E. coli* MG1655	LldR	*Ec*P$_{lldP}$	pEA016
			*Ec*LldR/P$_{lldP}$	pEA015
	P. putida KT2440	PdhR	*Pp*P$_{lldP}$	pEA010
			*Pp*PdhR/P$_{lldP}$	pEA011
	P. aeruginosa PAO1	PdhR	*Pa*P$_{lldP}$	pEA017
			*Pa*PdhR/P$_{lldP}$	pEA018
	P. fluorescens NCTC 10038	PdhR	*Pf*P$_{lldP}$	pEA024
			*Pf*PdhR/P$_{lldP}$	pEA025
	P. lactis DSM 29167	PdhR	*Pl*P$_{lldP}$	pEA026
			*Pl*PdhR/P$_{lldP}$	pEA027
II	*C. necator* H16	GntR	*Cn*P$_{H16_RS19190}$	pEA006
			*Cn*GntR/P$_{H16_RS19190}$	pEA007
	E. coli MG1655	RclR	*Ec*P$_{b0306}$	pEA005
			*Ec*RclR/P$_{b0306}$	pEA032
	C. necator H16	IclR	*Cn*P$_{H16_RS06900}$	pIE004
			*Cn*IclR/P$_{H16_RS06900}$	pIE005
III	*E. coli* MG1655	GlcC	*Ec*P$_{b2979}$	pEA003
			*Ec*GlcC/P$_{b2979}$	pEA004
	P. putida KT2440	GlcC	*Pp*P$_{PP_3745}$	pEA013
			*Pp*GlcC/P$_{PP_3745}$	pEA012
	C. necator H16	LysR	*Cn*P$_{H16_RS15430}$	pEA023
			*Cn*LysR/P$_{H16_RS15430}$	pEA021

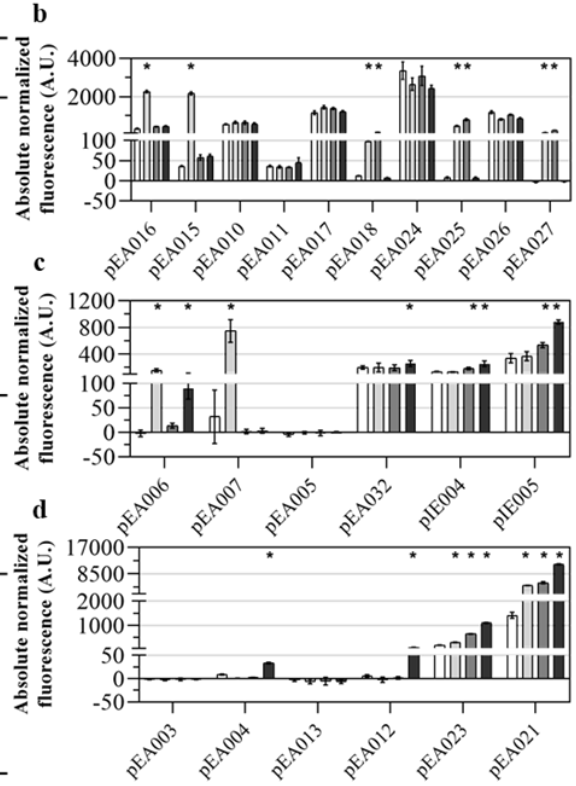

Fig. 3.3. Quantitative evaluation of lactic acid-inducible systems. **(a)** Summary of the identified inducible systems, including the system type, based on Fig. 3.1, system origin, TF name, and inducible promoter. Single time-point RFP fluorescence measurements (arbitrary units) were taken 6 h after the inducer addition of **(b)** Group I systems, **(c)** Group II systems, and **(d)** Group III systems. The RFP fluorescence output was determined in the absence of inducer (white) and extracellular supplementation with L-lactate (light gray), D-lactate (dark gray), and glycolate (black) to a final concentration of 5mM. Data is presented as mean ± SD, n = 3, *p ≤ 0.001 (unpaired *t*-test). This figure was used in [172]

The D-lactate specific inducible system has not been identified in *E. coli* MG1655, *C. necator* H16 or *Pseudomonas* spp. The most promising *Pf*PdhR/P_{lldP} (pEA025), *Pl*PdhR/P_{lldP} (pEA027), and *Pa*PdhR/P_{lldP} (pEA018) systems without D-lactic acid (124.2-, 78.3-, and 29.2-fold, respectively) were also induced with L-lactic acid (62.6-, 42.8-, and 23.9-fold, respectively). The TFs of these systems belong to the GntR family, act as repressors, and the function gene expression here is activated in the presence of either L- or D-lactic acid (Fig. 3.3a). The Inducible system *Pp*PdhR/P_{lldP} (pEA011) with a high level of homology to *Pa*PdhR/P_{lldP} did not show any statistically significant induction with L- and D-lactic acid when it was grown in MM with glucose as the carbon source (Fig. 3.3b). Possibly, the promoter P_{lldP} from *P. putida* is under catabolic repression in the presence of glucose in the growth medium. Previously, Zhang *et al.*[101] showed that lactate dehydrogenases are denoted by a higher activity when cells are cultured with lactic acid as the carbon source compared to glucose. Therefore, when L- or D-lactate was used as the sole carbon source, *Pp*P_{lldP} (pEA010) was slightly induced by D-lactate (see Supplementary Fig. S6). The obtained results show that, not only as previously reported, *lldPDE* from *E. coli* MG1655 cluster expression is associated with catabolic repression[176], but this association was also determined for *ykgEFG* from *E. coli* MG1655 and *lldPDE* from *P. putida* KT2440.

3.1.3. Parameterization and specificity determination of lactic acid inducible systems

*Ec*LldR/P_{lldP} (pEA015), *Cn*GntR/$P_{H16\_RS19190}$ (pEA007), *Pa*PdhR/P_{lldP} (pEA018), *Pf*PdhR/P_{lldP} (pEA025), and *Pl*PdhR/P_{lldP} (pEA027) lactic acid-inducible systems were subsequently evaluated for induction kinetics (see Supplementary Figs. S7 and S8). The cells were grown in MM containing 0.4% glucose (0.4% gluconate in the case of *C. necator*) and supplemented with the L-lactic acid and/or D-lactic acid at a final concentration of 5 mM, the fluorescence and absorbance were monitored over time. These systems were evaluated for a dose-response by using L-lactic acid or/and D-lactic acid concentrations between 0 and 5 mM (Fig. 3.4). Lactic acid-inducible systems parameters are provided in Table 3.1. Both L-lactic acid specific systems *Ec*LldR/P_{lldP} (pEA015) and *Cn*GntR/$P_{H16\_RS19190}$ (pEA007) exhibit low K_m values (below 1 mM), thereby indicating that low concentrations of L-lactic acid are required for the induction of these systems. The *Ec*LldR/P_{lldP} (pEA015) system gene expression can be tuned over the range of 9 µM-1 mM whereas *Cn*GntR/$P_{H16\_RS19190}$ (pEA007) system can be tuned over the range of 80 µM-1 mM. Inducible systems *Pa*PdhR/P_{lldP} (pEA018) and *Pf*PdhR/P_{lldP} (pEA025) showed similar affinities to L- and D-lactic acids, and the gene expression of these constructs can be tuned in the range of 9 µM-2 mM.

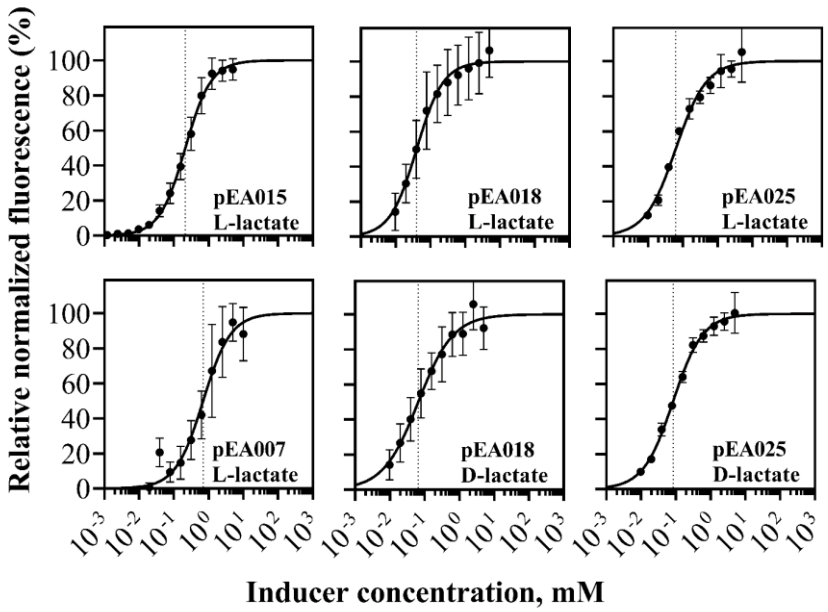

Fig. 3.4. Dose-response curves of L- and D-lactic acid-inducible systems. Relative normalized fluorescence of *E. coli* DH5*α*, *C. necator* H16, and *P. putida* KT2440 harboring *Ec*LldR/P_{lldP} (pEA015), *Cn*GntR/$P_{H16\_RS19190}$ (pEA007), *Pa*PdhR/P_{lldP} (pEA018), and *Pf*PdhR/P_{lldP} (pEA025) determined in response to various concentrations of either L- or D-lactate at 6 hours after inducer addition. The dose–response curves were fitted by using the Hill function as described in *Materials and Methods* Section. The maximum level of reporter output b_{max} was set to 100%**.** K_m is marked by using a dotted line. The cells were grown in MM containing 0.4% glucose (in the case of *C. necator* H16, SG-MM was supplemented with 0.4% gluconate). Data is presented as mean ± SD, n = 3 or 2. This figure was used in[172]

Table 3.1. Parameters of lactic acid-inducible systems

Inducible system (construct)	**Application host**	**Inducer**	**Dynamic range, in -fold[a]**	**K_m (mM)**	**Hill coefficient**
*Ec*LldR/P_{lldP} (pEA015)	*E. coli* DH5α	L-lactic acid	15.9 ± 1.3	0.22 ± 0.05	1.18 ± 0.06
*Pa*PdhR/P_{lldP} (pEA018)	*P. putida* KT2440	L-lactic acid	23.9 ± 10.9	0.04 ± 0.01	1.16 ± 0.08
		D-lactic acid	29.2 ± 17.8	0.07 ± 0.02	0.91 ± 0.04
*Pf*PdhR/P_{lldP} (pEA025)	*P. putida* KT2440	L-lactic acid	62.6 ± 6.5	0.06 ± 0.02	1.06 ± 0.21
		D-lactic acid	124.2 ± 46.2	0.08 ± 0.01	1.05 ± 0.21
*Pl*PdhR/P_{lldP} (pEA027)	*P. putida* KT2440	L-lactic acid	42.8 ± 9.4	ND	ND
		D-lactic acid	78.3 ± 11.9	ND	ND

Continued Table 3.1

*Cn*GntR/P$_{H16_RS19190}$ (pEA007)	*C. necator* H16	L-lactic acid	280.8 ± 57.7	0.67 ± 0.21	1.19 ± 0.10
*Cn*IclR/P$_{H16_RS06900}$ (pIE005)	*C. necator* H16	glycolic acid	2.6 ± 0.5	ND	ND
*Cn*LysR/P$_{H16_RS15430}$ (pEA021)	*C. necator* H16	D-lactic acid	3.9 ± 0.6	ND	ND

Data is presented as mean ± SD, n = 3. [a] – calculated by dividing the maximum level of fluorescence output by the basal level of fluorescence output.

The determination of the specificity of inducible systems can provide insight into TF affinity for compounds structurally similar to lactic acid and expand the list of analogous metabolites[2]. Consequently, *Ec*LldR/P$_{lldP}$ (pEA015), *Cn*GntR/P$_{H16_RS19190}$ (pEA007), *Pa*PdhR/P$_{lldP}$ (pEA018), and *Pf*PdhR/P$_{LctP}$ (pEA025) inducible systems were additionally tested with glyoxylate, 3-hydroxypropionate, and pyruvate (Fig. 3.5). Inducible system-reporter constructs were grown in MM containing 0.4% glucose (0.4% gluconate in the case of *C. necator* H16 was used), and the fluorescence output was monitored over time after the individual addition of each compound at 5 mM final concentration. The obtained results showed that the lactic acid-inducible systems did not induce other structurally similar compounds (glyoxylate, 3-hydroxypropionate, and pyruvate).

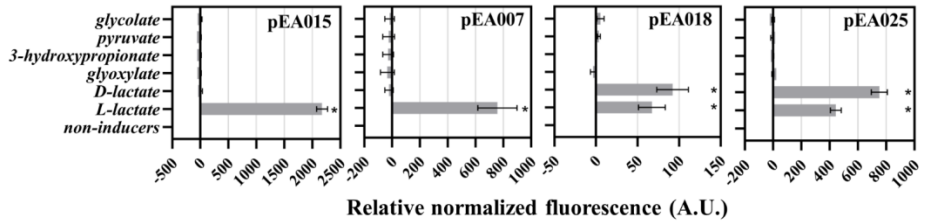

Fig. 3.5. Specificity determination of L- and D-lactic acid-inducible systems. Relative normalized fluorescence of *E. coli* DH5α harboring pEA015 (*Ec*LldR/P$_{lldP}$), *C. necator* H16 harboring pEA007 (*Cn*GntR/P$_{H16_RS19190}$), and *P. putida* KT2440 harboring pEA018 (*Pa*PdhR/P$_{lldP}$) and pEA025 (*Pf*PdhR/P$_{lldP}$). Single time-point fluorescence measurements were taken at 6 hours after addition of various compounds to a final concentration of 5 mM. Data is presented as mean ± SD, n = 3, *p ≤ 0.01 (unpaired *t*-test). This figure was used in[172]

3.1.4. Improvement of L-lactic acid-inducible system and determination of the inhibitory effect of D-lactic acid

To improve the expression of LldR TF from L-lactic acid inducible system *Ec*LldR/P$_{lldP}$, two constructs with additional modifications were assembled. The construct with P$_{lldP}$ and *lldR* under control of the synthetic promoter P$_{13}$ and the construct with P$_{lldP}$ and *lldR* under control of the arabinose inducible system *Ec*AraC/P$_{araBAD}$ were named pEA015 and pEA033, respectively. The construct pEA016 (*Ec*P$_{lldP}$) was used for negative control (Fig. 3.6a). Single time-point fluorescence measurements for *E. coli* DH5α harboring the described constructs were performed in the absence and presence of 5 mM L-lactate and 0.2% L-arabinose (in the case of pEA033). The absolute normalized fluorescence values showed a 59-fold

induction with pEA015 and an 18-fold induction with pEA033 (Fig. 3.6b). The obtained results indicated that the P_{13} promoter present in the pEA015 is stronger and that it gives a higher induction than the arabinose-controlled system presented in the pEA033, and higher levels of *lldR* can repress of *Ec*LldR/P_{lldP} in the absence of L-lactate.

To improve the inducible system *Ec*LldR/P_{lldP}, various RBSs for *lldR* expression regulation in the construct pEA015 containing TR gene under control of the constitutive promoter P_{13} were investigated. The theoretical translation rates of RBS variants were estimated by using an RBS calculator (available at https://salislab.net/software/)[177]. The absolute normalized fluorescence results obtained by using RBS variants showed that the sequences with different theoretical translation rates have a statistically significant effect on the gene expression and *Ec*LldR/P_{lldP} induction (see Supplementary Fig. S9). A significantly improved dynamic range of approximately 100- and 122-fold was achieved when RBSs with theoretical translation rates of 179032.18 and 51067.85 A.U., respectively, were introduced into pEA015 comparing to the approximately 59-fold induction obtained when using RBS with a theoretical translation rate of 19143.57 A.U.

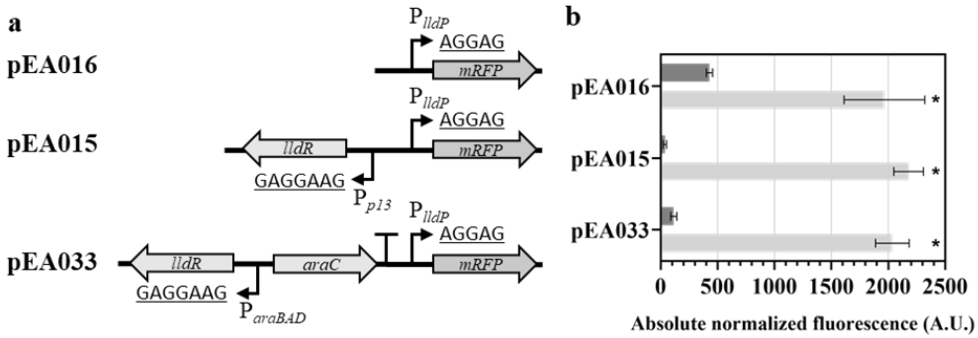

Fig. 3.6. Improvement of L-lactic acid-inducible system. **(a)** Schematic illustration of the different versions of the L-lactic acid-inducible system and their corresponding titles of plasmids. **(b)** Absolute normalized fluorescence of *E. coli* DH5α carrying different versions of the L-lactic acid-inducible system-reporter construct in the absence (dark gray) and presence (light gray) of 5mM L-lactate (pEA016 and pEA015) and 5mM L-lactate with 0.2% arabinose (pEA033). Data is presented as mean ± SD, n = 3, *p ≤ 0.001 (unpaired *t*-test). This figure was used in [172]

The inhibitory effect of D-lactate on the L-lactic acid inducible system *Ec*LldR/P_{lldP} was evaluated by testing different concentration mixtures of L-lactate and D-lactate (Fig. 3.7). The results showed that D-lactic acid inhibits RFP synthesis in mixtures of L-lactate and D-lactate when the concentration of D-lactate is two times lower than that of L-lactate, equal to L-lactate, or higher than the concentration of L-lactate. It is essential to note that when the mixtures contain 0.312 mM L-lactate, the inhibition effect of D-lactate starts from a concentration of 0.156 mM D-lactate (Fig. 3.7c). In addition, a shift of the fluorescence peak to a further hour was observed depending on the concentration of D-lactic acid in the mixture. Potentially, D-lactic acid inhibited the binding of L-lactic acid to LldR TF.

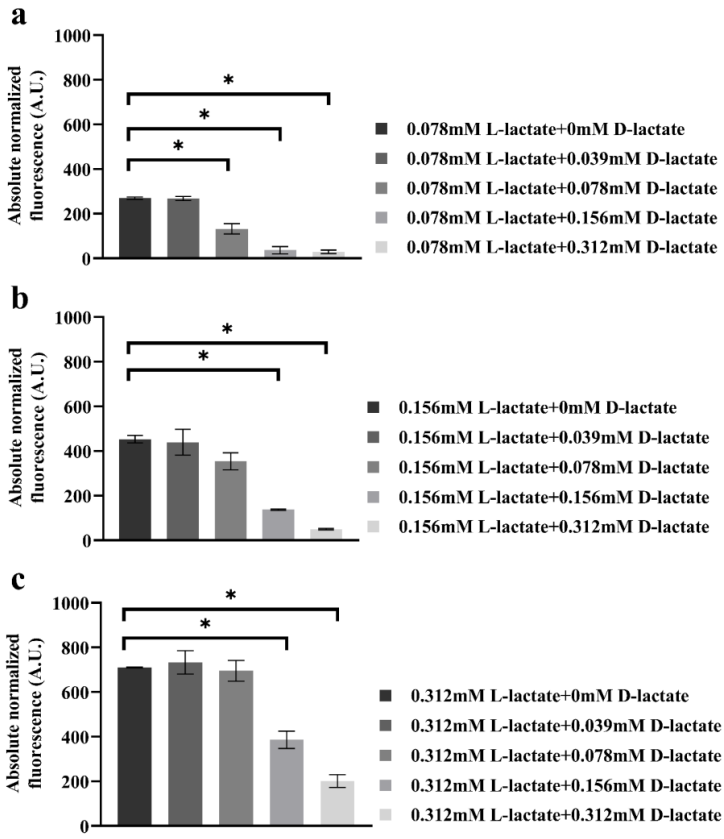

Fig. 3.7. Inhibitory effect of D-lactate on the L-lactic acid inducible system. Absolute normalized fluorescence of *E. coli* DH5α carrying pEA015 (*Ec*LldR/P_{lldP}) in the presence of different concentrations of L-lactate and different concentration mixtures of L-lactate and D-lactate. Data is presented as mean ± SD, n = 3, *p ≤ 0.001 (unpaired *t*-test)

3.1.5. Demonstration lactic acid-inducible systems of broad-host-range applicability

Lactic acid-inducible systems have not been studied previously in non-host organisms. To evaluate the applicability of the lactic acid-inducible gene expression systems to other chassis, inducible systems, including *Ec*LldR/P_{lldP} (pEA015), *Pf*PdhR/P_{LctP} (pEA025), and *Pl*PdhR/P_{LctP} (pEA027), were tested in *C. necator* H16 (betaproteobacterium) and *P. putida* KT2400 (gammaproteobacterium).

First, the inducible system *Ec*LldR/P_{lldP} (pEA015 and pEA033 plasmids) was tested in these strains. No significant induction was observed when plasmid-transformed cells were grown in MM with 0.4% glucose (*P. putida*) or gluconate (*C. necator*) as the carbon source and additionally added 5 mM L-lactate (see Supplementary Figs. S10 and S11a). However, when *lldR* TF was regulated by the arabinose system (pEA033) and *C. necator* cells grown on L-lactate as the carbon source, 57.5-fold induction was achieved compared to the construct grown with

gluconate as the carbon source (see Supplementary Fig. S11b). *Ec*LldR/P_{lldP} is activated in the presence of L-lactate as the sole carbon source in *C. necator* H16, and this is potentially related to carbon catabolite repression. *C. necator* H16 in SG-MM with gluconate as the carbon source form a protein complex which inhibits the expression of genes associated with non-preferred substrates, which is, in our case, the P_{lldP} promoter. When *C. necator* H16 harboring pEA033 in a MM with L-lactate as the carbon source probably does not inhibit the expression of genes associated with non-preferred substrates, as a result, changes in induction can be observed. These results correlate with the previously analyzed catabolic repression of the P_{lldP} promoter from *E. coli* MG1655 in the presence of glucose[176].

Inducible systems *Pf*PdhR/P_{lldP} (pEA025) and *Pl*PdhR/P_{lldP} (pEA027) mediated a significant increase in the reporter gene expression after both L- and D-lactate inducer addition in *P. putida* KT2400 (Fig. 3.8b). These systems also showed induction in *C. necator* H16. *Pf*PdhR/P_{LctP} system activated by L- and D-lactate, 7-fold and 14-fold, respectively, and *Pl*PdhR/P_{LctP} system activated 6-fold and 12-fold, by L- and D-lactate, respectively, in *C. necator* H16 (Fig. 3.8b).

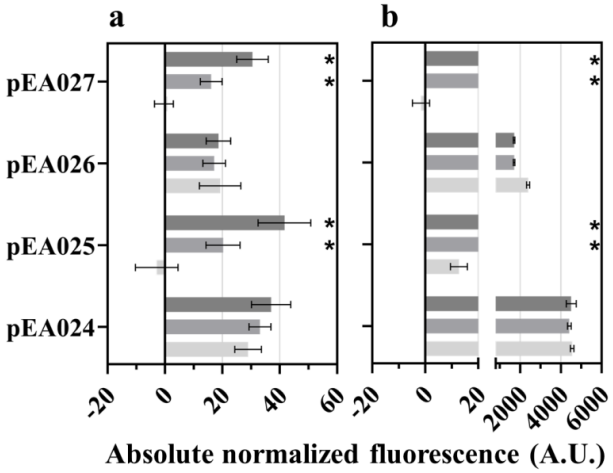

Fig. 3.8. Broad-host-range applicability of lactic acid inducible systems. Inducible systems *Pf*PdhR/P_{lldP} and *Pl*PdhR/P_{lldP} from *P. fluorescens* NCTC 10038 and *P. lactis* DSM 29167, respectively, mediate controllable gene expression in *C. necator* H16 and *P. putida* KT2440. Single time-point fluorescence measurements of **(a)** *C. necator* H16 and **(b)** *P. putida* KT2440 carrying the *Pf*PdhR/P_{lldP} and *Pl*PdhR/P_{lldP}-inducible gene expression systems composed of 'promoter only' (pEA024 and pEA026 constructs, respectively) and TF and promoter (pEA025 and pEA027 constructs, respectively). RFP fluorescence output was determined in the absence of an inducer (light gray) and 12 h after extracellular supplementation with L-lactate (medium gray) and D-lactate (dark gray) to a final concentration of 5 mM. Data is presented as mean ± SD, n = 3, *p ≤ 0.01 (unpaired *t*-test). This figure was used in[172]

3.2. Phenolic Acid-inducible Gene Expression Systems for Biosensors Development

In this work, it was chosen to characterize *Ec*MhpR/P_{mhpA}, *Ab*HcaR/$P_{ACIAD\_RS07960}$, *Bm*HcaR/$P_{NP80\_RS03060}$, *Pp*HcaR/$P_{PP\_RS17495}$, and *La*HcrR/P_{hcrA} inducible systems potentially induced by hydroxycinnamic acids. Part of the results discussed in this Subsection *3.2* is included in the article "Transcription factor-based biosensors for detection of naturally occurring phenolic acids" submitted to the *New BIOTECHNOLOGY* Journal.

3.2.1. Characterization of hydroxycinnamic acids-inducible gene expression systems

The bacterial degradation pathways of phenolic acids are a potential source of inducible gene expression systems. Previously, degradation of *m*-coumaric acid was described in *E. coli* MG1655[145], *C. testosteroni* TA441[178], and *R. globerulus* PWD1[179]. *m*-Coumaric acid is converted within six enzymatic reactions to acetyl-CoA in the presence of enzymes encoded by the *mhp*ABCDEF gene cluster (Fig. 1.7). Torres and colleagues demonstrated that MhpR TF binds to the P_{mhpA} and activates *mhp* cluster gene transcription[145].

The degradation pathways of other hydroxycinnamates, including caffeic acid, *p*-coumaric acid, and ferulic acid, were described in *A. baylyi* ADP1 and *P. fluorescens* BF13 (Fig. 1.7) and showed that HcaR TF belonging to the MarR TF family acts as a repressor, but this repression is initialized not by hydroxycinnamates, but rather by hydroxycinnamates-CoA thioesters, which are intermediate degradation compounds[143,144]. Acyl-CoA ligase encoded by the *fcs* gene and adjacent TR belonging to the MarR family were also identified in *B. multivorans* ATCC BAA-247 and *P. putida* KT2440.

Based on this knowledge, the putative *m*-coumaric acid inducible system from *E. coli* MG1655, and the putative *p*-coumaric acid inducible systems from *A. baylyi* ADP1, *B. multivorans* ATCC BAA-247, and *P. putida* KT2440 were evaluated and characterized. Putative *m*-coumaric and *p*-coumaric acids inducible systems containing promoters and TFs and only promoter regions were cloned into the reporter plasmid pBRC1 and pEV052, pEV053, pEV036, pEV035, pEV038, pEV039, pEV041, and pEV040 constructs were assembled (Fig. 3.9a). The fluorescence output measurements were performed on the host cells of these systems or the same class strain cells, *A. baylyi* ADP1 (gammaproteobacterium) constructs were cloned into *P. putida* KT2440 (gammaproteobacterium), *B. multivorans* ATCC BAA-247 (betaproteobacterium) constructs were cloned into *C. necator* H16 (betaproteobacterium). *E. coli* Top10, *P. putida* KT2440, and *C. necator* H16 strains carrying the inducible systems were grown in the LB medium, and the fluorescence output of the logarithmically growing cells was quantified at 6 h and 12 h after the addition of *m*-coumaric acid or *p*-coumaric acid, respectively.

As expected, the *Ec*MhpR/P_{mhpA} (pEV052) and *Ec*P_{mhpA} (pEV053) systems were induced 224- and 220-fold by *m*-coumaric acid, respectively, and high fluorescence values were observed with the construct only with the promoter due to the presence of TF in *E. coli* chromosomal DNA.

a

Coumaric acid	Origin	Regulator	Inducible system	Construct
m-Coumaric acid	*E. coli* MG1655	MhpR	*Ec*P$_{mhpA}$	pEV053
			*Ec*MhpR/P$_{mhpA}$	pEV052
p-Coumaric acid	*A. baylyi* ADP1	HcaR	*Ab*P$_{ACIAD_RS07960}$	pEV036
			*Ab*HcaR/P$_{ACIAD_RS07960}$	pEV035
p-Coumaric acid	*B. multivorans* ATCC BAA-247	HcaR	*Bm*P$_{NP80_RS03060}$	pEV038
			*Bm*HcaR/P$_{NP80_RS03060}$	pEV039
p-Coumaric acid	*P. putida* KT2440	HcaR	*Pp*P$_{PP_RS17495}$	pEV041
			*Pp*HcaR/P$_{PP_RS17495}$	pEV040

b

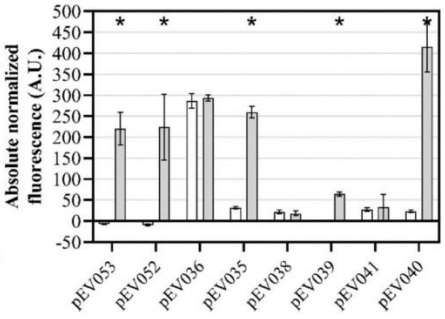

Fig. 3.9. Quantitative evaluation of coumaric acids inducible systems. **(a)** Summary of the identified inducible systems, including the system inducer, origin, TF name, and the corresponding plasmid identifiers. **(b)** Single time-point RFP fluorescence measurements were taken 6 h (in the case of pEV053 and pEV052) or 12 h (in the case of pEV036, pEV035, pEV038, pEV039, pEV041, and pEV040) after coumaric acid addition. RFP fluorescence output was determined in the absence of an inducer (white) and extracellular supplementation with the corresponding coumaric acid (light gray) to a final concentration of 5mM. Data is presented as mean ± SD, n = 3, $*p < 0.001$, unpaired two-tailed *t*-test

Table 3.2. Parameters of coumaric acids-inducible systems

Inducible system (construct)	Application host	Inducer	Dynamic range, in - fold	K_m (mM)	Hill coefficient
*Ec*MhpR/P$_{mhpA}$ (pEV052)	*E. coli* Top10	*m*-coumaric acid	223.9 ± 78.3	1.535 ± 0.064	1.53 ± 0.10
*Ab*HcaR/P$_{ACIAD_RS07960}$ (pEV035)	*P. putida* KT2440	*p*-coumaric acid	8.3 ± 1.1	1.527 ± 0.758	0.68 ± 0.07
*Bm*HcaR/P$_{NP80_RS03060}$ (pEV039)	*C. necator* H16	*p*-coumaric acid	64.6 ± 5.1	1.178 ± 0.179	2.65 ± 0.55
*Pp*HcaR/P$_{PP_RS17495}$ (pEV040)	*P. putida* KT2440	*p*-coumaric acid	16.2 ± 2.4	1.098 ± 0.173	2.22 ± 0.20

Data is presented as mean ± SD, n = 3.

The inducible systems *Ab*HcaR/P$_{ACIAD_RS07960}$ (pEV035), *Bm*HcaR/P$_{NP80_RS03060}$ (pEV039), and *Pp*HcaR/P$_{PP_RS17495}$ (pEA040) are regulated by HcaR belonging to the MarR TFs family. However, although the structural genes encoding acyl-CoA ligase have a high homology (with an identity of more than 80%) between these three bacteria, their TF homology does not reach 50% identity. Differences between TF activities are also revealed by fluorescence measurements, where *Ab*HcaR acts as a repressor, and the promoter only version construct (pEV036) mediated approximately 9-fold higher RFP synthesis in *P. putida* in comparison to the system composed of the TR and promoter (pEV035) in uninduced samples (Fig. 3.9b). Meanwhile, *Bm*HcaR

and *Pp*HcaR TFs potentially act as activators and promoter only version constructs pEV038 and pEV041, respectively, and RFP synthesis is less than 50 A.U. The *Ab*HcaR/P$_{ACIAD_RS07960}$ (pEV035), *Bm*HcaR/P$_{NP80_RS03060}$ (pEV039), and *Pp*HcaR/P$_{PP_RS17495}$ (pEA040) systems were induced 8-, 65- and 415-fold by *p*-coumaric acid at 12 h, respectively. The delayed induction is potentially related to *p*-coumaroyl-CoA acting as a systemic inducer, as previously described in the *Ab*HcaR/P$_{ACIAD_RS07960}$ system[144].

*Ec*MhpR/P$_{mhpA}$ (pEV052), *Ab*HcaR/P$_{ACIAD_RS07960}$ (pEV035), *Bm*HcaR/P$_{NP80_RS03060}$ (pEV039), and *Pp*HcaR/P$_{PP_RS17495}$ (pEA040)-inducible systems were evaluated for a dose-response by using *m*-coumaric acid or *p*-coumaric acids between 0 and 5 mM (Fig. 3.10). 5 mM concentration of the inducer usually saturates the systems. The parameters of coumaric acids-inducible systems are provided in Table 3.2. Coumaric acid-inducible systems have high K_m values (above 1 mM) and behave more like an on/off switch. The *Ec*MhpR/P$_{mhpA}$ (pEV052) system has a high dynamic range (about 224-fold), and its gene expression can be tuned over the range of 156 μM–1.25 mM. The inducible systems *Ab*HcaR/P$_{ACIAD_RS07960}$ (pEV035), *Bm*HcaR/P$_{NP80_RS03060}$ (pEV039), and *Pp*HcaR/P$_{PP_RS17495}$ (pEA040) showed a similar affinity to *p*-coumaric acid, and the gene expressions of these systems can be tuned in the range of 159 μM–2.5 mM.

*Ec*MhpR/P$_{mhpA}$ (pEV052), *Ab*HcaR/P$_{ACIAD_RS07960}$ (pEV035), *Bm*HcaR/P$_{NP80_RS03060}$ (pEV039), and *Pp*HcaR/P$_{PP_RS17495}$ (pEA040) inducible systems were tested with 21 different phenolic acids for the determination of system specificity. The *Ec*MhpR/P$_{mhpA}$ (pEV052) inducible system was statistically significantly induced only with *m*-coumaric acid of the tested phenolic acids (Fig. 3.11a). The *Ab*HcaR/P$_{ACIAD_RS07960}$ (pEA035) system reporter gene expression without *p*-coumaric acid was also statistically significantly induced with ferulic and caffeic acids and demonstrated 4- and 10-fold induction, respectively (Fig. 3.11b). *Bm*HcaR/P$_{NP80_RS03060}$ (pEV039) and *Pp*HcaR/P$_{PP_RS17495}$ (pEA040) systems without *p*-coumarate were induced 53-fold and 3-fold with caffeic acid, respectively, but these systems did not show induction with ferulic acid as could be expected (Figs. 3.11c and d).

To determine if *Ec*MhpR/P$_{mhpA}$, *Ab*HcaR/P$_{ACIAD_RS07960}$, *Bm*HcaR/P$_{NP80_RS03060}$, and *Pp*HcaR/P$_{PP_RS17495}$ inducible systems can be applied outside their host strain, the systems were tested in non-host microorganisms including *E. coli* Top10, *C. necator* H16, and *P. putida* KT2440. These systems did not show induction in non-host cells (data not shown). As described previously, hydroxycinnamoyl-CoA thioesters relieve repression of the *hca*ABCDE genes by HcaR TF belonging to the MarR family [144]. Potentially, other examined systems are also induced by metabolic intermediates, but not by hydroxycinnamic acids. This is also confirmed by the delayed induction observed after 3 h in the systems host cells. Generally, RFP expression started 30–40 min after the addition of the inducer[180,181]; and, in the case of these systems, a longer period is required for RFP maturing for an additional enzymatic reaction.

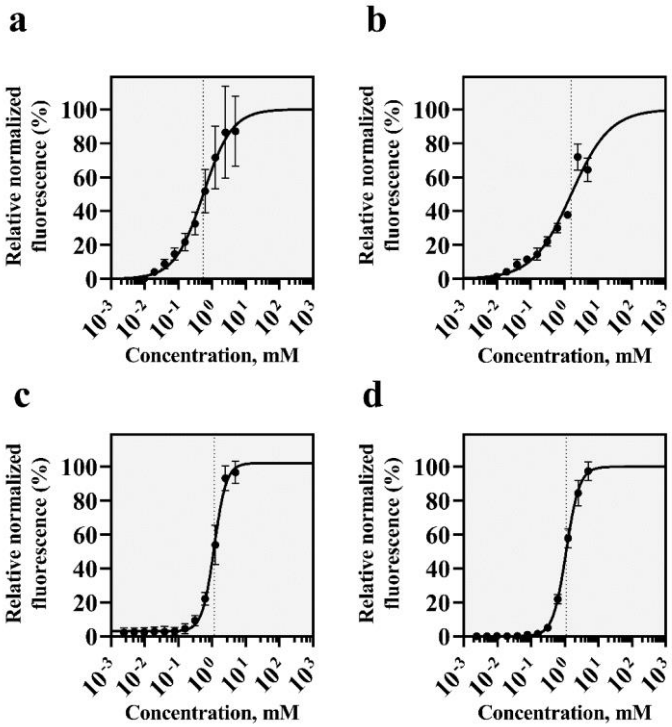

Fig. 3.10. Dose-response curves of coumaric acid-inducible systems. **(a)** Dose-response curve of *Ec*MhpR/P_{mhpA} inducible system in *E. coli* Top 10 determined in response to different concentrations of *m*-coumarate 6 h after inducer addition. Dose-response curve of **(b)** *Ab*HcaR/$P_{ACIAD\_RS07960}$ and **(d)** *Pp*HcaR/$P_{PP\_RS17495}$ inducible system in *P. putida* determined in response to different concentrations of *p*-coumaric acid 12 h after inducer addition. Dose-response curve of **(c)** *Bm*HcaR/$P_{NP80\_RS03060}$ inducible system in *C. necator* H16 determined in response to different concentrations of *p*-coumaric acid 12 h after inducer addition. The dose-response curves were fitted by using the Hill function. Data is presented as mean ± SD, n = 3

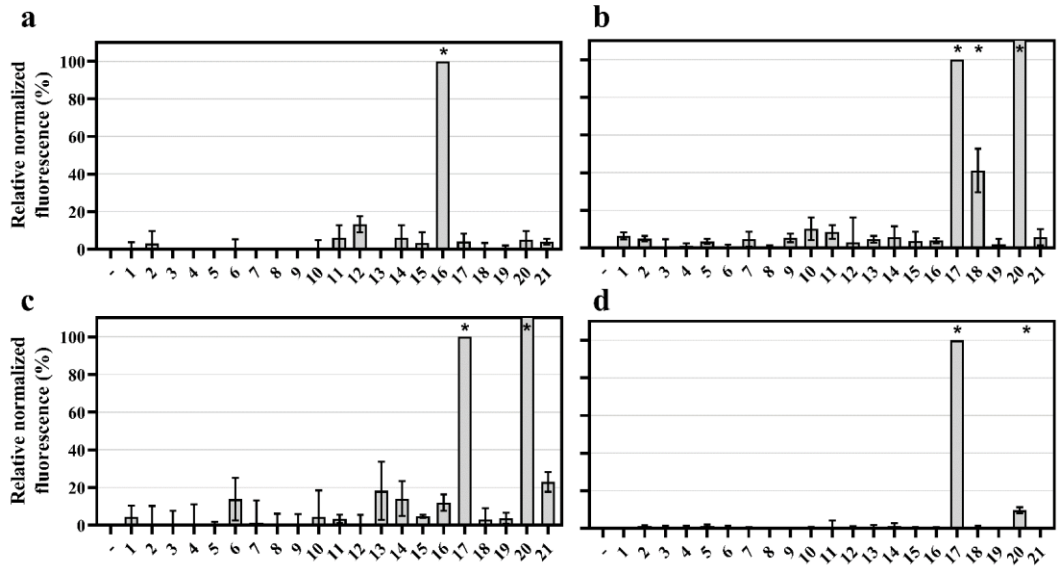

Fig. 3.11. Specificity determination of coumaric acid-inducible systems. Relative normalized fluorescence (%) of *E. coli* Top 10 harboring the **(a)** *Ec*MhpR/P_{mhpA} (pEV052) inducible system 6 h after addition of different phenolic acids at a final concentration of 5 mM relative to the fluorescence output obtained by adding 5 mM *m*-coumaric acid. Relative normalized fluorescence (%) of *P. putida* KT2440 harboring **(b)** *Ab*HcaR/$P_{ACIAD\_RS07960}$ (pEV035) and **(d)** *Pp*HcaR/$P_{PP\_RS17495}$ (pEV040), and *C. necator* H16 harboring **(c)** *Bm*HcaR/$P_{NP80\_RS03060}$ (pEV039) inducible systems 12 h after addition of different phenolic acids at a final concentration of 5 mM relative to the fluorescence output obtained by adding 5 mM *p*-coumaric acid. (-) uninduced sample. Error bars represent standard deviations of three biological replicates. Data is presented as mean ± SD, n = 3, *p ≤ 0.001 (unpaired *t*-test). The given numbers near to the columns correspond to the phenolic acids presented in Fig. 1.4: *o*-hydroxybenzoic acid (1), *m*-hydroxybenzoic acid (2), *p*-hydroxybenzoic acid (3), vanillic acid (4), isovanillic acid (5), gallic acid (6), protocatechuic acid (7), syringic acid (8), gentisic acid (9), *α*-resorcylic acid (10), *β*-resorcylic acid (11), *γ*-resorcylic acid (12), orsellinic acid (13), 6-methylsalicylic acid (14), *o*-coumaric acid (15), *m*-coumaric acid (16), *p*-coumaric acid (17), ferulic acid (18), sinapic acid (19), and caffeic acid (20)

Hydroxycinnamates can be decarboxylated and/or reduced with phenolic acid decarboxylase and hydroxycinnamate reductase in LAB. The reduction pathway has been described in several bacteria from the *Lactiplantibacillus* genus[142,182]. *hcrA* and *hcrB* genes were identified as encoding hydroxycinnamate reductase enzymes which can convert *o*-, *m*-, *p*-coumaric, ferulic, sinapic, and caffeic acids to 3-(2-hydroxyphenyl)propionic, 3-(3-hydroxyphenyl)propionic, phloretic, hydroferulic, hydrosinapic acids, and hydrocaffeic acids, respectively (Fig. 1.7).

hcrRABC operon in *L. argentoratensis* DSM 16365 was identified, and pEA048 and pEA049 constructs with only promoter P_{hcrA} and promoter P_{hcrA} with TR HcrR, respectively, were assembled. These constructs were tested in gammaproteobacteria *E. coli* Top10 (Fig. 3.12a) and *P. putida* KT2400 (Fig. 3.12c), and betaproteobacterium *C. necator* H16 (Fig. 3.12b). Analogous systems were not found in these chassis genomics DNAs when using BLAST. The response of the system *La*HcrR/P_{hcrA} (pEA049) to various hydroxycinnamic acids, including *o*-, *m*-, *p*-coumaric, ferulic, sinapic, caffeic, and chlorogenic acids, was evaluated. *La*HcrR/P_{HcrA} (pEA049) was induced approximately 1.6-fold by the tested hydroxycinnamic acids in *E. coli* Top10 (Fig. 3.12d). *La*HcrR/P_{HcrA} (pEA049) induction in *C. necator* H16 and *P. putida* KT2440 chassis produced a higher variation between different hydroxycinnamic acids. This system showed the highest 6.5-fold induction with *o*-coumaric acid in *C. necator* H16 cells, while, in *P. putida* KT2440 cells, it showed the highest 5-fold induction with *p*-coumaric acid (Fig. 3.12d). These results indicate that a hydroxycinnamates-inducible system can be investigated in three microorganisms: *E. coli* MG1655, *C. necator* H16, and *P. putida* KT2440, and this system HcrR TR acts as an activator. *La*HcrR/P_{HcrA} induction with caffeic acid was observed only in *C. necator* H16 cells. It is possible that *C. necator* H16 has a caffeic acid transport system into the cell.

Santamaría and colleagues in their publication also showed that the reduction was observed only on hydroxycinnamates, but not on cinnamic acid[142], and, therefore, HcrR TR can interact with the hydroxyl groups of hydroxycinnamates and allow transcription. Biosensor-aided discovery of lignin derivatives-degrading enzymes can expand the possibilities of lignin valorization to value-added products[7].

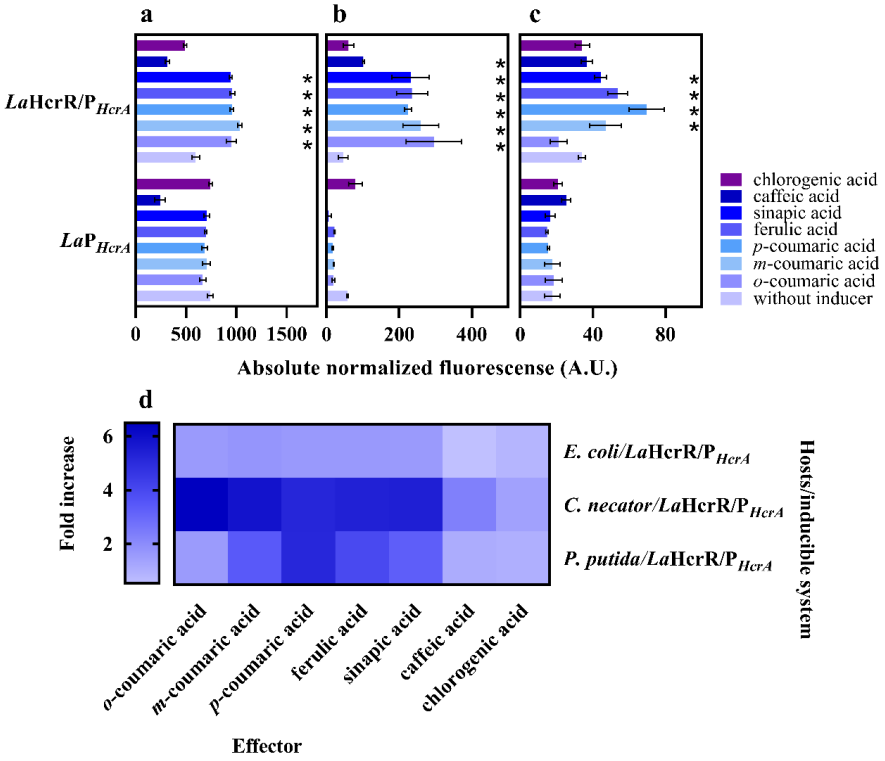

Fig. 3.12. Broad-host-range applicability of an inducible system of hydroxycinnamic acids. Absolute normalized fluorescence of *E. coli* Top10 **(a)**, *C. necator* H16 **(b)**, and *P. putida* KT2440 **(c)** harboring pEA048 with *La*P$_{HcrA}$ and pEA049 with *La*HcrR/P$_{HcrA}$. **(d)** The heat map illustrates n-fold induction between *La*HcrR/P$_{HcrA}$-inducible system and the corresponding effector. Single time-point fluorescence measurements were taken 6 h after the addition of different compounds to a final concentration of 1.25 mM. Additionally, 1 mM cysteine was added to 1.25 mM caffeic acid to slow this acid oxidation[183]. Data is presented as mean ± SD, n = 3, *p ≤ 0.001 (unpaired *t*-test)

3.3. Genetically Encoded Biosensors for Improved Optimization of L- and D-Lactic Acid Fermentation by *Lactobacillus* spp.

Optically pure L- and D-lactic acids play an important role in the production of biodegradable PLA. Alternative substrates including agricultural-food industry by-products are suitable for the cost-effectiveness production of these acids. In this study, the ability of *L. paracasei*, *L. lactis*, and *L. amylovorus* to ferment ORRF remaining after glucose syrup production were explored for the fermentation of L-, D-lactic acid, and a mixture of both, respectively. This substrate allowed the production of lactic acid without additional pretreatment and reached yields higher than 0.5 g/g. For the determination of L- and D-lactic acid optical isomers, we successfully validated previously constructed TR-based biosensors. This subsection also describes recommendations for the continuous production of D-lactic acid when using ORRF. The results confirm that the fermentation of industrial residues for the production of optically pure lactic acids is a promising avenue for the circular economy.

3.3.1. Fermentation of glucose syrup production residues by *Lactobacillus* spp. strains for lactic acid production

Glucose syrup is produced from wheat starch obtained from wheat flour. Starch solution intended for the production of syrups is liquefied and saccharified, and the resulting saccharified crude syrup is separated from the undesired by-products, for example, proteins and fatty acids via ultrafiltration processes. After ultrafiltration, proteins and fatty acids-rich undesired by-products remaining in the retentate enter the separator, where the upper phase of the by-products is separated, and the ORRF, as waste, is obtained. The initial ORRF has not only a high amount of proteins and fatty acids, but also a high concentration of glucose (207.39 g/kg). The biochemical compositions of ORRF are shown in Supplementary Table S4.

To obtain either L-lactic acid, D-lactic acid, or a mixture of both, LAB *L. paracasei*, *L. lactis*, or *L. amylovorus*, respectively, were attempted to be grown with ORRF as the sole carbon and nitrogen source; however, the growth and lactic acid production of all three LABs were extremely low compared to the MRS medium (Figs. 3.13a–c and 3.14a–c). LABs were grown in the MRS medium with 2% glucose. The production of L-, D-lactic acid and a mixture of both enantiomers and the consumption of glucose were monitored for 72 h (see Supplementary Fig. S12). *L. paracasei* and *L. amylovorus* produced L-lactic acid and a mixture of both enantiomers with a yield close to 1 g/g; then, *L. lactis* produced D-lactic acid with a yield of 0.88 g/g (see Supplementary Fig. S13).

To identify the growth limiting nutrients in ORRF, first of all, ORRF solution was supplemented with 10% MRS broth. This supplementation improved *L. paracasei*, *L. amylovorus*, and *L. lactis* growth (Fig. 3.13a–c), and the production of lactic acid increased from 38.80 ± 10.49 to 115.92 ± 13.40 mM, from 6.44 ± 3.31 to 64.96 ± 14.17 mM, and from 0 to 15.65 ± 2.46, respectively (Fig. 3.14a–c). To ascertain which component of MRS was the limiting factor in the ORRF solution, ORRF was supplemented with individual MRS broth components and their mixtures: 4 g/L of yeast extract, 8 g/L of meat extract, 1% vitamin supplement, 0.1% Tween 80, a mixture of 4 g/L of yeast extract and 8 g/L of meat extract, and a mixture of 4 g/L

of yeast extract, 8 g/L of meat extract, and 1% vitamin supplement. *L. paracasei* results showed that lactic acid production increased about 3-fold when an additional nitrogen source (yeast or meat extract) was added to ORRF (Fig. 3.14a). However, supplementation with vitamins and Tween 80 did not provide a significant increase in growth or lactic acid production in all the three strains (Fig. 3.13a–c and Fig. 3.14a–c). However, the addition of a nitrogen source in combination with Tween 80 had a positive effect on *L. amylovorus* and *L. lactis* growth and lactic acid production (Fig. 3.13e,f and Fig. 3.14e,f). The positive influence of Tween 80 on *Lactobacillus* growth had been observed previously[184,185].

To explore the optimal nitrogen source concentration for the *L. paracasei* strain, ORRF was supplemented with yeast extract from 1 to 30 g/L (Fig. 3.13d). Yeast extract was chosen as a budgetary alternative to meat extract[186]. The concentration of L-lactic acid increases when increasing the amount of the yeast extract in ORRF (Fig. 3.14d). *L. paracasei* can produce L-lactic acid from 92.58 ± 3.99 to 192.21 ± 4.26 mM. Similar results were obtained by[187], where the LAB growth and lactic acid productivity were claimed to be proportional up to a yeast extract dosage of approximately 30 g/L. However, higher levels of the yeast extract raise the total cost of lactic acid production, and, although the highest lactic acid titer can be achieved with ORWF supplemented with 30 g/L of the yeast extract, the yields ultimately remain unimproved (see Supplementary Fig. S13d).

L. amylovorus and *L. lactis* strains were grown on ORRF supplemented with 0.1% Tween 80 and with different concentrations of the yeast extract from 1 to 30 g/L. *L. amylovorus* produced from 61.84 ± 0.62 to 136.80 ± 1.98 mM of mixture of both lactic acids, while *L. lactis* produced from 13.97 ± 1.38 to 46.21 ± 0.34 of D-lactic acid, depending on the supplemented concentration of the yeast extract (Fig. 3.14e,f). The estimated yields revealed comparable results to the *L. paracasei* strain (see Supplementary Fig. S13e,f). For all three strains, the highest yield of lactic acid was obtained when ORRF was supplemented with 1 g/L of the yeast extract. The addition of the yeast extract eliminates the nitrogen deficiency in the medium and ensures the production of lactic acid. However, the optimal carbon and nitrogen ratio is essential for lactic acid production with a high yield[188].

It is important to remark that, usually, alternative substrates require additional enzymatic treatment for lactic acid production. For example, water-soluble carbohydrates remaining in sugarcane bagasse (lignocellulosic waste from the sugar industry) contain sucrose, which LAB cannot metabolize, and so it becomes necessary to hydrolyze sucrose to glucose and fructose with invertases[189]. Agricultural residues (e.g., rice straw), orange peel waste, or food waste, also require saccharification into fermentable sugars[91,95,190]. The ORRF used in this study for the production of lactic acid does not require additional enzymatic treatment because wheat starch was saccharified to glucose prior to ultrafiltration in the industrial process.

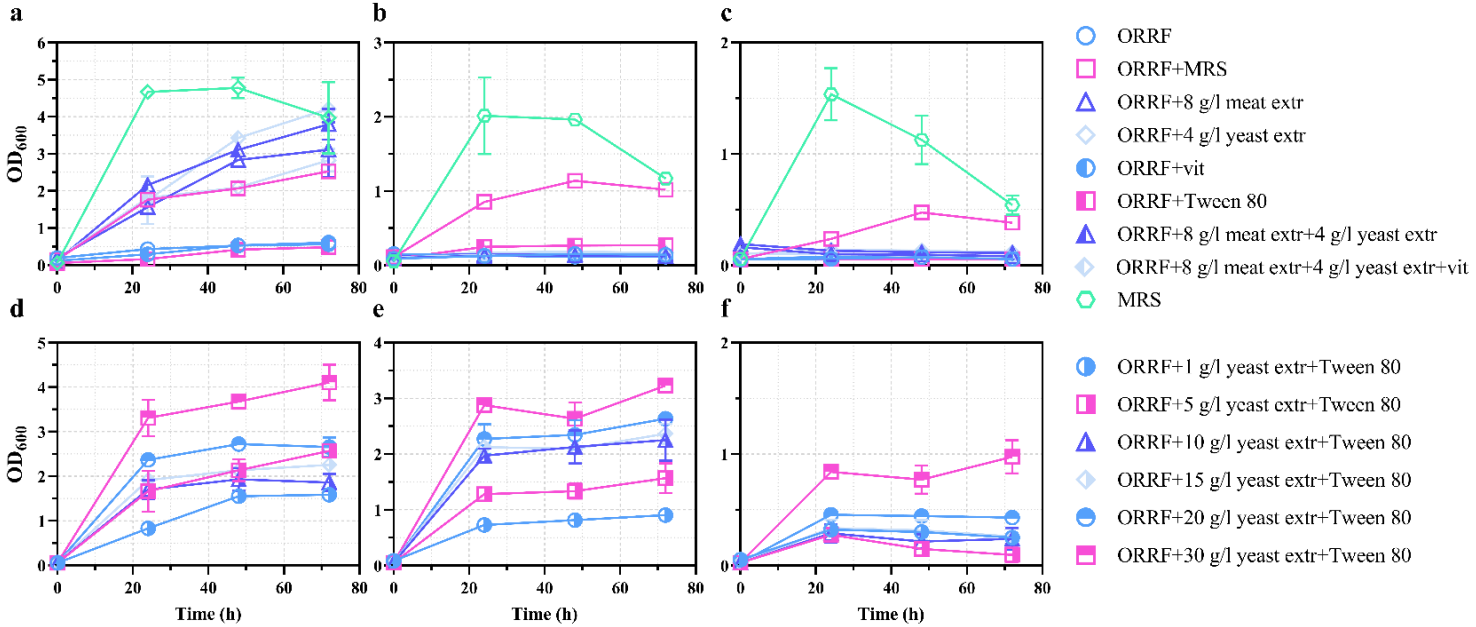

Fig. 3.13. Growth of **(a, d)** *L. paracasei*, **(b, e)** *L. amylovorus*, and **(c, f)** *L. lactis* on ORRF. Nutrient supplements are identified. Data is presented as mean ± SD, n = 2

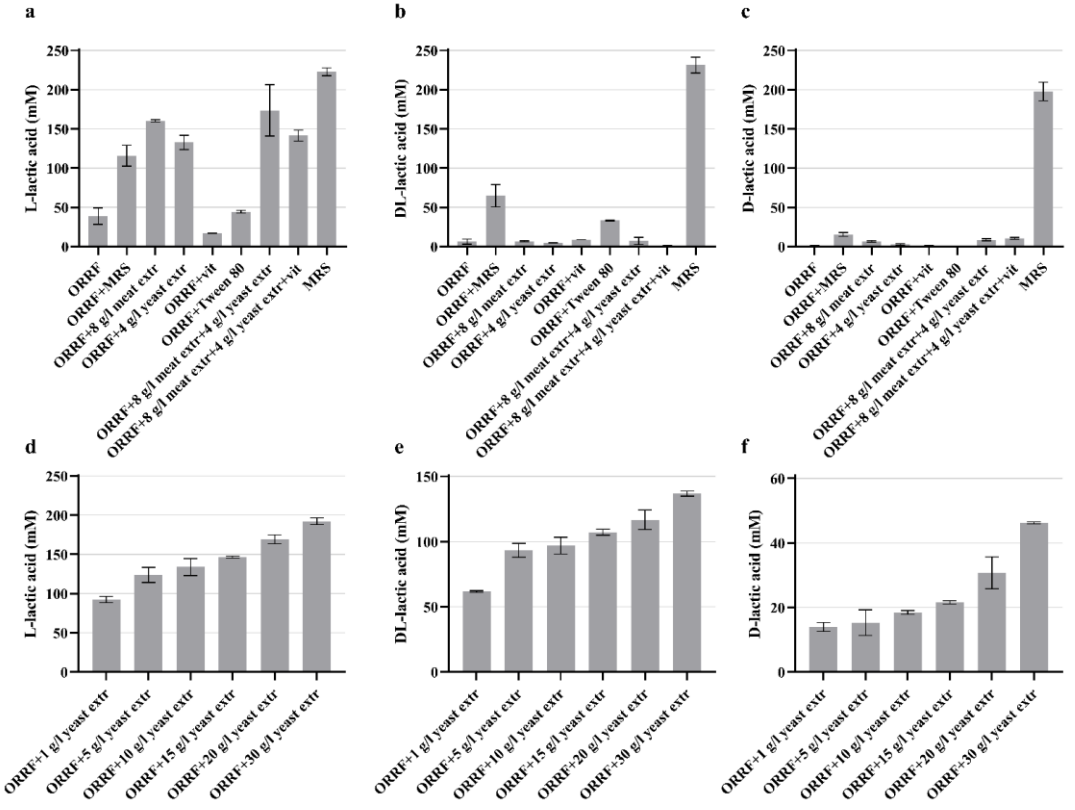

Fig. 3.14. Lactic acid concentrations (mM) produced by **(a, d)** *L. paracasei*, **(b, e)** *L. amylovorus*, and **(c, f)** *L. lactis* with ORRF (containing about 42 g/L glucose). Nutrient supplements used in lactic acid production are indicated. Data is presented as mean ± SD, n = 2

3.3.2. BLA1 and BLA2 as genetically encoded biosensors for L- and D-lactic acid determination

The ability of biosensors BLA1 (*E. coli*/*Ec*LldR/P_{lldP}; pEA015 plasmid) and BLA2 (*P. putida*/*Pf*PdhR/P_{lldP}; pEA025 plasmid) to detect the quantity of L- and D-lactic acid was tested in this thesis. BLA1 was characterized as specific for L-lactic acid and unresponsive to D-lactic acid, then BLA2 was characterized as showing a response to both L- and D-lactic acids (Fig. 3.5). LldR from *E. coli* MG1655 has a dual regulation role, because it acts as a repressor or an activator in the absence or presence of L-lactic acid, respectively (Fig. 3.15a)[108], while PdhR from *P. fluorescens* NCTC10038 acts as a repressor (Fig. 3.15b).

BLA1 and BLA2 were used for the analysis of L- and D-lactic acids in *L. paracasei* and *L. lactis* fermentations supernatant samples, respectively. For *L. amylovorus* samples, both BLA1 and BLA2 biosensors were used with additional recalculation, as described in the *Materials and Methods* Subsection *2.13*.

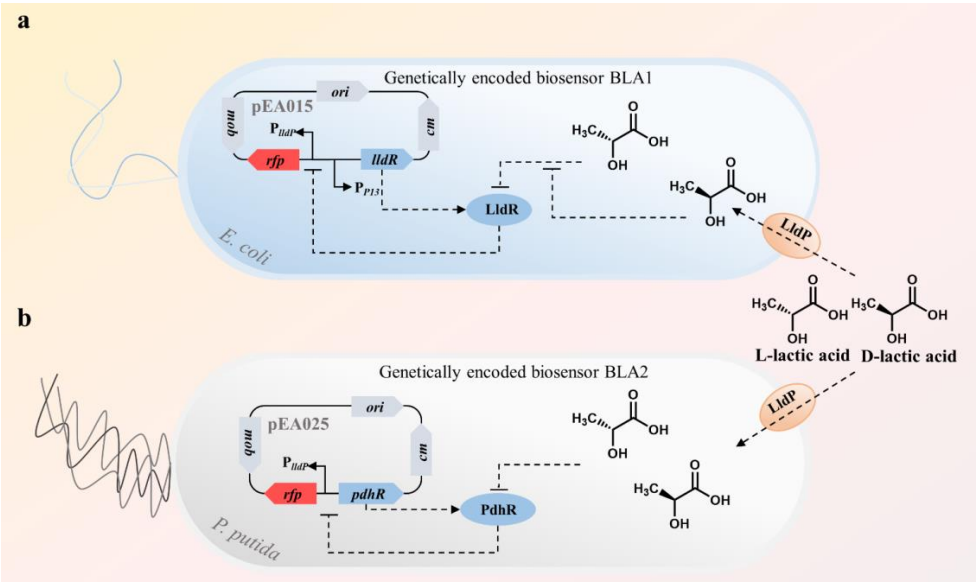

Fig. 3.15. Schematic representation of genetically encoded biosensors BLA1 **(a)** and BLA2 **(b)**

3.3.2.1. L- or D-lactic acid determination in biological sample with one of L- or D-lactic acid enantiomer and cross validation with HPLC analysis

To determine L- or D-lactic acid concentrations in *L. paracasei* and *L. lactis* fermentation supernatant samples, biosensors BLA1 and BLA2 were applied, respectively. The supernatant samples were collected during fermentation as described above at 72 h. The samples were analyzed in a 96-well plate by using a plate reader, whereas the fluorescence and absorbance were monitored over time by using biosensors BLA1 and BLA2. Standard lactic acids solutions of 0 to 20 mM were additionally tested during each analysis to construct a dose-response curve (Fig. 3.4),

as changes in the absolute normalized fluorescence and the instability of the K_m value were observed due to different cell growth rates influenced by environmental conditions. The concentrations obtained for L- and D-lactic acids in *L. paracasei* and *L. lactis* samples were compared with the results of the HPLC analysis (Fig. 3.16). The results show a fairly good correlation between both assays, with a correlation coefficient (r) of 0.84 for BLA1 (Fig. 3.16a) and 0.89 for BLA2 (Fig. 3.16b).

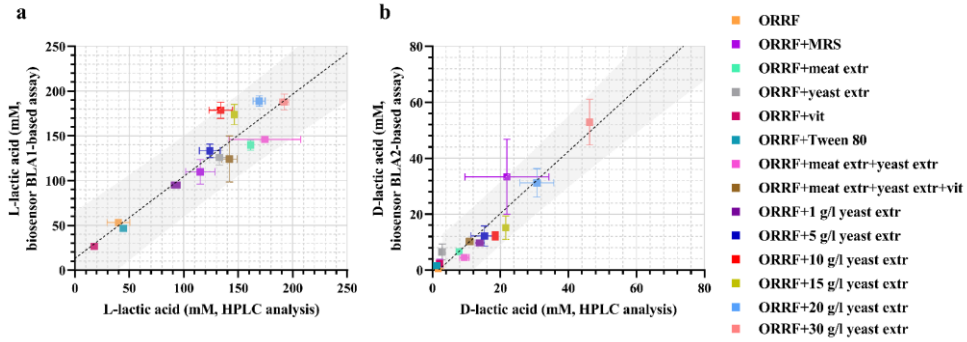

Fig. 3.16. Linear regression (black dotted line) analysis of the correlation between the HPLC analytical method **(a, b)** and whole-cells BLA1 **(a)** and BLA2 **(b)** biosensors. Linear regression analysis was performed to find the 95% prediction interval (gray area). L- and D-lactic acid values were obtained by testing *L. paracasei* **(a)** and *L. lactis* **(b)** 72 h fermentation supernatant samples, respectively. The substrate compositions of the tested samples are indicated. Data is presented as mean ± SD, n = 2

3.3.2.2. L- and D-lactic acid determination in biological sample with a mixture of lactic acid enantiomers and cross validation with enzyme-based analytical method

The quantification of L- and D-lactic acids in a racemic mixture requires methods based on chiral chromatography[191]. As an alternative, expensive L-and D-lactate dehydrogenase enzyme-based analytical methods can be used. In this work, the quantification of L- and D-lactic acid enantiomers in *L. amylovorus* samples with a racemic lactic acid mixture was completed, and it consisted of 3-step analysis. First, the total concentration of DL-lactic acids was determined with the BLA2 biosensor. Second, the concentrations of L-lactic acid in the mixtures were determined with the biosensor BLA1, while considering the inhibitory effect of D-lactic acid on fluorescence. Finally, the concentration of D-lactic acid in the mixture was calculated by subtracting the concentration of L-lactic acid from the total concentration of DL-lactic acids. The obtained values of L- and D-lactic acids were compared with the enzymatic D-/L-lactic acid assay kit method values (Fig. 3.17 and Fig. 3.18a).

A challenge was encountered in determining the concentration of L-lactic acid in the samples with a mixture of L- and D-lactic acids when using the biosensor BLA1. The inhibitory effect of D-lactic acid on the BLA1 biosensor was evaluated by testing different concentration mixtures of L-lactic acid and D-lactic acid (Fig. 3.7). To prevent the impact of the inhibitory effect on the accuracy of the estimation of L-lactic acid, the *L. amylovorus* fermentation sample was diluted to approximately 7 mM of

the total lactic acid with approximately 3 to 4 mM of D-lactic acid. This approach allowed reducing the inhibitory effect of D-lactic acid on the fluorescence output of the biosensor BLA1 (see Supplementary Fig. S14).

The obtained concentrations of L-lactic acids (with the biosensor BLA1) were compared with the results of the enzymatic analysis (Fig. 3.17a). The results show a very good correlation between both assays (r= 0.95). The correlation between the total concentration of DL-lactic acid obtained with the BLA2 biosensor and the enzymatic method was also good (r= 0.98), but the results obtained with the BLA2 biosensor were shifted towards higher concentrations (Fig. 3.17b). The recalculated concentrations of D-lactic acid by using the values obtained with biosensors were also shifted toward higher concentrations, and the correlation between these methods was lower (r= 0.84) (Fig. 3.18a). To better visualize the difference between the two groups of the data, Bland–Altman comparison plots[171] were further prepared (Fig. 3.18b), thereby providing the percentage difference of all the measurements obtained by the two analytical methods. D-lactic acid concentrations mean difference between the standard enzymatic method and the biosensors method was -24% with a 95% limit of agreement ranging from 70% to 117%. In addition, the Bland–Altman plot showed that 1/7 (< 13%) of the points were outside of the 95% limits of agreement, thus indicating the consistency between two methods once again (Fig. 3.18b).

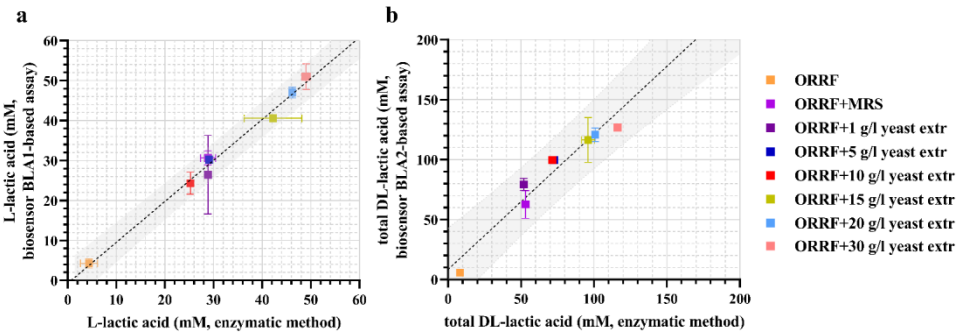

Fig. 3.17. Linear regression analysis (black dotted line) of the correlation between the enzymatic method **(a, b)** and the genetically encoded biosensors BLA1 **(a)** and BLA2 **(b)**. Linear regression analysis was performed to find the 95% prediction interval (gray area). The L-lactic acid and he total DL-lactic acid values were obtained by testing *L. amylovorus* 72 h fermentation supernatant samples, respectively. Compositions of substrates are indicated. Data is presented as mean ± SD, n = 2

The main advantage of the TF-based biosensors BLA1 and BLA2 is the ability to detect L- and D-lactic acid in samples with both enantiomers of lactic acid with sufficient accuracy, high performance, and a relatively low cost. Moreover, the detection limit of these biosensors is at the µmol level, which is similar to HPLC[23] and the enzymatic method; exclusively, the Förster resonance energy transfer (FRET)-based biosensor and LC-MS have a lower detection limit[192,193] (Table 1.1). According to calculations by Goers and colleagues (2017), genetically encoded biosensors are a significantly cheaper method (by about 30 times) compared to the commercial enzymatic method[33], and, as is known, complex equipment and

prohibitively expensive columns are required for the analysis of lactic acid enantiomers with HPLC or LC-MS[24].

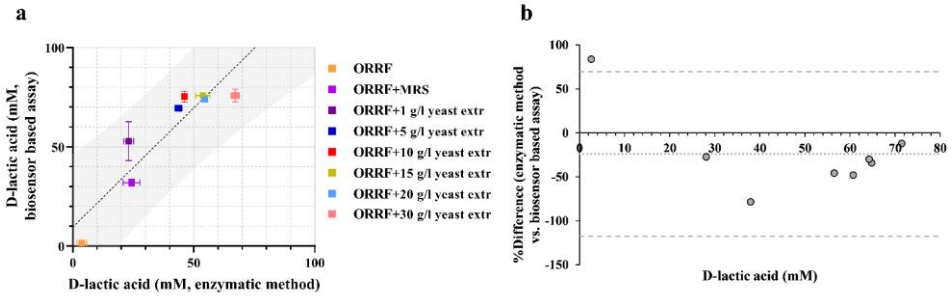

Fig. 3.18. (a) Regression analysis (black dotted line) of the correlation between the enzymatic method and the genetically encoded biosensors. Linear regression analysis was performed to find the 95% prediction interval (gray area). The D-lactic acid values were obtained by testing *L. amylovorus* fermentation supernatants with biosensors BLA1 and BLA2 and obtained with recalculation. Substrate compositions of the tested samples are indicated. Data is presented as mean ± SD, n = 2. **(b)** Bland–Altman comparison plot (n=8), showing the correlation between the biosensor and the commercial enzymatic method, determined D-lactic acid concentrations in *L. amylovorus* fermentation samples. The difference is plotted against average values, and the 95% limits of agreement (thick dashed lines) of the difference between the two methods of measurement are shown, as is the bias line (fine dashed lines)

3.3.2.3. BLA2 biosensor for rapid determination of optimal medium composition

Although the studies of optically pure L- and D-lactic acid fermentation using low-cost agro-industrial residues had been conducted previously, efficient production of D-lactic acid still remains a bottleneck[94]. The optimization of the medium formulation containing ORRF for the efficient production of D-lactic acid by *L. lactis* was described. The optimization of the medium formulation is accomplished by using a genetically encoded biosensor BLA2 as a rapid and high-throughput alternative to the traditional analytical methods. The previous results showed that *L. lactis* produces D-lactic acid by using ORRF as a carbon source supplemented with Tween 80 and yeast extract. However, ORRF supplementation with different concentrations of yeast extract from 1 g/L to 30 g/L did not improve the yields of D-lactic acid. 1 g/L of yeast extract resulted in a higher Cmol/Cmol yield than that in the medium supplemented with an increased yeast extract concentration (see Supplementary Fig. S13f). To optimize the formulation of the media, 27 different media supplemented with three different concentrations of ORRF, yeast extract, and Tween 80 were tested (see Supplementary Table S5). This cultivation experiment was performed with two replicates in a 96-well plate for 72 h, and the concentration of D-lactic acid was immediately determined with a plate reader by transferring the samples to a new 96-well plate with a BLA2 biosensor. A schematic representation of the experiment is presented in Fig. 3.19a. The results showed that the highest specific yields of D-lactic acid close to 0.22 were obtained by using 200 or 100 g/L of ORRF supplemented with 0.0625 g/L of the yeast extract and 0.025% or 0.00625% of Tween 80 (Fig. 3.19b).

Of the three Tween 80 concentrations tested, the highest concentration of D-lactic acid (about 11 mM) was obtained with 0.025% (see Supplementary Table S5).

This experiment showed that the genetically encoded biosensor platform can be a great tool for determining the optimal media composition for bacterial strains, thus allowing 96 different media compositions to be tested in a single trial. In addition, the biosensors BLA1 and BLA2 could be used in analogous studies in the selection of lactic acid producers, thereby contributing to the design-build-test-learn cycle[26,192].

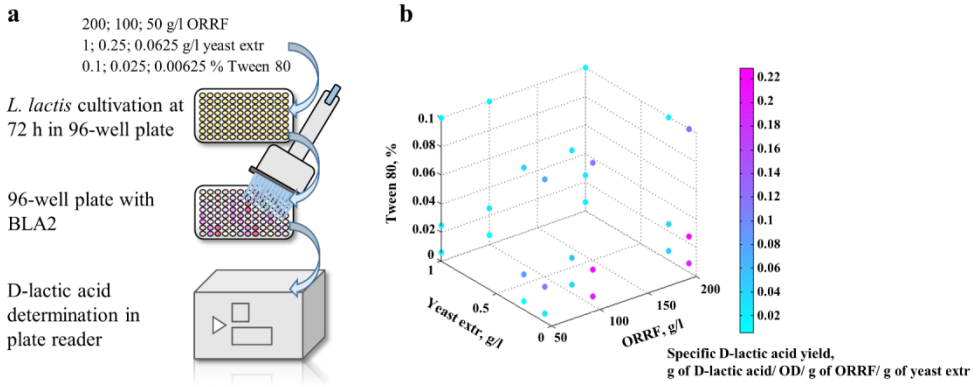

Fig. 3.19. (a) Flowchart of the experiment for the optimization of the medium formulation. **(b)** Interaction between the specific yield of D-lactic acid and the concentrations of Tween 80, yeast extract, and ORRF

3.3.3. Recommendations for continuous D-lactic acid fermentation with *L. lactis* by using glucose syrup production residues

This section describes recommendations for improving the D-lactic acid production by incorporating genetically encoded biosensors and a continuous fermentation strategy. As shown above, *L. lactis* can produce optically pure D-lactic acid when using ORRF supplemented with yeast extract and Tween 80. As a recommendation for an improved D-lactic acid production with ORRF by *L. lactis*, a process flow diagram with the basic information for the continuous production of D-lactic acid is presented (Fig. 3.20). The list of equipment included in the scheme with explanations is presented in Table 3.3. This diagram includes four parts: (i) determination of nutritional requirements (an additional step before fermentation), (ii) fermentation, (iii) downstream process for product recovery, and (iv) quantification of D-lactic acid.

In this work, in Subsection *3.3.2.3*, it was already established that the highest yield of D-lactic acid is obtained when using 200 g/L of ORRF supplemented with 0.0625 g/L of yeast extract and 0.025% of Tween 80 (Fig. 3.19b). Before pilot-scale continuous fermentation, rapid fermentation optimization can be performed. Search for a sustainable alternative and an inexpensive nitrogen source can be prepared with the genetically encoded biosensor BLA2. The yeast extract is the traditional source of nitrogen, but it can account for up to 38% of the total cost of lactic acid production [65]. Agricultural residues including: corn steep liquor[195], malt rootlets and soybean meal[85],

hydrolyzed rapeseed meal[196], cottonseed[197], and peanut meal[198] can replace expensive nitrogen sources. 96 different conditions can be tested for the cultivation of *L. lactic* when using the ORRF solution as a carbon source supplemented with alternative nitrogen sources in a 96-well plate. The D-lactic acid concentration in these samples can be measured simultaneously with the BLA2 biosensor when using a new 96-well plate with a plate reader. The selected optimal nitrogen source can be used in continuous D-lactic acid fermentation instead of the yeast extract.

L. lactis is maintained at -80°C in an ultra-low temperature freezer (F-1). Culture is transferred to an MRS agar plate (P-1) and incubated at 37 °C for 24 h. The grown cells are transferred to a sterile centrifuge tube (CT-1) with MRS broth and incubated at 37 °C for 24 h, without shaking. For the inoculum, the cell culture is transferred to culture flasks (CF-1) with sterile MRS broth and cultured at 37 °C without shaking. After 24 h of cultivation, cells are harvested by centrifugation (C-1) and washed twice. An inoculation size of 10% (v/v) is manually transferred to the bioreactor (B-1). A solution of ORRF is prepared with water at a ratio of 1:5 and left at 37 °C for 1 h with a shaking rate of 200 rpm in a T-1 tank. After shaking, the ORRF solution is sterilized in an autoclave (A-1), and centrifuged (C-2) to remove insoluble particles; then, the residue enters the waste stream, and the supernatant is stored in tank (T-2) and enters the blender (BL-1) through the peristaltic pump (P-1). The sterile nitrogen source and the salt solution are stored in T-3 and T-4, respectively, and they enter the blender (BL-1) through the peristaltic pumps (P-2 and P-3), where they are mixed with the ORRF solution. The 100 L bioreactor (B-1) (BR500-M1 microbial fermentator (*Labfirst Scientific Instruments*, China)) is supplemented with ORRF, nitrogen source, and a salt solution through a peristaltic pump (P-4); the pump flow rate is 1.6 L/min.

A bioreactor (B-1) connected to a membrane module (UF-1, NF-1, and IEX-1) is used for the continuous fermentation of D-lactic acid. In the bioreactor (B-1), the pH, the temperature, and the liquid level are monitored by using sensors (a, b, c). The temperature in the bioreactor is maintained at 37 °C by using a thermal jacket. Oxygen supply to the reactor and stirring (aeration) are not required because the *L. lactis* strain is microaerophilic, and bacteria cannot survive in an environment where the concentration of oxygen is high[199]. An included recirculation flow will return the unconsumed nutrients, for example, glucose, to the bioreactor (B-1). Cell suspension from the bioreactor (B-1) is pumped (P-5) into the ultrafiltration module (UF-1), where the D-lactic acid extraction processes begin. The peristaltic pump flow rate is 0.8 L/min. The ultrafiltration membrane (UF-1) separates and recycles the *L. lactis* cells to the bioreactor (B-1), while simultaneously removing D-lactic acid.

Efficient separation and purification processes are crucial in the industrial production of lactic acid[200]. The main purpose of the separation and purification methods is to isolate the substances from the fermentation medium (organic components (glucose, proteins, lipids), inorganic components (residual salt ions and water), and microbes)), and to obtain the highest purity of lactic acid. The downstream processes of lactic acid employ various purification techniques. Purification can be divided into the primary separation process (sedimentation, centrifugation, filtration), the preliminary purification (precipitation, distillation, membrane separation, liquid-liquid extraction, conventional filtration), and the further purification (ion-exchange

chromatography, evaporation, crystallization, reverse osmosis) [201,202,203,204]. Until now, calcium precipitation for the primary recovery has been the most common method for organic acid separation, but this method is costly and environmentally unfavorable because large amounts of gypsum are generated[201]. Reactive extraction is also not one of the most acceptable separation methods. Extraction is performed by using petroleum-based organic solvents, such as octanol, butanol, decanol, and ethanol. However, these solvents involve many problems, are toxic to LAB, are denoted by low process safety, and are problematic during the solvent regeneration process [203]. In recent years, reactive distillation, molecular distillation, membrane processes, and chromatography have become more widespread so that to avoid the disadvantages of the traditional separation processes [205,206,207,208]. Ion exchange is most commonly used to obtain pure lactic acid. It is selective, and it provides product recovery in a short period of time[209]. However, the ion exchange process requires the regeneration of ion exchange resin and the adjustment of the feed pH to increase the sorption, and the efficiency of the process requires a large amount of chemicals[210]. The emulsion liquid membrane-based separation technique is one of the most attractive methods for separating lactic acid from aqueous solutions with high extraction efficiency, and it is also denoted by low energy, and chemical consumption[205,208].

This process flow diagram shows the integrated membrane processes for lactic acid purification based on[211]. The integrated membrane separation process consists of ultrafiltration (UF-1), nanofiltration (NF-1), ion exchange (IEX-1 and IEX-1), and vacuum-assisted evaporation (VE-1). First, the cell suspension enters the ultrafiltration membrane (UF-1) by using a peristaltic pump (P-5) with 20 L/h of water flux, where bacterial cells are separated, and the remaining cells in the retentate are recycled to the bioreactor (B-1). The supernatant enters the nanofiltration membrane (NF-1) by using a peristaltic pump (P-6) with a 1 L/h water flux, where glucose is efficiently separated from lactic acid due to the difference in the molecular weights. The remaining glucose in the retentate is returned to the bioreactor (B-1). Residual monovalent inorganic ions present in the supernatant are removed by using an ion exchange resin (IEX-1). Finally, vacuum evaporation (VE-1) is used to concentrate D-lactic acid. High purity D-lactic acid (potentially >99%) is stored in the T-3 tank. Samples for lactic acid determination can be collected by using manual valves (V-2, V-3, and V-4). The yield of D-lactic acid during batch fermentation was approximately 0.5 Cmol/Cmol of glucose, and potentially the yield should increase further in continuous fermentation with recirculation flow. The concentration of D-lactic acid can be achieved up to 90 g/l during continuous fermentation, as per reference [212].

Table 3.3. Equipment used in the process flow diagram (Fig. 3.20).

Symbol	Equipment
F-1	-80 °C ultra-low temperature freezer
P-1	petri dish
CT-1	centrifuge tube with MRS broth
C-1, C-2	centrifuge
CF-1	culture flask
T-1, T-2, T-3	tank
A-1	autoclave
P-1, P-2, P-3, P-4, P-5, P-6, P-7	peristaltic pumps
V-1, V-2, V-3, V-4, V-5, V-6	manual valve
VA-1, VA-2, VA-3, VA-4, VA-5	valve
B-1	bioreactor (100 L)
UF-1	ultrafiltration membrane
NF-1	nanofiltration membrane
IEX-1	ion exchange resin
VE-1	vacuum evaporator
BL-1	blender (feed tank)
RO-1, RO-2	rotameter
PG-1, PG-2	pressure gauge
FD-1	flow distributor
a	pH probe
b	temperature probe
c	level sensor

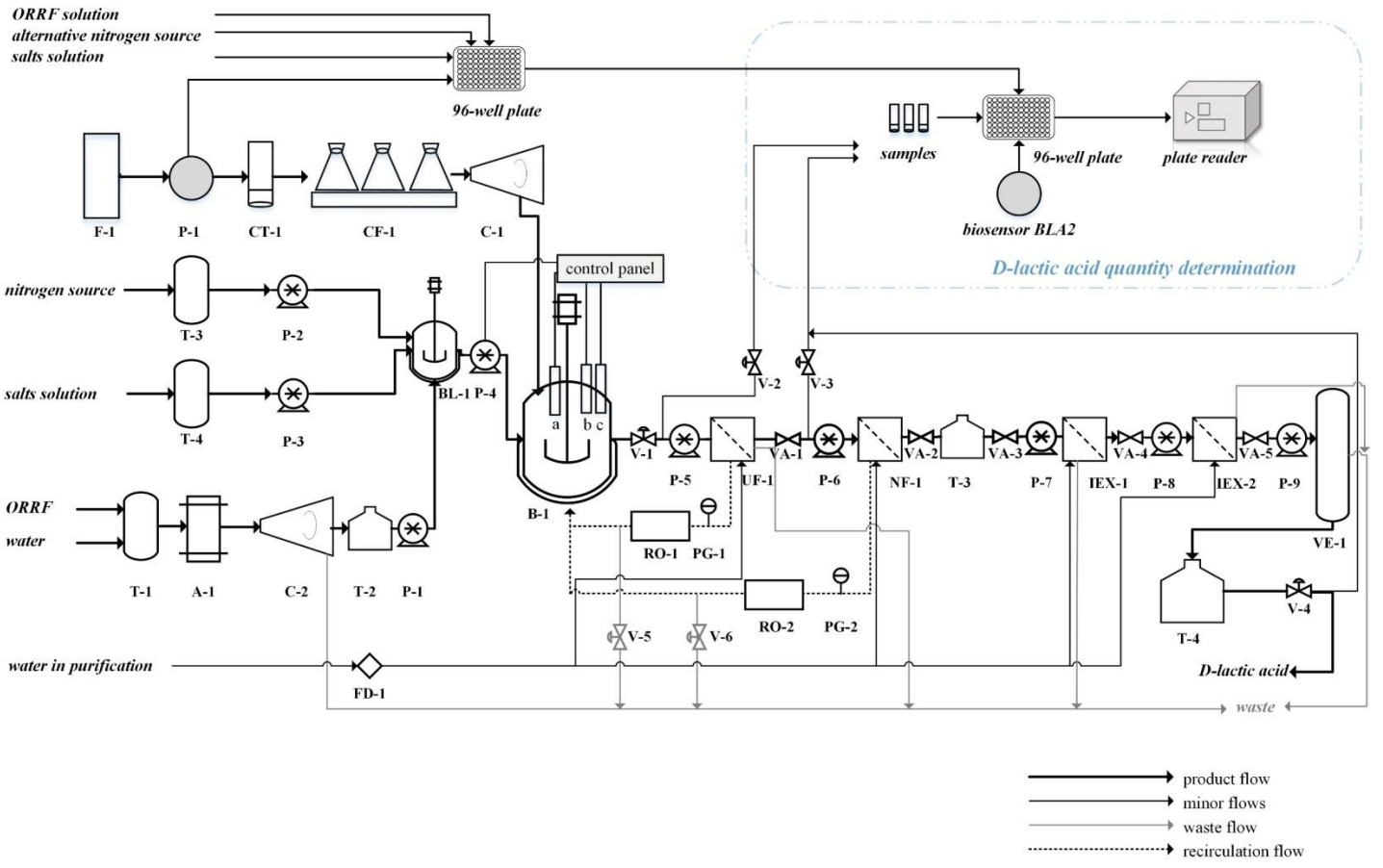

Fig. 3.20. Process flow diagram with basic information on the continuous fermentation of D-lactic acid by *L. lactis* using ORRF as the carbon source

4. CONCLUSIONS

1. Lactic acid-inducible systems *Ec*LldR/P_{lldP} and *Cn*GntR/$P_{H16\_RS19190}$ identified in the *E. coli* MG1655 and *C. necator* H16 genomes are specific for L-lactic acid, and their gene expression can be tuned in the ranges of 9 μM-1 mM and 80 μM-1 mM, respectively. Lactic acid-inducible systems *Pa*PdhR/P_{lldP}, *Pl*PdhR/P_{lldP}, and *Pf*PdhR/P_{lldP} identified in *Pseudomonas* spp. have similar affinities to L- and D-lactic acids, and their gene expression can be tuned in the range of 9 μM and 2 mM. Neither of the identified lactic acid-inducible systems from *E. coli* MG1655, *C. necator* H16, or *Pseudomonas* spp. responded solely to D-lactic acid.
2. The inducible system *Ec*MhpR/P_{mhpA} identified in *E. coli* MG1655 is specific for *m*-coumaric acid, and its gene expression can be tuned in the range of 156 μM and 1.25 mM. Inducible systems *Ab*HcaR/$P_{ACIAD\_RS07960}$, *Bm*HcaR/$P_{NP80\_RS03060}$, and *Pp*HcaR/$P_{PP\_RS17495}$ identified in *A. baylyi* ADP1, *B. multivorans* ATCC BAA-247, and *P. putida* KT2440 have a similar affinity for *p*-coumaric acid, and the gene expressions of these systems can be tuned in the range of 159 μM and 2.5 mM. The *Ab*HcaR/$P_{ACIAD\_RS07960}$ inducible system is also induced with ferulic and caffeic acids, whereas the *Bm*HcaR/$P_{NP80\_RS03060}$ and *Pp*HcaR/$P_{PP\_RS17495}$ systems without *p*-coumarate are induced with caffeic acid. The inducible system *La*HcrR/P_{HcrA} from *L. argentoratensis* DSM 16365 responds to several hydroxycinnamic acids, including *o*-coumaric, *m*-coumaric, *p*-coumaric, ferulic, and sinapic acids, and it has broad-host-range applicability in *E. coli*, *C. necator*, and *P. putida* chassis.
3. The inducible systems *Ec*LldR/P_{lldP} and *Pf*PdhR/P_{lldP} adapted as genetically encoded biosensors BLA1 and BLA2, respectively, have been validated as a rapid and high-throughput method for the determination of L- and D-lactic acids in biological samples.
4. A biosensor BLA2-based strategy to improve the optimization of D-lactic acid fermentation media with ORRF as a carbon source for *L. lactis* has been demonstrated, and the optimal medium formulation consisted of 200 g/L or 100 g/L ORRF supplemented with 0.0625 g/L of yeast extract and 0.00625% of Tween 80.

5. SANTRAUKA

5.1. ĮVADAS

Sintetinė biologija pirmą kartą buvo paminėta XX a. pradžioje mokslininko Stephano Leduco knygoje ir apibrėžta: „...arba mes sėkmingai kontroliuojame gyvybės reiškinį tiek, kad galime sukelti tą patį, kada tik norime, <...> arba mums pavyksta nustatyti skaitinį ryšį tarp eksperimentinės sąlygos ir biologinio rezultato“ (1). Taigi sintetinė biologija apima naujų biologinių sistemų kūrimą arba jau esamų transformavimą naudingais tikslais. Mikroorganizmai, įskaitant bakterijas, turi jutimo ir reguliavimo prietaisus, pagrįstus transkripcijos reguliatoriais (TR), kurie gali suaktyvinti genų ekspresiją reaguodami į metabolitų koncentracijų pokyčius (2). Viena iš sintetinės biologijos krypčių yra genetiškai užkoduotų biojutiklių, paremtų indukuojamomis genų ekspresijos sistemomis ir susidedančių iš TR ir gimininingų indukuojamų promotorių, kūrimas (3). Genetiškai užkoduoti biojutikliai pritaikomi kaip didelio našumo analizės metodai, siekiant suprasti genų ekspresijos valdymo mechanizmus. Būsimos programos apima jutiklių naudojimą intraląstelinių ir ekstraląstelinių metabolitų koncentracijoms stebėti, aukšto našumo atrankai, greitai kamienų evoliucijai, dinamiškai kelių kontrolei ir kryptingai laboratorinei evoliucijai (4,5,6). Genetiškai užkoduoti biojutikliai, skirti mažoms molekulėms nustatyti, suteikia galimybę susieti metabolitų koncentraciją su susijusio mikroorganizmo fenotipu (5,7).

Organinės rūgštys, įskaitant L- ir D-pieno rūgštis, yra svarbūs junginiai, naudojami įvairių medžiagų sintezei, tarp jų ir biologiškai skaidžių plastikų gamyboje, šie polimerai gali pakeisti tradicinius naftos pagrindu pagamintus plastikus (8,9). JAV Energetikos departamentas pieno rūgštį įvardijo kaip vieną iš 10 svarbiausių didelės vertės žaliųjų cheminių medžiagų (10). Literatūroje gausu pavyzdžių, aprašančių L- ir D-pieno rūgšties gamybą, pagrindinis šių rūgščių gamintojas yra pieno rūgšties bakterijos (PRB), pasiekiančios 1 g/g išeigą naudojant tradicinius substratus (11,12,13,14,15,16). Nors keletas sėkmingų tyrimų, naudojant lignoceliuliozės atliekas, žemės ūkio ir maisto pramonės likučius, buvo atlikti, tačiau optiškai grynų L- ir D-pieno rūgščių gamyba, naudojant šiuos alternatyvius substratus, išlieka iššūkiu. Fenolinės rūgštys yra antioksidantai, pasižymintys antimikrobiniu aktyvumu, paprastai naudojami farmacijos, kosmetikos ir chemijos pramonėje. Be to, fenolinės rūgštys gali būti pirmtakai kitų aukštos pridėtinės vertės junginių gamyboje, pavyzdžiui, katecholio, vanilino, mukono, adipino rūgščių ir kitų (17). Natūraliai hidroksicinamono rūgštis gali gaminti keletas bakterijų ir grybelių rūšių, tačiau kol kas yra pasiekiamos tik mažos išeigos, ir dažnai šie junginiai yra tarpiniai metabolinių reakcijų produktai (18). Pagrindinis efektyvios fenolinių rūgščių gamybos kelias yra genetiškai modifikuotų kamienų kūrimas.

Pieno rūgščių ir hidroksicinamono rūgščių fermentacija naudojant mikroorganizmus turi pranašumo lyginant su kitais gamybos metodais. Fermentacija nereikalauja organinių tirpiklių, brangių pirmtakų ar šiurkščių reakcijų sąlygų, be to, tik optiškai grynos L- ir D-pieno rūgštys gali būti gaunamos šio proceso metu. Mikroorganizmų ląstelių gamykloms yra reikalingi bakterijų kamienai, kurie gali naudoti ne tik tradicinius gliukoze papildytus substratus, bet taip pat ir nebrangias ne

maisto alternatyvas (glicerolį, lignoceliuliozę ar įvairų pramonių likučius). Alternatyvių substratų, tokių kaip žemės ūkio ir maisto pramonės atliekos, pavertimas į aukštos pridėtinės vertės medžiagas ne tik užtikrina efektyvią šių medžiagų gamybą, bet taip pat yra neatsiejama žiedinės ekonomikos dalis (19). Be to, mikroorganizmų priskyrimas atitinkamiems substratams reikalauja plačios kamienų paieškos arba genetiškai modifikuotų mikroorganizmų, efektyviai naudojančių žemės ūkio ir maisto pramonės atliekų sudedamąsias dalis ir išliekančių gyvybingų esant inhibitoriams, susidariusiems lignoceliuliozės apdorojimo metu, išvystymo.

Kamienų paieškai, vystymui, nebrangių ne maisto substratų pritaikymui reikalingi greiti ir didelio našumo analitiniai metodai. Tradiciniai analitiniai metodai, tokie kaip efektyvioji skysčių chromatografija (ESCh), skysčių chromatografija-masių spektrofotometrija ir komerciniai fermentiniai metodai, nors yra tikslūs ir plačiai taikomi, yra gana mažo našumo, brangūs ir reikalaujantys daug laiko, todėl naudinga būtų naudoti genetiškai užkoduotus biojutiklius, kurie gali aplenkti šiuos paminėtus trūkumus. Biojutikliai leidžia greitą kelių tūkstančių variantų charakterizavimą per trumpą laiką, todėl gali būti naudojami atrenkant mikroorganizmų kamienus ir jiems pritaikytus substratus efektyviai pieno ir hidroksicinamono rūgščių gamybai (20).

Šio darbo tikslas yra identifikuoti ir išvystyti pieno rūgštimis ir natūraliai aptinkamomis hidroksicinamono rūgštimis indukuojamas genų ekspresijos sistemas.

Šiam tikslui pasiekti buvo išsikelti šie uždaviniai:

1. Identifikuoti ir charakterizuoti L- ir D-pieno rūgštimis indukuojamas genų ekspresijos sistemas, aptiktas *E. coli* MG1655, *C. necator* H16 ir *Pseudomonas* spp. genomuose;
2. Identifikuoti ir charakterizuoti hidroksicinamono rūgštimis indukuojamas genų ekspresijos sistemas, aptiktas *E. coli* MG1655, *A. baylyi* ADP1, *B. multivorans* ATCC BAA-247, *P. putida* KT2440 ir *L. argentoratensis* DSM 16365 genomuose;
3. Išvystyti genetiškai užkoduotus biojutiklius BLA1, specifinį L-pieno rūgščiai, ir BLA2, indukuojamą L- ir D-pieno rūgštimis, ir palyginti jų veikimą su kitais analizės metodais;
4. Pritaikyti BLA2 genetiškai užkoduotą biojutiklį terpės sudėties optimizavimui su gliukozės sirupo gamybos likučiais, skirtą D-pieno rūgšties fermentacijai su *L. lactis*.

Mokslinio darbo naujumas

Apibūdintos ir detalizuotos identifikuotos L- ir D-pieno rūgščių indukuojamos sistemos, parodyta jų kinetika, dinaminis intervalas, specifiškumas ir pritaikymo galimybės skirtingų šeimininkų ląstelėse. Sistemų mechanizmų išaiškinimas leidžia suprasti genų funkcijas ir genų ekspresijos ir baltymų sintezės reguliavimą įvairiuose bakterijų kamienuose esant intraląsteliniams ir ekstraląsteliniams aplinkos pokyčiams. Pirmą kartą pastebėtos ir charakterizuotos pieno rūgštimis indukuojamos sistemos iš *C. necator* H16 ir *p*-kumaro rūgštimi indukuojama sistema iš *B. multivorans* ATCC BAA-247, be to, parodytas indukuojamos sistemos iš *L.*

argentoratensis DSM 16365 atsakas į kelias hidrokcinamono rūgštis skirtingų šeimininkų ląstelėse. Optiškai grynos L- ir D-pieno rūgštys ir jų mišinys buvo pagamintas su *Lactobacillus* spp., naudojant atliekas, likusias gliukozės sirupo gamybos metu. Pirmą kartą genetiškai užkoduoti BLA1 ir BLA2 biojutikliai pritaikyti nustatant L- ir D-pieno rūgštis biologiniuose mėginiuose su vienu pieno rūgšties enantiomeru ir su jų mišiniu, ši strategija patvirtinta tradiciniais analitiniais metodais. Be to, buvo parodytas greitas ir didelio našumo metodas, skirtas auginimo terpės sudėčiai optimizuoti naudojant alternatyvų anglies šaltinį.

Praktinė darbo vertė

Genetiškai užkoduoti biojutikliai, paremti indukuojamomis genų ekspresijos sistemomis, yra svarbus įrankis aukštos pridėtinės vertės junginių gamybai naudojant mikroorganizmus. Jie leidžia kontroliuoti natūralius, heterologinius genus ir biosintetinius kelius, taip pat tinka didelio našumo kamienų atrankai. Sukurti pieno rūgštimi indukuojami biojutikliai leidžia pakankamai tiksliai, efektyviai ir palyginti su mažomis sąnaudomis aptikti L- ir D-pieno rūgštį raceminiuose mišiniuose. Genetiškai užkoduoti biojutikliai gali būti puiki priemonė nustatant optimalią terpės sudėtį su gliukozės sirupo pramonės likučiais, kad būtų pagerinta L- ir D-pieno rūgšties fermentacija su *Lactobacillus* spp. Aukštos pridėtinės vertės cheminių medžiagų gamyba iš atsinaujinančių bioišteklių gali sumažinti neigiamą įprastų chemijos gamyklų poveikį ir išeikvotų naftos išteklių keliamus iššūkius.

Ginamieji disertacijos teiginiai

1. Pieno rūgštimis indukuojamos genų ekspresijos sistemos, identifikuotos *E. coli* MG1655, *C. necator* H16 ir *Pseudomonas* spp., panaudotos genetiškai užkoduotiems biojutikliams konstruoti, o išvystyti biojutikliai pritaikyti L- ir D-pieno rūgštims nustatyti biologiniuose mėginiuose su vienu L- arba D-pieno rūgšties enantiomeru arba su jų mišiniu.
2. Hidroksicinamono rūgštimis indukuojamos genų ekspresijos sistemos, identifikuotos *E. coli* MG1655, *A. baylyi* ADP1, *B. multivorans* ATCC BAA-247, *P. putida* KT2440 ir *L. argentoratensis* DSM 16365, pritaikytos genetiškai užkoduotiems biojutikliams vystyti.

Darbo aprobavimas ir publikavimas

Disertacijos darbo tema paskelbtos 3 mokslinės publikacijos recenzuojamuose mokslo leidiniuose „Web of Science" duomenų bazėje, indeksuotose leidiniuose su cituojamumo rodikliu (JCR SCIE). Disertacijos darbo tema įteiktos 2 mokslinės publikacijos recenzuojamuose mokslo leidiniuose „Web of Science" duomenų bazėje, indeksuotose leidiniuose su cituojamumo rodikliu (JCR SCIE). Darbo rezultatai pristatyti 4 tarptautinėse mokslinėse konferencijose.

Autorės ir bendraautorių mokslinis indėlis

Autorė sukonstravo ir charakterizavo genetiškai užkoduotus biojutiklius. Naglis Malys konsultavo dėl eksperimento eigos ir rezultatų analizės. Naglis Malys ir Kęstutis Baltakys konsultavo rankraščio rengimo eigos klausimais. Edita Mažonienė

ir Jurgita Kailiuvienė pateikė ir išanalizavo gliukozės sirupo gamybos atliekų sudėtį. Planuojant eksperimentus, susijusius su pieno rūgšties fermentacija, konsultavo Ilona Jonuškienė. Michailas Syrpas patarė dėl ESCh analizės.

Disertacijos struktūra

Disertaciją sudaro įvadas, literatūros apžvalga, rezultatai kartu su diskusija, medžiagos ir metodai, išvados, naudotos literatūros sąrašas, publikacijų disertacijos tema sąrašas ir papildoma informacija. Naudotos literatūros sąrašas apima 234 šaltinius, pagrindiniai rezultatai yra aptarti 152 puslapių, iliustruoti 21 lentelėje ir 27 paveiksluose. Papildoma informacija apima 7 lenteles ir 14 paveikslų.

5.2. MEDŽIAGOS IR METODAI

Potencialūs genų klasteriai, atsakingi už organinių ir fenolinių rūgščių metabolizmą, buvo rasti naudojantis literatūra ir GenBank duomenų baze (prieinama: https://www.ncbi.nlm.nih.gov/) (152). Prieinama informacija apie katabolinius kelius buvo analizuota KEGG kelių duomenų bazėje (prieinamoje: www.genome.jp/kegg/pathway.html) (153) ir BRENDA duomenų bazėje (prieinamoje: www.brenda-enzymes.org) (154). Tikslinių genų koduojamų baltymų homologija nustatyta naudojant BLAST (prieinama: https://blast.ncbi.nlm.nih.gov/Blast.cgi).

Fluorescencijos matavimai buvo atlikti naudojant Infinite M200 PRO („Tecan“, Austrija) mikroplokštelių skaitytuvą. 142,5 µl ląstelių kultūros ir 7,5 µl pasirinkto induktoriaus buvo pridėta į kiekvieną 96 plokštelės šulinėlį („Corning Incorporated“, USA arba „Thermo Scientific“, JAV). Raudonai fluorescuojančio baltymo (RFB) fluorescencija ir absorbcija buvo kiekybiškai įvertintos 15–20 val. ir jų vertės buvo pakoreguotos atitinkamai pagal terpės be ląstelių autofluorescenciją ir autoabsorbciją.

Absoliučiosios normalizuotos fluorescencijos vertės (*ANF*), gautos naudojant induktorius, apskaičiuotos pagal (148), naudojantis (5.2.1) formule:

$$ANF = \frac{FL_{mėginys} - FL_{terpė}}{OD_{mėginys} - OD_{terpė}}; \quad (5.2.1)$$

čia $FL_{mėginys}$ yra mėginio RFB fluorescencija, $FL_{terpė}$ yra terpės RFB fluorescencija, $OD_{mėginys}$ yra mėginio optinis tankis, $OD_{terpė}$ yra terpės optinis tankis.

Siekiant nustatyti sistemos parametrus, *ANF* vertės buvo nubrėžtos kaip induktoriaus koncentracijos funkcija naudojant GraphPad Prism 8 („GraphPad Software, Inc.“, JAV) ir netiesinis mažiausių kvadratų metodas pritaikytas naudojant Hillo funkciją (5.2.2) (113).

$$ANF = b_{max} \times \frac{I^h}{K_m^h + I^h} + b_{min}; \quad (5.2.2)$$

čia b_{max} yra didžiausias RFB sintezės greitis, b_{min} yra bazinis RFB sintezės lygis, I yra induktoriaus koncentracija, h yra Hillo koeficientas, K_m yra induktoriaus koncentracija, lygi pusei didžiausios reporterio išvesties.

Indukcija kartais arba dinaminis intervalas buvo apskaičiuoti padalijus indukuoto mėginio *ANF* vertę iš neindukuoto mėginio *ANF* vertės. Reliatyviosios normalizuotos fluorescencijos vertės santykiniais vienetais (snt. vnt.) buvo gautos atėmus neindukuotų ląstelių *ANF* vertes iš indukuotų ląstelių *ANF* verčių. Reliatyviosios normalizuotos fluorescencijos vertės (%) buvo apskaičiuotos naudojant *ANF* vertes esant tam tikrai induktoriaus koncentracijai pagal (5.2.3) formulę:

$$Reliatyvi\ normalizuota\ fluorescencija\ (\%) = 100 \times \left(\frac{ANF - b_{min}}{b_{max}}\right). \quad (5.2.3)$$

L- ir D-pieno rūgščių ir jų mišinio fermentacija buvo atlikta atitinkamai naudojant *L. paracasei*, *L. lactis* ir *L. amylovorus* kamienus. Daug organinių medžiagų turinti likutinė frakcija (ORRF), gauta iš sucukrinto kviečių krakmolo tirpalo gaminant gliukozės sirupą, buvo tiriama kaip galimas substratas pieno rūgšties

gamybai. Pramonėje krakmolo tirpalas yra skystinamas ir cukrinamas su alfa-amilazėmis ir gliukoamilazėmis ir gautas neapdorotas sirupas filtruojamas naudojant 30 nm porų dydžio filtrus. Taip gaunamas retentate likęs daug baltymų ir riebalų turintis nepageidaujamas šalutinis produktas. Šis šalutinis produktas patenka į specialų separatorių, kur yra atskiriamas jo viršutinis sluoksnis, šiame darbe vadinamas ORRF, kuris patenka į atliekas. ORRF buvo gautas iš „Roquette Amilina“ (Lietuva). Fermentacijai ORRF tirpalas buvo paruoštas ištirpinant tirpias daleles distiliuotame vandenyje, kurio pradinė koncentracija buvo 250 g/L, tirpalas inkubuotas 1 val. 37 °C 200 aps/min. Po inkubacijos, mišinys sterilintas autoklave 125 °C esant 1,5 atm slėgiui 15 min. ir centrifuguotas 11000 aps/min 5 min. Pašalintos vandenyje netirpios medžiagos, taip prarandant dalį baltymų ir riebalų. Likęs supernatantas surinktas, praskiestas iki 200 g/L koncentracijos ir naudotas bakterijoms auginti. ORRF tirpalas 200 g/L koncentracijos turi maždaug 42 g/L gliukozės.

BLA1 (paremtas *E. coli*/*Ec*LldR/P_{lldP} sistema, pEA015 konstruktu) ir BLA2 (paremtas *P. putida*/*Pf*PdhR/P_{lldP} sistema, pEA025 konstruktu) biojutikliai buvo naudoti L- ir D-pieno rūgščių koncentracijoms nustatyti biologiniuose mėginiuose. Fermentacijos supernatantų mėginiai buvo praskiesti 5, 10, 15, 10, 20 arba 30 kartų, priklausomai nuo numatomos pieno rūgšties koncentracijos. Fluorescencijos matavimai, *ANF* ir dozes atsako kreivės skaičiavimai atlikti kaip aprašyta aukščiau.

L-pieno rūgšties koncentracija, pagaminta su *L. paracasei*, buvo nustatyta naudojant BLA1 biojutiklį, D-pieno rūgšties koncentracija, pagaminta su *L. lactis*, buvo nustatyta su BLA2 biojutikliu. *L. amylovorus* mėginiai buvo analizuoti naudojant abu BLA1 ir BLA2 biojutiklius. BLA1 naudotas L-pieno rūgšties koncentracijai nustatyti, BLA2 – bendrai pieno rūgščių koncentracijai nustatyti. D-pieno rūgšties koncentracija apskaičiuota atimant L-pieno rūgšties koncentraciją iš bendros pieno rūgščių koncentracijos.

5.3. REZULTATAI IR JŲ APTARIMAS

5.3.1. Pieno rūgštimi indukuojamos genų ekspresijos sistemos

Šiame darbe buvo identifikuoti operonai, susidedantys iš mažiausiai dviejų genų, potencialiai susijusių su pieno rūgšties suvartojimu, ir geno, koduojančio TF iš *E. coli* MG1655, *C. necator* H16 ir *Pseudomonas* spp. Į šį sąrašą taip pat buvo įtraukti su glikolio rūgšties metabolizmu susiję genų klasteriai, nes anksčiau buvo patvirtinta apie jų dalyvavimą naudojant D-pieno rūgštį (101). Identifikuoti genų klasteriai buvo sugrupuoti remiantis keliomis taisyklėmis. Pirmiausia jie buvo išskirstyti į grupes pagal fermento tipą. Šios grupės buvo padalintos į pogrupius (1, 2, 3) pagal baltymų homologiją (į vieną grupę pateko sistemos, kurių funkcinių genų identiškumas didesnis nei 40%) ir TF šeimą. I grupei buvo priskirtos FMN-priklausomos, NAD-nepriklausomos L-pieno rūgšties dehidrogenazės (L-iLDHs; EC 1.1.2.3) ir FAD-priklausomos, NAD-nepriklausomos D-pieno rūgšties dehidrogenazės (D-iLDHs; EC 1.1.2.4), II grupei priskirtos 3-komponentų Fe-S NAD-nepriklausomos pieno rūgšties dehidrogenazės (iLDHs) (174) , susidedančios iš dviejų FAD ir Fe-S rišančių domenų 109), ir III grupėje operonai, susiję su glikolio rūgšties katabolizmu (5.3.1 pav.).

Identifikuotos potencialios pieno rūgštimi indukuojamos sistemos buvo klonuotos į modulinį reporterio vektorių pBRC1, siekiant ištirti atsaką į L, D-pieno rūgštis ir glikolio rūgštį. Įvertinimui su kiekviena indukuojama sistema buvo surinkti dviejų tipu konstruktai: tik promotoriaus versija ir TF kartu su indukuojamu promotoriumi, kai TF yra nukreiptas priešinga kryptimi nei RFB. Fluorescencijos išvesties matavimai buvo atlikti sistemų šeimininkų ląstelėse, išskyrus sistemas iš *P. aeruginosa* PAO1, *P. fluorescens* NCTC 10038 ir *P. lactis* DSM 29167, šie konstruktai buvo klonuoti į *P. putida* KT2440 ląsteles (5.3.2 pav.).

E. coli DH5α, *C. necator* H16, *P. putida* KT2440 kamienai, turintys indukuojamas sistemas, buvo auginti minimalioje terpėje, logaritmiškai augančių ląstelių fluorescencijos matavimai buvo kiekybiškai įvertinti praėjus 6 valandoms po induktoriaus pridėjimo. Iš vienuolikos analizuotų potencialių pieno rūgštimi indukuojamų sistemų buvo nustatytos dvi specifinės L-pieno rūgščiai. Kaip tikėtasi, *Ec*LldR/P_{lldP} (pEA015) sistema buvo indukuota 15,9 karto su L-pieno rūgštimi. Anksčiau buvo pranešta, kad ši sistema yra indukuojama 18,6 karto su 14 mM L-pieno rūgštimi. Šio tyrimo rezultatai atitiko Goers ir kolegų publikacijos rezultatus (33).

Palygintos *Cn*GntR/$P_{H16\_RS19190}$ (pEA007), *Ec*RclR/P_{b0306} (pEA032) ir *Cn*IclR/$P_{H16\_RS06900}$ (pIE005) indukuojamos sistemos iš II grupės (5.3.1 pav.), šios sistemos yra reguliuojamos skirtingų tipų TF, ir iš 3 komponentų sudarytas iLDH baltymas turi mažesnį nei 40 % identiškumą. Tai rodo genetinę įvairovę tarp skirtingų rūšių ir skirtingus genų raiškos reguliavimo mechanizmus. *Cn*GntR/$P_{H16\_RS19190}$ (pEA007) buvo indukuojama 280,8 karto su L-pieno rūgštimi. Tai rodo, kad GntR TF šeima dalyvauja reguliuojant su L-pieno rūgštimi susijusių katabolinių genų ekspresiją *C. necator* H16. *Ec*RclR/P_{b0306} (pEA032) yra indukuojama 2 kartus su glikolio rūgštimi (5.3.2 pav.), o promotoriaus P_{b0306} ekspresija yra paveikta anglies katabolitų represijos esant gliukozei ir aktyvuojama, kai L- ir D-pieno rūgštys yra naudojamos kaip anglies šaltiniai.

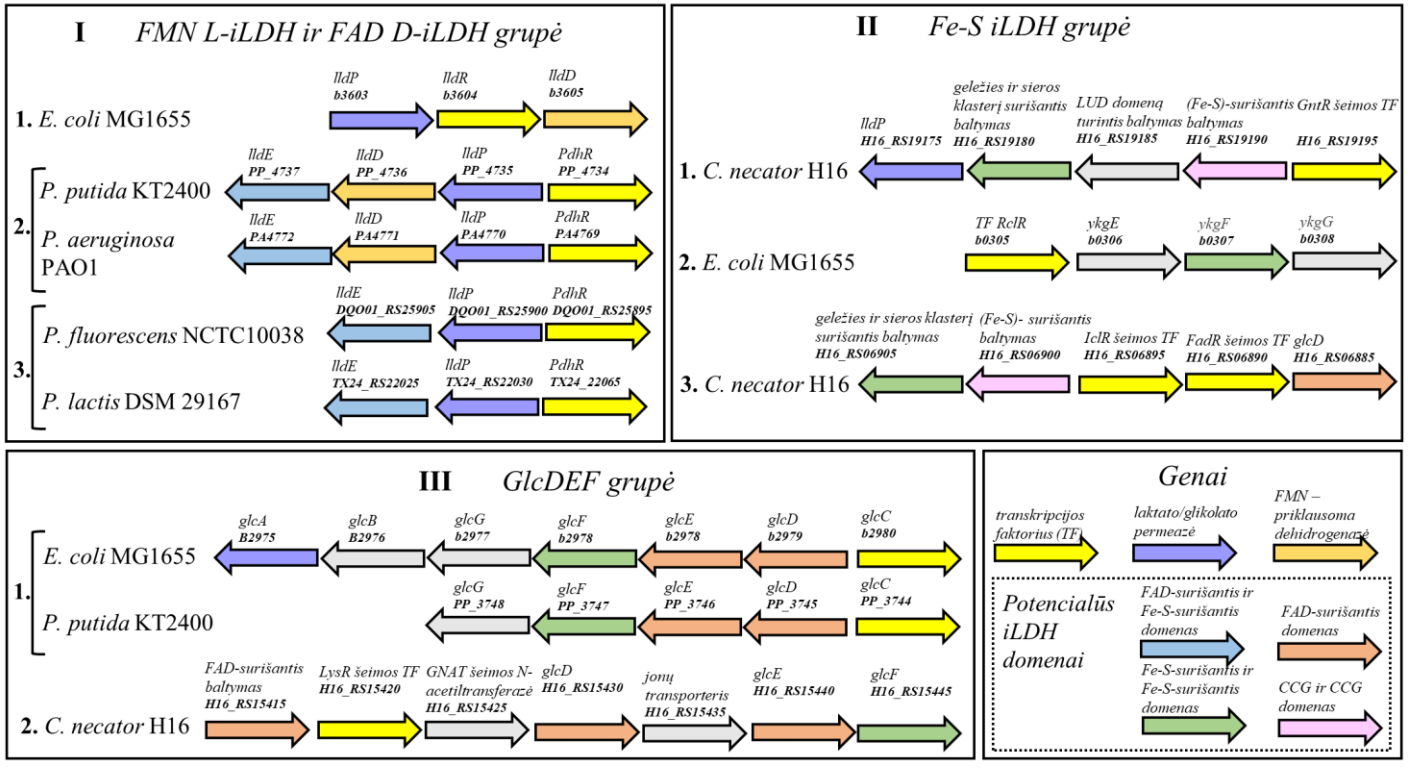

5.3.1 pav. Su pieno ir glikolio rūgšties katabolizmu susijusių genų klasterių organizacija *E. coli* MG1665, *C. necator* H16 ir *Pseudomonas* spp. Paveiksle nurodyti *lokus* žymenys, baltymų funkcijos ir baltymų domenai. Šis paveikslas buvo naudotas publikacijoje (172)

*Cn*IclR/$P_{H16\_RS06900}$ (pIE005) parodė 2 kartų indukcija su D-pieno rūgštimi ir 3 kartų indukcija su glikolio rūgštimi (5.3.2 pav.). Siekiant ištirti, ar IclR ekspresija yra slopinama duotomis sąlygomis ir ar IclR turi įtakos $P_{H16\_RS06900}$ promotoriaus aktyvacijai, IclR genas buvo kontroliuojamas stipriu sintetiniu P_{13} promotoriumi (175) ir indukuojama arabinozės sistema. Tačiau rezultatai parodė, kad IclR neturi įtakos indukuojamos sistemos *Cn*IclR/$P_{H16\_RS06900}$ atsakui į D-pieno rūgštį ir glikolio rūgštį. Šie rezultatai rodo, kad šios sistemos reguliacija nėra aiški.

III grupei priskirtos (5.3.1 pav.) *Ec*GlcC/P_{b2979} (pEA004) ir *Pp*GlcC/P_{PP_3745} (pEA012) indukuojamos sistemos parodė 4 ir 15 kartų indukciją su glikolio rūgštimi (5.3.2 pav.). Siekiant nustatyti *Cn*LysR/$P_{H16\_RS15430}$ glikolio rūgštimi indukuojamos sistemos reguliaciją, du $P_{H16\_RS15415}$ ir $P_{H16\_RS15430}$ promotorių regionai buvo įvertinti. Nustatyta, kad aukščiausios normalizuotos fluorescencijos vertės pasiekiamos, kai konstrukte yra abu $P_{H16\_RS15415}$ ir $P_{H16\_RS15430}$ promotorių regionai ir LysR TF su papildomais genais.

D-pieno rūgštimi indukuojama sistema nebuvo identifikuota *E. coli* MG1655, *C. necator* H16 ar *Pseudomonas* spp. Didžiausią potencialą turinčios *Pf*PdhR/P_{lldP} (pEA025), *Pl*PdhR/P_{lldP} (pEA027), *Pa*PdhR/P_{lldP} (pEA018) sistemos be D-pieno rūgšties taip pat buvo indukuojamos L-pieno rūgštimi. Šių sistemų TF priklauso GntR šeimai ir veikia kaip represoriai, funkcinių genų ekspresija yra aktyvuojama esant L- arba D-pieno rūgščiai (5.3.2 pav.). Indukuojama sistema *Pp*PdhR/P_{lldP} (pEA011), turinti aukštą homologiją su *Pa*PdhR/P_{lldP} (pEA018), neparodė statistiškai reikšmingos indukcijos su L- ir D-pieno rūgštimis, kai buvo auginta minimalioje terpėje su gliukoze kaip anglies šaltiniu (5.3.2 pav.). P_{lldP} promotorius iš *P. putida* galimai yra kataboliškai slopinamas, kai auginimo terpėje yra gliukozės. Kai L- ir D-pieno rūgštis buvo naudotos kaip vieninteliai anglies šaltiniai mitybinėje terpėje, *Pp*P_{lldP} (pEA010) buvo indukuojamas D-pieno rūgštimi. Šie rezultatai parodo, kad ne tik anksčiau aprašyto *lldPDE* klasterio iš *E. coli* MG1655 raiška yra susijusi su kataboliniu slopinimu, bet taip pat *ykgEFG* iš *E. coli* MG1655 ir *lldPDE* iš *P. putida* KT2440.

Pieno rūgštimi indukuojamų sistemų *Ec*LldR/P_{lldP} (pEA015), *Cn*GntR/$P_{H16\_RS19190}$ (pEA007), *Pa*PdhR/P_{lldP} (pEA018), *Pf*PdhR/P_{lldP} (pEA025), *Pl*PdhR/P_{lldP} (pEA027) dozės-atsakas buvo įvertintas naudojant L-pieno rūgšties ir / arba D-pieno rūgšties koncentracijas nuo 0 iki 5 mM (5.3.3 pav.). Abi L-pieno rūgštimi indukuojamos sistemos *Ec*LldR/P_{lldP} (pEA015) ir *Cn*GntR/$P_{H16\_RS19190}$ (pEA007) turi mažas K_m vertes (mažesnes nei 1 mM), tai rodo, kad šių sistemų indukcijai yra reikalingos mažos L-pieno rūgšties koncentracijos. *Ec*LldR/P_{lldP} (pEA015) sistemos genų raišką galima sureguliuoti 9 μM-1 mM intervale, o sistemos *Cn*GntR/$P_{H16\_RS19190}$ (pEA007) genų raišką galima sureguliuoti 80 μM-1 mM intervale. Indukuojamos sistemos *Pa*PdhR/P_{lldP} (pEA018) ir *Pf*PdhR/P_{lldP} (pEA025) parodė panašų gimiringumą su L- ir D-pieno rūgštimi, ir šių sistemų genų raiška gali būti sureguliuota 9 μM-2 mM intervale.

a

Sistemos tipas	Kilmė	Reguliatorius	Indukuojama sistema	Konstruktas
I	*E. coli* MG1655	LldR	*Ec*P$_{lldP}$	pEA016
			*Ec*LldR/P$_{lldP}$	pEA015
	P. putida KT2440	PdhR	*Pp*P$_{lldP}$	pEA010
			*Pp*PdhR/P$_{lldP}$	pEA011
	P. aeruginosa PAO1	PdhR	*Pa*P$_{lldP}$	pEA017
			*Pa*PdhR/P$_{lldP}$	pEA018
	P. fluorescens NCTC 10038	PdhR	*Pf*P$_{lldP}$	pEA024
			*Pf*PdhR/P$_{lldP}$	pEA025
	P. lactis DSM 29167	PdhR	*Pl*P$_{lldP}$	pEA026
			*Pl*PdhR/P$_{lldP}$	pEA027
II	*C. necator* H16	GntR	*Cn*P$_{H16_RS19190}$	pEA006
			*Cn*GntR/P$_{H16_RS19190}$	pEA007
	E. coli MG1655	RclR	*Ec*P$_{b0306}$	pEA005
			*Ec*RclR/P$_{b0306}$	pEA032
	C. necator H16	IclR	*Cn*P$_{H16_RS06900}$	pIE004
			*Cn*IclR/P$_{H16_RS06900}$	pIE005
III	*E. coli* MG1655	GlcC	*Ec*P$_{b2979}$	pEA003
			*Ec*GlcC/P$_{b2979}$	pEA004
	P. putida KT2440	GlcC	*Pp*P$_{PP_3745}$	pEA013
			*Pp*GlcC/P$_{PP_3745}$	pEA012
	C. necator H16	LysR	*Cn*P$_{H16_RS15430}$	pEA023
			*Cn*LysR/P$_{H16_RS15430}$	pEA021

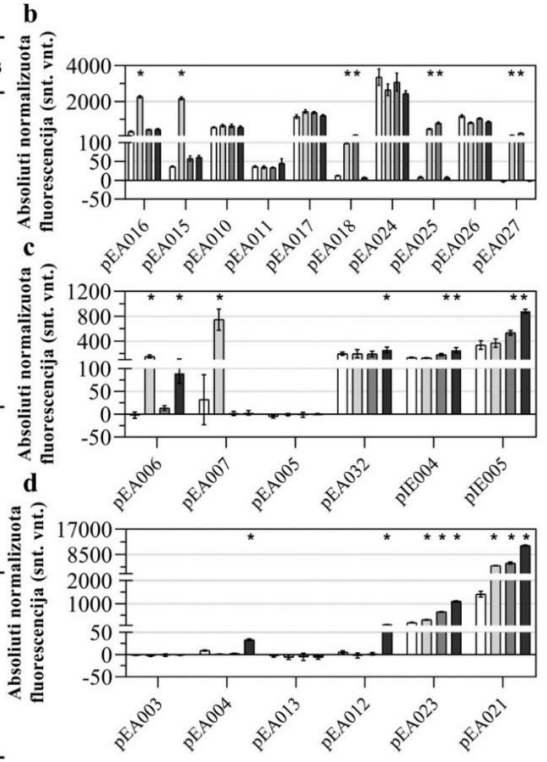

5.3.2 pav. Pieno rūgštimi indukuojamų sistemų kiekybinis įvertinimas. **(a)** Identifikuotų indukuojamų sistemų santrauka, apimanti sistemos tipą pagal 5.3.1 pav., sistemos kilmę, TF pavadinimą, indukuojamos sistemos sutrumpinimą, konstruktą. **(b)** I grupės sistemų, **(c)** II grupės sistemų ir **(d)** III grupės sistemų vieno laiko taško RFB fluorescencijos matavimai atlikti praėjus 6 val. po induktoriaus pridėjimo. RFB fluorescencijos matavimai buvo atlikti be induktoriaus (balti stulpeliai) ir papildžius su 5 mM L-laktatu (šviesiai pilki), 5 mM D-laktatu (tamsiai pilki) ir 5 mM glikoliatu (juodi). Stulpelinėse diagramose pateiktas duomenų vidurkis ir standartinis nuokrypis trijų biologinių pakartojimų, *p ≤ 0,001 (neporinis *t*-testas). Šis paveikslas buvo naudotas publikacijoje (172)

Indukuojamos sistemos *Ec*LldR/P_{lldP} (pEA015), *Cn*GntR/$P_{H16\_RS19190}$ (pEA007), *Pa*PdhR/P_{lldP} (pEA018) ir *Pf*PdhR/P_{LctP} (pEA025) specifiškumui nustatyti papildomai buvo pratestuotos su glioksilatu, 3-hidroksipropionatu ir piruvatu. Gauti rezultatai parodė, kad šios sistemos nėra indukuojamos su struktūriškai panašiais junginiais.

Siekiant įvertinti pieno rūgštimis indukuojamų sistemų pritaikomumą už šeimininkų ląstelių, *Ec*LldR/P_{lldP} (pEA015), *Pf*PdhR/P_{LctP} (pEA025) ir *Pl*PdhR/P_{LctP} (pEA027) indukuojamos sistemos buvo testuotos *C. necator* H16 ir *P. putida* KT2400 kamienuose. Vetinant rezultatus nustatyta, kad nebuvo jokio *Ec*LldR/P_{lldP} (pEA015 ir pEA033) sistemos atsako į L-pieno rūgštį, kai buvo patikrinta *C. necator* H16 ir *P. putida* KT2400 kamienuose. Tačiau indukcija buvo pastebėta, kai *lldR* TF buvo reguliuojamas arabinozės sistema (pEA033) ir *C. necator* H16 ląstelės augintos su L-laktatu kaip anglies šaltiniu. Toks *Ec*LldR/P_{lldP} sistemos reguliavimas yra susijęs su anglies katabolitų represija. O *Pf*PdhR/P_{lldP} (pEA025) ir *Pl*PdhR/P_{lldP} (pEA027) sistemos buvo indukuojamos L- ir D-pieno rūgštimis *P. putida* KT2400 ir *C. necator* H16 kamienuose.

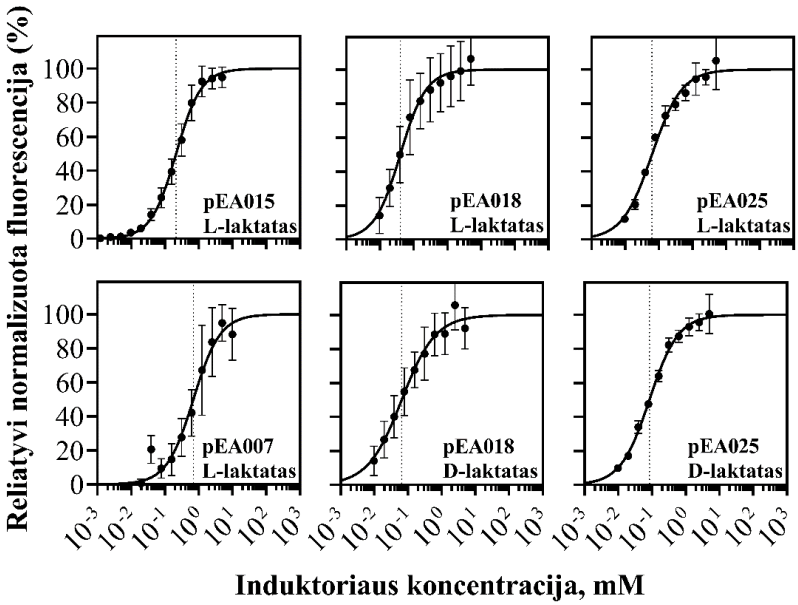

5.3.3 pav. L- ir D-pieno rūgščių indukuojamų sistemų dozės-atsako kreivės. Reliatyvi normalizuota fluorescencija *Ec*LldR/P_{lldP} (pEA015), *Cn*GntR/$P_{H16\_RS19190}$ (pEA007), *Pa*PdhR/P_{lldP} (pEA018) ir *Pf*PdhR/P_{lldP} (pEA025) sistemų praėjus 6 val. po L- ir D-pieno rūgšties skirtingų koncentracijų pridėjimo. K_m vertė pažymėta punktyrine linija. Pateiktas trijų biologinių pakartojimų vidurkis ir standartinis nuokrypis, *p ≤ 0,001 (neporinis *t*-testas). Šis paveikslas buvo naudotas publikacijoje (172)

5.3.2. Fenolinėmis rūgštimis indukuojamos genų ekspresijos sistemos

Fenolinių rūgščių sunaudojimo keliai bakterijose yra potencialus indukuojamų genų ekspresijos sistemų šaltinis. Anksčiau *m*-kumaro rūgšties sunaudojimas buvo aprašytas *E. coli* MG1655(145), *C. testosteroni* TA441(178) ir *R. globerulus* PWD1 (179). *m*-Kumaro rūgštis yra sunaudojama vykstant šešioms fermentinėms reakcijoms

esant *mhp*ABCDEF genų klasterio koduojamiems fermentams, galutinis šio metabolizmo produktas yra acetil-KoA. Torres ir kolegos parodė, kad MhpR TF jungiasi prie P_{mhpA} ir aktyvuoja *mhp* klasterio genų transkripciją (145). Kitų hidroksicinamono rūgščių, įskaitant kavos rūgštį, *p*-kumaro rūgštį ir ferulo rūgštį, sunaudojimo keliai buvo aprašyti *A. baylyi* ADP1 ir *P. fluorescens* BF13 ir parodyta, kad MarR šeimai priklausantis TF veikia kaip represorius, bet ši represija yra inicijuojama hidroksicinamatų-KoA tioesterių (tarpinių metabolitų), bet ne hidroksicinamono rūgščių (144). Remiantis šiomis žiniomis buvo pasirinkta įvertinti ir charakterizuoti potencialią *m*-kumaro rūgšties sistemą iš *E. coli* MG1655 ir *p*-kumaro rūgšties sistemas iš *A. baylyi* ADP1, *B. multivorans* ATCC BAA-247, *P. putida* KT2440.

m-Kumaro ir *p*-kumaro rūgštimis indukuojamos sistemos, sudarytos iš promotoriaus ir TF, ir tik iš promotorinės srities buvo klonuotos į pBRC1 reporterio plazmidę ir surinkti pEV052, pEV053, pEV036, pEV035, pEV038, pEV039, pEV041, pEV040 konstruktai. Fluorescencijos matavimai buvo atlikti sistemų šeimininkų ląstelėse arba tos pačios klasės kamienų ląstelėse. *A. baylyi* ADP1 konstruktai buvo klonuoti į *P. putida* KT2440 kamieną, o *B. multivorans* ATCC BAA-247 konstruktai klonuoti į *C. necator* H16 kamieną. *E. coli* Top10, *P. putida* KT2440 ir *C. necator* H16 kamienai su indukuojamomis sistemomis buvo auginti LB terpėje ir logaritmiškai augančių ląstelių fluorescencijos buvo kiekybiškai įvertintos praėjus 6 ir 12 valandų po *m*-kumaro ar *p*-kumaro rūgščių pridėjimo. Kaip ir buvo tikėtasi, *Ec*MhpR/P_{mhpA} (pEV052) ir *Ec*P_{mhpA} (pEV053) sistemos buvo indukuotos atitinkamai 224 ir 220 kartus su *m*-kumaro rūgštimi. Aukštos fluorescencijos vertės buvo pastebėtos ir su konstruktu be TF dėl esančios MhpR kopijos *E. coli* chromosominėje DNR.

Indukuojamos sistemos *Ab*HcaR/$P_{ACIAD\_RS07960}$ (pEV035), *Bm*HcaR/$P_{NP80\_RS03060}$ (pEV039) ir *Pp*HcaR/$P_{PP\_RS17495}$ (pEA040) yra reguliuojamos TR, priklausančio MarR šeimai, tačiau nors struktūriniai genai, koduojantys acil-KoA ligazę, turi aukštą identiškumą (daugiau nei 80 %) tarp šių bakterijų, TF identiškumas nesiekia 50 %. Sistemų skirtumai taip pat atsiskleidžia fluorescencijos matavimų rezultatuose, *Ab*HcaR veikia kaip represorius, promotoriaus vieno versijos konstruktas (pEV036) turi apie 9 kartus didesnę RFB sintezę *P. putida* ląstelėse nei sistema, sudaryta iš TF ir indukuojamojo promotoriaus (pEV035), lyginant neindukuotus mėginius. *Bm*HcaR and *Pp*HcaR TF potencialiai veikia kaip aktyvatoriai, ir promotoriaus vieno versijos konstruktų pEV038 ir pEV041 RFB sintezė yra mažesnė nei 50 A.U. *Ab*HcaR/$P_{ACIAD\_RS07960}$ (pEV035), *Bm*HcaR/$P_{NP80\_RS03060}$ (pEV039) ir *Pp*HcaR/$P_{PP\_RS17495}$ (pEA040) sistemos buvo indukuotos atitinkamai 8, 65 ir 415 karto su *p*-kumaro rūgštimi po 12 valandų. Uždelsta indukcija gali būti siejama su sistemų tikraisiais induktoriais, tarpiniais metabolizmo produktais, *p*-kumaroil-KoA tioesteriais, kaip anksčiau buvo pademonstruota *Ab*HcaR/$P_{ACIAD\_RS07960}$ sistemoje (144).

Buvo įvertinta šių indukuojamų sistemų kinetika ir dozės atsakas naudojant *m*-kumaro ir *p*-kumaro rūgščių skirtingas koncentracijas nuo 0 iki 5 mM. Kumaro rūgštimis indukuojamos sistemos turi aukštas K_m vertes, apie 1 mM, ir veikia kaip įjungimo / išjungimo jungikliai. *Ec*MhpR/P_{mhpA} (pEV052) sistema turi aukštą

dinaminį intervalą, ir jos genų raiška gali būti sureguliuota 156 μM–1,25 mM intervale (5.3.4pav., a). Indukuojamos sistemos *Ab*HcaR/$P_{ACIAD\_RS07960}$ (pEV035), *Bm*HcaR/$P_{NP80\_RS03060}$ (pEV039), *Pp*HcaR/$P_{PP\_RS17495}$ (pEA040) parodė panašų gimiringumą su *p*-kumaro rūgštimi, ir šių sistemų genų raiška gali būti sureguliuota 159 μM–2,5 mM intervale (5.3.4 pav., b–d).

Indukuojamos sistemos *Ec*MhpR/P_{mhpA} (pEV052), *Ab*HcaR/$P_{ACIAD\_RS07960}$ (pEV035), *Bm*HcaR/$P_{NP80\_RS03060}$ (pEV039) ir *Pp*HcaR/$P_{PP\_RS17495}$ (pEA040) buvo išbandytos su 21 fenoline rūgštimi, siekiant nustatyti sistemų specifiškumą. *Ec*MhpR/P_{mhpA} (pEV052) sistema buvo specifinė *m*-kumaro rūgščiai. *Ab*HcaR/$P_{ACIAD\_RS07960}$ (pEA035) sistema be *p*-kumaro rūgšties buvo indukuojama ir ferulo, ir kavos rūgštimis. *Bm*HcaR/$P_{NP80\_RS03060}$ (pEV039) ir *Pp*HcaR/$P_{PP\_RS17495}$ (pEA040) sistemos be *p*-kumaro rūgšties buvo indukuojamos ir kavos rūgštimi.

Siekiant nustatyti, ar *Ec*MhpR/P_{mhpA}, *Ab*HcaR/$P_{ACIAD\_RS07960}$, *Bm*HcaR/$P_{NP80\_RS03060}$ ir *Pp*HcaR/$P_{PP\_RS17495}$ sistemos gali veikti kituose, ne šeimininkų, ar tos pačios klasės bakterijose, sistemos buvo išbandytos *E. coli* Top10, *C. necator* H16 ir *P. putida* KT2440 kamienuose, tačiau indukcija nebuvo matoma. Potencialiai šias tirtas sistemas indukuoja ne hidroksicinamono rūgštys, o tarpiniai šių rūgščių metabolizmo produktai, tai gali patvirtinti matoma uždelsta indukcija po 3 val. sistemų šeimininkų ląstelėse.

hcrRABC operonas buvo identifikuotas *L. argentoratensis* DSM 16365 ir pEA048 ir pEA049 konstruktai buvo surinkti atitinkamai tik su promotoriumi P_{hcrA} ir promotoriumi P_{hcrA}, ir HcrR TR. Šie konstruktai buvo pratestuoti *E. coli* Top10, *C. necator* H16 ir *P. putida* KT2400 ląstelėse. *La*HcrR/P_{HcrA} (pEA049) sistema, rodanti atsaką į skirtingas hidroksicinamono rūgštis, įskaitant *o*-, *m*-, *p*-kumaro, ferulo, sinapo, kavos ir chlorogeninę rūgštį, buvo įvertinta. Rezultatai parodė, kad hidroksicinamono rūgštimis indukuojama sistema gali būti tiriama trijuose skirtinguose mikroorganizmuose, *E. coli* MG1655, *C. necator* H16 ir *P. putida* KT2440, ir šios sistemos TF veikia kaip aktyvatorius. Lignino darinius skaidančių fermentų atradimas gali išplėsti lignino apdorojimo galimybes ir pritaikymą aukštos pridėtinės vertės produktų gamyboje (7).

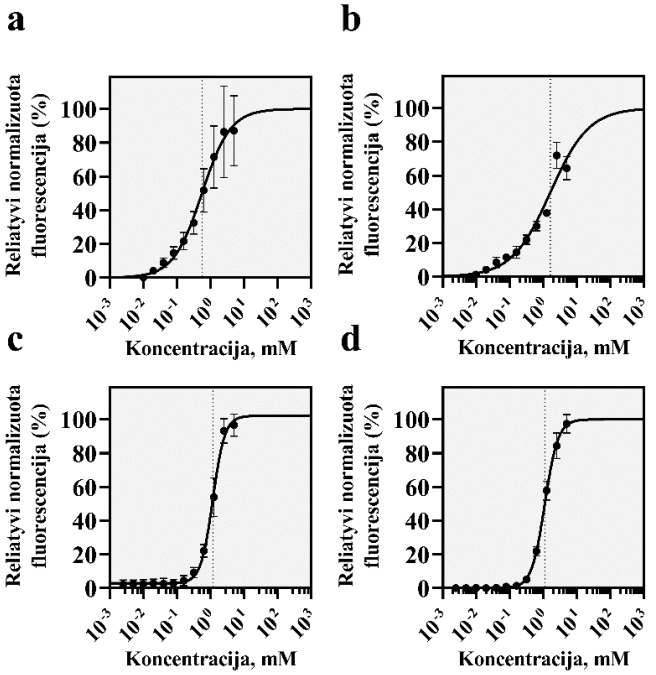

5.3.4 pav. Kumaro rūgštimi indukuojamų sistemų dozės-atsako kreivės. Reliatyvi normalizuota fluorescencija **(a)** *E. coli*/*Ec*MhpR/P_{mhpA} (pEV052) sistemos praėjus 6 val. po *m*-kumaro rūgšties skirtingų koncentracijų pridėjimo. Reliatyvi normalizuota fluorescencija **(b)** *P. putida*/*Ab*HcaR/$P_{ACIAD\_RS07960}$ (pEV035), **(c)** *C. necator*/*Bm*HcaR/$P_{NP80\_RS03060}$ (pEV039) ir **(d)** *Pp*HcaR/$P_{PP\_RS17495}$ (pEV040) sistemų praėjus 12 val. po *p*-kumaro rūgšties skirtingų koncentracijų pridėjimo. K_m vertė pažymėta punktyrine linija. Pateiktas trijų biologinių pakartojimų vidurkis ir standartinis nuokrypis, $*p \leq 0{,}001$ (neporinis *t*-testas)

5.3.3. Genetiškai užkoduoti biojutikliai pagerintai pieno rūgščių analizei

Daug organinių medžiagų turinti likutinė frakcija (ORRF) kaip atliekos buvo gauta gliukozės sirupo gamybos metu iš daug baltymų ir riebalų rūgščių turinčios nereikalingų, šalutinių produktų frakcijos, likusios retentate po žalio sirupo ultrafiltracijos. ORRF buvo naudotas kaip substratas optiškai grynų L-pieno rūgšties, D-pieno rūgšties ir jų mišinio gamybai su PBR *L. paracasei, L. lactis* ir *L. amylovorus*. Gauti rezultatai parodė, kad PBR augimas ir pieno rūgšties gamyba (5.3.5 pav.), naudojant ORRF kaip vienintelį anglies ir azoto šaltinį, yra labai maži, palyginti su MRS terpe. Siekiant nustatyti, kurių maistinių medžiagų trūkumas riboja PBR augimą, ORRF buvo papildytas skirtingais MRS terpės komponentais ir jų mišiniais: 4 g/L mielių ekstraktu, 8 g/L mėsos ekstraktu, 1% vitaminų kompleksu, 0,1 % Tween 80, 4 g/L mielių ekstraktu ir 8 g/L mėsos ekstrakto mišiniu, 4 g/L mielių ekstrakto, 8 g/L mėsos ekstrakto ir 1 % vitaminų komplekso mišiniu, 1–30 g/L mielių ekstrakto ir 0,1 % Tween 80 mišiniu. *L. paracasei* kamieno rezultatai parodė, kad L-pieno rūgšties gamyba padidėjo apie tris kartus pridėjus į ORRF papildomai azoto šaltinio, mielių arba mėsos ekstrakto (5.3.5 pav., a). O azoto šaltinis kartu su Tween 80 turėjo teigiamą

poveikį *L. amylovorus* ir *L. lactis* augimui ir pieno rūgšties gamybai (5.3.5 pav. e, f) Su visais trimis PBR kamienais pieno rūgščių koncentracija didėjo didinant mielių ekstrakto koncentraciją nuo 1 iki 30 g/L ORRF tirpale (5.3.5 pav., d–f). Tačiau didžiausios pieno rūgščių išeigos buvo gautos, kai ORRF buvo papildyta 1 g/L mielių ekstrakto. Mielių ekstrakto pridėjimas pašalino azoto trūkumą terpėje ir padėjo užtikrinti geresnę pieno rūgščių gamybą, anglies ir azoto santykis terpėje yra svarbus siekiant gaminti pieno rūgštis su didele išeiga.

Šiame darbe buvo testuotas biojutiklių BLA1 (paremtas *E. coli*/*Ec*LldR/P_{lldP} indukuojama sistema, esančia pEA015 plazmidėje) ir BLA2 (paremtas *P. putida*/*Pf*PdhR/P_{lldP} indukuojama sistema, esančia pEA025 plazmidėje) gebėjimas nustatyti L- ir D-pieno rūgšties koncentracijas biologiniuose mėginiuose. BLA1 buvo naudotas nustatant L-pieno rūgšties koncentraciją *L. paracasei* fermentacijos supernatantų mėginiuose, BLA2 naudotas nustatant D-pieno rūgštį *L. lactis* fermentacijos supernatantų mėginiuose. *L. amylovorus* fermentacijos mėginių analizė buvo atlikta naudojant abu BLA1 ir BLA2 biojutiklius.

Supernatantų mėginiai buvo surinkti 72 fermentacijos valandą. Mėginiai analizuoti 96 šulinėlių plokštelėse naudojant plokštelių skaitytuvą, fluorescencija ir absorbcija buvo stebėtos laikui bėgant naudojant BLA1 ir BLA2 biojutiklius. Gautos L-pieno rūgšties ir D-pieno rūgšties koncentracijos buvo palygintos su ESCh analizės rezultatais. Gauti rezultatai parodė gana gerą koreliaciją tarp dviejų tyrimų, koreliacijos koeficientas (r) buvo lygus 0,84 su BLA1 ir 0,89 su BLA2 (5.3.6 pav.).

L- ir D-pieno rūgšties kiekybinis nustatymas *L. amylovorus* mėginiuose su raceminiu pieno rūgšties mišiniu buvo atliktas naudojant trijų žingsnių analizę. Pirma, bendra DL-pieno rūgšties koncentracija buvo nustatyta naudojantis BLA2 biojutikliu. Antra, L-pieno rūgšties koncentracija mišinyje buvo nustatyta naudojantis BLA1 biojutikliu, atsižvelgiant į D-pieno rūgšties, esančios mišinyje, slopinamąjį poveikį fluorescencijai. Galiausiai, D-pieno rūgšties koncentracija mišinyje buvo apskaičiuota atimant L-pieno rūgšties koncentraciją iš bendros DL-pieno rūgščių koncentracijos. Skaičiavimams patvirtinti gautos vertės buvo palygintos su fermentinio D-/L-pieno rūgšties tyrimo rinkinio vertėmis (5.3.7 pav.). Gauti rezultatai parodė, kad labai gera koreliacija (r = 0,95) yra tarp L-pieno rūgšties verčių, gautų su BLA1 biojutikliu, ir fermentiniu metodu gautų rezultatų (5.3.7 pav., a). Koreliacija tarp bendros DL-pieno rūgščių koncentracijos, gautos su BLA2 biojutikliu, ir fermentinio metodo, taip pat buvo gera (r = 0,98), tačiau rezultatai, gauti naudojant BLA2 biojutiklį buvo pasislinkę link didesnių koncentracijų (5.3.7 pav., b). Perskaičiavus D-pieno rūgšties koncentracijas naudojant vertes, gautas su biojutikliais, rezultatai taip pat parodė verčių poslinkį link didesnių koncentracijų, ir koreliacija tarp šių metodų buvo mažesnė (r = 0,84).

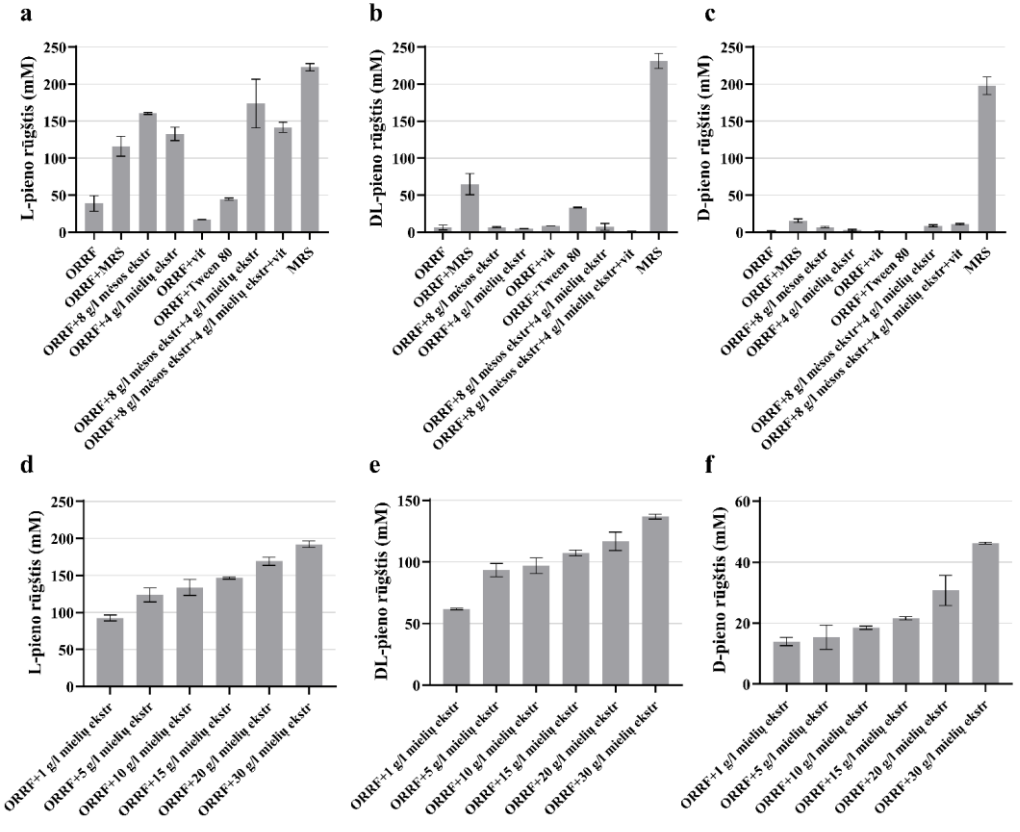

5.3.5 pav. Pieno rūgščių koncentracijos, gautos su **(a, d)** *L. paracasei*, **(b, e)** *L. amylovorus* **(c, f)** *L. lactis*, naudojant ORRF, turintį apie 42 g/L gliukozės. Nurodyti pieno rūgšties gamyboje naudoti maisto medžiagų papildai. Stulpelinėse diagramose pateiktas dviejų biologinių pakartojimų duomenų vidurkis ir standartinis nuokrypis

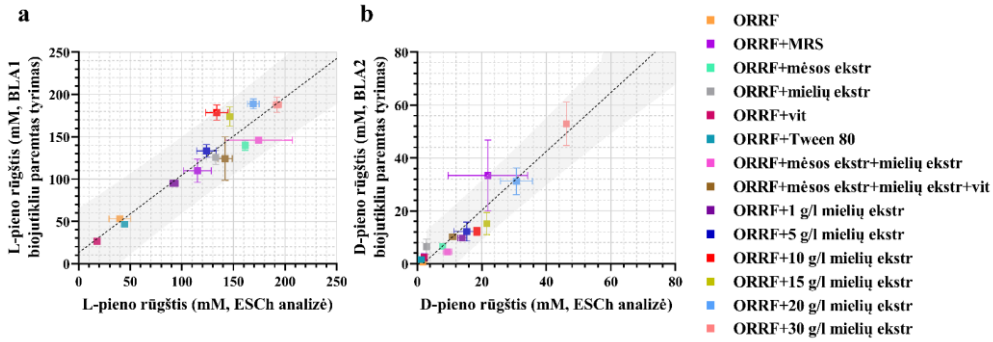

5.3.6 pav. Tiesinės regresijos analizė (juoda punktyrinė linija) tarp ESCh metodo **(a, b)** ir genetiškai užkoduotų biojutiklių BLA1 **(a)** ir BLA2 **(b)**. Tiesinė regresijos analizė atlikta siekiant rasti 95 % prognozės intervalą (pilka sritis). L- ir D-pieno rūgščių reikšmės gautos tiriant *L. paracasei* **(a)** ir *L. lactis* **(b)** 72 val. fermentacijos supernatantų mėginius. Tiriamų mėginių substratų sudėtis nurodyta dešinėje pusėje. Pateiktas dviejų biologinių pakartojimų duomenų vidurkis ir standartinis nuokrypis

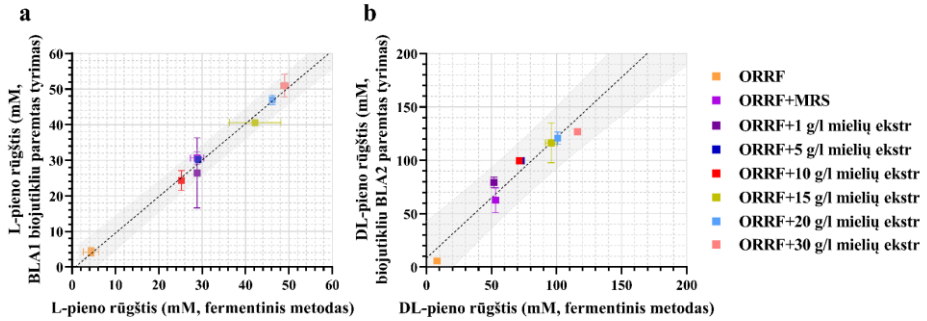

5.3.7 pav. Tiesinės regresijos analizė (juoda punktyrinė linija) tarp fermentinio metodo **(a, b)** ir genetiškai užkoduotų biojutiklių BLA1 **(a)** ir BLA2 **(b)**. Tiesinė regresijos analizė atlikta siekiant rasti 95 % prognozės intervalą (pilka sritis). L-pieno rūgšties ir bendros DL-pieno rūgščių koncentracijos reikšmės gautos tiriant *L. amylovorus* 72 val fermentacijos supernatantų mėginius. Tiriamų mėginių substratų sudėtis nurodyta dešinėje pusėje. Pateiktas dviejų biologinių pakartojimų duomenų vidurkis ir standartinis nuokrypis

Šiame darbe taip pat buvo aprašytas terpės, turinčios ORRF, optimizavimas efektyviai D-pieno rūgšties gamybai su *L. lactis*. Terpės sudėties optimizavimas buvo atliktas su genetiškai užkoduotu BLA2 biojutikliu kaip greita ir aukšto našumo alternatyva tradiciniams analitiniams metodams. Testuotos 27 skirtingos terpės, papildytos su skirtingomis ORRF, mielių ekstrakto ir Tween 80 koncentracijomis. Šis auginimo eksperimentas buvo atliktas dviem pakartojimais 96 šulinėlių plokštelėje 72 val., o D-pieno rūgšties koncentracija nedelsiant nustatyta plokštelių skaitytuvu, perkeliant mėginius į naują 96 šulinėlių plokštelę su BLA2 biojutikliu. Scheminis eksperimento atvaizdavimas pateiktas 5.3.8 pav., a. Gauti rezultatai parodė, kad didžiausia specifinė D-pieno rūgšties išeiga, artima 0,22, buvo gauta naudojant 200

arba 100 g/L ORRF, papildytos 0,0625 g/L mielių ekstrakto ir 0,025 % arba 0,00625 % Tween 80 (5.3.8 pav., b).

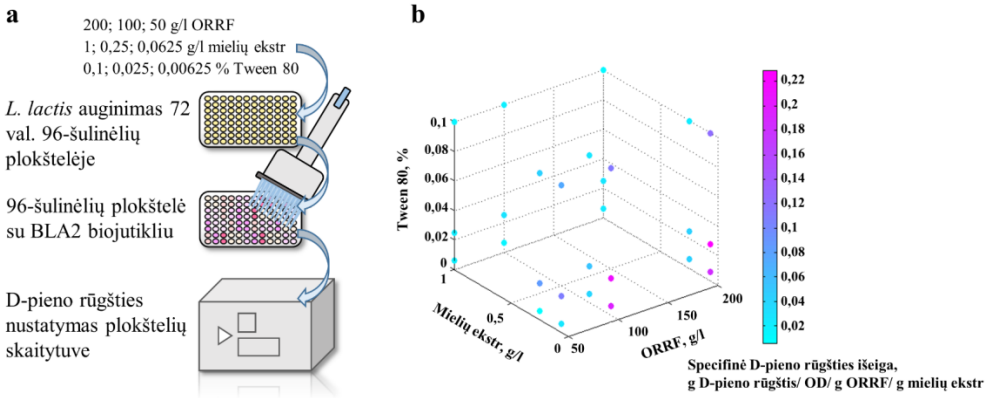

5.3.8 pav. (a) Scheminis eksperimento atvaizdavimas, kuris buvo skirtas terpės sudėčiai optimizuoti. **(b)** D-pieno rūgšties specifinės išeigos ir Tween 80, mielių ekstrakto ir ORRF koncentracijų sąveika

5.3.4. Rekomendacijos nepertraukiamai D-pieno rūgšties fermentacijai su *L. lactis* naudojant gliukozės sirupo gamybos likučius

Šiame skyriuje aprašomos pagerintos nepertraukiamos D-pieno rūgšties fermentacijos rekomendacijos. *L. lactis* gali gaminti optiškai gryną D-pieno rūgštį naudojant ORRF, papildytą mielių ekstraktu ir Tween 80. Proceso eigos schema su pagrindine informacija nepertraukiamai D-pieno rūgšties gamybai pateikta 5.3.9 paveiksle. Schemą sudaro keturios dalys: i) mitybinių poreikių nustatymas (papildomas etapas prieš fermentaciją), ii) fermentacija, iii) produkto gryninimo procesas ir iv) D-pieno rūgšties koncentracijos nustatymas.

Prieš didesnės apimties nepertraukiamą fermentaciją gali būti atliekama greita nebrangių substratų ir alternatyvių azoto šaltinių paieška naudojant genetiškai užkoduotus biojutiklius. Mielių ekstraktas yra tradicinis azoto šaltinis, tačiau jo naudojimas padidina pieno rūgšties gamybos sąnaudas. Žemės ūkio likučiai gali pakeisti brangius azoto šaltinius, jų paiešką atitinkamiems kamienams galima atlikti naudojant genetiškai užkoduotus biojutiklius, kaip buvo pademonstruota 5.3.3 poskyryje, kai plokštelių skaitytuve 96 skirtingos sudėties mėginiai gali būti išmatuoti per vieną kartą. Atrinktas optimalus azoto šaltinis toliau naudojamas nepertraukiamoje D-pieno rūgšties fermentacijoje pakeičiant mielių ekstraktą.

100 l talpos bioreaktorius (B-1) (mikrobinis fermentatorius BR500-M1 („Labfirst Scientific Instruments“, Kinija)) papildomas ORRF, azoto šaltiniu ir druskos tirpalu naudojant peristaltinį siurblį (P-4) su 1,6 L/min srauto greičiu. Į bioreaktorių (B-1) rankiniu būdu perkeliama 10 % (v/v) *L. lactis* ląstelių, užaugintų kultivavimo kolboje (CF-1) sterilioje MRS terpėje 37 °C. Bioreaktorius (B-1), sujungtas su membranų moduliu (UF-1, NF-1, IEX-1), naudojamas nepertraukiamai D-pieno rūgšties fermentacijai. Bioreaktoriuje (B-1) pH, temperatūra ir skysčio lygis

stebimas naudojant jutiklius (a, b, c). Bioreaktoriuje palaikoma 37 °C temperatūra naudojant temperatūros palaikymo gaubtuvą.

Po fermentacijos pieno rūgšties gryninimas atliekamas naudojant membraninį atskyrimo metodą, aprašytą (211). Fermentacijos mišinys iš bioreaktoriaus pumpuojamas 0,8 L/min greičiu į ultrafiltracijos membraną (UF-1) naudojant peristaltinį siurblį (P-5), ultrafiltracijos membrana (UF-1) atskiria *L. lactis* ląsteles iš fermentacijos mišinio, ir ląstelės grąžinamos į bioreaktorių (B-1). Supernatantas patenka į nanofiltracijos membraną (NF-1), kur likusi gliukozė atskiriama nuo pieno rūgšties dėl molekulinių masių skirtumo. Likusi gliukozė retentante grąžinama į bioreaktorių (B-1). Likę druskų jonai supernatante atskiriami naudojant jonų mainų dervą (IEX-1 ir IEX-2). Pabaigoje D-pieno rūgščiai sukoncentruoti naudojamas vakuuminis garintuvas (VE-1). Aukšto grynumo, potencialiai >99 %, D-pieno rūgštis saugoma T-3 talpoje. Mėginiai pieno rūgščiai nustatyti gali būti surenkami naudojant rankinius vožtuvus (V-2, V-3 ir V-4). Šio proceso metu pagamintos D-pieno rūgšties koncentracija gali siekti iki 90 g/L (remiantis literatūra (212)).

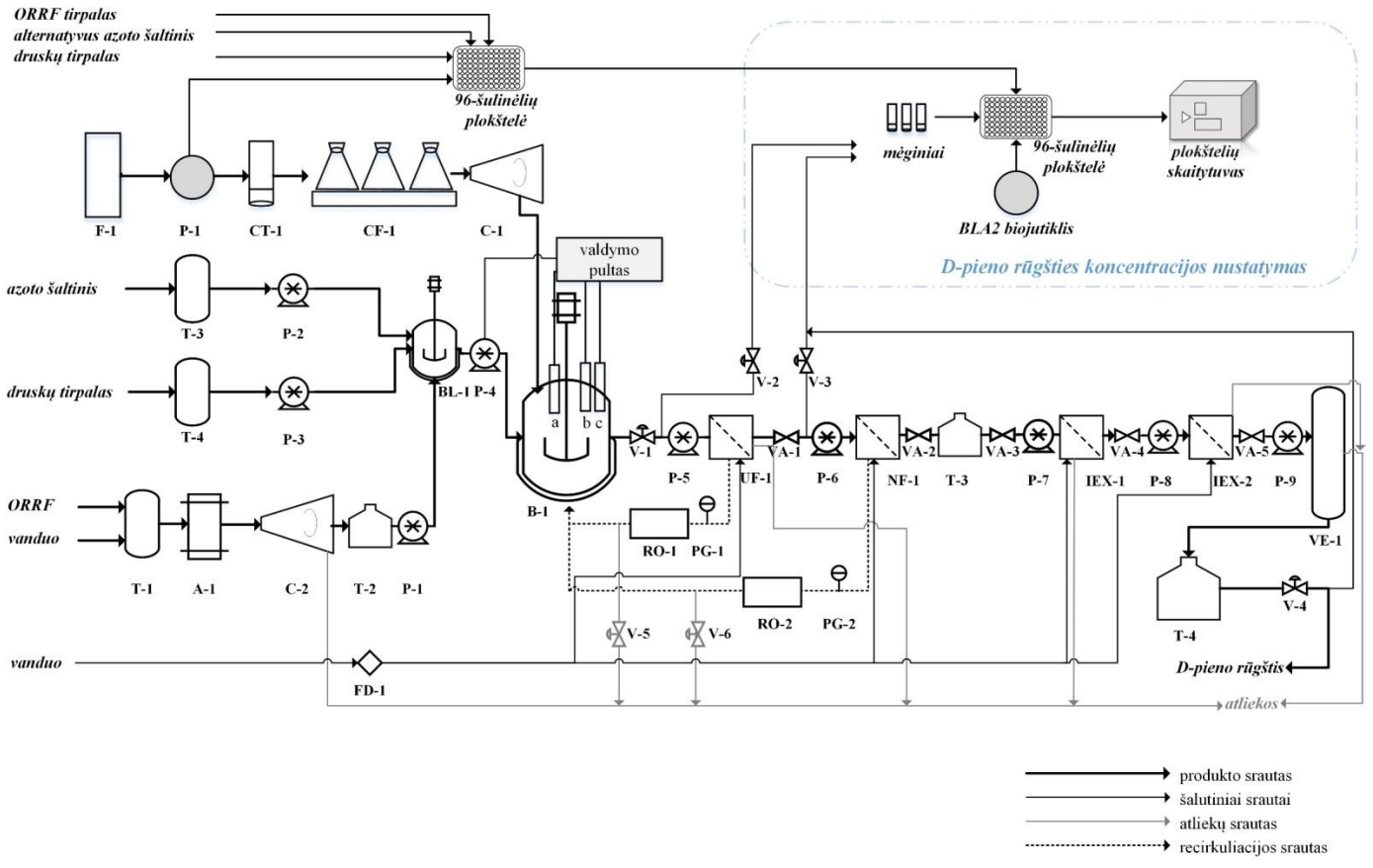

5.3.9 pav. Proceso eigos diagrama su pagrindine informacija nepertraukiamai D-pieno rūgšties fermentacijai su *L. lactis* naudojant ORRF kaip anglies šaltinį

5.4. IŠVADOS

1. Pieno rūgštimis indukuojamos sistemos *Ec*LldR/P_{lldP} ir *Cn*GntR/$P_{H16\_RS19190}$, identifikuotos *E. coli* MG1655 ir *C. necator* H16 genomuose, yra specifinės L-pieno rūgščiai, ir jų genų raiška gali būti sureguliuota atitinkamai 9 µM-1 mM ir 80 µM-1 mM intervaluose. Pieno rūgštimis indukuojamos sistemos *Pa*PdhR/P_{lldP}, *Pl*PdhR/P_{lldP} ir *Pf*PdhR/P_{lldP}, identifikuotos *Pseudomonas* spp., turi panašų gimiringumą su L- ir D-pieno rūgštimis, ir jų genų raiška gali būti sureguliuota 9 µM–2 mM intervaluose. Nenustatyta nė vienos iš *E. coli* MG1655, *C. necator* H16 ir *Pseudomonas* spp. genomuose identifikuotų pieno rūgštimis indukuojamų sistemų atsako specifiškai tik į D-pieno rūgštį.
2. *Ec*MhpR/P_{mhpA} indukuojama sistema, identifikuota *E. coli* MG1655 genome, yra specifinė *m*-kumaro rūgščiai, ir jos genų raiška gali būti sureguliuota 156 µM–1,25 mM intervale. Indukuojamos sistemos *Ab*HcaR/$P_{ACIAD\_RS07960}$, *Bm*HcaR/$P_{NP80\_RS03060}$ ir *Pp*HcaR/$P_{PP\_RS17495}$, identifikuotos *A. baylyi* ADP1, *B. multivorans* ATCC BAA-247 ir *P. putida* KT2440, yra panašaus gimiringumo su *p*-kumaro rūgštimi, ir jų genų raiška gali būti sureguliuota 159 µM–2,5 mM intervaluose. Sistema *Ab*HcaR/$P_{ACIAD\_RS07960}$ taip pat yra indukuojama ferulo ir kavos rūgštimis, o *Bm*HcaR/$P_{NP80\_RS03060}$ ir *Pp*HcaR/$P_{PP\_RS17495}$ sistemos be *p*-kumaro rūgšties yra indukuojamos kavos rūgštimi. Indukuojama sistema *La*HcrR/P_{HcrA} iš *L. argentoratensis* DSM 16365 rodo atsaką į keletą hidroksicinamono rūgščių, įskaitant *o*-kumaro, *m*-kumaro, *p*-kumaro, ferulo ir sinapo rūgštis, ir gali būti pritaikyta tokiuose kamienuose, kaip *E. coli*, *C. necator* ir *P. putida.*
3. *Ec*LldR/P_{lldP} ir *Pf*PdhR/P_{lldP} indukuojamos sistemos buvo pritaikytos kaip genetiškai užkoduoti BLA1 ir BLA2 biojutikliai ir patvirtintos kaip greitas ir didelio našumo metodas L- ir D-pieno rūgštims biologiniuose mėginiuose nustatyti su vienu pieno rūgšties enantiomeru arba su jų mišiniu.
4. Pademonstruota BLA2 biojutikliu paremta strategija skirta D-pieno rūgšties fermentacijos terpės optimizavimui pagerinti su *L. lactis* naudojant ORRF kaip anglies šaltinį. Nustatyta optimali terpės sudėtis: 200 g/L arba 100 g/L ORRF, papildytos 0,0625 g/L mielių ekstrakto ir 0,00625 % Tween 80.

REFERENCES

1. LEDUC S. *La biologie synthétique*. A. Paris, Poinat, 1912.
2. HANKO E. K. R., MINTON N. P. and N. MALYS. A transcription factor-based biosensor for detection of itaconic acid. *ACS Synthetic Biology.* 2018, 7 (5), 1436-1446. DOI 10.1021/acssynbio.8b00057.
3. BHALERAO, K. D. Synthetic gene networks: the next wave in biotechnology? *Trends in Biotechnology*. 2009, 27 (6), 368-374. DOI 10.1016/j.tibtech.2009.03.003.
4. BOADA Y., VIGNONI A., PICO J. and P. CARBONELL. Extended metabolic biosensor design for dynamic pathway regulation of cell factories. *iScience.* 2020, 23 (7), 101305. DOI 10.1016/j.isci.2020.101305.
5. YU W. et al. Genetically encoded biosensors for microbial synthetic biology: From conceptual frameworks to practical applications. *Biotechnology Advances.* 2023, 62, 108077. DOI 10.1016/j.biotechadv.2022.108077.
6. ZHANG F. and J. D. KEASLING. Biosensors and their applications in microbial metabolic engineering. *Trends in Microbiology*. 2011, 19 (7), 323-329. DOI 10.1016/j.tim.2011.05.003.
7. ALVAREZ-GONZALEZ G. and N. DIXON. Genetically encoded biosensors for lignocellulose valorization. *Biotechnology for Biofuels*. 2019, 12, 246. DOI 10.1186/s13068-019-1585-6.
8. JANSSEN M. *Systems perspectives on biorefineries*. Chalmers University of Technology, 2013.
9. SALUSJÄRVI L., HAVUKAINEN S., KOIVISTOINEN O. and M. TOIVARI. Biotechnological production of glycolic acid and ethylene glycol: current state and perspectives. *Applied Microbiology and Biotechnology*. 2019, 103, 2525–2535. DOI 10.1007/s00253-019-09640-2.
10. BOZELL J. J. and G. R. PETERSEN. Technology development for the production of biobased products from biorefinery carbohydrates—the US Department of Energy's "Top 10" revisited. *The Royal Society of Chemistry.* 2010, 12 (4), 539-555. DOI 10.1039/b922014c.
11. BAI D.M. *et al.* Fed-batch fermentation of *Lactobacillus lactis* for hyper-production of L-lactic acid. *Biotechnology Letters*. 2003, **25** (21), 1833–1835. DOI 10.1023/a:1026276925649.
12. MOON S.-K., WEE Y.-J. and G.-W. CHOI. A novel lactic acid bacterium for the production of high purity L-lactic acid, *Lactobacillus paracasei* subsp. *paracasei* CHB2121. *Journal of Bioscience and Bioengineering*. 2012, 114 (2), 155-159. DOI 10.1016/j.jbiosc.2012.03.016.
13. ABDEL-RAHMAN M. A., HASSAN S. E.-D., AZAB M. S., MAHIN A.-A. and M. A. GABER. High improvement in lactic acid productivity by new alkaliphilic bacterium using repeated batch fermentation integrated with increased substrate concentration. *BioMed Research International.* 2019, 7212870. DOI 10.1155/2019/7212870.

14. TASHIRO Y. et al. Continuous D-lactic acid production by a novel thermotolerant *Lactobacillus delbrueckii* subsp. *lactis* QU 41. *Applied Microbiology and Biotechnology*. 2011, 89 (6), 1741–1750. DOI 10.1007/s00253-010-3011-7.

15. ABDEL-RAHMAN M. A., TASHIRO T., ZENDO T., SAKAI K. and K. SONOMOTO. *Enterococcus faecium* QU 50: a novel thermophilic lactic acid bacterium for high-yield l-lactic acid production from xylose. *FEMS Microbiology Letters*. 2015, 362 (2), 1-7. DOI 10.1093/femsle/fnu030.

16. TANAKA K. et al. Two different pathways for D-xylose metabolism and the effect of xylose concentration on the yield coefficient of L-lactate in mixed-acid fermentation by the lactic acid bacterium *Lactococcus lactis* IO-1. *Applied Microbiology and Biotechnology*. 2022, 60 (1-2), 160–167. DOI 10.1007/s00253-002-1078-5.

17. PUGH S., MCKENNA R., OSMAN M., THOMPSON B. and D. R. NIELSEN. Rational engineering of a novel pathway for producing the aromatic compounds *p*-hydroxybenzoate, protocatechuate, and catechol in *Escherichia coli*. *Process Biochemistry*. 2014, 49 (11), 1843-1850. DOI 10.1016/j.procbio.2014.08.011.

18. VALANCIENE E. et al. Advances and prospects of phenolic acids production, biorefinery and analysis. *Biomolecules*. 2020, 10 (6), 874. DOI 10.3390/biom10060874

19. SRIVASTAVA R. K. et al. Biorefineries development from agricultural byproducts: Value addition and circular bioeconomy. *Sustainable Chemistry and Pharmacy*. 2023, 32, 100970. DOI 10.1016/j.scp.2023.100970.

20. LI C. et al. Advances and prospects of transcription-factor-based biosensorsin high-throughput screening for cell factories construction. *Food bioengineering*. 2022, 1 (2), 1-13. DOI 10.1002/fbe2.12019.

21. GREENWALD E. C., MEHTA S. and J. ZHANG. Genetically encoded fluorescent biosensors illuminate the spatiotemporal regulation of signaling networks. *Chemical Reviews*. 2018, 118 (24), 11707–11794. DOI 10.1021/acs.chemrev.8b00333.

22. FERREIRA P. S., VICTORELLI F. D., FONSECA-SANTOS B. and M. CHORILLI. A review of analytical methods for *p*-coumaric acid in plant-based products, beverages, and biological matrices. *Critical Reviews in Analytical Chemistry*. 2019, 49, 21-31. DOI 10.1080/10408347.2018.1459173.

23. CHEN S.F., MOWERY R. A., CASTLEBERRY V. A., WALSUM G. P. V. and C. K. CHAMBLISS. High-performance liquid chromatography method for simultaneous determination of aliphatic acid, aromatic acid and neutral degradation products in biomass pretreatment hydrolysates. *Journal of Chromatography A*. 2006, 1104 (1-2), 54-61. DOI 10.1016/j.chroma.2005.11.136.

24. HENRY H., MARMY CONUS N., STEENHOUT P., BÉGUIN A. and O. BOULAT. Sensitive determination of D-lactic acid and L-lactic acid in urine by high-performance liquid chromatography–tandem mass spectrometry. *Biomedical Chromatography*. 2012, 26 (4), 425-428. DOI 10.1002/bmc.1681.

25. MORASKIE M. et al. Microbial whole-cell biosensors: Current applications, challenges, and future perspectives. *Biosensors and Bioelectronics*. 2021, 191, 113359. DOI 10.1016/j.bios.2021.113359.

26. HOSSAIN G. S., SAINI M., MIYAKE R., LING H. and M. W. CHANG. Genetic biosensor design for natural product biosynthesis in microorganisms. *Trends in Biotechnology: Cell Press*. 2020, 38 (7), 797-810. DOI 10.1016/j.tibtech.2020.03.013.

27. SCHMITT R. E., MOLITOR H. R. and T. WU. Voltammetric method for the determination of lactic acid using a carbon paste electrode modified with cobalt phthalocyanine. *International Journal of Electrochemical Science*. 2012, **7** (11), 10835-10841. DOI 10.1016/S1452-3981(23)16906-9.

28. PUNDIR C. S. NARWAL V. and B. BATRA. Determination of lactic acid with special emphasis on biosensing methods: a review. *Biosensors and Bioelectronics*. 2016, 86, 777-790. DOI 10.1016/j.bios.2016.07.076.

29. CHEN S.-F., MOWERY R. A., CASTLEBERRY V. A., WALSUM G. P. V. and C. K. CHAMBLISS. High-performance liquid chromatography method for simultaneous determination of aliphatic acid, aromatic acid and neutral degradation products in biomass pretreatment hydrolysates. *Journal of Chromatography A*. 2006, 1104 (1-2), 54-61. DOI 10.1016/j.chroma.2005.11.136.

30. IBÁÑEZ, A. B. and S. BAUER. Analytical method for the determination of organic acids in dilute acid pretreated biomass hydrolysate by liquid chromatography-time-of-flight mass spectrometry. *Biotechnology for Biofuels*. 2014, **7**, 145. DOI 10.1186/s13068-014-0145-3.

31. FOROUZANFAR S. et al. Highly sensitive lactic acid biosensors based on photoresist derived carbon. *IEEE Sensors Journal*. 2020, 20 (16), 8965-8972. DOI 10.1109/JSEN.2020.2988383.

32. CERRATO-ALVAREZ M., BERNALTE E., BERNALTE-GARCÍA M. J. and E., Pinilla-Gil. Fast and direct amperometric analysis of polyphenols in beers using tyrosinase-modified screen-printed gold nanoparticles biosensors. *Talanta*. 2019, 193, 93-99. DOI 10.1016/j.talanta.2018.09.093.

33. GOERS L. et al. Whole-cell *Escherichia coli* lactate biosensor for monitoring mammalian cell cultures during biopharmaceutical production. *Biotechnology and Bioengineering*. 2017, 114 (6), 1290-1300. DOI 10.1002/bit.26254.

34. SIEDLER S. et al. Development of bacterial biosensor for rapid screening of yeast *p*-coumaric acid production. *ACS Synthetic Biology*. 2017, 6 (10), 1860-1869. DOI 10.1021/acssynbio.7b00009.

35. LIU Y., LIU Y. and M. WANG. Design, optimization and application of small molecule biosensor in metabolic engineering. *Frontiers in Microbiology*. 2012, 8. DOI 10.3389/fmicb.2017.02012.

36. MANNAN A. A., LIU D., ZHANG F. and D. OYARZÚN. A. Fundamental design principles for transcription-factor-based metabolite biosensors. *ACS Synthetic Biology* 6 (10), 1851-1859 (2017). DOI 10.1021/acssynbio.7b00172.

37. ARIS H. et al. Modeling transcriptional factor cross-talk to understand parabolic kinetics, bimodal gene expression and retroactivity in biosensor design. *Biochemical Engineering Journal*. 2019, 144, 209-216. DOI 10.1016/j.bej.2019.02.005.

38. PALMER A. E., QIN Y., PARK J. G. and J. E. MCCOMBS. Design and application of genetically encoded biosensors. *Trends in Biotechnology*. 2011, 29 (3), 144–152. DOI 10.1016/j.tibtech.2010.12.004.

39. BEREPIKI A., KENT R., MACHADO L. F. M. and N. DIXON. Development of high-performance whole cell biosensors aided by statistical modeling. *ACS Synthetic Biology*. 2020, 9, 576−589. DOI 10.1021/acssynbio.9b00448.

40. DING N. et al. Programmable cross-ribosome-binding sites to fine-tune the dynamic range of transcription factor-based biosensor. *Nucleic Acids Research*. 2020, 48 (18), 10602-10613. DOI 10.1093/nar/gkaa786.

41. FLACHBART L. K., SOKOLOWSKY S. and J. MARIENHAGEN. Displaced by deceivers: prevention of biosensor cross-talk is pivotal for successful biosensor-based high-throughput screening campaigns. *ACS Synthetic Biology*. 2019, 8 (8), 1847-1857. DOI 10.1021/acssynbio.9b00149.

42. BINDER S. et al. A high-throughput approach to identify genomic variants of bacterial metabolite producers at the single-cell level. *Genome Biology*. 2012, 13, R40. DOI 10.1186/gb-2012-13-5-r40.

43. NGUYEN N. H., KIM J.-R. and S. PARK. Application of transcription factor-based 3-hydroxypropionic acid. *Biotechnology and Bioprocess Engineering*. 2018, 23, 564-572. DOI 10.1007/s12257-018-0390-6.

44. MAHR R. et al. Biosensor-driven adaptive laboratory evolution of l-valine production in *Corynebacterium glutamicum*. *Metabolic Engineering*. 2015, 32, 184-194. DOI 10.1016/j.ymben.2015.09.017.

45. MAHR R. and FRUNZKE J. Transcription factor-based biosensors in biotechnology: current state and future prospects. *Applied Microbiology and Biotechnology*. 2016, 100 (1), 79-90. DOI 10.1007/s00253-015-7090-3.

46. DOONG S. J., GUPTA A. and K. L. J. PRATHER. Layered dynamic regulation for improving metabolic pathway productivity in *Escherichia coli*. *Proceedings of the National Academy of Sciences of the United States of America*. 2018, 115 (12), 2964-2969. DOI 10.1073/pnas.1716920115.

47. DAVID F., NIELSEN J. and V. SIEWERS. Flux control at the malonyl-CoA node through hierarchical dynamic pathway regulation in *Saccharomyces cerevisiae*. *ACS Synthetic Biology*. 2016, 5 (3), 224-233. DOI 10.1021/acssynbio.5b00161.

48. LEAVITT J. M. et al. Biosensor-enabled directed evolution to improve muconic acid production in *Saccharomyces cerevisiae*. *Biotechnology Journal*. 2017, 12 (10), 1600687. DOI 10.1002/biot.201600687.

49. BENTLEY G. J. et al. Engineering glucose metabolism for enhanced muconic acid production in *Pseudomonas putida* KT2440. *Metabolic Engineering*. 2020, 59, 64-75. DOI 10.1016/j.ymben.2020.01.001.

50. BECKER J., LANGE A., FABARIUS J. and C. WITTMANN. Top value platform chemicals: bio-based production of organic acids. *Current Opinion in Biotechnology*. 2015, 36, 168-175. DOI 10.1016/j.copbio.2015.08.022.

51. LORENZO R. D. D., SERRA I., PORRO D. and P. BRANDUARDI. State of the art on the microbial production of industrially. *Catalysts*. 2022, 12 (2), 234. DOI 10.3390/catal12020234.

52. INTASIAN P. et al. Enzymes, in vivo biocatalysis, and metabolic engineering for enabling a circular economy and sustainability. *Chemical Review*. 2021, 121 (17), 10367–10451. DOI 10.1021/acs.chemrev.1c00121.

53. VARADARAJAN S. and D. J. MILLER. Catalytic upgrading of fermentation-derived organic acids. *Biotechnology Progress*. 1999, 15 (5), 845-854. DOI 10.1021/bp9900965.

54. DESHMUKH K. et al. Biopolymer composites with high dielectric performance: interface engineering in *Biopolymer composites in electronics*, edited by Sadasivuni, K. K., Ponnamma, D., Kim, J., Cabibihan, J.-J. & AlMaadeed, M. A. Elsevier, 2017.

55. KLOTZ S., KAUFMANN N., KUENZ A. and U. PRÜßE. Biotechnological production of enantiomerically pure d-lactic acid. *Applied Microbiology and Biotechnology*. 2016, 100 (22), 9423–9437. DOI 10.1007/s00253-016-7843-7.

56. KERVRAN M. et al. Thermal degradation of polylactic acid (PLA)/polyhydroxybutyrate (PHB) blends: A systematic review. *Polymer Degradation and Stability*. 2022, 201, 109995. DOI 10.1016/j.polymdegradstab.2022.109995.

57. RESEARCH GRAND VIEW. *Lactic Acid Market Size, Share & Trends Analysis Report By Raw Material (Sugarcane, Corn, Cassava), By Application (PLA, Food & Beverages, Personal Care, Pharmaceuticals), By Region, And Segment Forecasts, 2022 - 2030.* San Francisco: Grand View Research, 2021.

58. RESEARCH GRAND VIEW. *Lactic acid market size worth $5.8 billion by 2030.* San Francisco: Grand View Research, 2022.

59. RESEARCH GRAND VIEW. *Polylactic acid market size worth $2,709.61 million by 2030.* San Francisco: Grand View Research, 2022.

60. RESEARCH GRAND VIEW. *Polylactic acid market size, share and trends analysis report by end use (packaging, agriculture, transport, electronics, textile, others), by region, and segment forecasts, 2022 - 2030.* San Francisco: Grand View Research, 2022

61. GARVIE E. I. Bacterial lactate dehydrogenases. *Microbiological Reviews*. 1980, 44 (1), 106-139. DOI 10.1128/mr.44.1.106-139.1980.

62. MURAKAMI N. et al. L-lactic acid production from glycerol coupled with acetic acid metabolism by *Enterococcus faecalis* without carbon loss. *Journal of Bioscience and Bioengineering*. 2016, 121 (1), 89-95. DOI 10.1016/j.jbiosc.2015.05.009.

63. CHEN X. et al. Influence of rice straw-derived dissolved organic matter on lactic acid fermentation by *Rhizopus oryzae*. *Journal of Bioscience and Bioengineering*, 2018, 125 (6), 703-709. DOI 10.1016/j.jbiosc.2018.01.004.

64. CHEN P.-T. et al. Exploring fermentation strategies for enhanced lactic acid production with polyvinyl alcohol-immobilized *Lactobacillus plantarum* 23 using microalgae as feedstock. *Bioresource Technology*. 2020, 308, 123266. DOI 10.1016/j.biortech.2020.123266.

65. DE LA TORRE I., ACEDOS M. G., LADERO M. and V. E.,SANTOS. On the use of resting *L. delbrueckii* spp. *delbrueckii* cells for D-lactic acid production from orange peel wastes hydrolysates. *Biochemical Engineering Journal*. 2019, 145, 162-169. DOI 10.1016/j.bej.2019.02.012.

66. ANGERMAYR S. A. et al. Exploring metabolic engineering design principles for the photosynthetic production of lactic acid by *Synechocystis* sp. PCC6803. *Biotechnology for Biofuels*. 2014, 7 (1), 99. DOI 10.1186/1754-6834-7-99.

67. HENARD C. A. et al. Bioconversion of methane to lactate by an obligate methanotrophic bacterium. *Scientific Reports*. 2016, 6, 21585. DOI 10.1038/srep21585.

68. HIDESE R., MATSUDA M., OSANAI T., HASUNUMA T. and A. KONDO. Malic enzyme facilitates D-lactate production through increased pyruvate supply during anoxic dark fermentation in *Synechocystis* sp. PCC 6803. *ACS Synthetic Biology*. 2020, 9 (2), 260-268. DOI 10.1021/acssynbio.9b00281.

69. LEE J. K. et al. Efcient production of d-lactate from methane in a lactate-tolerant strain of *Methylomonas* sp. DH-1 generated by adaptive laboratory evolution. *Biotechnology for Biofuels*. 2019, 12 (1), 234. DOI 10.1186/s13068-019-1574-9.

70. BIZZINI A. et al. Glycerol is metabolized in a complex and strain-dependent manner in *Enterococcus faecalis*. *Journal of Bacteriology*. 2010, 192 (3), 779–785. DOI 10.1128/JB.00959-09.

71. DOI Y. Glycerol metabolism and its regulation in lactic acid bacteria. *Applied Microbiology and Biotechnology*. 2019, 103, 5079–5093. DOI 10.1007/s00253-019-09830-y.

72. WANG Y., LIAO J., CHIANG C. and Y. CHAO. A simple strategy to efectively produce d-lactate in crude glycerol-utilizing *Escherichia coli*. *Biotechnology for Biofuels*. 2019, 273. DOI 10.1186/s13068-019-1615-4.

73. JÖNSSON L. and C. MARTÍN. Pretreatment of lignocellulose: Formation of inhibitory by-products and strategies for minimizing their effects. *Bioresource Technology*. 2016, 199, 103-112. DOI 10.1016/j.biortech.2015.10.009.

74. CUBAS-CANO E., LOPEZ-GOMEZ J. P., GONZALEZ-FERNANDEZ C., BALLESTEROS I. and E. TOMAS-PEJO. Towards sequential bioethanol and L-lactic acid co-generation: Improving xylose conversion to L-lactic acid in presence of lignocellulosic ethanol with an evolved *Bacillus coagulans*. *Renewable Energy*. 2020, 153, 759-765. DOI 10.1016/j.renene.2020.02.066.

75. YADAV N., PRANAW K. and S. K. KHARE. Screening of lactic acid bacteria stable in ionic liquids and lignocellulosic by-products for bio-based lactic acid production. *Bioresource Technology Reports*. 2020, 11, 100423. DOI 10.1016/j.biteb.2020.100423.

76. KARNAOURI A., ASIMAKOPOULOU G., KALOGIANNIS K. G., LAPPAS A. and E. TOPAKAS. Efficient D-lactic acid production by *Lactobacillus delbrueckii* subsp. *bulgaricus* through conversion of organosolv pretreated lignocellulosic biomass. *Biomass and Bioenergy*. 2020, 140, 105672. DOI 10.1016/j.biombioe.2020.105672.

77. QIU Z., GAO Q. and J. BAO. Constructing xylose-assimilating pathways in *Pediococcus acidilactici* for high titer D-lactic acid fermentation from corn stover feedstock. *Bioresource Technology*. 2017, 247 (Part B), 1369-1376. DOI 10.1016/j.biortech.2017.05.128.

78. YUAN S. et al. Production of optically pure l(+)-lactic acid from waste plywood chips using an isolated thermotolerant *Enterococcus faecalis* SI at a pilot scale. *Journal of Industrial Microbiology & Biotechnology*. 2018, 45 (11), 961–970. DOI 10.1007/s10295-018-2078-5.

79. JOHNSON C. W. and G. T. BECKHAM. Aromatic catabolic pathway selection for optimal production of pyruvate and lactate from lignin. *Metabolic Engineering*. 2015, 28, 240-247. DOI 10.1016/j.ymben.2015.01.005.

80. NGUYEN C. M. et al. Production of l-lactic acid from a green microalga, *Hydrodictyon reticulum*, by *Lactobacillus paracasei* LA104 isolated from the traditional Korean food, makgeolli. *Bioresource Technology*. 2012, 110, 552-559. DOI 10.1016/j.biortech.2012.01.079.

81. NGUYEN C. M. et al. D-lactic acid production from dry biomass of *Hydrodictyon reticulatum* by simultaneous saccharification and co-fermentation using *Lactobacillus coryniformis* subsp. *torquens*. *Biotechnology Letters*. 2012, 34 (12), 2235–2240. DOI 10.1007/s10529-012-1023-3.

82. CHEN C.-Y. et al. Microalgae-based carbohydrates for biofuel production. *Biochemical Engineering Journal*. 2013, 78, 1-10. DOI 10.1016/j.bej.2013.03.006.

83. KWAN T. H., HU Y. and C. S. K. LIN. Techno-economic analysis of a food waste valorisation process for lactic acid, lactide and poly(lactic acid) production. *Journal of Cleaner Production.* 2018, 181, 72-87. DOI 10.1016/j.jclepro.2018.01.179.

84. PEINEMANN J. C., DEMICHELIS F., FIORE S. and D. PLEISSNER. Techno-economic assessment of non-sterile batch and continuous production of lactic acid from food waste. *Bioresource Technology*. 2019, 289, 121631. DOI 10.1016/j.biortech.2019.121631.

85. PEJIN J. et al. Possibility of L-(+)-lactic acid fermentation using malting, brewing, and oil production by-products. *Waste Management*. 2018, 79, 153-163. DOI 10.1016/j.wasman.2018.07.035.

86. UNBAN K., KHANONGNUCH R., KANPIENGJAI A., SHETTY K. and C. KHANONGNUCH, Utilizing gelatinized starchy waste from rice noodle factory as substrate for L(+)-lactic acid production by amylolytic lactic acid bacterium *Enterococcus faecium* K-1. *Applied Biochemistry and Biotechnology*. 2020, 192, 353–366. DOI 10.1007/s12010-020-03314-w.

87. GULLÓN B., YÁÑEZ R., ALONSO J. L. and J. C. PARAJÓ. L-lactic acid production from apple pomace by sequential hydrolysis and fermentation. *Bioresource Technology.* 2008, 99 (2), 308-319. DOI 10.1016/j.biortech.2006.12.018.

88. NAKANO S., UGWU C. U. and Y. TOKIWA. Efficient production of D-(-)-lactic acid from broken rice by *Lactobacillus delbrueckii* using $Ca(OH)_2$ as a neutralizing

agent. *Bioresource Technology*. 2012, 104, 791-794. DOI 10.1016/j.biortech.2011.10.017.

89. CINGADI S., SRIKANTH K., E.V.R. A. and S. SIVAPRAKASAM. Statistical optimization of cassava fibrous waste hydrolysis by response surface methodology and use of hydrolysate based media for the production of optically pure d-lactic acid. *Biochemical Engineering Journal*. 2015, 102, 82-90. DOI 10.1016/j.bej.2015.02.006.

90. QIU Z. et al. Enhanced cellulosic d-lactic acid production from sugarcane bagasse by pre-fermentation of water-soluble carbohydrates before acid pretreatment. *Bioresource Technology*. 2023, 368, 128324. DOI 10.1016/j.biortech.2022.128324.

91. MA K. et al. D-lactic acid production from agricultural residues by membrane integrated continuous fermentation coupled with B vitamin supplementation. *Biotechnology for Biofuels and Bioproducts*. 2022, 15, 24. DOI 10.1186/s13068-022-02124-y.

92. GARRIGUES C., MERCADE M., COCAIGN-BOUSQUET M., LINDLEY N. D. and P. LOUBIERE. Regulation of pyruvate metabolism in *Lactococcus lactis* depends on the imbalance between catabolism and anabolism. *Biotechnology and Bioengineering*. 2001, 74 (2), 108-115. DOI 10.1002/bit.1100.abs.

93. GÄNZLE M. G. Lactic metabolism revisited: metabolism of lactic acid bacteria in food fermentations and food spoilage. *Current Opinion in Food Science*. 2015, 2, 106-117. DOI 10.1016/j.cofs.2015.03.001.

94. AUGUSTINIENE E. et al. Bioproduction of L- and D-lactic acids: advances and trends in microbial strain application and engineering. *Critical Reviews in Biotechnology*. 2022, 42 (3), 342-360. DOI 10.1080/07388551.2021.1940088.

95. DE LA TORRE I., LADERO M. and V. E. SANTOS. D-lactic acid production from orange waste enzymatic hydrolysates with *L. delbrueckii* cells in growing and resting state. *Industrial Crops and Products*. 2022, 146, 112176. DOI 10.1016/j.indcrop.2020.112176.

96. FORTUNE BUSINESS INSIGHTS, 2019. *Glycolic acid market size.* Maharashtra.

97. NANCUCHEO I. and JOHNSON D. B. Production of glycolic acid by chemolithotrophic iron- and sulfur-oxidizing bacteria and its role in delineating and sustaining acidophilic sulfide mineral-oxidizing consortia. *Applied and Environmental Microbiology*. 2010, 76 (2), 461–467. DOI 10.1128/AEM.01832-09.

98. KATAOKA M., SASAKI M., HIDALGO A.-R. G. D. NAKANO, M. and S. SHIMIZU. Glycolic acid production using ethylene glycol-oxidizing microorganisms. *Bioscience, Biotechnology and Biochemistry*. 2001, 65 (10), 2265-2270. DOI 10.1271/bbb.65.2265.

99. SALUSJÄRVI L. et al. Production of ethylene glycol or glycolic acid from D-xylose in *Saccharomyces cerevisiae*. *Applied Microbiology and Biotechnology.* 2017, 101 (22), 8151-8163. DOI 10.1007/s00253-017-8547-3.

100. ZHANG Z. et al. Ethylene glycol and glycolic acid production from xylonic acid by *Enterobacter cloacae*. *Microbial Cell Factories*. 2020, 19, 89. DOI 10.1186/s12934-020-01347-8.

101. ZHANG Y. et al. Coexistence of two D-lactate-utilizing systems in *Pseudomonas putida* KT2440. *Environmental Microbiology Reports*. 2016, 8 (5), 699–707. DOI 10.1111/1758-2229.12429.

102. CAM Y. et al. Engineering of a synthetic metabolic pathway for the assimilation of (d)-xylose into value-added chemicals. *ACS Synthetic Biology*. 2016, 5 (7), 607-618. DOI 10.1021/acssynbio.5b00103.

103. KOIVISTOINEN O. M. et al. Glycolic acid production in the engineered yeasts *Saccharomyces cerevisiae* and *Kluyveromyces lactis*. *Microbial Cell Factories*. 2013, 12 (1), 82. DOI 10.1186/1475-2859-12-82.

104. JIANG T., GAO C., MA C. and P. XU. Microbial lactate utilization: enzymes, pathogenesis, and regulation. *Trends in Microbiology*. 2014, 22 (10), 589-599. DOI 10.1016/j.tim.2014.05.008.

105. JIANG G. R., NIKOLOVA S. and D. P. CLARK. Regulation of the *ldhA* gene, encoding the fermentative lactate dehydrogenase of *Escherichia coli*. *Microbiology*. 2001, 147 (9), 2437–2446. DOI 10.1099/00221287-147-9-2437.

106. LIN Y.-C., CORNELL W. C., JO J., PRICE-WHELAN A. and DIETRICH, L. E. P. The *Pseudomonas aeruginosa* complement of lactate dehydrogenases enables use of D- and L-lactate and metabolic cross-feeding. *American Society for Microbiology*. 2018, 9 (5), e00961-18. DOI 10.1128/mBio.00961-18.

107. GAO C. et al. NAD-independent L-lactate dehydrogenase required for L-lactate utilization in *Pseudomonas stutzeri* A1501. *Journal of Bacteriology*. 2015, 197 (13), 2239-2247. DOI 10.1128/JB.00017-15.

108. AGUILERA L. et al. Dual role of LldR in regulation of the lldPRD operon, involved in L-lactate metabolism in *Escherichia coli*. *Journal of Bacteriology*. 2008, 180 (8), 2997–3005. DOI 10.1128/JB.02013-07.

109. JIANG T. et al. A bacterial multidomain NAD-independent D-Lactate dehydrogenase utilizes flavin adenine dinucleotide and Fe-S clusters as cofactors and quinone as an electron acceptor for D-lactate oxidization. *Journal of Bacteriology*. 2017, 199 (22), e00342-17. DOI 10.1128/JB.00342-17.

110. PELLICER M.-T., BADÍA J., AGUILAR J. and L. BALDOMÀ. *glc* Locus of *Escherichia coli*: Characterization of genes encoding the subunits of glycolate oxidase and the glc regulator protein. *Journal of Bacteriology*. 1996, 178 (7), 2051-2059. DOI 10.1128/jb.178.7.2051-2059.1996.

111. NUNEZ M. F., PELLICER M. T., BADIA J., AGUILAR J. and L. BALDOMA. The gene *yghK* linked to the *glc* operon of *Escherichia coli* encodes a permease for glycolate that is structurally and functionally similar to L-lactate permease. *Microbiology*. 2001, 147, 1069–1077. DOI 10.1099/00221287-147-4-1069.

112. LIN J.-L., WAGNER J. M. and H. S. ALPER. Enabling tools for high-throughput detection of metabolites: Metabolic engineering and directed evolution applications. *Biotechnology Advances*. 2017, 35 (8), 950-970. DOI 10.1016/j.biotechadv.2017.07.005.

113. HANKO E. K. R., MINTON N. P. and N. MALYS. Design, cloning and characterization of transcription factor-based inducible gene expression systems. *Methods in Enzymology*. 2019, 621, 153-169. DOI 10.1016/bs.mie.2019.02.018.

114. GAO Y.-G. et al. Structural and functional characterization of the LldR from *Corynebacterium glutamicum*: a transcriptional repressor involved in L-lactate and sugar utilization. *Nucleic Acids Research*. 2008, 36 (22), 7110–7123. DOI 10.1093/nar/gkn827.

115. GAO C. et al. Lactate utilization is regulated by the FadR-type regulator LldR in *Pseudomonas aeruginosa*. *Journal of Bacteriology*. 2012, 194 (10), 2687-2692. DOI 10.1128/JB.06579-11.

116. CHAI Y., KOLTER, R. and R. LOSICK. A widely conserved gene cluster required for lactate utilization in *Bacillus subtilis* and its involvement in biofilm formation. *Journal of Bacteriology*. 2009, 191 (8), 2423–2430. DOI 10.1128/JB.01464-08.

117. CHIU K.-C., LIN C.-J. and G.-C. SHAW. Transcriptional regulation of the L-lactate permease gene *lutP* by the LutR repressor of *Bacillus subtilis* RO-NN-1. *Microbiology*. 2014, 160, 2178–2189. DOI 10.1099/mic.0.079806-0.

118. RAJEEV L. et al. LurR is a regulator of the central lactate oxidation pathway in sulfate-reducing *Desulfovibrio* species. *PLoS ONE*. 2019, 14 (4), e0214960. DOI 10.1371/journal.pone.0214960.

119. SCHOELMERICH M. C. et al. Regulation of lactate metabolism in the acetogenic bacterium *Acetobacterium woodii*. *Environmental Microbiology*. 2018, 20 (12), 4587–4595. DOI 10.1111/1462-2920.14412.

120. LYNCH A. S. and C. C. E. LIN. Transcriptional control mediated by the ArcA two-component response regulator protein of *Escherichia coli*: characterization of DNA binding at target promoters. *Journal of Bacteriology*. 1996, 178 (21), 6238–6249. DOI 10.1128/jb.178.21.6238-6249.1996.

121. DONG J. M., TAYLOR J. S., LATOUR D. J., IUCHI S. and E. C. C. LIN. Three overlapping lct genes involved in L-lactate utilization by *Escherichia coli*. *Journal of Bacteriology*. 1993, 175 (20), 6671-6678. DOI 10.1128/jb.175.20.6671-6678.1993.

122. LICHTENEGGER S. *et al.*, Characterization of lactate utilization and its implication on the physiology of *Haemophilus influenzae*. *International Journal of Medical Microbiology*. 2014, 304 (3-4), 490-498. DOI 10.1016/j.ijmm.2014.02.010.

123. XU X. et al. A selective fluorescent L-lactate biosensor based on an L-lactate-specific transcription regulator and förster resonance energy transfer. *Biosensors*. 2022, 12 (12), 1111. DOI 10.3390/bios12121111.

124. SINGH K., AINALA S. K., KIM Y. and S. PARK. A novel D(−)-lactic acid-inducible promoter regulated by the GntR-family protein D-LldR of *Pseudomonas fluorescens*. *Synthetic and Systems Biotechnology*. 2019, 4 (3), 157–164. DOI 10.1016/j.synbio.2019.08.004.

125. XU S., ZHANG L., ZHOU S. and Y. DENG. Biosensor-based multigene pathway optimization for enhancing the production of glycolate. *Applied and Environmental Microbiology*. 2021, 87 (12), e00113-21. DOI 10.1128/AEM.00113-21.

126. FUTURE MARKET INSIGHTS. *Salicylic acid market size is estimated to be valued at US$ 417.8 million in 2022, with a CAGR of 6.9% from 2022 to 2032* . Newark: Future Market Insights Inc., 2022.

127. RESEARCH NESTER. *p-Hydroxycinnamic Acid Market Analysis by Product (Purity, and Modified p-Coumaric Acid); and by End-User (Chemical Industry, Food Industry, Cosmetic Industry, and Pharmaceutical Industry) – Global Supply & Demand Analysis & Opportunity Outlook 2021- 2031.* New York: Research Nester, 2022.

128. BOO Y. C. *p*-Coumaric acid as an active ingredient in cosmetics: a review focusing on its antimelanogenic effects. *Antioxidants (Basel)*. 2019, 8 (8), 275. DOI 10.3390/antiox8080275.

129. ALDABA-MURUATO L. R. et al. Therapeutic perspectives of *p*-coumaric acid: Anti-necrotic, anti-cholestatic and anti-amoebic activities. *World Academy of Sciences Journal*. 2021, 3 (5), 47. DOI 10.3892/wasj.2021.118.

130. CONTARDI M. et al. Low molecular weight ε-caprolactone-pcoumaric acid copolymers as potential biomaterials for skin regeneration applications. *PLoS ONE*. 2019, 14 (4), e0214956. DOI 10.1371/journal.pone.0214956.

131. RAMÍREZ-MORALES J. E. et al. Lignin aromatics to PHA polymers: nitrogen and oxygen are the key factors for *Pseudomonas*. *ACS Sustainable Chemistry & Engineering*. 2021, 9 (31), 10579–10590. DOI 10.1021/acssuschemeng.1c02682.

132. DEY T. B., CHAKRABORTY S., JAIN K. K., SHARMA A. and R. C. KUHAD Antioxidant phenolics and their microbial production by submerged and solid state fermentation process: A review. *Trends in Food Science & Technology*. 2016, 53, 60-74. DOI 10.1016/j.tifs.2016.04.007.

133. FLOURAT A. L. et al. Accessing *p*-hydroxycinnamic acids: chemical synthesis, biomass recovery or engineered microbial production? *ChemSusChem*. 2020, 14 (1), 118-129. DOI 10.1002/cssc.202002141.

134. BHAN N., XU P. and M. A. G. KOFFAS. Pathway and protein engineering approaches to produce novel and commodity small molecules. *Current Opinion in Biotechnology*. 2013, 24 (6), 1137-1143. DOI 10.1016/j.copbio.2013.02.019.

135. SUN X., LI X., SHEN X., WANG J. and Q. YUAN. Recent advances in microbial production of phenolic compounds. *Chinese Journal of Chemical Engineering*. 2021, 30, 54-61. DOI 10.1016/j.cjche.2020.09.001.

136. LIU Q. et al. Rewiring carbon metabolism in yeast for high level production of aromatic chemicals. *Nature Communications*. 2019, 10, 4976. DOI 10.1038/s41467-019-12961-5.

137. KOGURE T., SUDA M., HIRAGA K. and M. INUI. Protocatechuate overproduction by *Corynebacterium glutamicum* via simultaneous engineering of native and heterologous biosynthetic pathways. *Metabolic Engineering*. 2021, 65, 232-242. DOI 10.1016/j.ymben.2020.11.007.

138. WEILAND F., KOHLSTEDT M. and C. WITTMANN. Guiding stars to the field of dreams: Metabolically engineered pathways and microbial platforms for a sustainable lignin-based industry. *Metabolic Engineering*. 2022, 71, 13-41. DOI 10.1016/j.ymben.2021.11.011.

139. BASU A. and P. S. PHALE. Inducible uptake and metabolism of glucose by the phosphorylative pathway in *Pseudomonas putida* CSV86. *FEMS Microbiology Letters.* 2006, 259 (2), 311–316. DOI 10.1111/j.1574-6968.2006.00285.x.

140. PARK H., MCGILL,S. L., ARNOL, A. D. and R. P. CARLSON. Pseudomonad reverse carbon catabolite repression, interspecies metabolite exchange, and consortial division of labor. *Cellular and Molecular Life Sciences*. 2022, **77**, 395–413. DOI 10.1007/s00018-019-03377-x.

141. TRAN N. P. et al. Phenolic acid-mediated regulation of the *padC* gene, encoding the phenolic acid decarboxylase of *Bacillus subtilis*. *Journal of Bacteriology*. 2008, 190 (9), 3213–3224. DOI 10.1128/JB.01936-07.

142. SANTAMARÍA L., REVERÓN I., LÓPEZ DE FELIPE F., DE LAS RIVAS B. and R. MUÑOZ. Unravelling the reduction pathway as an alternative metabolic route to hydroxycinnamate decarboxylation in *Lactobacillus plantarum*. *Applied and Environmental Microbiology*. 2018, 84 (15), e01123-18. DOI 10.1128/AEM.01123-18.

143. CALISTI C., FICCA A. G., BARGHINI P. and RUZZI M. Regulation of ferulic catabolic genes in *Pseudomonas fluorescens* BF13: Involvement of a MarR family regulator. *Applied Microbiology and Biotechnology*. 2008, 80 (3), 475-483. DOI 10.1007/s00253-008-1557-4

144. PARKE D. and N. ORNSTON. Hydroxycinnamate (*hca*) catabolic genes from *Acinetobacter* sp. strain ADP1 are repressed by HcaR and are induced by hydroxycinnamoyl-coenzyme A thioesters. *Applied and Environmental Microbiology.* 2003, 69 (9), 5398-5409. DOI 10.1128/AEM.69.9.5398-5409.2003.

145. TORRES B., PORRAS G., GARCIA J. L. and E. DIAZ. Regulation of the *mhp* cluster responsible for 3-(3-hydroxyphenyl)propionic acid degradation in *Escherichia coli*. *Journal of Biological Chemistry*. 2003, 278 (30), 27575-85. DOI 10.1074/jbc.M303245200

146. LIU H. et al. Bacterial conversion routes for lignin valorization. *Biotechnology Advances*. 2022, 60, 108000. DOI 10.1016/j.biotechadv.2022.108000.

147. BECKER J. and C. WITTMANN. A field of dreams: Lignin valorization into chemicals, materials, fuels, and health-care products. *Biotechnology Advances*. 2019, 37 (6), 107360. DOI 10.1016/j.biotechadv.2019.02.016.

148. HANKO E. K. R. et al. A genome-wide approach for identification and characterisation of metabolite-inducible systems. *Nature Communications*. 2020, 11, 1213. DOI 10.1038/s41467-020-14941-6.

149. LEE S., KANG M., BAE J.-H., SOHN J.-H. and B. H. SUNG. Bacterial valorization of lignin: strains, enzymes, conversion pathways, biosensors, and perspectives.

Frontiers in Bioengineering and Biotechnology. 2019, 7, 209. DOI 10.3389/fbioe.2019.00209

150. LI J. et al. Construction of a *p*-coumaric and ferulic acid auto-regulatory system in *Pseudomonas putida* KT2440 for protocatechuate production from lignin-derived aromatics. *Bioresource Technology*. 2022, 344, 126221. DOI 10.1016/j.biortech.2021.126221.

151. MACHADO L. F. M. and N. DIXON. Development and substrate specificity screening of an *in vivo* biosensor for the detection of biomass derived aromatic chemical building blocks. *Chemical Communications*. 2016, 52, 11402-11405. DOI 10.1039/c6cc04559f.

152. BENSON D. A. et al. GenBank. *Nucleic Acids Research*. 2012, 41 (D1), D36–D42. DOI 10.1093/nar/gkm929.

153. KANEHISA M., FURUMICHI M., TANABE M., SATO Y. and MORISHIMA K. KEGG: New perspectives on genomes, pathways, diseases and drugs. *Nucleic Acids Research*. 2017, 45 (D1), D353-D361. DOI 10.1093/nar/gkw1092.

154. JESKE L., PLACZEK S., SCHOMBURG I., CHANG A. and D. SCHOMBURG. BRENDA in 2019: a European ELIXIR core data resource. *Nucleic Acids Research*. 2019, D1, D542-D549. DOI 10.1093/nar/gky1048.

155. DURFEE T. et al. The complete genome sequence of *Escherichia coli* DH10B: insights into the biology of a laboratory workhorse. *Journal of Bacteriology*. 2008, 190 (7), 2597-2606. DOI 10.1128/JB.01695-07.

156. CHEN J., LI Y., ZHANG K. and H. WANG. Whole-genome sequence of phage-resistant strain *Escherichia coli* DH5α. *Genome Announcements*. 2018, 6 (10), e00097-18. DOI 10.1128/genomeA.00097-18.

157. BLATTNER F. R. et al. The complete genome sequence of *Escherichia coli* K-12. *Science*. 1997, 277 (5331), 1453-1462. DOI 10.1126/science.277.5331.1453.

158. MAKKA, N. S. and L. E. CASIDA JR. *Cupriavidus necator* gen. nov., sp. nov.; a nonobligate bacterial predator of bacteria in soil. *International Journal of Systematic and Evolutionary Microbiology*. 1987, 37 (4), 323-326. DOI 10.1099/00207713-37-4-323.

159. NELSON K. E. et al. Complete genome sequence and comparative analysis of the metabolically versatile *Pseudomonas putida* KT2440. *Environmental Microbiology*. 2002, 4 (12), 799-808. DOI 10.1046/j.1462-2920.2002.00366.x.

160. HUGH R., GUARRAIA L. and HATT H. The proposed neotype strains of *Pseudomonas fluorescens* (Trevisan) Migula 1895. *International Journal of Systematic and Evolutionary Microbiology*. 1964, 14 (4), 145-155. DOI 10.1099/0096266X-14-4-145.

161. VON NEUBECK M. et al. *Pseudomonas lactis* sp. nov. and *Pseudomonas paralactis* sp. nov., isolated from bovine raw milk. *International Journal of Systematic and Evolutionary Microbiology*. 2017, 67 (6), 1656-1664. DOI 10.1099/ijsem.0.001836.

162. CARR E. L., KAMPFER P., PATEL, B. K. C., GÜRTLER, V. and R. J. SEVIOUR. Seven novel species of *Acinetobacter* isolated from activated sludge. *International Journal of Systematic and Evolutionary Microbiology*. 2003, 53 (4). DOI 10.1099/ijs.0.02486-0.

163. VANDAMME P. et al. Occurrence of multiple genomovars of *Burkholderia cepacia* in cystic fibrosis patients and proposal of *Burkholderia multivorans* sp. nov. *International Journal of Systematic and Evolutionary Microbiology*. 1997, 47 (4), 1188-1200. DOI 10.1099/00207713-47-4-1188.

164. BRINGEL F. et al. *Lactobacillus plantarum* subsp. *argentoratensis* subsp. nov., isolated from vegetable matrices. *International Journal of Systematic and Evolutionary Microbiology*. 2005, 55, 1629–1634. DOI 10.1099/ijs.0.63333-0.

165. WEISS N., SCHILLINGER U. and O. KANDLER. *Lactobacillus lactis*, *Lactobacillus leichmannii* and *Lactobacillus bulgaricus*, subjective synonyms of *Lactobacillus delbrueckii*, and description of *Lactobacillus delbrueckii* subsp. *lactis* comb. nov. and *Lactobacillus delbrueckii* subsp. *bulgaricus* comb. nov. *Systematic and Applied Microbiology*. 1983, 4 (4), 552-557. DOI 10.1016/S0723-2020(83)80012-5.

166. NAKAMURA L. K. *Lactobacillus amylovorus*, a new starch-hydrolyzing species from cattle waste-corn fermentations. *International Journal of Systematic and Evolutionary Microbiology*. 1981, 31 (1), 56-63. DOI 10.1099/00207713-31-1-56.

167. COLLINS M. D., PHILLIPS B. A. and P. ZANONI. Deoxyribonucleic acid homology studies of *Lactobacillus casei*, *Lactobacillus paracasei* sp. nov., subsp. *paracasei* and subsp. *tolerans*, and *Lactobacillus rhamnosus* sp. nov., comb. nov. *International Journal of Systematic and Evolutionary Microbiology*. 1989, 39 (2), 105-108. DOI 10.1099/00207713-39-2-105.

168. SAMBROOK J. F. and D. W. RUSSELL. *Molecular Cloning: A Laboratory Manual, 3rd ed., Vols 1,2 and 3*. Cold Spring Harbor Laboratory Press, New York, 2001.

169. SCHLEGEL H. G., KALTWASSER H. and G. GOTTSCHALK. Ein Submersverfahren zur Kultur wasserstoffoxydierender Bakterien: Wachstumsphysiologische Untersuchungen. *Archiv für Mikrobiologie*. 1962, 38, 209–222. DOI 10.1007/BF00422356.

170. AUSUBEL F. M. et al. *Current Protocols in Molecular Biology*. John Wiley & Sons, 1988.

171. GIAVARINA D. Understanding Bland Altman analysis. *Biochemia medica*. 2015, 25 (2), 141-151. DOI 10.11613/BM.2015.015.

172. AUGUSTINIENE E. and MALYS N. Identification and characterization of L- and D-lactate-inducible systems from *Escherichia coli* MG1655, *Cupriavidus necator* H16 and *Pseudomonas* species. *Scientific Reports*. 2022, 12, 2123. DOI 10.1038/s41598-022-06028-7.

173. SWEENEY J., MURPHY C. D. and MCDONNELL K. Towards an effective biosensor for monitoring AD leachate: a knockout *E. coli* mutant that cannot catabolise lactate. *Applied Microbiology and Biotechnology*. 2015, 99, 10209–10214. DOI 10.1007/s00253-015-6887-4.

174. PINCHUK G. E. et al. Genomic reconstruction of *Shewanella oneidensis* MR-1 metabolism reveals a previously uncharacterized machinery for lactate utilization. *Proceedings of the National Academy of Sciences of the United States of America*. 2009, **106** (8), 2874-2879. DOI 10.1073/pnas.0806798106.

175. ALAGESAN S. et al. Functional genetic elements for controlling gene expression in *Cupriavidus necator* H16. *Applied and Environmental Microbiology*. 2018, 84 (19), e00878-18. DOI 10.1128/AEM.00878-18**.**

176. ZÚÑIGA A. *et al.*, Engineered L-lactate responding promoter system operating in glucose-rich and anoxic environments. *ACS Synthetic Biology*. 2021, 10 (12), 3527–3536. DOI 10.1021/acssynbio.1c00456.

177. REIS A. C. and H. M. SALIS. An automated model test system for systematic development and improvement of gene expression models. *ACS Synthetic Biology*. 2020, 9 (11), 3145-3156. DOI 10.1021/acssynbio.0c00394.

178. ARAI H. et al. Genetic organization and characteristics of the 3-(3-hydroxyphenyl)propionic acid degradation pathway of *Comamonas testosteroni* TA441. *Microbiology*. 1999, 145, 2813–2820. DOI 10.1099/00221287-145-10-2813.

179. BARNES M. R., DUETZ W. A. and P. A. WILLIAMS. A 3-(3-hydroxyphenyl)propionic acid catabolic pathway in *Rhodococcus globerulus* PWD1: cloning and characterization of the hpp operon. *Journal of Bacteriology*. 1997, 179 (19), 6145-6153. DOI 10.1128/jb.179.19.6145-6153.1997.

180. HANKO E. K. R., MINTON N. P. and N. MALYS. Characterisation of a 3-hydroxypropionic acid-inducible system from *Pseudomonas putida* for orthogonal gene expression control in *Escherichia coli* and *Cupriavidus necator*. *Scientific Reports*. 2017, **7**, 1724. DOI 10.1038/s41598-017-01850-w.

181. MATULIS P. and N. MALYS. Nanomolar biosensor for detection of phenylacetic acid and L-phenylalanine. *Biochemical Engineering Journal*. 2023, 191, 108765. DOI 10.1016/j.bej.2022.108765.

182. BARTHELMEBS L., DIVIES C. and J.-F. CAVIN. Knockout of the *p*-coumarate decarboxylase gene from *Lactobacillus plantarum* reveals the existence of two other inducible enzymatic activities involved in phenolic acid metabolism. *Applied and Environmental Microbiology*. 2000, 66 (8), 3368-3375. DOI 10.1128/aem.66.8.3368-3375.2000.

183. CILLIERS J. J. L. and V. L. SINGLETON. Caffeic acid autoxidation and the effects of thiols. *Journal of Agricultural and Food Chemistry*. 1990, 38 (9), 1789–1796. DOI 10.1021/jf00099a002.

184. COELHO L. F., LIMA C. J. B. D., BERNARDO M. P., ALVAREZ G. M. and J. CONTIERO. Improvement of L(+)-lactic acid production from cassava waste water by *Lactobacillus rhamnosus* B 103. *Journal of the Science of Food and Agriculture*. 2010, **90** (11), 1944 - 1950. DOI 10.1002/jsfa.4039.

185. AUGCHARARAT K. et al. Improvement of enantiomeric L-lactic acid production from mixed hexose-pentose sugars by coculture of *Enterococcus mundtii* WX1 and

Lactobacillus rhamnosus SCJ9. *Fermentation.* 2021, **7** (2), 95. DOI 10.3390/fermentation7020095.

186. GALI K. K. et al. Bioprospecting of cassava fibrous waste as a precursor for stereospecific lactic acid production: inhibition insights for value addition and sustainable utilization. *Biomass Conversion and Biorefinery*. 2023, 13, 2255–2265. DOI 10.1007/s13399-020-01272-1.

187. OH H., WEE Y.-J., YUN J.-S. and H.-W. RYU. Lactic acid production through cell-recycle repeated-batch bioreactor. *Applied Biochemistry and Biotechnology*. 2003, 107 (1-3), 603-613. DOI 10.1385/abab:107:1-3:603.

188. YANKOV D. Fermentative lactic acid production from lignocellulosic feedstocks: from source to purified product. *Frontiers in Chemistry.* 2022, 10, 823005. DOI 10.3389/fchem.2022.823005.

189. QIU Z. et al. Enhanced cellulosic D-lactic acid production from sugarcane bagasse by pre-fermentation of water-soluble carbohydrates before acid pretreatment. *Bioresource Technology*. 2023, 368, 128324. DOI 10.1016/j.biortech.2022.128324.

190. RAWOOF S. A. A., KUMAR P. S., DEVARAJ K., DEVARAJ, T. and S. SUBRAMANIAN. Enhancement of lactic acid production from food waste through simultaneous saccharification and fermentation using selective microbial strains. *Biomass Conversion and Biorefinery*. 2022, 12 (12), 5947-5958. DOI 10.1007/s13399-020-00998-2.

191. CHANKVETADZE B. Recent trends in preparation, investigation and application of polysaccharide-based chiral stationary phases for separation of enantiomers in high-performance liquid chromatography. *TrAC Trends in Analytical Chemistry*. 2020, 122, 115709. DOI 10.1016/j.trac.2019.115709.

192. XU X. et al. A selective fluorescent L-lactate biosensor based on an L-lactate-specific transcription regulator and Förster resonance energy transfer. *Biosensors.* 2022, 12 (12), 1111. DOI 10.3390/bios12121111.

193. IBÁÑEZ A. B. and S. BAUER. Analytical method for the determination of organic acids in dilute acid pretreated biomass hydrolysate by liquid chromatography-time-of-flight mass spectrometry. *Biotechnology for Biofuels*. 2014, **7** (1), 145. DOI 10.1186/s13068-014-0145-3.

194. LI J.-W., ZHANG X.-Y., WU H. and Y.-P. BAI. Transcription factor engineering for high-throughput strain evolution and organic acid bioproduction: A review. *Frontiers in Bioengineering and Biotechnology*. 2020, **8** (98). DOI 10.3389/fbioe.2020.00098.

195. DE LIMA C. J. B., COELHO L. F., BLANCO K. C. and J. CONTIERO. Response surface optimization of D(-)-lactic acid production by *Lactobacillus* SMI8 using corn steep liquor and yeast autolysate as an alternative nitrogen source. *African Journal of Biotechnology*. 2009, 8, 5842-5846. DOI 10.5897/AJB09.627.

196. BROCK S., KUENZ A. and U. PR€UßE. Impact of hydrolysis methods on the utilization of agricultural residues as nutrient source for D-lactic acid production by *Sporolactobacillus inulinus*. *Fermentation*. 2019, 5 (1), 12. DOI 10.3390/fermentation5010012.

197. LI Y., WANG L., JU J., YU B. and Y. MA. Efficient production of polymer-grade D-lactate by *Sporolactobacillus laevolacticus* DSM442 with agricultural waste cottonseed as the sole nitrogen source. *Bioresource Technology*. 2013, 142, 186-191. DOI 10.1016/j.biortech.2013.04.124.

198. WANG L. et al. Highly efficient production of D-lactate by *Sporolactobacillus* sp. CASD with simultaneous enzymatic hydrolysis of peanut meal. *Applied Microbiology and Biotechnology*. 2011, 89, 1009–1017. DOI 10.1007/s00253-010-2904-9.

199. CONDON S. Responses of lactic acid bacteria to oxygen. *FEMS Microbiology Reviews*. 1897, 3 (3), 269-280. DOI 10.1016/0378-1097(87)90112-1.

200. LÓPEZ-GARZÓN C. S. and A. J. J. STRAATHOF. Recovery of carboxylic acids produced by fermentation. *Biotechnology Advances*. 2014, 32 (5), 873-904. DOI 10.1016/j.biotechadv.2014.04.002.

201. MIN D.-J., CHOI K. H., CHANG Y. K. and J.-H. KIM. Effect of operating parameters on precipitation for recovery of lactic acid from calcium lactate fermentation broth. *Korean Journal of Chemical Engineering*. 2011, 28 (10), 1969-1974. DOI 10.1007/s11814-011-0082-9.

202. LUX S. and M. SIEBENHOFER. Investigation of liquid–liquid phase equilibria for reactive extraction of lactic acid with organophosphorus solvents. *Chemical Technology & Biotechnology*. 2013, 88 (3), 462-467. DOI 10.1002/jctb.3847.

203. UDACHAN I. S. and A. K. SAHOO. A study of parameters affecting the solvent extraction of lactic acid from fermentation broth. *Brazilian Journal of Chemical Engineering*. 2014, 31 (3), 821-827. DOI 10.1590/0104-6632.20140313s00002495.

204. LI Q.-Z. et al. Recovery processes of organic acids from fermentation broths in the biomass-based industry. *Journal of Microbiology and Biotechnology*. 2016, 26 (1), 1-8. DOI 10.4014/jmb.1505.05049.

205. SCHOLLER C., CHAUDHURI J. B. and D. L. PYLE. Emulsion liquid membrane extraction of lactic acid from aqueous solutions and fermentation broth. *Biotechnology and Bioengineering*. 1993, 42 (1), 50–58. DOI 10.1002/bit.260420108.

206. KUMAR R., NANAVATI H., NORONHA S. B. and S. M. MAHAJANI. A continuous process for the recovery of lactic acid by reactive distillation. *Journal of Chemical Technology and Biotechnology*. 2006, 81, 1767–1777. DOI 10.1002/jctb.1603.

207. ALEXANDRI M., SCHNEIDER R. and J. VENUS. Membrane technologies for lactic acid separation from fermentation broths derived from renewable resources. *Membranes (Basel). 2018*, 8 (4), 94. DOI 10.3390/membranes8040094.

208. MANZAK A. and O. TUTKUN. The extraction of lactic acid by emulsion type of liquid membranes using alamine 336 in escaid 100. *The Canadian Journal of Chemical Engineering*. 2011, 89 (6), 1458-1463. DOI 10.1002/cjce.20501.

209. GHAFFAR T. et al. Recent trends in lactic acid biotechnology: a brief review on production to purification. *Journal of Radiation Research and Applied Sciences*. 2014, **7** (2), 222-229. DOI 10.1016/j.jrras.2014.03.002.

210. WASEWAR K. L. Separation of lactic acid: recent advances. *Chemical and Biochemical Engineering Quarterly*. 2005, 19 (2), 159-172. DOI 10.15255/CABEQ.2014.522.

211. LEE H. D. et al. Separation and purification of lactic acid from fermentation broth using membrane-integrated separation processes. *Industrial & Engineering Chemistry Research*. 2017, 56 (29), 830. DOI 10.1021/acs.iecr.7b02011.

212. LÓPEZ-GÓMEZ J. P., ALEXANDRI M., SCHNEIDER R. and J. VENUS. A review on the current developments in continuous lactic acid fermentations and case studies utilising inexpensive raw materials. *Process Biochemistry*. 2019, 79, 1-10. DOI 10.1016/j.procbio.2018.12.012.

213. FREI C. S., QIAN S. and P. C. CIRINO. New engineered phenolic biosensors based on the AraC regulatory protein. *Protein Engineering, Design and Selection*. 2018, 31, 213–220. DOI 10.1093/protein/gzy024.

214. QIAN S., LI Y. and P. C. CIRINO. Biosensor-guided improvements in salicylate production by recombinant *Escherichia coli*. *Microb. Cell Factories.* 2019, 18, 18. DOI 10.1186/s12934-019-1069-1.

215. MACHADO L. F. M., CURRIN A. and N. DIXON. Directed evolution of the PcaV allosteric transcription factor to generate a biosensor for aromatic aldehydes. *Journal of Biological Engineering*. 2019, 13, 91. DOI 10.1186/s13036-019-0214-z.

216. HIROMOTO T. et al. Characterization of MobR, the 3-hydroxybenzoate-responsive transcriptional regulator for the 3-hydroxybenzoate hydroxylase gene of *Comamonas testosteroni* KH122-3s. *Journal of Molecular Biology.* 2006, 364 (5), 863-877. DOI 10.1016/j.jmb.2006.08.098.

217. QUINN J. A., MCKAY D. B. and B. ENTSCH. Analysis of the *pobA* and *pobR* genes controlling expression of *p*-hydroxybenzoate hydroxylase in *Azotobacter chroococcum*. *Gene.* 2001, 264 (1), 77-85. DOI 10.1016/s0378-1119(00)00599-0.

218. DIMARCO A. A., AVERHOFF B. and L. N. ORNSTON. Identification of the transcriptional activator *pobR* and characterization of its role in the expression of *pobA*, the structural gene for *p*-hydroxybenzoate hydroxylase in *Acinetobacter calcoaceticus*. *Journal of Bacteriology.* 1993, 175 (14), 4499-4506. DOI 10.1128/jb.175.14.4499-4506.1993.

219. CASTAÑO-CEREZO S., FOURNIÉ M., URBAN P., FAULON J.-L. and G. TRUAN. Development of a biosensor for detection of benzoic acid derivatives in *Saccharomyces cerevisiae*. *Frontiers in Bioengineering and Biotechnology*. 2020, **7**, 372. DOI 10.3389/fbioe.2019.00372.

220. JHA R. K., CHAKRABORTI S., KERN T. L., FOX D. T. and C. E. M. STRAUSS. Rosetta comparative modeling for library design: Engineering alternative inducer specificity in a transcription factor. *Proteins.* 2015, 83 (7), 1327–1340. DOI 10.1002/prot.24828.

221. JHA R. K. et al. Sensor-enabled alleviation of product inhibition in chorismate pyruvate-lyase. *ACS Synthetic Biology*. 2019, 8 (4), 775–786. DOI 10.1021/acssynbio.8b00465.

222. KUNJAPUR A. M. and K. L. J. PRATHER. Development of a vanillate biosensor for the vanillin biosynthesis pathway in *E. coli*. *ACS Synthetic Biology.* 2019, **8** (9), 1958–1967. DOI 10.1021/acssynbio.9b00071.

223. MEYER A. J., SEGALL-SHAPIRO T. H., GLASSEY E., ZHANG J. and C. A. VOIGT. *Escherichia coli* "Marionette" strains with 12 highly optimized small-molecule sensors. *Nature Chemical Biology*. 2019, 15, 196–204. DOI 10.1038/s41589-018-0168-3.

224. D'AMBROSIO V. et al. Directed evolution of VanR biosensor specificity in yeast. *Biotechnology Notes.* 2020, 1, 9-15. DOI 10.1016/j.biotno.2020.01.002.

225. ARAKI T. et al. The syringate *o*-demethylase gene of *Sphingobium* sp. strain SYK-6 is regulated by DesX, while other vanillate and syringate catabolism genes are regulated by DesR. *Applied and Environmental Microbiology*. 2020, 86 (22), e01712-20. DOI 10.1128/AEM.01712-20.

226. AMBRI F. et al. High-resolution scanning of optimal biosensor reporter promoters in yeast. *ACS Synthetic Biology.* 2020, 9 (2), 218–226. DOI 10.1021/acssynbio.9b00333.

227. STRACHAN C. R. et al. Metagenomic scaffolds enable combinatorial lignin transformation. *Proceedings of the National Academy of Sciences of the United States of America*. 2014, 111 (28), 10143-10148. DOI 10.1073/pnas.1401631111.

228. VARMAN A. M. et al. Hybrid phenolic-inducible promoters towards construction of self-inducible systems for microbial lignin valorization. *Biotechnology for Biofuels*. 2018, 11, 182. DOI 10.1186/s13068-018-1179-8.

229. NOGALES J. et al. Unravelling the gallic acid degradation pathway in bacteria: the *gal* cluster from *Pseudomonas putida*. *Molecular Microbiology*. 2011, 79 (2), 359–374. DOI 10.1111/j.1365-2958.2010.07448.x.

230. JHA R. K., KERN T. L., FOX D. T. and STRAUSS C. E. M. Engineering an *Acinetobacter* regulon for biosensing and high-throughput enzyme screening in *E. coli* via flow cytometry. *Nucleic Acids Research*. 2014, 42 (12), 8150–8160. DOI 10.1093/nar/gku444.

231. JHA R. K. et al. A protocatechuate biosensor for *Pseudomonas putida* KT2440 via promoter and protein evolution. *Metabolic Engineering Communications*. 2018, 6, 33-38. DOI 10.1016/j.meteno.2018.03.001.

232. PACHECO-SÁNCHEZ D., MOLINA-FUENTES Á., MARÍN P., DÍAZ-ROMERO A. and S. MARQUÉS. DbdR, a new member of the LysR family of transcriptional regulators, coordinately controls four promoters in the *Thauera aromatica* AR-1 3,5-dihydroxybenzoate anaerobic degradation pathway. *Applied and Environmental Microbiology*. 2019, 85 (2), e02295-18. DOI 10.1128/AEM.02295-18.

233. KASAI D. et al. γ-Resorcylate catabolic-pathway genes in the soil actinomycete *Rhodococcus jostii* RHA1. *Applied and Environmental Microbiology.* 2015, 81 (21), 7656-7665. DOI 10.1128/AEM.02422-15.

234. JIANG T., LI C. and Y. YAN. Optimization of a *p*-coumaric acid biosensor system for versatile dynamic performance. *ACS Synthetic Biology*. 2021, 10 (1), 132–144. DOI 10.1021/acssynbio.0c00500.

CURRICULUM VITAE

Personal information

Name, Surname	**Ernesta Augustinienė**
Date of birth	20 August 1994
Email	ernesta.augustiniene@ktu.lt
ORCID	0000-0001-9002-3545

Education

2019 – 2023	Doctoral studies, Chemical Engineering, Kaunas University of Technology, Faculty of Chemical Technology
2017 – 2019	Master's degree in Industrial Biotechnology, Kaunas University of Technology, Faculty of Chemical Technology
2013 – 2017	Bachelor's degree in Biotechnology, Vytautas Magnus University, Faculty of Natural Sciences

Work Experience

June 2019 – *present*
Project Junior Researcher at Kaunas University of Technology, Faculty of Chemical Technology, Bioprocess Research Center
July 2018 – August 2018
Laboratory Specialist at AB *Kauno grūdai*
May 2017/05 – August 2017
Receptionist at UAB *Diagnostikos laboratorija*

LIST OF PUBLICATION AND CONFERENCES

Publications related to the topic of the dissertation published in journals indexed in the *Clarivate Analytics Web of Science* with Impact Factor

1. **Augustiniene, Ernesta**; Malys, Naglis. Identification and characterization of L- and D-lactate inducible systems from *Escherichia coli* MG1655, *Cupriavidus necator* H16 and *Pseudomonas* species //Scientific Reports. Berlin: Springer Nature. ISSN 2045-2322. 2022, Vol. 12, iss. 1, art. No. 2123, p. 1-11. DOI:10.1038/s41598-022-06028-7. Impact Factor: 4.9

2. **Augustiniene, Ernesta**; Valanciene, Egle; Matulis, Paulius; Syrpas, Michail; Jonuskiene, Ilona; Malys, Naglis. Bioproduction of l- and d-lactic acids: advances and trends in microbial strain application and engineering // Critical reviews in biotechnology. Abingdon: Taylor & Francis. ISSN 0738-8551. eISSN 1549-7801. 2022, Vol. 42, iss. 3, p. 342-360. DOI: 10.1080/07388551.2021.1940088. Impact Factor: 9.0

3. Valanciene, Egle; Jonuskiene, Ilona; Syrpas, Michail; **Augustiniene, Ernesta**; Matulis, Paulius; Simonavicius, Andrius; Malys, Naglis. Advances and prospects of phenolic acids production, biorefinery and analysis // Biomolecules. Basel: MDPI. ISSN 2218-273X. 2020, Vol. 10, iss. 6, art. No. 874, p. 1-41. DOI: 10.3390/biom10060874. Impact Factor: 5.5

4. **Augustiniene, Ernesta**; Kutraite, Ingrida; Valanciene, Egle; Matulis, Paulius; Jonuskiene, Ilona; Malys, Naglis. Transcription factor-based biosensors for detection of naturally occurring phenolic acids // New BIOTECHNOLOGY. Impact Factor: 5.4 **(submitted)**

5. **Augustiniene, Ernesta**; Jonuskiene, Ilona; Kailiuviene, Jurgita; Mažonienė, Edita; Baltakys, Kęstutis; Malys, Naglis. Biosensor-assisted optimization of L- and D-lactic acid production from wheat starch by *Lactobacillus* spp. // Microbial Cell Factories. Impact Factor: 6.4 **(submitted)**

Other publication published in journals indexed in the *Clarivate Analytics Web of Science* with Impact Factor

1. Matulis, Paulius; Kutraite, Ingrida; **Augustiniene, Ernesta**; Valanciene, Egle; Jonuskiene, Ilona; Malys, Naglis. Development and characterization of indole-responsive whole-cell biosensor based on the inducible gene expression system from *Pseudomonas putida* KT2440 // International journal of molecular sciences. Basel: MDPI. ISSN 1661-6596. eISSN 1422-0067. 2022, Vol. 23, iss. 9, art. No. 4649, p. 1-12. DOI:10.3390/ijms23094649. Impact Factor: 5.6

2. Syrpas, Michail; Valanciene, Egle; **Augustiniene, Ernesta**; Malys, Naglis. Valorization of Bilberry (*Vaccinium myrtillus* L.) pomace by enzyme-assisted extraction: process optimization and comparison with conventional solid-liquid extraction // Antioxidants. Basel: MDPI. ISSN 2076-3921. 2021, Vol. 10, iss. 5, art. No. 773, p. 1-15. DOI: 10.3390/antiox10050773. Impact Factor: 7.0

Presentations in international conferences

1. **Augustiniene, Ernesta**; Malys, Naglis. Identification and characterization of L- and D-lactic acid-inducible systems for transcription factor-based biosensor development // Open Readings 2021: 64th international conference for students of physics and natural sciences, March 16-19, Vilnius, Lithuania: abstract book / editors: Š. Mickus, R. Platakytė, S. Pūkienė. Vilnius: Vilnius University Press. 2021, P7-35, p. 452.

2. **Augustiniene, Ernesta**; Kutraitė, Ingrida; Malys, Naglis. Identification and characterization of *p*-coumarate and ferulate-inducible systems for transcription factor-based biosensors development // Open Readings 2022: 65th international conference for students of physics and natural sciences, March 15-18: abstract book / editors: Š. Mickus, S. Pūkienė, L. Naimovičius. Vilnius: Vilnius University Press. 2022, P5-4, p. 311.

3. **Augustiniene, Ernesta**; Malys, Naglis. Towards whole-cell biosensor development for monitoring L-and D-lactic acids. 6th Applied synthetic biology in Europe, Edinburgh, United Kingdom, 2-4 November 2022: programme and abstracts. 2022, poster 67, p. 116.

4. **Augustiniene, Ernesta**; Malys, Naglis. Development of transcription factor-based biosensors for L-and D-lactic acids. VIII Baltic Genetics Congress. Biologija, 2023, Vol. 69, No. 1, p. 25. ISSN 2029-0578.

ACKNOWLEDGMENTS

I would like to acknowledge my supervisor Prof. Dr. Kęstutis Baltakys for the provided study opportunities and consultation throughout the preparation of my PhD thesis. My sincere appreciation is sent to my thesis scientific advisor Prof. Dr. Naglis Malys for responsible consultations, suggestions, and feedback that encourage interest and improvement.

This project would not have been possible without the collaboration with Dr. Edita Mažonienė, Jurgita Kailiuviene, and the company *Roquette Amilina*, I would like to express my gratitude for providing glucose syrup production industrial waste and carrying out their composition analyses.

I would like to thank Assoc. Prof. Dr. Michail Syrpas for assistance with HPLC analysis. I feel especially thankful to Assoc. Prof. Dr. Ilona Jonuškienė for continuous help, support, and guidance. Finally, thank you Dr. Eglė Valančienė, Ingrida Kutraitė, and Paulius Matulis for all the discussions, help, and for creating a supportive environment.

SUPPLEMENTARY INFORMATION

Supplementary Tables

Supplementary Table S1. L-lactic acid production using alternative substrates

Microorganism (relevant characteristics)	Carbon source	Fermentation mode	Concentration (g/L)	Yield (g/g) consumed substrate	Productivity (g/(Lh))	References
E. faecalis QU 11	glycerol	fed-batch, fermentation coupled with acetic acid reduction to ethanol	55.3	**0.97**	0.772	[62]
E. faecalis SI	acid-impregnated steam explosion-treated plywood chips (glucose)	batch, SHF	59.81	**0.97**	1.07	[78]
L. rhamnosus ATCC 7469	brewer's spent grain hydrolysate (glucose)	fed-batch, SHF	58.01	**0.88**	1.19	[85]
E. faecium K-1	gelatinised starchy waste	batch, 37 °C amylolytic microorganism	87.2	**0.88**	1.82	[86]
L. rhamnosus ATCC 9595 (CECT288)	apple pomace (glucose, fructose)	batch, SHF	32.5	**0.88**	5.41	[87]

Supplementary Table S2. Previously reported hydroxybenzoic and hydroxycinnamic acids-inducible gene expression systems. The dataset is based on the research reported in literature; it does not include patented information and is not complete.

Phenolic acid	Inducible systems	Source	Host	Observed induction factor	System specificity	Analysis method	Application	Reference
Hydroxybenzoic acid-inducible gene expression systems								
o-hydroxybenzoic acid	*Cn*NahR/$P_{H16\_RS08125}$	*C. necator* H16	*E. coli* TOP10; *P. putida* KT2440; *C. necator* H16	about 100-fold induction (*E. coli* TOP10 and *P. putida* KT2440); 650.8-fold induction (*C. necator* H16)	specific	RFP fluorescence measurement	N/A	[148]
o-hydroxybenzoic acid	*Ec*AraC-TAL10/P_{BAD}	*E. coli*	*E. coli* HF19	218-fold induction	partially specific (responds to vanillic acid)	negative-FACS sorting	N/A	[213]
o-hydroxybenzoic acid	*Ec*AraC-TAL10/P_{BAD}	*E. coli*	*E. coli* HF19	200-fold induction	partially specific (responds to vanillic acid)	GFP fluorescence measurement	high-throughput screening tool; improved salicylate production	[214]

Continued Supplementary Table S2

m-hydroxybenzoic acid	*Sc*PcaV(mutPCA1)/P_{PV}	*S. coelicolor*	*E. coli* BL21	2.8-fold induction	partially specific (responds to *p*-hydroxybenzoic acid, protocatechuic acid)	eGFP fluorescence measurement	PcaV directed evolution	[215]
m-hydroxybenzoic acid	*Ct*MobR/P_{mobA}	*C. testosteroni* KH122-3s	*E. coli* TG-1	11.6-fold induction	partially specific (responds to *o*-hydroxybenzoic acid and *p*-hydroxybenzoic acid)	β-galactosidase assay	N/A	[216]
p-hydroxybenzoic acid	*Ac*pobR/P_{pobA}	*A. chroococcum* ATCC 9043	*E. coli* DH5α	40% activity	N/A	*p*-hydroxybenzoate hydroxylase activity measurement	N/A	[217]
p-hydroxybenzoic acid	*Ac*pobR/P_{pobA}	*A. calcoaceticus* ADP1 (*A. baylyi* ADP1)	*A. calcoaceticus* ADP4005 (pZR427)	275.5-fold induction	N/A	β-galactosidase assay	N/A	[218]
p-hydroxybenzoic acid	*Rps*HbaR/P_{CYC1} (sBAD biosensor)	*R. palustris*	*S. cerevisiae* CEN.PK 2C-1	3-fold induction	nonspecific	mCitrine yellow fluorescence measurement	*in vivo* pHBA detection in genetically modified *S. cerevisiae* strain	[219]

Continued Supplementary Table S2

p-hydroxybenzoic acid	*Ab*PobR/P_{pobA}	*A. baylyi* ADP1	*E. coli*	30-fold induction	N/A	GFP fluorescence measurement	N/A	[220]
p-hydroxybenzoic acid	*Pp*PobR-DM/P_{pobA}	*P. putida* KT2440	*P. putida* CJ182	7-fold induction	N/A	sfGFP fluorescence measurement	high-throughput screening tool; muconate production	[221]
p-hydroxybenzoic acid	*Sc*PcaV(mutPCA1)/P_{PV}	*S. coelicolor*	*E. coli* BL21	3.6-fold induction	partially specific (responds to *m*-hydroxybenzoic acid, protocatechuic acid)	eGFP fluorescence measurement	PcaV directed evolution	[215]
vanillic acid	*Cc*VanR/P_{VanO}	*C. crescentus*	*E. coli* DH5α	14-fold induction	N/A	RFP fluorescence measurement	*O*-methyltransferases enzymes screening	[222]
vanillic acid	*Cc*$VanR^{AM}$ /P_{VanCC}	*C. crescentus*	*E. coli* DH10B	1200-fold induction	specific	YFP fluorescence measurement	N/A	[223]
vanillic acid	*Ec*AraC-Van6/P_{BAD}	*E. coli*	*E. coli* HF19	170-fold induction	partially specific (responds to *o*-hydroxybenzoic acid)	negative-FACS sorting	N/A	[213]

Continued Supplementary Table S2

vanillic acid	*Cc* TEF1p:VanR/$P_{TEF1p2xVanO}$	*C. crescentus*	*S. cerevisiae* CEN.PK113–11C	3.7-fold induction	N/A	GFP fluorescence measurement	N/A	[224]
vanillic acid	*Sp*DesX/P_{SLG_25010}	*Sphingobium* sp. SYK-6	*Sphingobium* sp. SYK-6 pSDA2	12-fold induction	N/A	β-galactosidase assay	N/A	[225]
vanillic acid	*Cc*VanR/P_{VanO_83}	*C. crescentus*	*S. cerevisiae* CEN.PK102-5B	8.6-fold induction	N/A	yeGFP fluorescence measurement	N/A	[226]
vanillic acid	*Ec*EmrR/P_{emrRAB}	*E. coli* K12	*E. coli* Mach1	1-fold induction	partially specific (responds to vanillin, *p*-coumaric acid, *o*-hydroxybenzoic acid)	GFP fluorescence measurement	high-throughput screening tool	[227]
vanillic acid	*Ec*P_{vtac}	*E. coli* pNW33N	*E. coli* Mach1	9.5-fold induction	partially specific (responds to coumaric acid)	mCherry fluorescence measurement	N/A	[228]
isovanillic acid	N/A	N/A	N/A	N/A	N/A	N/A	N/A	N/A
gallic acid	*Pp*GalR/$P_{PP\_RS13150}$	*P. putida* KT2440	*P. putida* KT2440	2300-fold induction	N/A	β-galactosidase assay	N/A	[229]
protocatechuic acid	*Ab*PcaU^{AM}/P_{3B5}	*A. baylyi* ADP1 pAJM.690	*E. coli* DH10B	360-fold induction	specific	YFP fluorescence measurement	N/A	[223]

Continued Supplementary Table S2

protocatechuic acid	*Cn*PcaQ/$P_{H16\_RS30145}$	*C. necator* H16	*E. coli* TOP10 *P. putida* KT2440 *C. necator* H16	100-fold induction (*E. coli* TOP10 and *P. putida* KT2440) 77.2-fold induction (*C. necator* H16)	partially specific (*p*-hydroxybenzoic acid)	RFP fluorescence measurement	N/A	[148]
protocatechuic acid	*Sc*PcaV/P_{PV}	*S. coelicolor*	*E. coli* DH5α	521-fold induction	N/A	sfGFP fluorescence measurement	N/A	[39]
protocatechuic acid	*Ab*PcaU/P_{pcaI}	*A. baylyi* ADP1	*E. coli* BL21-Gold(DE3)	14-fold induction	N/A	GFP fluorescence measurement	high-throughput screening tool	[230]
protocatechuic acid	*Sc*PcaV(mutPCA1)/P_{PV}	*S. coelicolor*	*E. coli* BL21	3-fold induction	partially specific (responds to *p*-hydroxybenzoic acid, *m*-hydroxybenzoic acid)	eGFP fluorescence measurement	PcaV directed evolution	[215]
protocatechuic acid	*Ab*PcaU/P_{pcaI}	*A. baylyi* ADP1	*P. putida* KT2440	12-fold induction	partially specific (responds to catechol)	sfGFP fluorescence measurement	protocatechuic acid production real-time monitoring	[231]
syringic acid	*Sp*DesX/P_{SLG_25010}	*Sphingobium* sp. SYK-6	*Sphingobium* sp. SYK-6 pSDA2	12-fold induction	N/A	β-galactosidase assay	N/A	[225]

Continued Supplementary Table S2

gentisic acid	N/A	N/A	N/A	N/A	N/A	N/A	N/A	N/A
α-resorcylic acid	*Ta*DbdR/P_{dbhL}	*T. aromatica* AR-1	*T. aromatica* AR-1	2-fold induction	N/A	β-galactosidase assay	N/A	[232]
β-resorcylic acid	N/A	N/A	N/A	N/A	N/A	N/A	N/A	N/A
γ-resorcylic acid	*Rj*TsdR/P_{tsdB}	*R. jostii* RHA1	*R. jostii* RHA1	N/A	N/A	N/A	N/A	[233]
orsellinic acid	N/A	N/A	N/A	N/A	N/A	N/A	N/A	N/A
6-methylsalicylic acid	N/A	N/A	N/A	N/A	N/A	N/A	N/A	N/A
Hydroxycinnamic acids-inducible gene expression systems								
o-coumaric acid	N/A	N/A	N/A	N/A	N/A	N/A	N/A	N/A
m-coumaric acid	*Ec*MhpR/P_{mhpA}	*E. coli* DH5α	*E. coli* AFMCRAL	7-fold induction	N/A	β-galactosidase assay	N/A	[145]
p-coumaric acid	*Bs*PadR/P_{BSU_34400}	*B. subtilis* subsp. *subtilis* str. 168	*E. coli* XL1-blue	130-fold induction	of the tested chemicals, only *p*-coumaric acid acted as an inducer	YFP fluorescence measurement	yeast cell sorting for *p*-coumaric acid production	[34]
p-coumaric acid	*Pp*PadR/P_{padC} (KT11)	*B. subtilis* subsp. *subtilis* str. 168	*P. putida* KT2440	134.8-fold induction	partially specific (responds to ferulic acid)	mCherry fluorescence measurement	PCA production under the auto-regulatory system	[150]
p-coumaric acid	*Bs*K64A(PadR mutant)/P_{padC}	*B. subtilis*	*E. coli* BW25113 (F′)	1000-fold induction (1.3-fold higher than wild type PadR)	partially specific (responds to ferulic acid)	eGFP fluorescence measurement	N/A	[234]

Continued Supplementary Table S2

p-coumaric acid	*Sp*FerC/P_{LC}	*Sphingobium* sp. SYK-6	*E. coli* BL21	25-fold induction	partially specific (responds to feruli, sinapic and caffeic acids)	eGFP fluorescence measurement	N/A	[151]
p-coumaric acid	*Ab*HcaR/$P_{ACIAD\_RS07960}$	*A. baylyi* ADP1	*A. baylyi* ADP1	approximately 100-fold induction	partially specific (responds to ferulic and caffeic acids)	β-galactosidase assay	N/A	[144]
ferulic acid	*Sp*FerC/P_{LC}	*Sphingobium* sp. SYK-6	*E. coli* BL21	26.2-fold induction	partially specific (responds to *p*-coumaric, sinapic and caffeic acids)	eGFP fluorescence measurement	lignin degradation screening after treatment with feruloyl esterase enzymes	[151]
ferulic acid	*Sp*FerC/P_{LC}	*Sphingobium* sp. SYK-6	*E. coli* DH5α	118-fold induction	N/A	sfGFP fluorescence measurement	N/A	[39]
sinapic acid	*Sp*FerC/P_{LC}	*Sphingobium* sp. SYK-6	*E. coli* BL21	15.4-fold induction	partially specific (responds to *p*-coumaric, sinapic and caffeic acids)	eGFP fluorescence measurement	N/A	[151]
caffeic acid	*Sp*FerC/P_{LC}	*Sphingobium* sp. SYK-6	*E. coli* BL21	11.2-fold induction	partially specific (responds to *p*-coumaric, sinapic and caffeic acids	eGFP fluorescence measurement	N/A	[151]

Supplementary Table S3. Homology of proteins involved in lactic acid catabolism

Group [a]	Protein used for homology search	Protein sequence coverage (identity) in (%)						
		*Ec*LldR/P$_{lld\ P}$	*Pp*PdhR/P$_{lld\ P}$	*Pa*PdhR/P$_{lld\ P}$	*Pf*PdhR/P$_{Lct\ P}$	*Pl*PdhR/P$_{Lct\ P}$	*Cn*GntR/P$_{H16_RS19190}$	*Ec*GlcC/P$_{b2979}$
I	*Ec*LldP (b3603)	100 (100)	99 (66.37)	99 (65.18)	99 (65.48)	99 (64.95)	100 (65.13)	99 (63.08)
	*Ec*LldD (b3605)	100 (100)	98 (84.74)	95 (86.58)	ND	ND	ND	ND
	*Ec*LldR (b3604)	100 (100)	97 (41.09)	90 (41.91)	94 (40.32)	97 (40.16)	81 (34.86)	86 (31.20)
	*Pp*LldE (PP_4737)	ND	100 (100)	99 (81.69)	99 (84.49)	99 (84.92)	ND	ND
		*Cn*GntR/P$_{H16_RS19190}$		*Ec*RclR/P$_{b0306}$		*Cn*IclR/P$_{H16_RS06900}$		
II	*Cn*LldF (H16_RS19180)	100 (100)		97 (39.79)		97 (38.96)		
	*Cn*LldG (H16_RS19185)	100 (100)		40 (31.07)		ND		
	*Cn*LldE (H16_RS19190)	100 (100)		91 (34.85)		90 (40.51)		
	*Cn*GntR (H16_RS19195)	100 (100)		NS with *Ec*RclR		NS with *Cn*IclR; 67 (36.77) with *Cn*FadR		
		*Ec*GlcC/P$_{b2979}$		*Pp*GlcC/P$_{PP_3745}$		*Cn*LysR/P$_{H16_RS15430}$		
III	*Ec*GlcD (b2979)	100 (100)		100 (80.76)		96 (61.20)		
	*Ec*GlcE (b2978)	100 (100)		100 (64.29)		96 (47.37)		
	*Ec*GlcF (b2978)	100 (100)		100 (72.73)		99 (55.05)		
	*Ec*GlcC (b2980)	100 (100)		95 (62.14)		NS with *Cn*LysR		

[a]groups were designated as in Fig. 3.1

Supplementary Table S4. Biochemical compositions of ORRF

Biochemical composition	**ORRF**
Protein, amino acids, nucleic acids (g/kg)	123
Carbohydrates (g/kg)	223
Glucose (g/kg)	207
Xylose (g/kg)	9
Arabinose (g/kg)	2
Other carbohydrates (g/kg)	5
Lipids (g/kg)	179
Free fatty acids (g/kg)	114
Lysophospholipids (g/kg)	16
Phosphodiglycerides (g/kg)	36
Diglycerides (g/kg)	3
Triglycerides (g/kg)	7
Fatty alcohols (g/kg)	3
Organic acids (g/kg)	27.6
Lactate (g/kg)	1.0
Acetate (g/kg)	0
Other organic acids (g/kg)	25.9
Glycerol (g/kg)	3

Supplementary Table S5. Different medium compositions and obtained D-lactic acid concentrations of two biological replicates

Sample	ORRF, g/L	Yeast extract, g/L	Tween 80, %	D-lactic acid, mM	
1	200	1	0.1	4.880	4.304
2	200	1	0.025	11.401	10.663
3	200	1	0.00625	9.659	8.580
4	200	0.25	0.1	1.464	1.326
5	200	0.25	0.025	3.413	2.999
6	200	0.25	0.00625	2.852	2.661
7	200	0.0625	0.1	2.000	1.941
8	200	0.0625	0.025	4.101	3.542
9	200	0.0625	0.00625	2,315	3.643
10	100	1	0.1	4.176	2.478
11	100	1	0.025	4.926	4.023
12	100	1	0.00625	2.304	2.071
13	100	0.25	0.1	1.072	0.725
14	100	0.25	0.025	1.797	1.940
15	100	0.25	0.00625	1.628	1.286
16	100	0.0625	0.1	1.072	0.872
17	100	0.0625	0.025	2.010	1.823
18	100	0.0625	0.00625	1.739	1.554
19	50	1	0.1	1.275	1.196
20	50	1	0.025	1.746	1.544
21	50	1	0.00625	1.669	0.582
22	50	0.25	0.1	0.827	0.673
23	50	0.25	0.025	2.158	0.720
24	50	0.25	0.00625	0.074	0.115
25	50	0.0625	0.1	0.315	0.276
26	50	0.0625	0.025	0.343	0.459
27	50	0.0625	0.00625	0.093	0.114

Supplementary Table S6. Construction of plasmids

Construct name	Ligation method	Oligonucleotide primers pairs	Source	Amplified region	Vector backbone	Restriction enzymes
Constructs for lactic acids-inducible gene expression systems assays						
pEA003	restriction enzyme-based cloning	EA021 and EA022	*E. coli* MG1655 gDNA	glycolic acid-inducible promoter	pBRC1 (constructed based on 180)	AatII/NdeI
pEA004	restriction enzyme-based cloning	EA021 and EA023	*E. coli* MG1655 gDNA	glycolic acid-inducible system	pBRC1	AatII/NdeI
pEA005	restriction enzyme-based cloning	EA024 and EA025	*E. coli* MG1655 gDNA	lactic acid-inducible promoter	pBRC1	AatII/NdeI
pEA006	restriction enzyme-based cloning	EA026 and EA027	*C. necator* H16 gDNA	lactic acid-inducible promoter	pBRC1	AatII/NdeI
pEA007	restriction enzyme-based cloning	EA026 and EA028	*C. necator* H16 gDNA	lactic acid-inducible system	pBRC1	AatII/NdeI
pEA010	restriction enzyme-based cloning	EA032 and EA033	*P. putida* KT2440 gDNA	lactic acid-inducible promoter	pBRC1	AatII/NdeI
pEA011	restriction enzyme-based cloning	EA032 and EA034	*P. putida* KT2440 gDNA	lactic acid-inducible system	pBRC1	AatII/NdeI
pEA012	restriction enzyme-based cloning	EA035 and EA037	*P. putida* KT2440 gDNA	glycolic acid-inducible system	pBRC1	AatII/NdeI
pEA013	restriction enzyme-based cloning	EA035 and EA038	*P. putida* KT2440 gDNA	glycolic acid-inducible promoter	pBRC1	AatII/NdeI
pEA014	Hifi DNA assembly	EA013 and EA016; EG017 and N78	pIE005; *C. necator* H16 gDNA	lactic acid inducible promoter and *rfp*; *iclR* TF with constitutive promoter P_{13}	pBRC1	AscI/NdeI

Continued Supplementary Table S6

pEA015	Hifi DNA assembly	EA045 and EA041; EA039 and EA038	*E. coli* MG1655 gDNA	L-lactic acid inducible promoter and *lldR* with constitutive promoter P_{13}	pBRC1	AatII/NdeI
pEA015_60	Hifi DNA assembly	EA060C and EA038C	pEA015	*lldR* with a modified RBS sequence	pBRC1	AatII/SpeI
pEA015_61	Hifi DNA assembly	EA061C and EA038C	pEA015	*lldR* with a modified RBS sequence	pBRC1	AatII/SpeI
pEA015_62	Hifi DNA assembly	EA062B and EA038C	pEA015	*lldR* with a modified RBS sequence	pBRC1	AatII/SpeI
pEA015_63	Hifi DNA assembly	EA063B and EA038C	pEA015	*lldR* with a modified RBS sequence	pBRC1	AatII/SpeI
pEA016	restriction enzyme-based cloning	EA040 and EA041	*E. coli* MG1655 gDNA	L-lactic acid inducible promoter	pBRC1	AatII/NdeI
pEA017	restriction enzyme-based cloning	EA042 and EA043	*P. aeruginosa* PAO1 gDNA	lactic acid inducible promoter	pBRC1	AatII/NdeI
pEA018	restriction enzyme-based cloning	EA042 and EA044	*P. aeruginosa* PAO1 gDNA	lactic acid inducible system	pBRC1	AatII/NdeI
pEA019	Hifi DNA assembly	EA046 and EA047	*C. necator* H16 gDNA	lactic acid inducible system	pBRC1	AatII/NdeI
pEA020	Hifi DNA assembly	EA047 and EA049; EA046 and EA048	*C. necator* H16 gDNA	FadR family TF; lactic acid inducible promoter	pBRC1	AatII/NdeI
pEA021	Hifi DNA assembly	EA050 and EA051	*C. necator* H16 gDNA	glycolic acid inducible system	pBRC1	AatII/NdeI

Continued Supplementary Table S6

pEA022	Hifi DNA assembly	EA050 and EA052	*C. necator* H16 gDNA	glycolic acid inducible promoter	pBRC1	AatII/NdeI
pEA023	Hifi DNA assembly	EA053 and EA051	*C. necator* H16 gDNA	glycolic acid inducible promoter	pBRC1	AatII/NdeI
pEA024	Hifi DNA assembly	EA054 and EA056	*P. fluorescens* NCTC 10038 gDNA	lactic acid inducible promoter	pBRC1	AatII/NdeI
pEA025	Hifi DNA assembly	EA054 and EA055	*P. fluorescens* NCTC 10038 gDNA	lactic acid inducible system	pBRC1	AatII/NdeI
pEA026	Hifi DNA assembly	EA057 and EA058	*P. lactis* DSM 29167 gDNA	lactic acid inducible promoter	pBRC1	AatII/NdeI
pEA027	Hifi DNA assembly	EA057 and EA059	*P. lactis* DSM 29167 gDNA	lactic acid inducible system	pBRC1	AatII/NdeI
pEA028	Hifi DNA assembly	EA079 and EA078; EA077 and EA076; EA013 and EA016	pIE005; pBRC1	*iclR* TF; arabinose-inducible system; lactic acid inducible promoter and *rfp*	pBRC1	AscI/BamHI
pEA030	Hifi DNA assembly	EA086 and EA085; EA087 and EA052; EA051 and EA053	*C. necator* H16 gDNA	LysR family TF; glycolic acid-inducible promoters	pBRC1	AatII/NdeI
pEA032	Hifi DNA assembly	EA089 and EA090	*E. coli* MG1655 gDNA	lactic acid inducible system	pBRC1	AatII/NdeI
pEA033	Hifi DNA assembly	EA038 and EA081; EA088 and EA083; EA013 and EA084	pEA015; pBRC1	*lldR* TF; arabinose-inducible system; L-lactic acid inducible promoter and *rfp*	pBRC1	AscI/BamHI

Continued Supplementary Table S6

Constructs for phenolic acids-inducible gene expression systems assays						
pEV035	Hifi DNA assembly	EV092 and EV093	*A. baylyi* ADP1 gDNA	*p*-coumaric acid inducible system and HcaK putative hydroxycinnamates transporter	pBRC1	AatII/NdeI
pEV036	Hifi DNA assembly	EV094 and EV093	*A. baylyi* ADP1 gDNA	*p*-coumaric acid inducible promoter and HcaK putative hydroxycinnamates transporter	pBRC1	AatII/NdeI
pEV038	Hifi DNA assembly	EV097 and EV098	*B. multivorans* ATCC BAA-247 gDNA	putative *p*-coumaric acid inducible promoter and TF	pBRC1	AatII/NdeI
pEV039	Hifi DNA assembly	pEV099 and pEV100; pEV101 and pEV102; pEV044 and pEV045	*B. multivorans* ATCC BAA-247 gDNA; pBRC1	*p*-coumaric acid inducible system and TF; *rfp*	pBRC1	AatII/ BamHI
pEV040	Hifi DNA assembly	EV104 and EV103	*P. putida* KT2440 gDNA	*p*-coumaric acid inducible system	pBRC1	AatII/NdeI
pEV041	Hifi DNA assembly	EV104 and EV105	*P. putida* KT2440 gDNA	*p*-coumaric acid-inducible promoter	pBRC1	AatII/NdeI
pEA048	Hifi DNA assembly	EA132 and EA133	*L. argentoratensis* DSM 16365 gDNA	hydroxycinnamic acids-inducible promoter	pBRC1	AatII/NdeI
pEA049	Hifi DNA assembly	EA133 and EA134	*L. argentoratensis* DSM 16365 gDNA	hydroxycinnamic acids-inducible system	pBRC1	AatII/NdeI
pEV052	Hifi DNA assembly	EV106 and EV107	*E. coli* MG1655 gDNA	*m*-coumaric acid-inducible system	pBRC1	AatII/NdeI
pEV053	Hifi DNA assembly	EV107 and EV108	*E. coli* MG1655 gDNA	*m*-coumaric acid-inducible promoter	pBRC1	AatII/NdeI

The antibiotic resistance gene (chloramphenicol) for plasmids pEA010, pEA011, pEA012, pEA013, pEA017, pEA018, pEA024, pEA025, pEA026, pEA027, pEV035, pEV036, pEV040, pEV041, pEA048, and pEA049 was changed to tetracycline. Oligonucleotide primers IK003 and IK004 were used to amplify the tetracycline resistance gene from pME6000 (*Addgene*, USA), and cloned into the above mentioned plasmids by PmeI and AscI restriction sites.

Supplementary Table S7. Oligonucleotide primers

Primer name	Primer sequence (5' → 3')
Primers for lactic acids-inducible constructs	
N78	cagatatcggccggcctggcgcgccataaaacgaaaggctcagtcgaaagactgggcctttcgttttatgacgtcgac gtctggcgattcggccttcagg
EA013	ccttactcgagtttggatcc
EA016	agatggaaaaaagagaaatgttgcttgc
EA017	catttctctttttttccatctttccctttaatcatccggctcgtataatgtgtggagacttgaattcactagtttaactttaagaag gagatatatctatgtccgacgcagaca
EA021	atatatcatatgtaggcttcgctttgttgtgttgtgtg
EA022	atatgacgtctcccggacctcgtgcaca
EA023	atatgacgtcctaactcaggttcatctccagc
EA024	atatgacgtcataaaaccgccagaaatcaggg
EA025	atatatcatatgtaatactccattacttcatgcccat
EA026	atatatcatatgtcgctccggacgtgctg
EA027	atatgacgtcgaccgactccacgcgtc
EA028	atatgacgtctggtaggaccaatgcctgc
EA032	ttgccaggtttgcatatggg
EA033	atatgacgtccacatgctctccacaaaccc
EA034	atatgacgtccggtactgcccataaaagcc
EA035	atatatcatatgctcactcgcaacggtttttg
EA037	atatggcgcgccataaaacgaaaggctcagtcgaaagactgggcctttcgttttatgacgtcgacgtccctgtggctga ccattgagt
EA038	gcctttcgttttatgacgtctcatgcgtttttctccctcgaatg
EA038C	gcctttcgttttatgacgtctcatgcgtttttctccctcgaatg
EA039	ttccctttaatcatccggctcgtataatgtgtggagacttgaattcactagtttaactttaagaaggagatatatctaatgatt gttttacccagacg
EA040	aggaatcatccacgttaaggacgtcctttaccagacatctccccccac
EA041	acgtcttcgctactcgccatatgaggtctcctggagtccacg
EA042	atatatcatatgggttggctccctaattgt
EA043	atatgacgtctcccgacacccttacccg
EA044	atatgacgtctagtcttcctgcacgctgc
EA045	gccggatgattaaaagggaactttaccagacatctccccccac
EA046	acgtcttcgctactcgccatatgcgacttctccagacccgaaac
EA047	gcctttcgttttatgacgtcaatggtggtgtcgtctcagg
EA048	gtctgcgtcggacatagatg
EA049	catctatgtccgacgcagacgcctgaaggccgaatcgc
EA050	gcctttcgttttatgacgtcgccggtctcctcgtaagc
EA051	acgtcttcgctactcgccatatgcgactcctgtggggcct
EA052	atatatcatatgggtctccggcgggtc

Continued Supplementary Table S7

EA053	atatgacgtccgacatggtctgcttcctg
EA054	cgtcttcgctactcgccatatggggtggcccctaattg
EA055	gggcctttcgttttatgacgtctccttgtgacactgtagccttg
EA056	gggcctttcgttttatgacgtcttactgacgcacctgatcaaacc
EA057	cgtcttcgctactcgccatatggggtggcccctga
EA058	gggcctttcgttttatgacgtcttactgacgcacctgatcaaacc
EA059	gggcctttcgttttatgacgtcaatccttgtgacggtgtagc
EA060C	ggagacttgaattcactagtacaagcagttataaggaggttattttatgattgttttacccagacgc
EA061C	ggagacttgaattcactagtataagaagacttaaggacaaaattgtatgattgttttacccagacgc
EA062B	ggagacttgaattcactagtctttcacagctcatcaagaggaatccatgattgttttacccagacgc
EA063B	ggagacttgaattcactagttaaatacctattggacggagaagctcatgattgttttacccagacgc
EA076	tgtctgcgtcggacatatgtatatctccttcttaaaagatcttttgaattcc
EA077	catttctctttttttccatctttaagcagaaggccatcctgacggatggccttttgcgtttctacttatgacaacttgacggcta
EA078	atgtccgacgcagacaagt
EA079	ggcctttcgttttatgacgtc
EA081	atgattgttttacccagacgc
EA083	tctgggtaaaacaatcatatgtatatctccttcttaaaagatcttttgaattcc
EA084	agatatatctccttcttaaagttaaactagtg
EA085	gcctttcgttttatgacgtctaccagtccaggctcag
EA086	gacccgccggagacccatggcctccatgttcaacc
EA087	caggaagcagaccatgtcggtagaaacgcaaaaaggccatccgtcaggatggccttctgcttaagccggtctcctcg taagc
EA088	cactagtttaactttaagaaggagatatatctgtagaaacgcaaaaaggccatccgtcaggatggccttctgcttaattat gacaacttgacggcta
EA089	ataacgtcttcgctactcgccatatgccactccttgtggtggc
EA090	gcctttcgttttatgacgtcatggatttttcttcctttgttgcc
Primers for phenolic acids-inducible constructs	
EV044	atggcgagtagcgaagac
EV045	aagcaccggtggagtgac
EV092	gggcctttcgttttatgacgtctaaattaatgccgagcttaagaaagctg
EV093	cgtcttcgctactcgccatatgttttctccttgaatgacaaattgtgc
EV094	gggcctttcgttttatgacgtcttatctatcaactgaacttgaacgtagcat
EV097	cgtcttcgctactcgccatatgtggcggaaaacgtgcgc
EV098	gggcctttcgttttatgacgtctaagaacgtgtcggaatcgatatcg
EV099	gggcctttcgttttatgacgtctaaggtacctgatcgcgcgacg
EV100	cgtcttcgctactcgccatatgcgttctccaatgacagcgc

Continued Supplementary Table S7

EV101	gtcactccaccggtgcttaactcggtaccaaattccagaaaagaggcctcccgaaaggggggccttttttcgtttatcg gtggcggaaaacgt
EV102	ccttactcgagtttggatccgtcgtctccaaacctggac
EV103	gggcctttcgttttatgacgtcgactgagtcagtcccggtag
EV104	cgtcttcgctactcgccatatgtctgcactcttgttgttcgagg
EV105	gggcctttcgttttatgacgtccaggtttcatgctcctcgatca
EV106	gggcctttcgttttatgacgtcccattcgatggtgtcaacgt
EV107	cgtcttcgctactcgccatatgagtacctcacgactcggaca
EV108	gggcctttcgttttatgacgttattccgtctgctcattgttctgc
EA132	gggcctttcgttttatgacgtcaaagcgccttcctctcgc
EA133	cgtcttcgctactcgccatatgttcagatcctttcaggatgatttaaacagtcg
EA134	gggcctttcgttttatgacgtctcatgaaattgttgacgattgtgcc
Primers for antibiotic resistence gene replacement	
IK003	tcgttttatggcgcgccaggccggccaattagaaggccgccagagagg
IK004	actagtactgtttaaaccgctcacaattccacacaa

Supplementary Figures

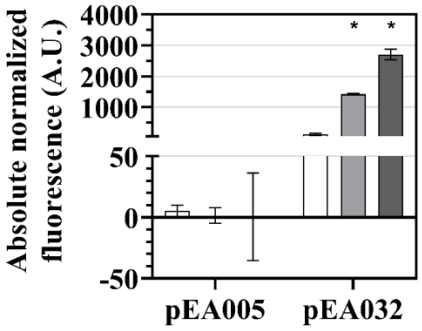

Supplementary Fig. S1. Absolute normalized fluorescence of *E. coli* DH5α harboring the constructs pEA005 (*Ec*P$_{b0306}$) and pEA032 (*Ec*RclR/P$_{b0306}$). Cells were grown with glucose (white), L-lactate (light gray), and D-lactate (dark gray) as the carbon source. Single time-point fluorescence measurements were taken at 6 h. Data is presented as mean ± SD, n = 3, *p ≤ 0.01 (unpaired *t*-test). This figure was used in [172]

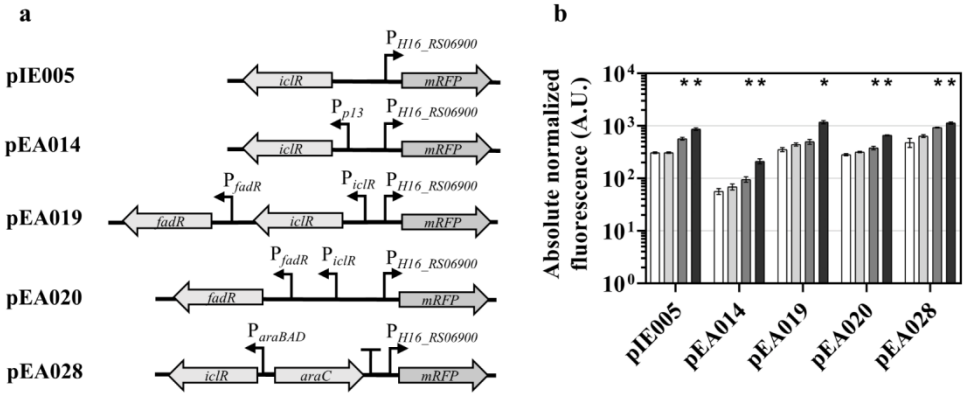

Supplementary Fig. S2. (a) Schematic illustration of the different versions of the *Cn*IclR/P$_{H16_RS06900}$ system and their corresponding plasmid identifiers. **(b)** Absolute normalized fluorescence of *C. necator* H16 carrying different versions of the *Cn*IclR/P$_{H16_RS06900}$ system construct in the absence of inducer (white) and presence of L-lactate (light gray), D-lactate (dark gray), and glycolate (black) of 5 mM. In the case of pEA028, the inducer culture was additionally supplemented with 0.2% L-arabinose. Cells were grown in SG-MM containing 0.4% gluconate. Data is presented as mean ± SD, n = 3, *p ≤ 0.01 (unpaired *t*-test). This figure was used in [172]

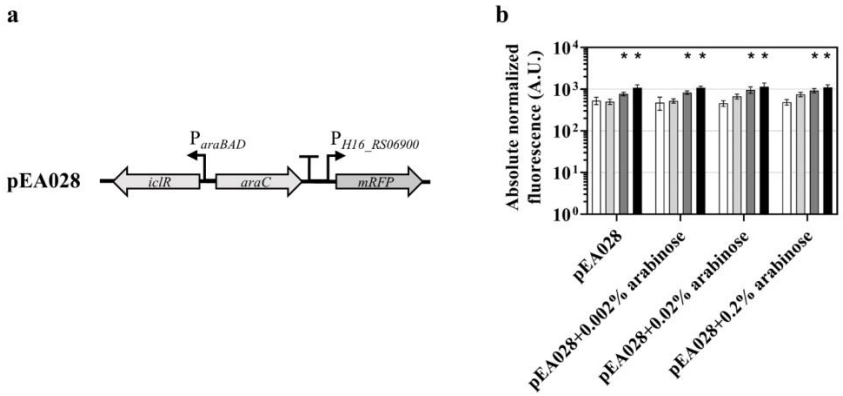

Supplementary Fig. S3. (a) Schematic illustration of the *Cn*IclR/$P_{H16\_RS06900}$ system with an adjustable L-arabinose system. **(b)** Absolute normalized fluorescence of *C. necator* H16 carrying pEA028 vector with different arabinose concentration in the absence of inducer (white) and presence L-lactate (light gray), D-lactate (dark gray), and glycolate (black) of 5 mM. Cells were grown in SG-MM containing 0.4% gluconate. Data is presented as mean ± SD, n = 3, *p ≤ 0.01 (unpaired *t*-test). This figure was used in [172]

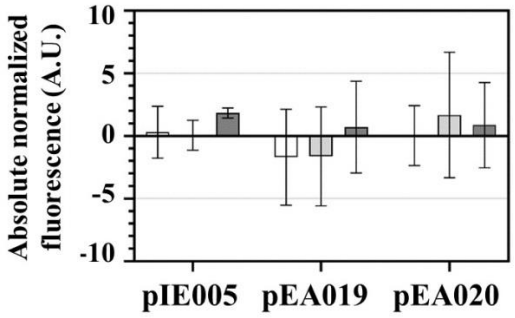

Supplementary Fig. S4. Absolute normalized fluorescence of *E. coli* DH5α harboring constructs pIE005, pEA019, and pEA020 with *Cn*IclR/$P_{H16\_RS06900}$, *Cn*IclRFadR/$P_{H16\_RS06900}$, and *Cn*FadR/$P_{H16\_RS06900}$, respectively. RFP fluorescence output was determined in the absence of inducer (white) and at 6 h after extracellular supplementation with D-lactate (light gray) and glycolate (dark gray) of 5 mM. Cells were grown in MM containing 0.4% glucose. Data is presented as mean ± SD, n = 3, *p ≤ 0.01 (unpaired *t*-test). This figure was used in[172]

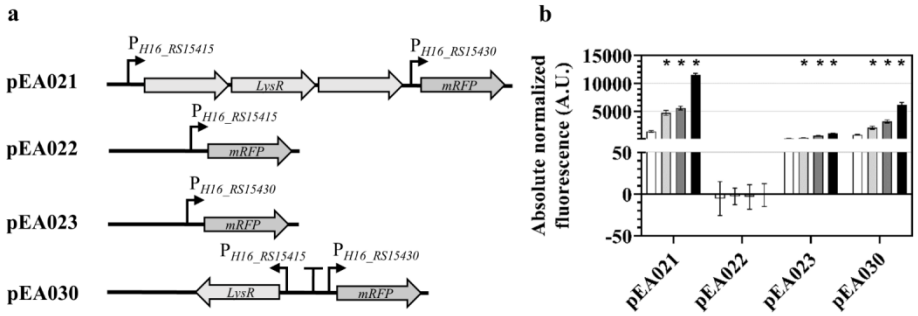

Supplementary Fig. S5. (a) Schematic illustration of the different versions of the *Cn*LysR/$P_{H16\_RS15430}$ inducible system and their corresponding plasmid identifiers. (**b**) Absolute normalized fluorescence of *C. necator* H16 carrying different versions of the inducible system/reporter construct without (white) and with extracellular supplementation of either L-lactate (light gray), D-lactate (dark gray), or glycolate (black) of 5 mM. Cells were grown in SG-MM containing 0.4% gluconate. Data is presented as mean ± SD, n = 3, *p ≤ 0.01 (unpaired *t*-test). This figure was used in [172]

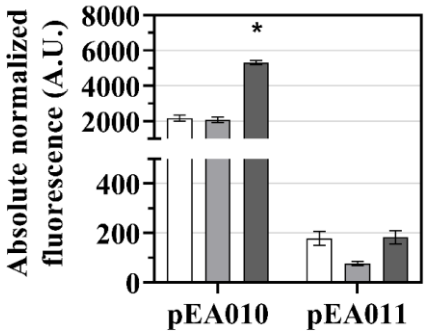

Supplementary Fig. S6. Absolute normalized fluorescence of *P. putida* KT2440 harboring constructs pEA010 and pEA011 with *Pp*P_{lldP} and *Pp*PdhR/P_{lldP}, respectively. Cells were grown with glucose (white), L-lactate (light gray), and D-lactate (dark gray) as carbon source. Single time-point fluorescence measurements were taken at 12 h. Data is presented as mean ± SD, n = 3, *p ≤ 0.01 (unpaired *t*-test). This figure was used in [172]

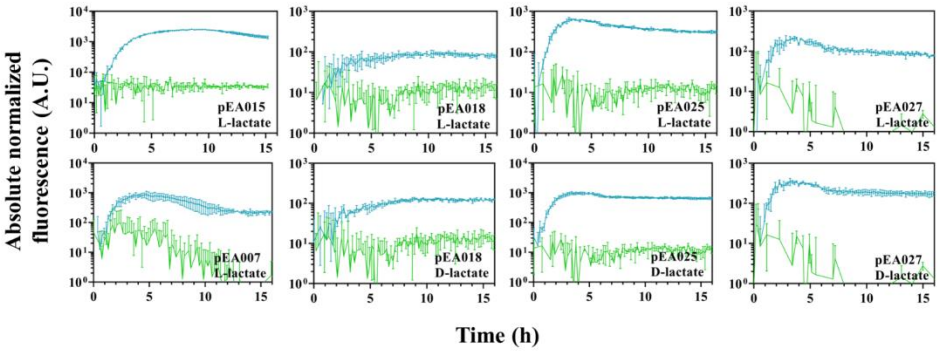

Supplementary Fig. S7. Induction kinetics of the identified lactic acid-inducible systems. Absolute normalized fluorescence of *E. coli* DH5α harboring pEA015 with *Ec*LldR/P_{lldP}, *C. necator* H16 harboring pEA007 with *Cn*GntR/$P_{H16\_RS19190}$, and *P. putida* KT2400 harboring pEA018, pEA025, and pEA027 with *Pa*PdhR/P_{lldP}, *Pf*PdhR/P_{lctP}, and *Pl*PdhR/P_{lctP}, respectively. Cells were grown in MM containing 0.4% glucose (in the case of *C. necator* H16, supplemented with 0.4% gluconate) for 16 hours. RFP-fluorescence output was determined in the absence of inducer (green) and in the presence of either L- or D-lactate (blue), which were added at time 0 hours to a final concentration of 5 mM. Data is presented as mean ± SD, n = 3. This figure was used in [172]

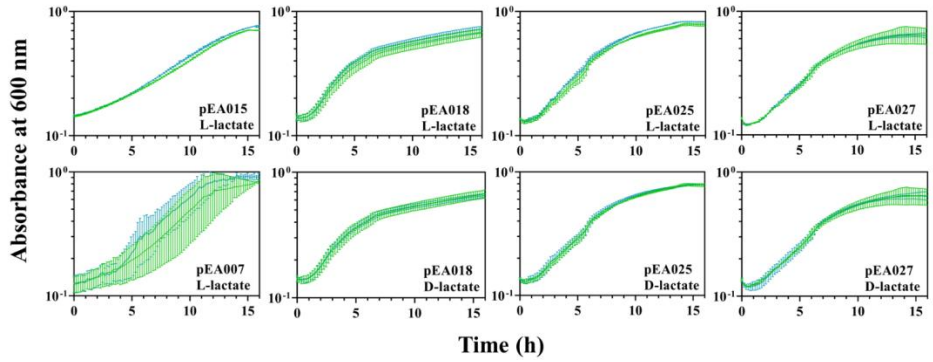

Supplementary Fig. S8. Cell growth dynamics. Graphs represent the optical density over time in cell cultures of *E. coli* DH5α harboring pEA015 with *Ec*LldR/P_{lldP}, *C. necator* H16 harboring pEA007 with *Cn*GntR/$P_{H16\_RS19190}$, and *P. putida* KT2400 harboring constructs pEA018, pEA025, and pEA027 with *Pa*PdhR/P_{lldP}, *Pf* PdhR/P_{lctP}, and *Pl*PdhR/P_{lctP}, respectively. Cells were grown in MM containing 0.4% glucose (in the case of *C. necator* H16, supplemented with 0.4% gluconate) for 16 hours. Absorbance was measured in the absence of inducer (green) and in the presence of either L- or D-lactate (blue), which were added at time 0 hours to a final concentration of 5 mM. Data is presented as mean ± SD, n = 3. This figure was used in [172]

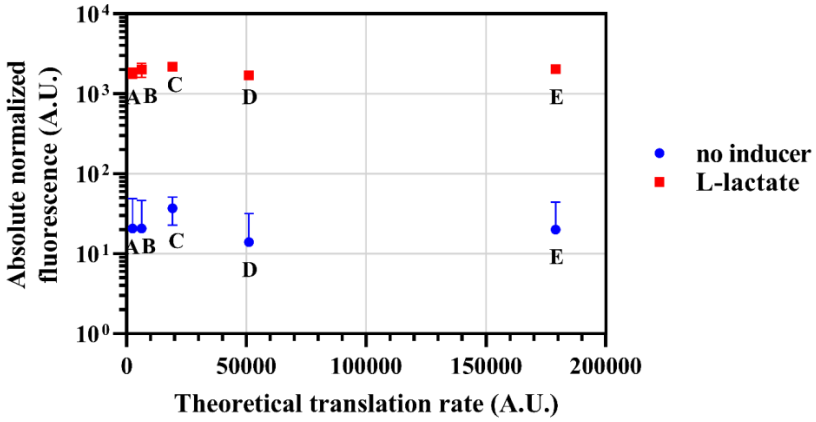

Supplementary Fig. S9. Influence of *lldR* theoretical translation rate on the dynamic range of the *Ec*LldR/P_{lldP}-inducible system. Absolute normalized fluorescence values of *E. coli* DH5α carrying variants of the *Ec*LldR/P_{lldP}-inducible system with different RBS sequences upstream to the *lldR* gene are compared to the corresponding theoretical translation rates. Plasmid constructs containing *Ec*LldR/P_{lldP}-inducible system with different RBS sequence variants were as follows: A-pEA015-63; B-pEA015-62; C-pEA015; D-pEA015-61; E-pEA015-60. Cells were grown in MM containing 0.4% glucose. Data is presented as mean ± SD, n =3. This figure was used in [172]

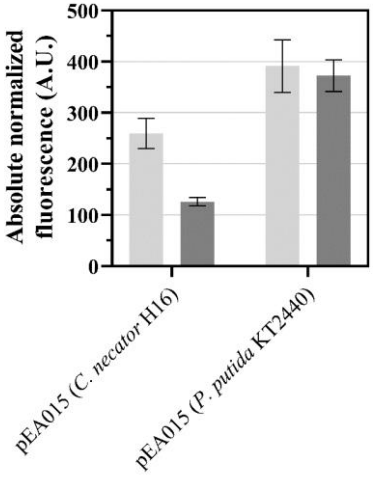

Supplementary Fig. S10. Absolute normalized fluorescence of *C. necator* H16 and *P. putida* KT2440 carrying pEA015 (*Ec*LldR/P_{lldP}). RFP fluorescence output was determined in the absence of ligand (light gray) and 6 h after extracellular supplementation with L-lactate to a final concentration of 5 mM (dark gray). *P. putida* cells were grown in MM containing 0.4% glucose (in the case of *C. necator* H16, SG-MM was supplemented with 0.4% gluconate). Data is presented as mean ± SD, n =3. This figure was used in [172]

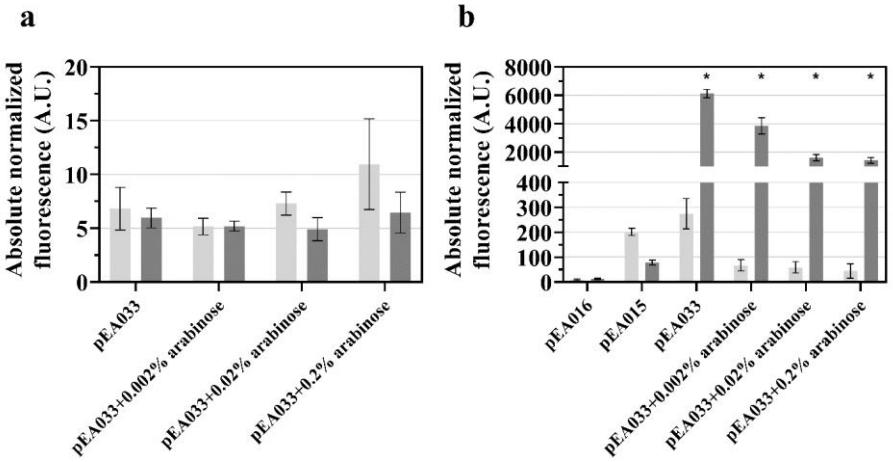

Supplementary Fig. S11. Absolute normalized fluorescence of *C. necator* H16 harboring different versions of L-lactic acid-inducible systems (*Ec*LldR/P_{lldP}). **(a)** *C. necator* H16 cells were grown in SG-MM with 0.4% gluconate in the absence of inducer (light gray) and extracellular supplementation with L-lactate of 5 mM (dark gray). **(b)** *C. necator* H16 cells were grown with gluconate (light gray) and L-lactate (dark gray) as a carbon source. In the case of pEA033, the culture was supplemented with different concentrations of L-arabinose. Single time-point fluorescence measurements were taken at 6 h. Data is presented as mean ± SD, n = 3, *p ≤ 0.01 (unpaired *t*-test). This figure was used in [172]

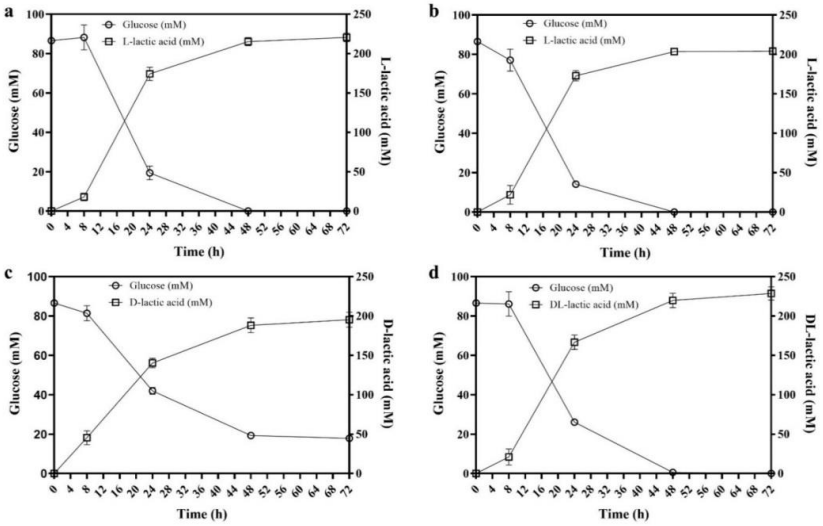

Supplementary Fig. S12. Lactic acid production and glucose utilization during fermentation by **(a)** *L. paracasei* (microaerophilic conditions), **(b)** *L. paracasei* (aerobic conditions), **(c)** *L. lactis* (microaerophilic conditions), and *L. amylovorus* (microaerophilic conditions) with MRS medium with 2% glucose. Data is presented as mean ± SD, n = 3

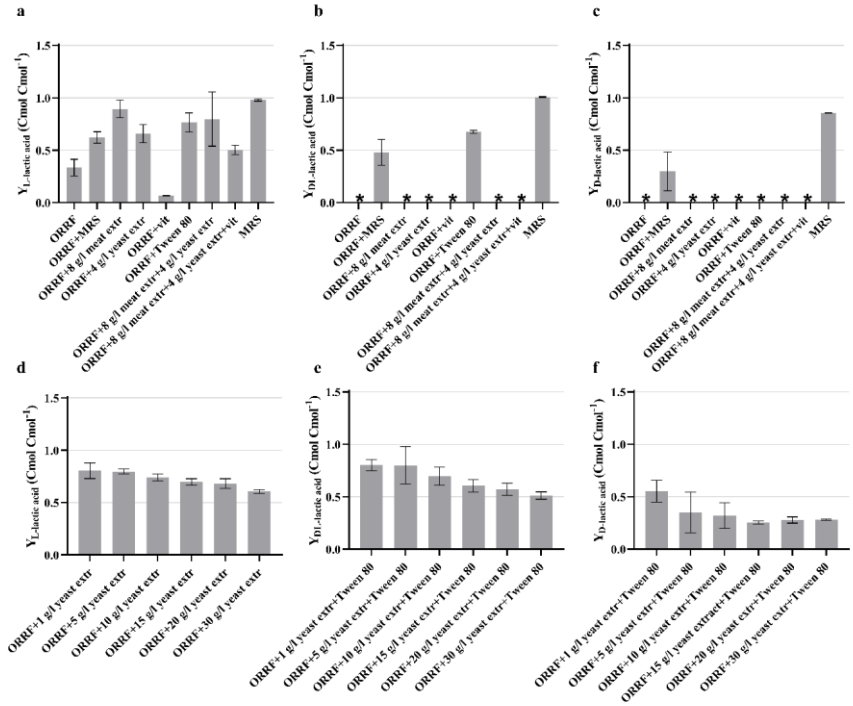

Supplementary Fig. S13. Lactic acid yields (Cmol Cmol^{-1} on glucose) produced by **(a, d)** *L. paracasei*, **(b, e)** *L. amylovorus*, and **(c, f)** *L. lactis* on 200 g/L ORRF (containing about 42 g/L glucose) at 72 h. Nutrient supplements used in lactic acid production are indicated. *-no growth was observed, and yields were not estimated. Error bars represent standard deviations of two biological replicates. Data is presented as mean ± SD, n = 2

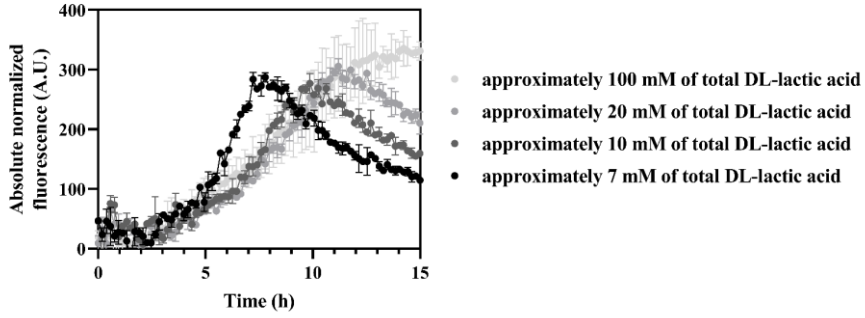

Supplementary Fig. S14. Absolute normalized fluorescence of genetically encoded biosensor BLA1 in MM with 0.4% glucose supplemented with different dilutions of *L. amylovorus* fermentation samples collected at 72 h. *L. amylovorus* was grown by using 200 g/L of ORRF supplemented with 20 g/L of yeast extract and 0.1% Tween 80. Data is presented as mean ± SD, n = 3

UDK 577.21+53.082.9+661.746.2](043.3)

SL344. 2023-09-15, xx leidyb. apsk. l. Tiražas 14 egz. Užsakymas 144.
Išleido Kauno technologijos universitetas, K. Donelaičio g. 73, 44249 Kaunas
Spausdino leidyklos „Technologija“ spaustuvė, Studentų g. 54, 51424 Kaunas